PARTICULATE STARCH,

ITS EFFECTS AS A FILLER

IN HIGH DENSITY POLYETHYLENE

BY

Seyed Ali HASHEMI (BSc. MSc.)

Department of Non-Metallic Materials,
Brunel University, Uxbridge,
Middlesex, England, G.B.

A THESIS SUBMITTED IN FULFILMENT

OF THE REQUIREMENT FOR THE DEGREE

OF DOCTOR OF PHILOSOPHY AT BRUNEL

UNIVERSITY

April 1983

I CERTIFY THAT ALL THE

EXPERIMENTAL WORK DESCRIBED

IN THIS THESIS WAS CARRIED

OUT BY MYSELF

S. A. Hashemi

ABSTRACT

Rapid advances continue in the acquisition of new fundamental knowledge of starch and a vigorous expansion in the use of starch is proceeding in both food and non-food applications. Results are here reported on starch-filled high density polyethylene which reveal reinforcement effects of starch on the thermoplastic. This significant development makes starch a most promising organic filler.

This work is primarily a study of the mechanical and thermal properties of starch-filled high density polyethylene and attempts to identify changes caused in the structure of this polymer due to starch filler. Particular attention has also been given to changes in crystallinity and microscopic appearance.

Because preliminary studies showed that enhanced effects were obtained when using starches of small particle size, much effort was given to developing a simple method of extraction of starches from the many varieties of Taro (Colocasia esculenta) plants in order to get the best possible yield and freedom from agglomerates. Because of the absence of recorded data it was necessary to study the physical properties of these starches.

The theory and application of small-angle light scattering was reviewed because of its value as a technique for the characterization of starches and spherulitic polymer studies. One hundred and twelve Taro starches were characterized in terms of average particle sizes by the above technique. Starches with particle sizes ranging from 3 micron to 50 micron were investigated in order to establish the size/effect relationship in starch polymer composites.

Methods of increasing the adhesion between filler and polymer matrix have also been studied, as has also the stripping of amylopectin from starch grains by cold acid treatment. Acid treatment, surprisingly, produced composites of increased mechanical strength in high density polyethylene, implying that a true reinforcing filler has been created.

Results from differential scanning calorimetry and x-ray diffraction studies revealed that an increase in degree of crystallinity in high density polyethylene was associated with the presence of starch.

Acknowledgements

The author wishes to express his sincere appreciation to Mr. G.J.L.Griffin, Director of Ecological Materials Research Institute, for his guidance during this entire investigation.

The author would like to record his gratitude to Dr. W.G.Griffin for valuable suggestions and discussions on the subject.

I am indebted to Professor M. Bevis, Head of Department of Non-Metallic materials for his personal support and encouragement.

Thanks are due to technical staff of the Department of Non-Metallic Materials and the Experimental Techniques Centre.

I am indebted to my colleagues, former and present, who during the course of investigation helped me to gain experience.

The author wishes to express his gratitude to his brother, Dr. S.R.Hashemi for financial support received during the past five years.

Finally, I wish to thank Mrs. J. Bradbury for typing the scripts.

CONTENTS

Contents

Contents

Contents

Contents

Contents

CHAPTER 1

INTRODUCTION

1.0 Introduction

Organic plastics additives offer advantages to the plastics processor, to the user, and to society as a whole. A wide range of these additives may be used to give plastic products improved mechanical properties, better surface quality for some applications and when desired, biodegradability (1 - 7). Additional benefits may include lower product cost, processing energy savings and reduced wear on processing machines.

The use of these additives makes it possible to replace a part of the polymer which is an ever more costly petrochemical product, by starch, an easily renewable natural product available in nearly every country. In many cases the user benefits from a product which for the same price may be lighter and have a better appearance. Some of the additives are formulated to trigger and accelerate the biodegradation process of plastic bags and disposable articles when they are based underground and in refuse dumps, or simply discarded as litter.

Starch in its usual commercial form is totally unsuited for use with plastics. The starch must first be selected for the appropriate grain size according to the application. Then it must be carefully dried and rendered hydrophobic. The excellent compatibility of these additives with many different plastics and the ease and simplicity of processing makes it possible to use starch in a variety of uses on different polymers. Specially

treated starch has been tested in polyethylene, polypropylene, polystyrene, polyurethane, ethylene vinylacetate copolymers, polyester, PVC and ABS. Plastic containing the additives have been made into film for bags, mulch film, injection mouldings, blow mouldings, sheets for thermoforming, and foams, plastisols, and polymer solutions. The latter are used for coating fabrics, paper, cellophane, etc. and have not only given a better surface with starch additive, but in some cases the starch has made it possible to increase the speed of the coating process.

Each new application must be carefully examined to find the proper balance of physical and chemical properties, appearance, material cost, processing cost and other factors required. Starch particles from different plants have different sizes and shapes, making it possible to choose the best-suited type of starch for each use. For every thin film, small particle size starches like rice or taro may be needed, whereas wheat and maize starch give good results with most blown films.

Several detailed investigations of the properties of starch-filled plastics have already been carried out (3 & 9). However, some questions have been raised concerning the relationship between structure/composition of the starch-filled plastics and the physico-chemical properties of these materials which have been investigated in the present work. Emphasis is placed, in this thesis, on experiments designed to elucidate the mechanisms by

which means starch-polymer interactions result in properties of the composite markedly different from the unfilled polymer properties. In particular attention has been directed towards increasing our understanding of the thermal, and mechanical properties of starch-filled HDPE and the way in which the microscopic structure of the starch-polymer interface affects these properties. An extensive tabulation of mechanical properties of starch-filled LDPE has been presented in the thesis of Linero (9).

Linero in his work has drawn several conclusions about starch fillers and their possible influence on the matrix polymer. We can summarise his experimental results on starch filled plastics in three different systems, as follows:

If the matrix polymer is amorphous like polystyrene, the starch acts as an extender, and the transformation of the starch character from hydrophilic to hydrophobic increases substantially the compatability of the two materials. It is also expected that particle size and particle size distribution should play a fundamental role in determining the properties of the composite.

In the case of a crystalline polymer like low density polyethylene, the most important facts are particle size and particle size distribution. It is therefore advisable to use small particles and a narrow particle size distribution. A hydrophobic coat around the particles also helps processability and leads to a material with a higher yield strength (the increase in yield strength

appeared to be abnormally high and suggest a significant change in the physical properties of the matrix polymer itself). Linero concluded that when working with resins with active groups like an acidic unsaturated polyester resin, for example, the most important fact to consider is the chemical compatibility at the interface. It is preferable to treat the granules with sodium hydroxide solution under very mild conditions to increase their wettability by the resin. Mild alkaline treatment avoids weakening the starch granular structure.

Following Linero's work, the present work was aimed at obtaining a deeper understanding of the effect on the starch fillers on the properties of high-density polyethylene (HDPE). The first step was to choose particle sizes and shapes, recommended by Linero as producing optimal properties with the aim of testing some of Linero's speculation in the composite and to study such systems. In order to measure the particle size of starches, a study using light scattering on the basis of the Stein's technique (10), utilizing radiation of one wavelength in the range of visible light has been undertaken.

The physical and mechanical properties of polymers are profoundly dependent on their degree of crystallinity, for example, the tensile strength and stiffness of polymer fibres are directly related to the degree of alignment of the molecular chains parallel to the

fibre axes and hence to the degree of crystallinity. Likewise the stress at which the polymer starts to cold-draw (yield strength) increases with the degree of crystallinity. The changes in crystallinity have been studied by differential scanning calorimetry (D.S.C.). This technique has been widely used to determine the crystallinity of semi crystalline polymers.

Morphological changes of starch-filled plastic have been investigated using light microscopy, scanning electron microscopy (S.E.M.) and transmission electron microscopy.

CHAPTER 2

GENERAL REVIEW

2.00 General Review

2.1 Structure of starch

Starch and cellulose are both naturally occurring polymers composed of the same structural unit D-glucose (fig. 2.1). Their physical and chemical properties have been studied extensively (11,12) and major industries have been created dealing with their utilization. In starch the units are α-linked, whereas in cellulose they are β-linked and consequently the polymer structures are different in conformation. The cellulose occurs in plant cell walls in fibrillar form and is now a fairly well understood structure both on the molecular as well as on the supermolecular (ultra structural) level. Starch, however, occurs in granular form and its internal ultrastructural organization is not well known; nor has exact determination of its molecular conformation been achieved.

2.1.1 Native Starch structure

Most starches consist of two chemically distinct components, amylose and amylopectin, and these two are present in varying amounts in starch from different botanical sources.

Amylose is a linear polymer whereas amylopectin is a branched polymer (fig. 2.1). Most common cereal starches of the non-waxy types contain about 25% amylose. The amylose stains bright blue with iodine, and it has been shown by Bear (13) and by Rundle and

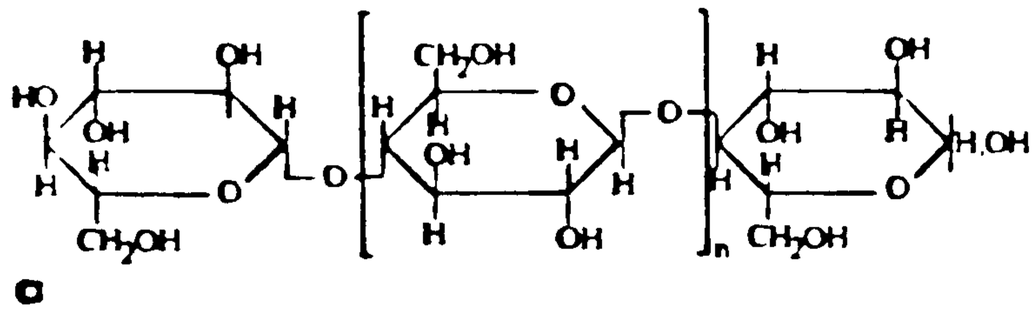

(a) cellulose

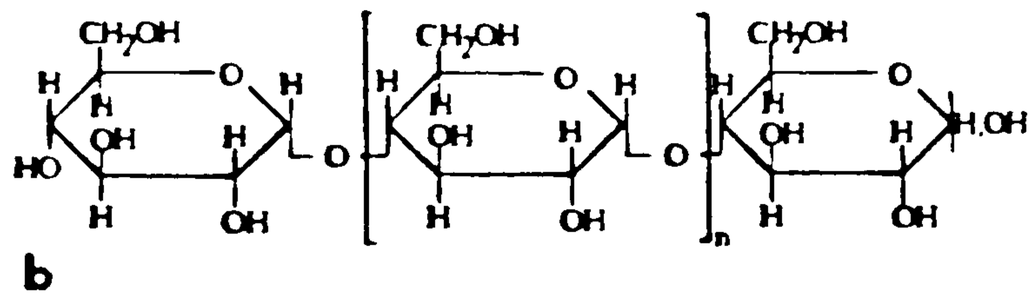

(b) amylose

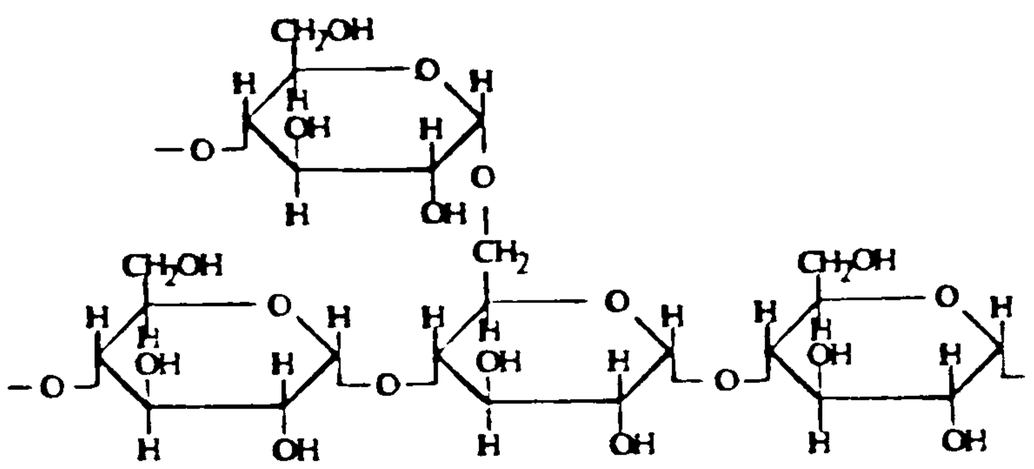

(c) amylopectin branching point

(d) C1 conformation

Fig (2.1) Amylose is a linear polymer of 1-4 linked α- D - glucose residue in the C1 conformation whereas a mylopectin contains additional α-(1-6) - glycosidic branching link.

co-workers (14) using x-ray crystallography, to have a helical structure in its crystalline complexes. This establishment of a helical conformation in starch was not well received at the time, but is currently accepted for many natural products. Unit-cell dimensions would indicate a helix containing about 6 D-glucose residue per turn. These dimensions are such that the iodine molecule (15) could be accommodated within the helix; this suggestion has been offered previously by Hames (16) and by Freudenburg and associates (17). Various methods can be used to determine the ratio of amylose to amylopectin (11). However, in order to study the composition a breakdown of the matrix structure is always necessary and it is difficult to ascertain whether a complete characterization of the two fractions, amylose and amylopectin, is possible in view of chemical hydrolysis occurring during the analysis procedure. The ratio of two fractions varies depending on the starch variety. Table (2.1) shows some of these ratios which were calculated by C. Ogbonna (18) for taro starches. The most common starch yielding plant species, as for example potato, corn or wheat, contain 70-80% of amylopectin, but certain "waxy" varieties of rice and corn are nearly 100% amylopectin.

Despite the differences in the content of linear and branched components, the starches are fairly uniform in microscopic appearance. The size and the shape of the granules are dependent on their growth conditions (14) and thus, to a certain extent dependent on the starch variety.

Table (2.1) showing Amylose content and Gelation temperature of 109 varieties of Taro (18)

Class No.	Horticultural Varieties	Amylose Content (%)	Gelation Temp. (^{o}C)
1	Tsurunoko	23	74
2	Akado	28	70
3	Miyako	28	71
4	Iliuaua	18	72
5	Bun-Long	22	71
6	Awau	18	72
7	Kakakura-Ula	22	72
11	Mana Uliuli	28	71
12	Mana Ulaula	43	71
13	Mano Lauloa	20	69
14	Mano Keokeo	22	70
16	Piko Lehua-apei	32	69
17	Piko Ulaula	18	69
18	Piko Kea	33	69
19	Piko Keokeo	19	69
20	Piko Uaua	27	70
22	Piko Eleele	10	69
23	Elepaio	40	70
24	Uahiapele	22	68
25	Manapiko	20	69
26	Tahitian	20	70
27	Kai Uliuli	27	72
28	Kai Ala	23	72
29	Kai Kea	43	70
30	Apuwai	28	70
31	Apu	33	71
32	Piialii	27	72

Class No.	Horticultural Varieties	Amylose Content (%)	Gelation Temp. (^{o}C)
33	Paakai	23	70
34	Moana	29	70
38	Lauloa Palakea-eleele	23	70
39	Lauloa Palakea-ula	16	72
40	Lauloa Palakea-papamu	29	72
41	Lauloa Palakea-keokeo	21	72
42	Lauloa Keokeo	31	74
43	Eleele Makoko	21	72
44	Eleele Naioea	29	72
45	Manini-Owali	28	70
46	Kumu eleele	29	72
47	Nawao	29	70
48	Ulaula Kumu	27	70
49	Ulaula poni	19	70
50	Ulaula Moano	30	71
51	Niue - Ulaula	25	71
52	Oopukai	29	71
53	Manini Uliuli	26	70
54	Manini Kea	28	70
55	Manini Toretore	32	69
56	Papakolea - Koae	21	69
58	Nihopuu	25	71
59	Manini- Opelu	29	69
62	Ohe	16	73
63	Lehua Maoli	26	72
64	Lehua Keokeo	19	75
66	Lehua Palaii	19	72
67	Apowale	26	70
68	Wahiwa	16	69
69	Papapeuo	25	70
70	Kuoho	25	73
71	Leo	20	72

Class No.	Horticultural Varieties	Amylose Content (%)	Gelation Temp. (^{o}C)
72	Maea	23	69
73	Haokea	21	72
74	Kalalau	14	70
75	Hapuu	20	70
79	Mana Eleele	24	70
80	Mana Okoa	24	69
81	White Moi	21	69
84	Pololu	42	70
85	Piialii Ula	16	70
86	Red Moi	26	69
87	Kai KBS	9	69
101	Pola Samoa	28	69
103	Talo Manua	23	73
104	Lauloa Dala	28	72
105	Manakea Mata	24	71
106	Matangi Fauna	28	70
107	Sasa Uliuli	23	70
108	Mana Lanu-Mahata I	22	71
109	A'alii	22	71
110	Pula Mumu	39	73
111	Vaevae ula-uki	28	68
113	Falan	23	75
114	Sasa Paepae	23	72
115	Matale I	43	69
117	Katuangamea I	28	72
118	Katuangamea II	28	72
119	Teatea I	19	69
120	Teatea II	27	69
121	Yan 614	27	70
128	Pilipino Red-stem	24	74
129	Pilipino short-stem	28	70

Class No.	Horticultural Varieties	Amylose Content (%)	Gelation Temp. (°C)
131	Fai Fassi I	16	71
132	Taro Hoia	9	74
133	L73-365	3	74
135	L73-369	17	75
137	Manu Lanu-Mehata II	21	74
139	Fa Eleele	27	70
142	KBS Bun-Long	16	70
148	Sawa Pah-Uetata	22	74
149	Burra	29	73
151	Fai Fassi II	28	71
153	Yellow Benahi	26	73
155	Pang Daga	22	70
157	Kaladao	22	73
159	Purple Manalua	25	69
165	N3-396	20	70
167	N365-1	31	70
171	N7-391	15	70
173	N8-398	23	74
174	N7-398	26	72
175	N330	21	68

2.1.2 (X-ray diffraction patterns obtained from starch granules) In contrast to the situation with cellulose, little information regarding the structure of starch has been gained from application of X-ray diffraction methods (20). However, Katz and his co-workers (21) have shown that starches offer a variety of diffraction patterns, and much can be expected from the study of this diffraction data. Most X-ray investigations of starches have been limited to powder patterns which indicate in many instances a surprising degree of crystalline organization, are relatively weak and diffuse and have offered no great wealth of information. In the absence of knowledge concerning geometrical relationships between visible structure and diffraction pattern, and between separate diffractions, the problem has been a very difficult one. Bear and French (13) made progress by obtaining accurate information for a number of related patterns and by comparing line positions and intensities in these. It was possible to draw some conclusions regarding the structures responsible for them. Certain questions arose out of the crystallographic studies of Bear and French (13). These are stated below and some answers are indicated. Since starch granules are not in the ordinary sense pure crystalline materials, is it necessary to assume that all the diffraction rings are caused by a single crystalline starch component. The answer seems to be, yes. Although crystalline structures might perhaps be present in the parts of the granule, the major fraction of the granule is far less ordered as shown by Sterling (22) on the basis of X-ray diffraction analysis, the

granule as a whole might best be described as a mesomorphic structure, that is, a structure which is intermediate between the crystalline and the amorphous and in which the polymer chains tend to align parallel to the radial direction but with far less ordering in tangential direction (23). The granular growth progress by apposition (24) and is regulated by various enzymes which may determine the size and shape of granules (25). The growth processes are still not fully understood, when more information regarding the growth of the granule becomes available, the morphology of the mature granule may be better understood. X-ray diffraction analysis has shown that the starch granule is poly or crypto-crystalline and possesses a smaller degree of crystallinity than native cellulose such as, for example, cotton cellulose (22). Originally, X-ray patterns obtained from starch were designated A, B and C. the A type pattern being characteristic for cereal starches, the B type pattern being characteristic for tuber starches and the intermediate C type pattern being characteristic for bean and root starches (26). These different crystalline structures are interconvertible by heat/moisture treatment (27) and it is suggested that the degree of hydration determines the molecular conformation and associated obtained in the native granule (19). The branched amylopectin is able to crystallize (as is the linear amylose). The waxy starch varieties show as strong a crystalline pattern as other starches. In order to determine the exact crystalline conformation for each case, A, B, or C, it is necessary to obtain fibre diffraction diagrams, and this has not been

achieved for the native starch grain. Crystalline patterns similar to or identical with the B-type pattern of the native granule have been obtained from oriented amylose film (26). The quality and quantity of data on these patterns may make it possible to determine the structure of B-amylose (28). On the basis of work done it has been proposed that the B-conformation is a helix with six glucose residue patterns. It has also been proposed that V-amylose, a sixfold helical structure obtained by precipitation of amylose from solutions of organic solvents, is directly convertible to B-amylose on hydration. The other question which arises out of the work of French (13) concerns the relation between the A and B types of diffraction pattern. They may represent very different modifications or be indicative of only slight variations in the starch chain organization. These authors assumed that in going from an A to a B pattern only relatively slight alterations in unit cell dimensions and angles are necessary. As a consequence diffraction rings in corresponding locations on the two patterns are taken to have arisen from the corresponding atomic planes of the similar structures.

2.2 Acid treatment of Starch

In 1874, Nageli (29) described the preparation of an acid-resistant polysaccaride by protracted heterogeneous hydrolysis of potato starch granules by aqueous sulphuric acid at room temperature. Material obtained by heterogeneous aqueous and hydrolysis of starch granules, which was called amylodextrin, has been prepared and described in varying degrees of detail by other authors (30,31).

Kainuma and French (32) have assembled the following list of properties for amylodextrin:

(1) Amylodextrin dissolves readily in hot water to form a true solution rather than a paste. The Lintner process (33) for making soluble starch, by heterogeneous aqueous acidic hydrolysis in the cold, is simply an abbreviated Nageli type treatment.

(2) Amylodextrin can be recrystallized either from an aqueous solution in the cold, especially by freezing, or by adding organic agents such as methanol, ethanol, or acetone to a concentrated aqueous solution. Depending on the style of recrystallization, amylodextrin can give A, B. or V-type patterns of exceptional sharpness (34).

(3) Native potato amylodextrin (i.e. the insoluble residue of the original starch granules that has not been dissolved or re-crystallized) retains the external microscopic form, polarization cross, birefringence, retardation pattern, and X-ray diffraction pattern (35) of the parent starch.

(4) The average molecular size, as indicated by the number of groups reducing is in the range of 15-30 glucose units.

(5) Degradation by B-amylase gives about 80% hydrolysis to maltose.

(6) Although the native amylodextrin granules stain weakly, if at all, with dilute iodine solution, dissolved amylodextrin gives a red or purple iodine stain.

(7) The specific rotation of anhydrous amylodextrin is about $(\alpha)_D \doteq 195$ (H_2O).

(8) Amylodextrin is exceedingly resistant to further heterogeneous hydrolysis at room temperature, a portion of it remaining undissolved after years of acid treatments.

The heterogeneous hydrolysis of starch granules by aqueous acid is clearly a complicated process. It certainly cannot be regarded as the simple, uniform erosion of material from the granule surface. . Rather this heterogeneous hydrolysis preferentially attacks the more amorphous, gel-like portions of the starch granule (36) whether they be at the surface or in the interior. The crystalline portions are protected against acidic attack by at least two factors. First, the packing of the starch chains within the crystalline regions may be so dense that it does not permit the ready penetration of hydrated protons and accompanying anions. The gel-like, amorphous part of starch granules can readily take up acid molecules, with consequent local glycosidic hydrolysis. The crystallites would only be attacked at the surface of the crystallite or at its junction with an amorphous region. Such a picture is similar to that advanced for heterogeneous hydrolysis of cellulose (37,38).

The second factor is that, for hydrolysis to occur, it is necessary for the glucosidic unit to undergo a change in conformation from a chair to a half chair (39,40). As long as the glucose units are held in a crystalline matrix, such a conformational change would require a very high energy of activation, and hence would have a very low probability. This argument would still hold to some degree even for a glucosidic unit at the crystallite surface.

A high tendency to aggregate, as with amylose and the high-amylose starches, does not induce a high perfection of crystallinity. Here, the amylose molecules form strong and numerous inter-molecular bridges which mitigate against forming long "runs" of ordered association, necessary for good polymer crystallization. However, the disordered regions again form an amorphous gel so that they can be penetrated by acid. Cleavage of just a few molecular chains permits extensive "annealing" or, at least, ordering of the newly released chain ends. Such processes are well known in the case of cellulose where it is reported that a small amount of heterogeneous hydrolysis markedly sharpens the X-ray crystallinity of a sample (41,42). The iodine reaction of starch granules probably involves amylose molecules that run through the amorphous or gel regions. When iodine penetrates into these regions, it can react readily and energetically with the amylose, possibly even tearing some of it out of the ordered structures.

However, with the amylodextrins, the gel regions have been substantially removed, and there is no point of initiation for an iodine complex, even though there are still many long molecules present in the crystalline arrangement. The native amylodextrins from low-amylose starches (potato or waxy maize) are virtually insoluble in cold water, but dissolve readily in hot water to give clear solutions. Dilute (1%) solutions remain clear on cooling to room temperature, but more concentrated solutions (10% deposit part

of the amylodextrin in solid form.

As remarked by Nageli, dilute solutions of potato amylodextrin stain a purple colour with iodine. Such a reaction indicates that there are some fairly long amylose chains present, in the neighbourhood of 40 glucose units or more. However, the proportion of such long chains may be very small and they would still tend to dominate the iodine stain, in comparison with the more weakly reacting shorter chains that stain red or yellow.

Amylose on heterogeneous acid hydrolysis gives a degraded product that is almost insoluble in boiling water. On cooling the heated suspension, the insoluble residue settles out and may be readily removed by centrifugation, leaving a clear supernatant. The high-amylose starches (wrinkled pea) behave similarly.

Kainuma and French (32) found that amylose and the high-amylose starches give the weakest and most diffuse x-ray pattern, indicative of a low degree and perfection of crystallinity, and yet these same starches are still very insoluble even after prolonged acid treatment. Moreover, the extent of erosion of the amylose material during acid treatment is very much less than that of the "normal" and low-amylose starches. These observations suggest that it cannot be solely crystalline organization that protects the starch chains from attack. Rather, whatever organization protects starch chains against an acidic hydrolysis also gives them a high tendency to aggregate.

2.3 Microscopy of starches

Microscopy has been widely and beneficially applied in the study of starches.

2.3.1 Light microscope

In its simplest form, the light microscope is used in conjunction with a tungsten filament lamp which can provide either reflected or transmitted illumination. The latter is generally the more useful. Lower power magnification (< x100) is useful in assessing such methods as extent of aggregation or purity, medium power (x100 to x400) is suitable for the identification and study of individual and small arrays of granules. Higher powers (up to x1500) may be required for studying granule surface details and contaminants in gels. The modern microscope generally has a turret carrying several objectives, permitting easy change of magnifying power.

Light microscopy offers a ready means of observing starch and several text books (43 - 45) have been written to provide full descriptive data on starch.

Leeuwenhock (46), in 1719, seems to be the first to have studied starch granules microscopically, and made fascinating observations on the swelling phenomena shown by the starch granule when heated in water.

Nageli (47) on the basis of light microscopic studies, developed intuitively the concept of "micelli" as a grade of organization of starch molecules, with a crystalline character, in the construction of the starch granule. Several other concepts and models of starch granules have been based on microscopic observation, so our knowledge of the physical structure and behaviour of the starch granule has grown parallel to the development of microscopy techniques.

The microscope has also been traditionally employed for identifying the species of unknown starch, to detect adulteration and to provide information on granule aggregation.

Under polarized light most starch grains show a characteristic "Maltese cross" and the location of the hilum. For examination under the light microscope the starch sample should be mounted in diluted glycerol or Canada Balsam. The following features may be observed:

1. presence of foreign matter
2. the nature of aggregates or " lumps" of particles if these are present
3. the size and shape of the granules
4. the presence of layers or "rings"
5. the position of the hilum
6. the presence of fissures and cavities
7. the response to various stains and reagents
8 the gelatinization temperature
9. the appearance of the granules in polarized light

Electron microscopy may be used to help in the determination of the structure of materials.

2.3.2 Conventional Transmission Electron Microscopy (CTEM)

In most cases the CTEM can be used to derive information of several different kinds which extend right across the various areas of science concerned with elucidating micro-structure. The external surface of a body can be studied and information obtained concerning the external morphology of the specimen and also microscopic details of the surface roughness can be investigated. Materials of interest here are small particles in which the form of the natural surface has a direct bearing on the properties and uses of the material. However, even in material in which surface properties are not important, much information about the constitution of the material can be obtained by studying a prepared surface. Possibly one of the earliest applications of the CTEM was to study the size, shape and dispersion of small particles. Here, of course, transmission of electrons is not essential and the microscope is used as super optical microscope of great magnifying power and depth of focus, avoiding the problem which shadow micrographs of particles and fibres involve.

2.3.3 Scanning Electron Microscopy (SEM)

In contrast to CTEM, the field of application of SEM is wide. The requirements for suitable specimens are much less stringent than for TEM and virtually anything that does not decompose in the vacuum of the instrument can be examined.

Yamachi and French (48) have examined starch crystallites by electron microscopy to learn details of the structure of starch-forming molecules and their organization in starch granules.

The SEM has also been used to study the shape, size and surface topography of various starches as well as the internal morphology. Hall and Sayre (49) have reported in recent publications the sizes and surface details of a great variety of starches from different sources, using SEM.

2.4 Characterization and analysis of starches

Starches used by food and non food industries were obtained from several cereal grain and tuber crops. Molecular composition and inherent properties of the native starches are related to their origin; however, physical as well as chemical properties may be altered by the recovery process and by physical modification if the preparation of chemical derivatives are both applied to the isolated starch.

Analytical methods in the following sections are divided into two categories: i) general methods, ii) physical property methods. With exceptions, these methods can be applied to all starch products.

i) General Methods

2.4.1 Moisture

Under normal ambient temperature and humidity conditions, the

equilibrium moisture content of most unmodified cereal starches is about 12%, whereas that of some of the root starches, notably potato starch, is considerably higher - up to 18%. The value for modified and derivatized starches often varies from those of the parent starches, and most manufacturers dry their products so that final moisture contents are near the equilibrium value, thus preventing significant weight change during storage and transit.

Moisture or volatile contents of unmodified and modified starches are most commonly determined by drying to constant weight in a vacuum oven at 100-120°C(50-52). Air oven techniques (53) are sometimes employed although less accurate. Reference is usually made to the iodemetric titration method to calibrate these procedures. The Karl Fischer Method (54) method is frequently applied to starch products containing other volatiles which would be included in the weight loss obtained by oven drying, and it is similarly applied to those products showing evidence of decomposition at customary drying temperatures. Karl Fischer moisture value on starch products containing no other volatiles are in good agreement with the air oven results (55).

2.4.2 pH

Since the pH of a starch product affects the physical properties of pastes, most unmodified starches are adjusted to a pH level of about 5.0 during the final stages of processing. Some modified and derivatized starches, on the other hand, may be adjusted to a

somewhat higher pH value. pH is measured in the conventional manner by pH meters. Above pH 11 alkali metal substitution in the surface hydroxy groups reduces hydrogen bonding to the point of rapid swelling in water with eventual gelation. At the other extreme, pH values of starch slurries much below pH5 lead to progressive hydrolysis and destruction of the starch structure. These limits, associated with temperature, set important conditions upon the handling conditions for wet starch.

ii) physical property

2.4.3 Colour

Starches produced in commercial plants are isolated from cereal and root crops which contain significant amounts of protein, fibre, fat and other minor components. The colour of corn (maize) starch the major starch produced in the United States, is related primarily to non starch residues, particularly pigments associated with protein (glutin). The colour is minimized by processing methods that give products having the lowest possible concentrations of non starch components, or by bleaching starches recovered from corn or other pigment-free crops.

Starch colour is often assessed by visual comparison with a standard product, or by matching against certified colour standards such as the Munsel colour disks (56).

2.4.4 Density

Commercial starches are obtained in powder, "crystal", flake and

lump forms by several commercial methods resulting in a variety of agglomerate sizes and shapes. These physical differences, together with differences in origin and type and/or degree of modification or derivation, affect absolute density of starch products to a minor degree, but they affect bulk density to a large degree.

Densities of starches can be determined by the liquid displacement technique of Schochand Leach (57).

Using either water or xylene depending on sample characteristics, Linero (9) calculated the densities of potato, tapioca, maize, rice and taro, 1.425, 1.515, 1.202, 1.424, 1.591, g cm^{-3} respectively This variation could be explained in terms of the creation of a void in the starch granule during drying.

2.5 Starch varieties and their properties

Taro, one of the oldest cultivated crops in the world, has long been a staple food of the natives of all the Polynesian islands as well as the West Indies and the Orient.

Since Taro is propagated almost exclusively by vegetative means, each locality has tended to perpetuate its own forms, or "horticultural varieties". Some of these forms have remained localized; others have spread, and many of them have been given new names (58).

Taro is a member of the Arum family, Araceae, which contains about 100 genera and 1500 species, most of which are subtropical or tropical. They tend to be aquatic, but some are epiphytic. Among the more familiar plants in this family are the callalily, the anthurium, and the ornamental caladiums.

Taro belongs to the genus Colocasia, a word which has been connected through the Greek with the ancient Egyptian name of Taro "culcas". The scientific name of Taro is Colocasia esculenta.

Taro literature was examined for information about Taro starch, and as a guide to the growth of interest in the material worldwide. The properties of Taro starch are presented, as available from the literature and supplemented by new observations. The significance of particle size is considered as it relates to the fields of application of starches other than as foods, and especially in the plastics and related industries.

2.5.1. (a) Properties of Taro starch

Apart from occasional descriptions of particle size, there was little detailed published information on the properties of Taro starch itself prior to the publication of the paper by Higashihara, Umeki, and Yamaoto (59). Working with colocasia antiquorum Schott var, exulenta engler, they separated their starch from grated coat with 0.2M sodium chloride, at pH 8.6, washed it with water and finally deproteinized it by steeping for 24 hours these times in 0.3 percent sodium hydroxide.

The particle size as determined by electron microscopy, was 1 to 2 microns, where Radley (60) quotes figures of 1 to 3 micron obtained by optical microscopy. The gelatinization temperature was high ($73^{o}C$ to $74^{o}C$) compared with rice ($63^{o}C$ to $64^{o}C$). Earlier figures are quoted by Radley (60) as part of an argument that particle size alone does not determine gelation temperature by starches in water.

2.5.1. (b) Thermal Stability of Taro

The ability of starches to withstand exposure to elevated temperatures as dry powders is of little interest to the starch industry at present, but it is crucial to the successful application of starches as fillers in plastics. This has now been investigated using standard (Stanton & Co.) differential thermal analysis apparatus by Griffin, and some of his results are recorded in figure (2.2), for a series of common starches and Taro. The odd exothermic behaviour of Taro starch when treated in air was immediately apparent. No other starch in this group of common commercial materials exhibited the same behaviour, even a sample of 1 micron particle size starch from saponaria vaccaria followed the familiar pattern. A re-run of the DTA of Taro in an atmosphere of oxygen-free nitrogen showed an inverted curve (figure 2.3), clearly implying that the effect was one of accelerated oxidation.

As far as plastics applications are concerned, there is no special difficulty because the common polymers are seldom processed at temperatures exceeding $230^{o}C$ and air is largely excluded.

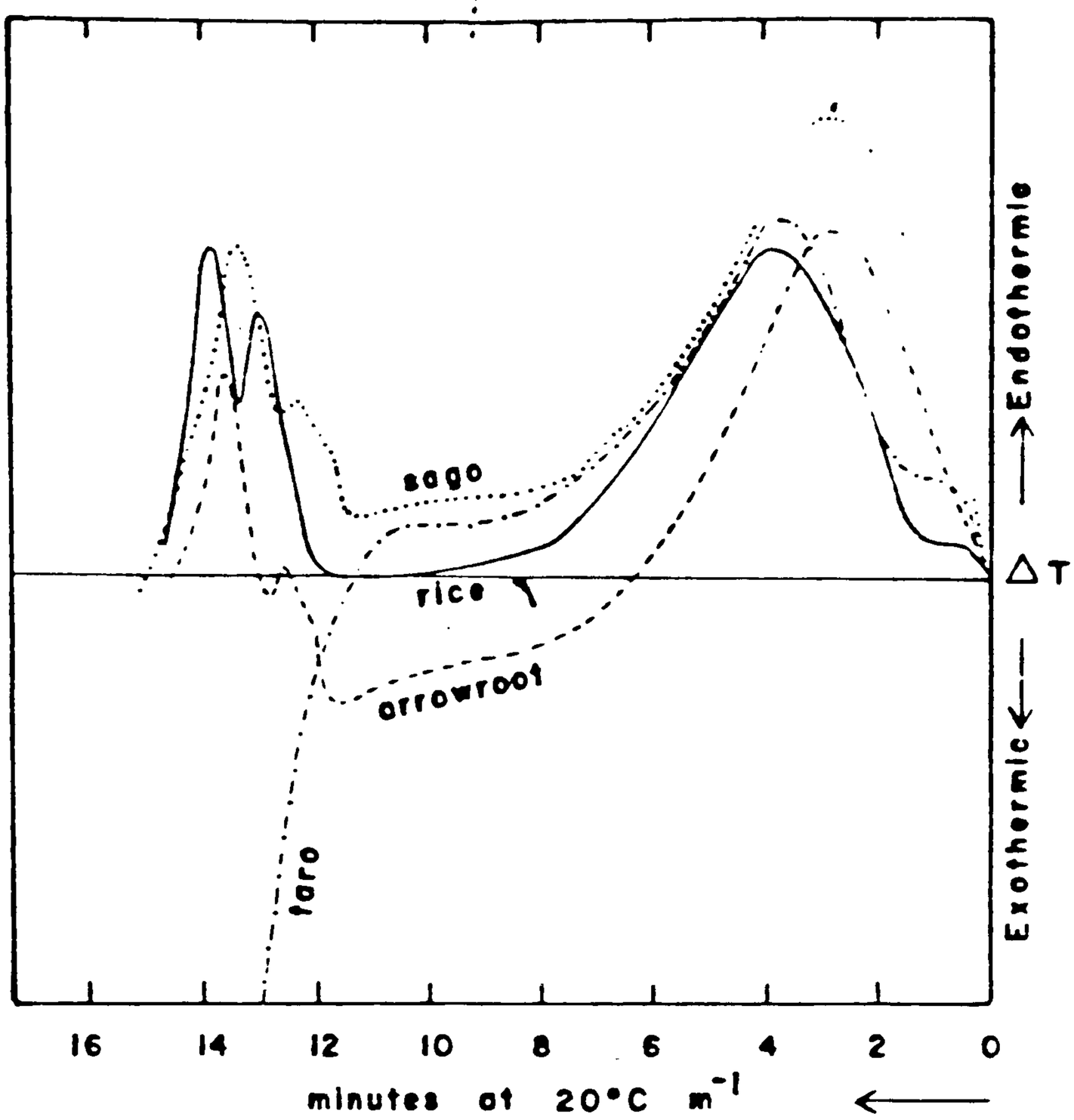

Fig (2.2) Comparison between the thermal stabilities of three common starches and taro starch, traced from DTA apparatus recordings. The samples were all heated in air.

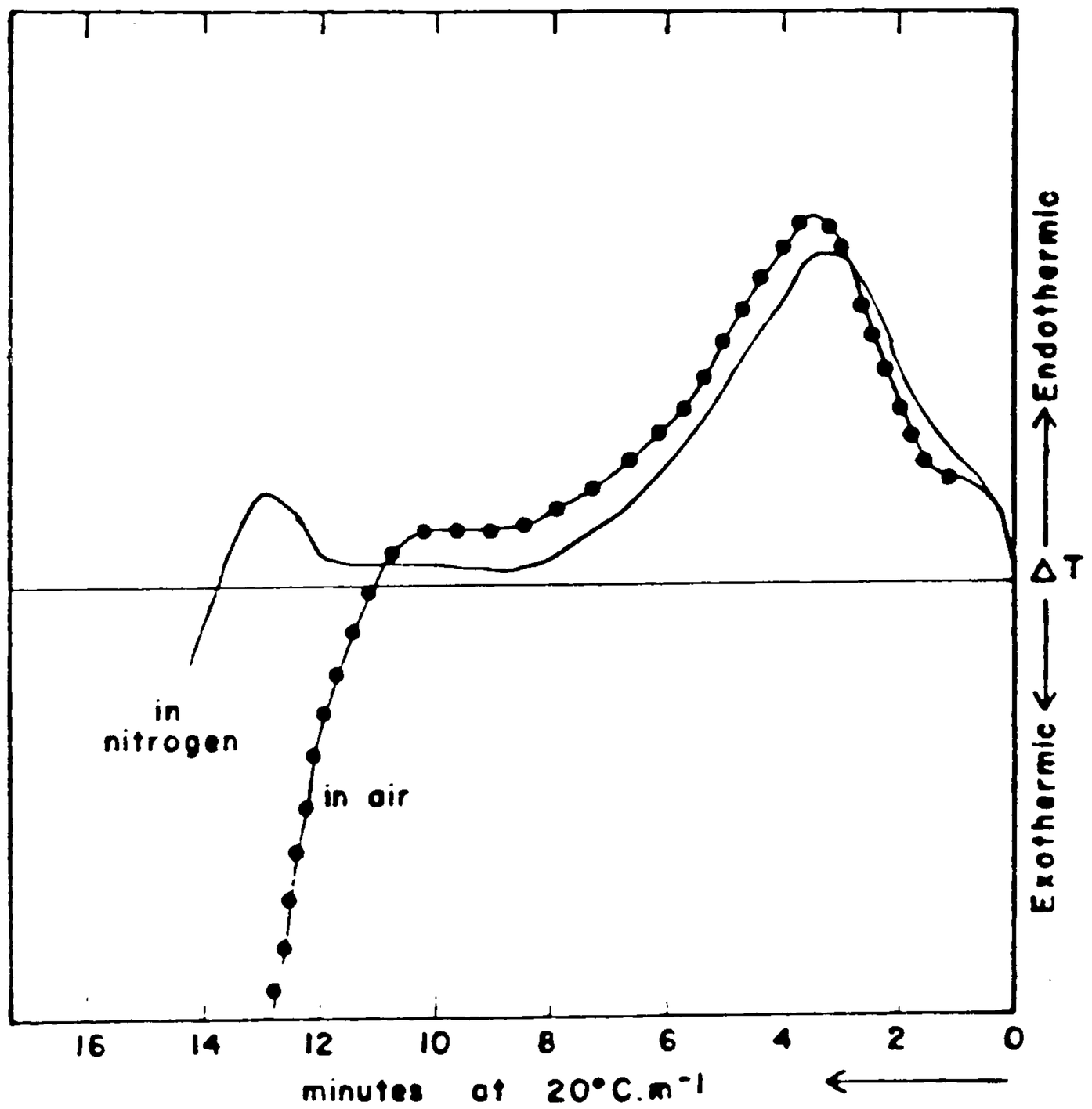

Fig (2.3) Effect of atmosphere on the thermal stability of taro starch, traced from DTA apparatus recordings, with the samples heated in air and in oxygen-free nitrogen, respectively.

2.6 Starch as a component of plastic compositions

2.6.1 Achieving compatibility

The technical literature contains many hundreds of references to the preparation of chemical derivations of starches which owe their origin to the exploitation of the plentiful reactive groups on the chemical structure of the starch molecule. In most cases the procedures described involve taking the starch into solution followed by chemical reaction, then precipitation of the derivative, followed in turn by filtration and drying operations to recover the product. Simple as this sounds, it proves impossible to create a dry "ready" product at a cost approaching that of the common plastics materials because of the expense involved in chemical reagents, process water energy, and handling costs, even though the starting material, starch, may be obtained at one half of the cost of the polymers.

Recently Griffin (61) reported a treatment of starch which was acceptable to the plastics industry with the minimum of added cost. Primarily, the lack of compatibility of normal commercial starch with plastics is determined by the proportion of free water commonly present (9 to 17 percent), and in the physicochemical antipathy between the starch surface and the polymer. The former is remediable by a straightforward drying operation. The latter offers more difficulty because the polysaccharides are intrinsically polar and hydrophylic materials in contrast to the polymers, which are low in polarity and are essentially oleophilic, or hydrophobic. This problem has been overcome by chemically modifying the starch

surface so as to obscure the influence of the hydroxyl groups, but the modification is restricted to the surface layer only, this being the only part in contact with the polymer matrix. By using this approach to the interface problem the desired effect can be achieved with the most minute amount of chemical additive. The net effect is to produce a polymer-compatible starch filler at reasonable cost.

Linero (9) examined several physical and chemical methods of treatment of starches with reagents that should form a hydrophobic coat and should increase the wettability of the starch granules by the polymer melts. He prepared starch granules with a hydrophobic surface by a dry process using the following coating agents:

	Formula
Coating agents polymethyl hydrogen siloxane (DC 1107)	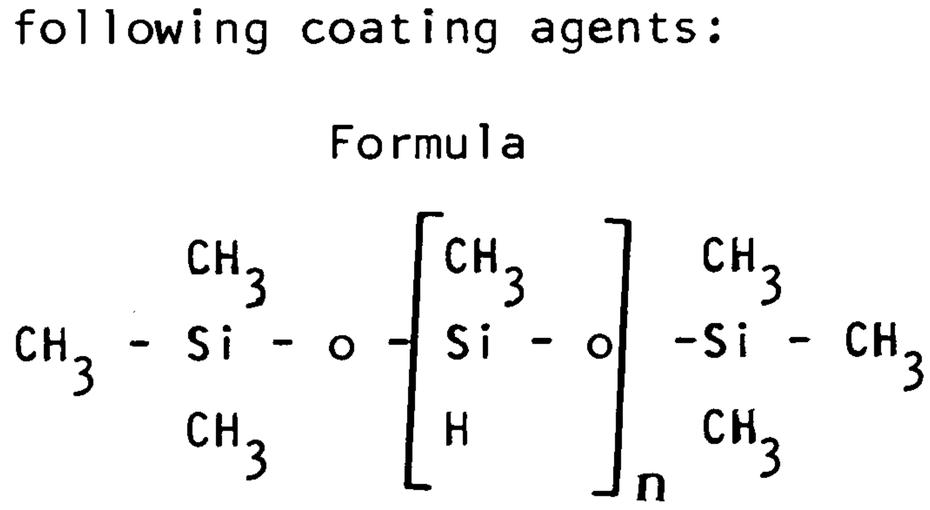
Alkyl succinic anhydrides (Kg,K12,N18 & J18)	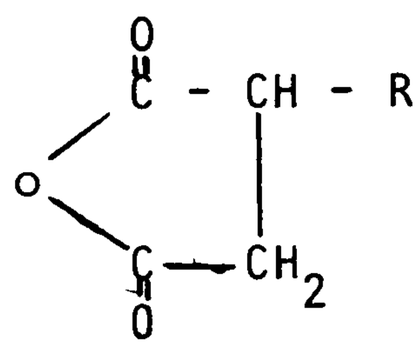

The catalysts used to accelerate the cure of DC1107, which was recommended by Watt (62) and Dow Corning (63) were as follows:

a. Fatty acid salts of lead, zinc or calcium

b. Tin salts in form of a stabilised stannous octoate (Stannous 2-ethyl hexoate) solution with a trade name of Nuocure - 28.

2.6.2 The effect of tropical starches on the physical properties of polyethylene.

Griffin reported (64) the physical benefits to be achieved are illustrated by a typical set of test results on injection moulded samples of starch filled low density polyethylene (fig 2.4).

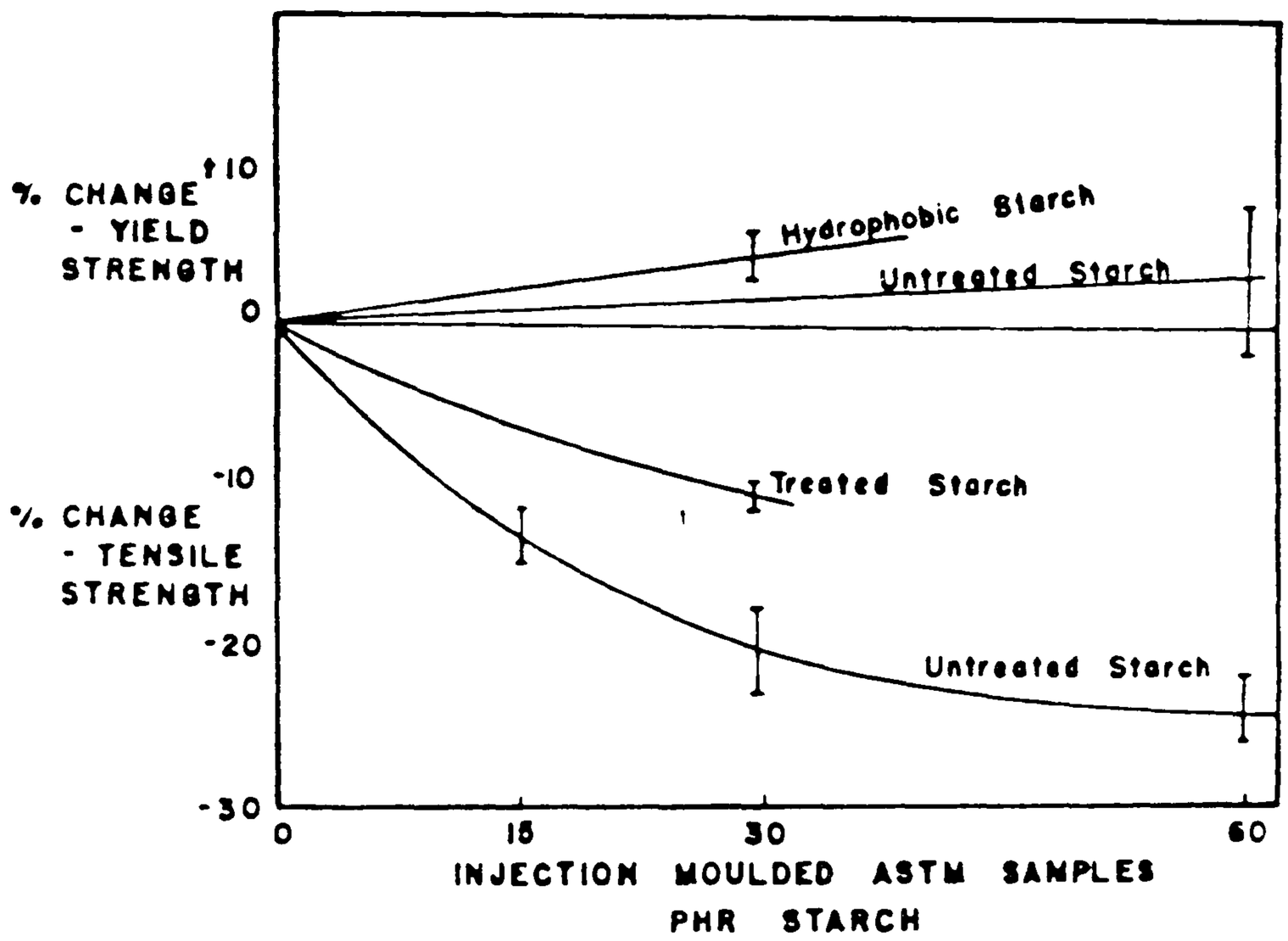

Fig (2.4) Strength of maize starch/low density polyethylene composites showing the general increase in yield strength and decrease in tensile strength with increasing starch content. The A samples are made from hydrophobic starch showing the benefit of this pretreatment. B samples use untreated starch. All samples were injection moulded to ASTM standard form.

2.6.3 The effect of DC1107/Zn - stearate surface treatment on tapioca starch filled polystyrene.

Linero (9) analyzed the mechanical properties of the starch/ polymer composite mouldings as a function of the nature of the starch-polymer interface in order to understand the factors which determined the strength of the mouldings at starch concentration of 30 phr. He showed the variation of flexural strength of tapioca-starch filled polystyrene injection moulding as a function of the coating concentration and it is illustrated in (figure 2.5).

The peculiar variation of the flexural strength of the composite mouldings with the rubbery silicone layer at the interface is a demonstration that the effect of filler on the mechanical properties of an amorphous and unreactive polymer is determined principally by the thickness and physical properties of the coating agent around the filler. It has been said that the presence of a monolayer of liquid between carefully polished contacting solids will result in a strong adhesion (65).

This statement could describe the variation in flexural strength of (figure 2.5).

Linero (9) also reported on the effect of starch on the tensile and yield properties of ethylene/vinyl acetate co-polymers. He selected a variety of commercial ethylene/vinyl acetate co-polymers to cover a broad range of ductilities.

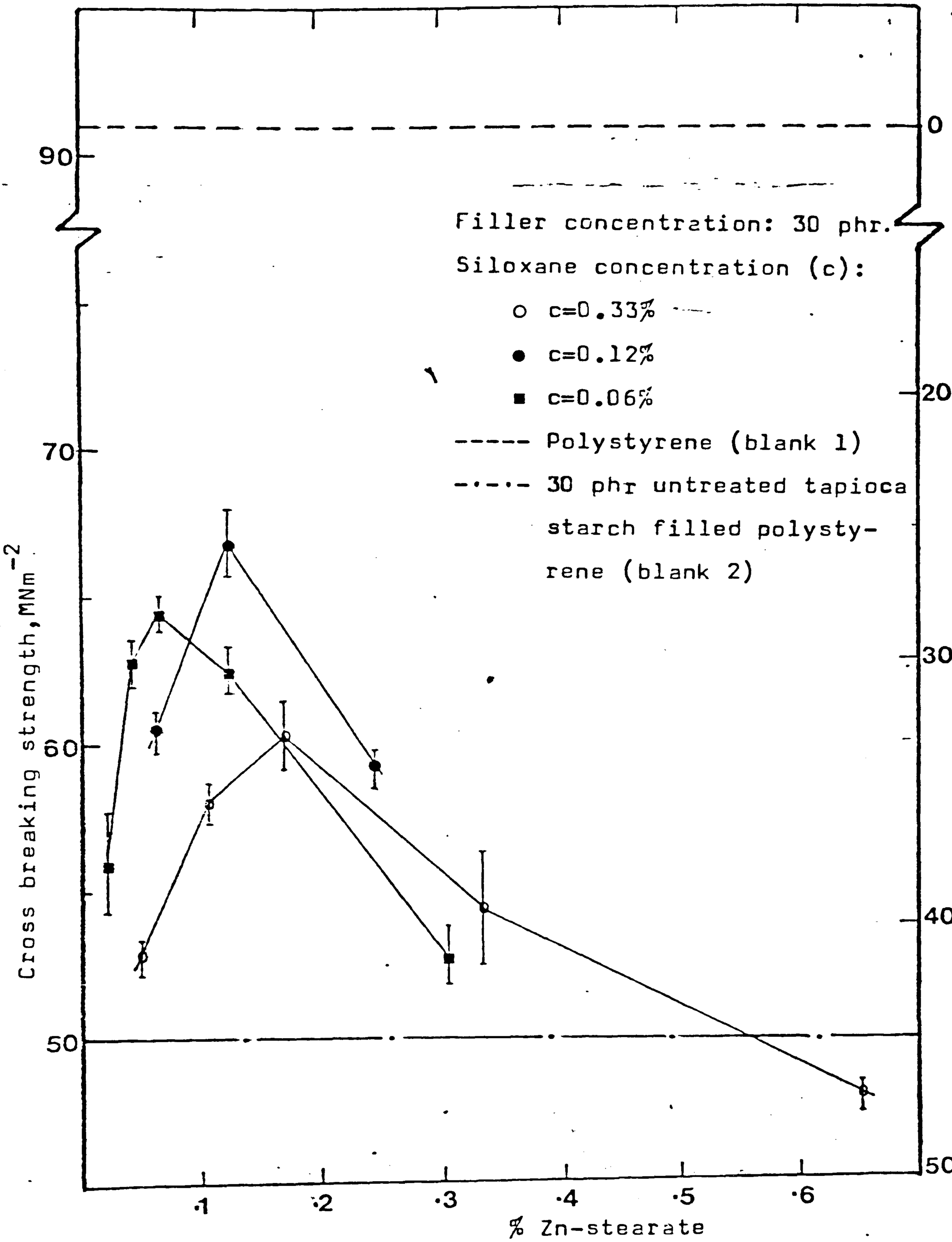

Fig (2.5) Changes in cross breaking strength of 30 phr tapioca starch-filled polystyrene with concentration of siloxane (%;starch basis) and Zn-stearate. Injection moulding samples tested according to the specification of ASTM D790-71.

Table (2.2) Tensile and yield properties at 23°C. of tapioca starch filled polyethylene at various percentages of vinyl acetate (%VA)

Polymer (%VA)	Starch (30 phr)	Tensile strength σ_b, (PSI)	Yield strength σ_y, (PSI)	Elongation at break (%)
LDPE QI388 (0%)	None	2376	1461	57
	Tapioca-A	2204	1660	34
	Tapioca-B	2363	1800	36
	Tapioca-C	2317	1771	38
	Tapioca-D	2290	1883	30
Petrothene 294 (4%)	None	2041	1145	92
	Tapioca-A	1797	1250	69
	Tapioca-B	1827	1300	59
	Tapioca-C	1896	1385	59
Ultrathene UE631 (20%)	None	2115	-	98
	Tapioca-A	1608	-	94
	Tapioca-B	1702	-	76
	Tapioca-C	1722	-	97

Tapioca A: Untreated tapioca starch with less than 1% moisture.

Tapioca B: Tapioca starch dry-coated with 0.12 gr. Silox-ane/0.12 gr. Zn-stearate for each 100 gr. star

Tapioca C: Tapioca starch dry- coated with 0.3 gr. J-18/ 100 gr. starch.

Tapioca D: Tapioca starch wet-treated with J-18.

Table (2.2) shows the tensile strength at break, yield strength and elongation at break, for three grades of resin containing 0%, 4% and 20% of vinyl acetate (VA) as co-monomer. These polymers were filled with a loading of 30 phr. Tapioca starch, tapioca starch treated with siloxane, and also two other treatments were evaluated such as, J18 using a wet or dry process.

His results, table (2.2) shows the tensile strength at break of the filled polymer was reduced by all the starches, but most of all by the untreated starch, whereas the siloxane treated starch filler in polyethylene Q1388 had a relatively slight effect on this property.

The treated and untreated starch increased the yield strength of their respective composites. Because of the success of these trials he extended his work to find out the influence of starch concentration and particle size distribution on the properties of the LDPE. His result shows the smaller the granule size the greater the yield point.

2.7 Small angle light scattering for measurement of particle size.

Radiation methods of analysis are among the most useful for obtaining information on structural ordering in crystalline polymers. One of the newest of such methods is small angle light scattering (SALS) (66) which utilizes radiation of wavelengths in the range of visible light (4000-8000Å). Structural aggregates of the order of 0.1 micron

can be investigated and important knowledge regarding the structure of the material may often be acquired from the distribution of the scattered light or the scattering envelope. The latter can be obtained in a rapid and convenient manner by using high intensity lasers as light sources and photographic film for collecting the scattered light (67). The scattering method is fast and non-destructive and allows the following of deformations in solid material which may take place in a fraction of a second (68). It is useful in elucidating the structure of materials and relating it to physical properties of the polymer. Consequently, more and more investigators are utilizing light scattering methods in conjunction with other structural methods such as optical and electron microscopy and electron and x-ray diffraction for obtaining supramolecular structural information.

Crystallization in high polymers may be followed by observing the change in the scattering envelope during the process (69). Unoriented polymer often contains small crystalline regions which are roughly spherical in shape and where the crystallites have their optic arcs in a fixed orientation with respect to the radius of the sphere (70). Such spherulitic systems have been extensively explored by the scattering technique. Stein et al (10,71,72) have shown how distinct scattering envelopes are created which are dependent on the orientation of the spherulites optic arcs. For example, on the basis of scattering data they have recently proposed an internal organization of polytetra fluoroethylene spherulites (72). Samuels (73) has used the technique to distinguish between different kinds of spherulites of the same polymer. The shape of the

scattering envelope depends on the shape of the scattering bodies. Thus, Picot (74) distinguished disc-like spherulites from spherical ones, purely on the basis of scattering envelopes. One of the most extensive scattering studies of spherulites is due to Keijzers (75). He showed how much systems might be characterized by means of "correlation" distance, as originally introduced by Debye and Bueche (76) for the characterization of density fluctuations, in solids, and later extended by other authors (77,78) to include anisotropy fluctuations as well. It is, however, often necessary to record absolute scattered intensities by means of a photometer in order to obtain the required information. Unfortunately, this eliminates the advantages of the rapidity of the photographic procedure.

Natural polymers have also been investigated by light scattering (79,80). Among these, starch is spherulitic and it has been demonstrated (81) that scattering envelopes, comparable to those produced by spherulitic synthetic polymer films, can be obtained. In a sample of starch the spherulites are separate and are not part of a polymer matrix as is the case for synthetic polymer films. Thus, various aspects of the scattering theory of Stein et al (10,71) investigated by Borch (23), and the scattering bodies, were irradiated singly as well as collectively. This allows a convenient isolation of the scattering area and the obtaining of scattered intensities without interference from other structures in the scattering beam; a procedure which is normally difficult to achieve using a solid polymer film.

2.7.1 Theory of SALS

A theory describing the observed small-angle light scattering SALS) from optically anisotropic spheres was first derived in the 1960's (10). This theory described the scattering behaviour under two experimental optical conditions denoted H_v SALS and V_v SALS. The first, H_vSALS, occurs when an analyzer and polarizer are crossed. Here scattering is dependent only on the size and shape of the scattering particle. The second V_v SALS, requires that the polarizer and analyzer be parallel. Scattering is much more complicated under V_v SALS conditions, as it depends on factors other than the size of the birefringent scatterers.

A spherulite is a three-dimensional, spherically symmetrical aggregate of crystalline and non crystalline polymer. Thus any theory which purports to describe SALS behaviour of spherulites must use as its model the known three-dimensional structure of the spherulite as observed by light and electron microscopy. The amplitude method for calculating the intensity envelope of scattered radiation is most useful for the theoretical small angle light scattering approach since it requires a model for its derivation. By choosing a model which realistically represents the known morphological characteristics of the spherulites, the observed SALS behaviour from spherulites should be predictable.

Since the underformed spherulite is spherical, the simplest model to which to apply the amplitude method to describe the observed

scattering behaviour would be that of a uniform isotropic sphere of polarizability αo and Radius Ro. Starting with this model, the following expression is obtained for the scattering intensity (82)

$$I = AV_0^2\alpha_0^2[(3/U^3)\ (\sin U - U\cos U)]^2$$

where I is the intensity, A is a proportionality constant, and Vo is the volume of the isotropic sphere. The shape factor is

$$U = (4\pi Ro/\lambda')\ \ Sin\ (\theta/2) \qquad (2.0)$$

λ' denoting the wavelength of light in the medium, and θ the polar scattering angle fig (2.6)

The undeformed spherulite is not isotropic, instead it has different radial and tangential refractive indices due to the ordered arrangements of anistropic crystallites along its radii. Thus a more reasonable model with which to represent the undeformed spherulite is that of an anisotropic sphere.

Stein and Rhodes (10) first considered the problem of the SALS patterns to be expected from a homogeneous anisotropic sphere in an isotropic or anisotropic medium. They assumed in their derivation that the optic axis was parallel to the radial fibril axis, and that there was rotational symmetry in the plane perpendicular to the fibril axis (a uniaxial indication). Later, Van Aartsent (83) rederived their equations and extended them to include the case where the

angle between the optic axis and the radial fibril direction (defined as β) could be 90^{o}. The correct form of the equations relating the intensity of the scattered light to the optical parameters, for the case where the optic axis is parallel to the radial fibril axis (this corresponds to Stein and Rhodes original restrictions, inc., $\beta = 0^{o}$ are:

$$I_{V_s} = A\rho^2 V_0^2 (3/U^3)^2 \{(\alpha_1 - \alpha_{s1})(\mathrm{Si}U - \sin U) + (\alpha_2 - \alpha_{s2}) \times (2\sin U - U\cos U - \mathrm{Si}U) + (\alpha_1 - \alpha_2)[\cos^2(\theta/2)/\cos\theta]\cos^2\mu \times (4\sin U - U\cos U - 3\mathrm{Si}U)\}^2 \quad (2.1)$$

$$I_{H_s} = A\rho^2 V_0^2 (3/U^3)^2 \{(\alpha_1 - \alpha_2)[\cos^2(\theta/2)/\cos\theta]\sin\mu\cos\mu \times (4\sin U - U\cos U - 3\mathrm{Si}U)\}^2 \quad (2.2)$$

where V_o is the volume of the anisotropic sphere, θ and μ are the radial and azimuthal scattering angles, and A is a proportionality constant. SiU is

$$\mathrm{Si}U = \int_o^U (\mathrm{Sin}\,x / x)\,dx \quad (2.3)$$

and is solved as a series expansion sum for computational purposes. U has the same definition as in the isotropic sphere model (eg (2.0) with Ro now the radius of the anisotropic sphere. U has the same definition for both the isotropic and anisotropic sphere models, since U depends only on the shape of the model. ρ is a geometric polarization correction term defined as

$$\rho = \cos\theta\,(\cos^2\theta + \sin^2\theta\cos^2\mu)^{-1/2} \qquad (2.4)$$

The term $\alpha_1, \alpha_2, \alpha_{s1}$, , and α_{s2} are polarizability terms. In Van Aartsen's derivation, (83) the polarizabilities of the cylindrically symmetrical volume elements are α_1 , in the direction of the optic axis and α_2 perpendicular to it. The symbols α_{s1} , and α_{s2} represent here the polarizability of the surrounding medium in the α_1 and α_2 directions respectively. When β , the angle between the optic axis and the spherulite radial-fibril direction is zero (i.e. the optic axis is parallel to the radial fibril direction), $\alpha_1 = \alpha_r$, where α_r is the polarizability parallel to the radial fibril direction, and $\alpha_2 = \alpha_t$, where α_t is the polarizability perpendicular to the radial fibril direction. Thus, for the case of $\beta = 0°$ the polarizability term in the expression for H_v SALS (equation 2.2) becomes $(\alpha_r - \alpha_t)$, , while the polarizability terms in the V_v SALS expression (eg 2.1) are:

$$\begin{aligned}(\alpha_1 - \alpha_{s1}) &= (\alpha_r - \alpha_{sr})\\ (\alpha_2 - \alpha_{s2}) &= (\alpha_t - \alpha_{st})\\ (\alpha_1 - \alpha_2) &= (\alpha_r - \alpha_t)\end{aligned} \qquad (2.5)$$

Here α_{sr} and α_{st} are the polarizabilities of the surroundings in the radial and tangential directions, respectively. The distinction that the term $(\alpha_1 - \alpha_2)$ equals $(\alpha_r - \alpha_t)$ was overlooked by Van Aartsen (83) and thus he concluded that equations (2.1) and

(2.2) were "directly comparable" to that derived by Stein and Rhodes earlier. However, in the Stein-Rhodes equations for IH_v and I_{Vv} the term $(\alpha_1 - \alpha_2)$ is written as $(\alpha_t - \alpha_r)$. . Though this small error will have no effect on the evaluation of Hv SALS patterns, it has serious consequences for the evaluation of Vv SALS, patterns (84).

The equations describing the intensity distribution of scattered light for the case when the optic axis is perpendicular to radial fibril direction $(\beta = 90°)$, , have the form (84):

$$I_{V_r} = A'\rho^2 V_0^2 (3/U^3)^2 \{(\alpha_2 - \alpha_{s2})(\mathrm{Si}U - U\cos U) + (\alpha_1 - \alpha_{s1})(2\sin U - U\cos U - \mathrm{Si}U) + (\alpha_2 - \alpha_1)[\cos^2(\theta/2)/\cos\theta]\cos^2\mu(4\sin U - U\cos U - 3\mathrm{Si}U)\}^2 \quad (2.6)$$

$$I_{H_r} = A'\rho^2 V_0^2 (3/U^3)^2 \{(\alpha_2 - \alpha_1)[\cos^2(\theta/2)/\cos\theta]\sin\mu\cos\mu \times (4\sin U - U\cos U - 3\mathrm{Si}U)\}^2 \quad (2.7)$$

When $\beta = 90^{\circ}$, the radial polarizability α_r equals α_2 .

Now, however, since the polarizability α_1 , is in the direction of the optic axis, and the optic axis is perpendicular to the radius and rotates randomly about it; then will be two polarizabilities perpendicular to the radius, α_1 in the optic axis direction, and α_2 in the direction perpendicular to the radius and to the optic axis, with random rotation of the optic axis about the radius. The

effective tangential polarizability will therefore be $(\alpha_1 + \alpha_2)/2$: If this substitution is made, it then follows for the case where

$$\alpha_{s1} = \alpha_{s2}$$

$$(\alpha_2 - \alpha_s) = \alpha_r - \alpha_s \quad .$$

$$\alpha_t = (\alpha_1 + \alpha_2)/2$$

$$\alpha_1 = 2\alpha_t - \alpha_r$$

$$(\alpha_1 - \alpha_s) = (2\alpha_t - \alpha_r) - \alpha_s = 2(\alpha_t - \alpha_s) - (\alpha_r - \alpha_s)$$

$$(\alpha_2 - \alpha_1) = \alpha_r - (2\alpha_t - \alpha_r) = (\alpha_r - 2\alpha_t + \alpha_r) = 2(\alpha_r - \alpha_t)$$

Thus, for the case $\beta = 90°$, the polarizability term in the expression for H_V SALS (eq. 2.7 becomes $2(\alpha_r - \alpha_t)$, while the first two terms in the V_V SALS expression (eq. 2.6) becomes:

$$\begin{aligned}(\alpha_2 - \alpha_s)(\mathrm{Si}U - U\cos U) + (\alpha_1 - \alpha_s)[2\sin U - U\cos U - \mathrm{Si}U] \\ = (\alpha_r - \alpha_s)(\mathrm{Si}U - U\cos U) + [2(\alpha_t - \alpha_s) \\ - (\alpha_r - \alpha_s)][2\sin U - U\cos U - \mathrm{Si}U] \\ = (\alpha_r - \alpha_s)[\mathrm{Si}U - U\cos U - 2\sin U + U\cos U + \mathrm{Si}U] \\ + 2(\alpha_t - \alpha_s)[2\sin U - U\cos U - \mathrm{Si}U] = 2(\alpha_r - \alpha_s) \\ \times (\mathrm{Si}U - \sin U) + 2(\alpha_t - \alpha_s)(2\sin U - U\cos U - \mathrm{Si}U)\end{aligned}$$

Since $(\alpha_2 - \alpha_1) = 2(\alpha_r - \alpha_t)$,

$$I_{V_r} = A'\rho^2V_0^2(3/U^3)^2\{2(\alpha_r - \alpha_s)(\mathrm{Si}U - \sin U) + 2(\alpha_t - \alpha_s)(2\sin U - U\cos U - \mathrm{Si}U) + 2(\alpha_r - \alpha_t) \times [\cos^2(\theta/2)/\cos\theta]\cos^2\mu(4\sin U - U\cos U - 3\mathrm{Si}U)\}^2$$

The constant multiplier A' in eqs. (2.6) and (2.7) is defined by Van Aartsen $4A' = 4(A/4) = A$, and

$$I_{V_r} = A\rho^2V_0^2(3/U^3)^2\{(\alpha_r - \alpha_s)(\mathrm{Si}U - \sin U) + (\alpha_t - \alpha_s)(2\sin U - U\cos U - \mathrm{Si}U) + (\alpha_r - \alpha_t) \times [(\cos^2(\theta/2)/\cos\theta)]\cos^2\mu(4\sin U - U\cos U - 3\mathrm{Si}U)\}^2 \qquad (2.8)$$

Also, eq. (2.7) is now

$$I_{H_r} = A\rho^2V_0^2(3/U^3)^2\{(\alpha_r - \alpha_t)[\cos^2(\theta/2)/\cos\theta)]\sin\mu\cos\mu \times (4\sin U - U\cos U - 3\mathrm{Si}U)\}^2 \qquad (2.9)$$

Equation (2.1) and (2.8), for I_{Vv} and eqs (2.2) and 2.9) for $I H_V$ are now identical when examined in terms of the fibril polarizabilities α_r and α_t.

in the H_V SALS relations, eqs. (2.2) and (2.9) the magnitude of A and $(\alpha_r - \alpha_t)$ affect only the absolute magnitude of the calculated intensity and not the position of θ max.

Thus these parameters do not influence the calculation of spherulite size from the H_v SALS patterns.

Therefore the correct form of three dimensional small-angle light scattering equations for anisotropic spheres are equations (2.8 and (2.9).

The characteristic behaviour of the H_v SALS pattern is determined theoretically by the form of the shape factor, U.
In an undeformed film the spherulite is spherical in shape and the shape factor takes the form of eq. (2.0). Owing to the dependence of the terms $(3/U^3)(4\ \sin U - U\cos U - 3\mathrm{Si}U)$ in the H_v equation on U, a maximum intensity will always be observed at a value of $U = 4.09$. This means the average spherulite radius can be obtained from the H_v SALS pattern, since the distance from the centre of the H_v SALS pattern to the intensity maximum of one of the lobes, in conjunction with the known sample - to film distance, is a measure of the polar angle θmax. Once the value of the polar angle, θmax has been obtained, the value of Ro can be calculated by using the equation;

$$Ro(\text{sphere}) = 1.025\lambda/\pi \sin(\theta max/2) \qquad (2.10)$$

Since the polar angle θmax, at which maximum intensity appears, is inversely proportional to the radius Ro, of the spherulite, small spherulites will have a clover-leaf pattern with maxima at large radial angles while large spherulites will have maxima at small radial angles. These H_v SALS patterns were obtained by keeping the sample-to-film distance constant during the experiment.

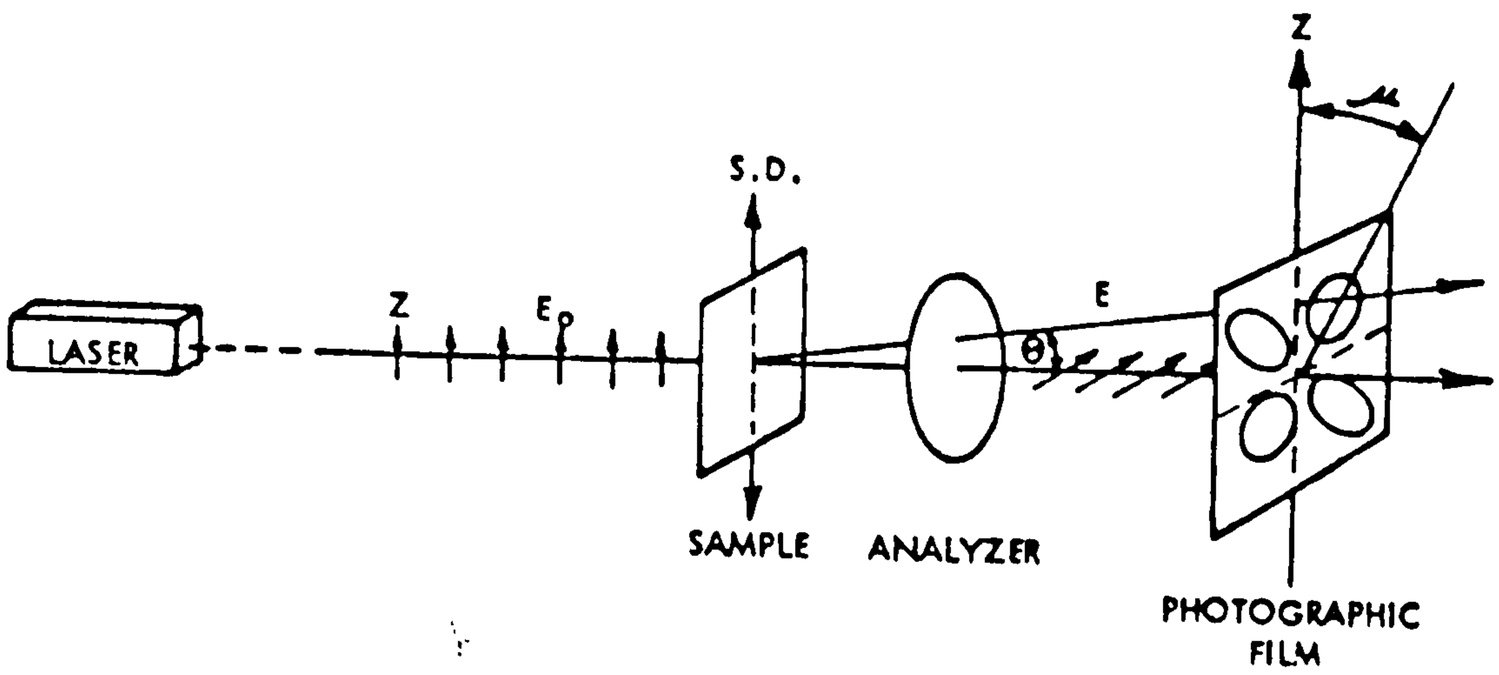

Fig. (2.6) Schematic diagram of the SALS system

2.8.0 Thermal analysis and the influence of thermal history on polymer fusion curves.

The technique of differential thermal analysis has been applied to many problems related to the melting behaviour of polymers. Melting points are usually derived by this means and the crystallite size distribution qualitatively inferred from the overall breadth and shape of the curves (85-87). However, due to the influence of kinetic factors in bulk crystallization, the temperature-crystallinity dependence of a semi crystalline polymer is not uniquely determined by its component structures and may be varied over a wide range according to the thermal pretreatment of the sample. Nevertheless, a proper understanding and interpretation of the effect of thermal history on polymer melting phenomena can lead to the determination of thermodynamically significant quantities which cannot be measured directly. The true maximum melting point, for example, can be obtained by extrapolation of observed melting points as a function of successively increasing annealing temperature (88,89). The

wealth of structural information which is, in principle, extractable from the shape of a fusion curve (90,91), might similarly be obtained in practice if the inevitable influence of thermal history were sufficiently well understood.

A common application of differential scanning calorimetry is the determination of the weight fraction of crystalline material in semi-crystalline polymers. The method is based upon the measurement of the polymer samples heat of fusion ΔHf, in calories per gram and the plausible assumption is made that this quantity is proportional to the crystalline content. If by some process of extrapolation, estimation, or analogy with model compounds, the heat of fusion, ΔHf^{o} of a hypothetical 100% crystalline sample is known, then the weight-fraction crystallinity is taken as

$$\Delta Hf \; / \; \Delta Hf^{o}$$

2.8.1 Application of Differential Scanning Calorimetry (D.S.C.)

The applications of differential scanning calorimetry are described in a great number of studies described in the literature, since all the applications of conventional differential thermal analyses are directly applicable to the calorimetric technique of DSC (provided they are within the operating range of the instrument).

Most of these applications can be extended by the use of DSC to include quantitative as well as qualitative observations.

Polymer research and characterization is one of the major applications of DSC. As a consequence of the research carried out to date, routine methods have been developed for the determination of thermodynamic projections, particularly specific heats (92) and heats of fusion (93); for the qualitative and quantitative analysis of polymer blends and copolymers (94); for distinguishing folded-chain from extended-chain morphologies (95); for determining the effect of comonomers or chain substituents on morphology and general thermal behaviour (96); for evaluating the effects and effectiveness of additives such as plasticizers, antioxidants, and accelerators, catalysts, nucleating agents (97) etc; for determining the degree of cure of thermosets (98); for the determination of crystallinity (99), thermal stability (100) and crystallization rates (101), and for control of textile fibre and other polymer processing operations.

CHAPTER 3

EXPERIMENTAL WORK

3.0.0 Sources of raw materials

All the starches used were commercial except Taro starches, which are not yet commercially available. Dry slices of taro starches were obtained from the Department of the Food Science and Technology of the University of Hawaii, Honolulu, USA; the U.S. Department of Agriculture Field Station at Kauai, and the Department of Botany at North Eastern University, Boston.

Sources of the starting starches are listed in table (3.1).

High density polyethylene was obtained from British Petroleum trade name Rigidan, Grade 002-40

Table 3.1

Starch	Source
Potato	Tunnel-Avebe Ltd.
Maize	CPC (UK) Ltd.
Rice	CAT (UK) Ltd.
Taros	Dr. Ramon de la Pena, U.S. Dept. of Agriculture, Kauai Branch Station, Kapaa, Kauai, Hawaii, USA
and	Prof. M. S. Strauss, Dept. of Botany North Eastern University, Boston, USA

3.1.0 Extraction and purification of starch granules from plants of the yams.

In the search for other sources of small starch granules to continue the study of the effect of granule size on the properties of thermoplastics, it was found that taro root which contained the desired small granules size starch was readily available as a cheap food crop in named tropical countries. Out of 112 different Taro starches which were examined, four could be manufactured commercially from Taro cultivars currently grown as commercial crops, these being:

1. Colocasia esculenta var. Bun Long
2. Un-named cultivar ex W. Samoa
3. Colocasia esculenta var. Lehua Moai.
4. Colocasia esculenta var. White Moi.

The raw materials were provided as dried slices of corm.

5 kg samples were ground to a fine powder using a pin mill made by Kek & Co. Ltd. The resulting powder was suspended in water and stirred thoroughly for half an hour. It was then screened through a sieve of mesh size (120 μ) in order to remove the cellulose fibres. The starch was then recovered from the sieved suspension by the use of a simple continuous bowl-type centrifuge with repeated washing. The starch was resuspended in water and then stirred for four hours with the addition of hydrogen peroxide as a bleach. The slurry was allowed to settle overnight, the suspenatent was removed and the moisture content of the starch paste was measured. The moisture content was further reduced by using a bucket-centrifuge

(6000 rpm for 15 min) and the pellet was dried in an air-circulating oven at 50°C for 24 hours to reduce the moisture content to below 8%. The resulting pellet was further dried in an oven at 100°C for 72 hours. The extraction method is shown schematically in flow sheet (1).

The other three starches were prepared in the same way, Other Taro starches were prepared for the author on a much smaller scale by C. Ogbonna using a similar method.

Flow sheet (1) Taro extraction

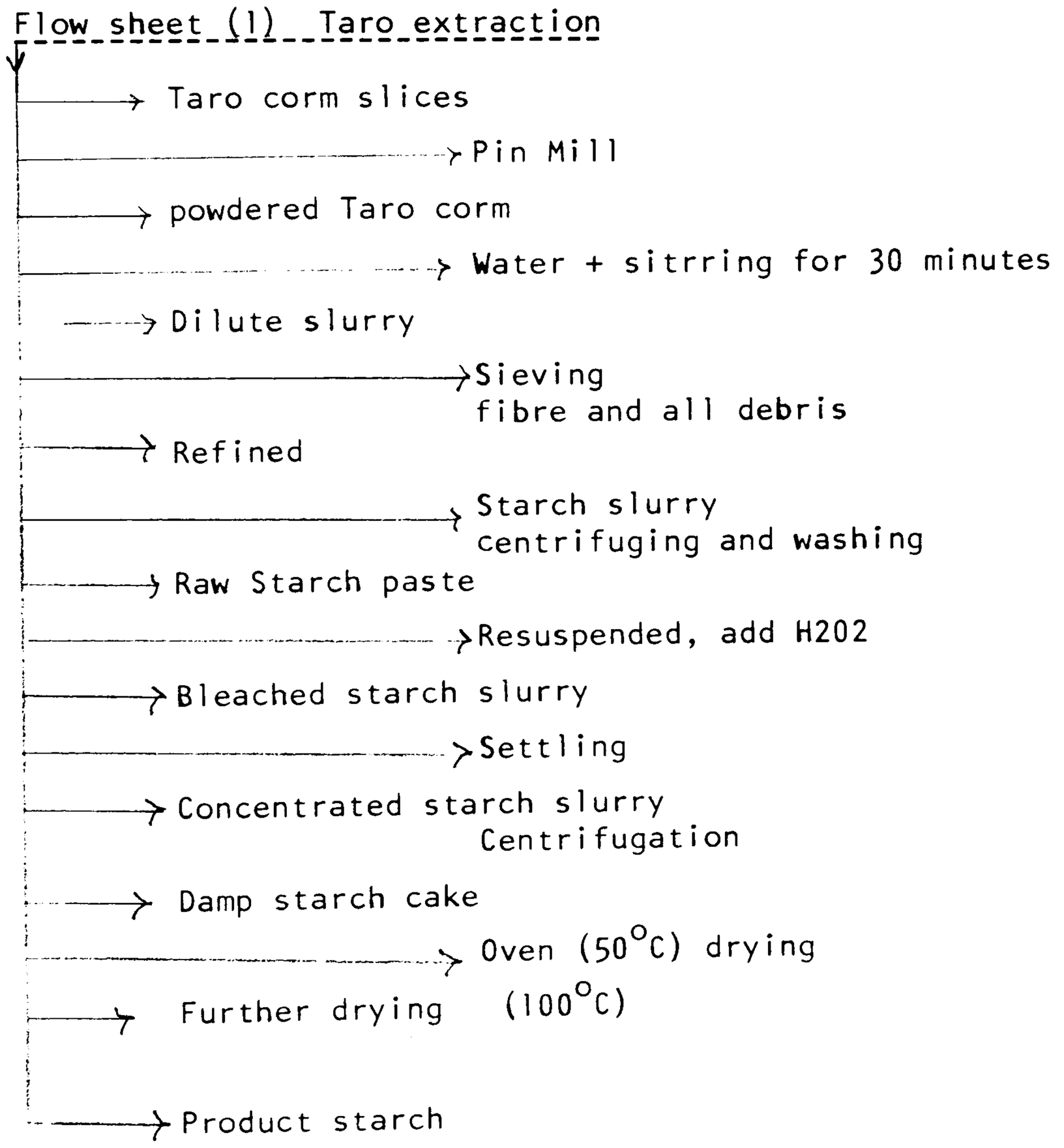

3.2 Modification procedures required to render starch granules compatible with polyethylene.

Dry treatment of starch with silicone coating agents.

Starch granules with a hydrophobic surface were prepared by a dry process using silicone coating agents as suggested by Griffin (61).

Polydimethyl hydrogen siloxane (DC1107) was chosen, a polydimethyl siloxane in which some of the methyl substituents have been replaced byhydrogen atoms in order to confer greater reactivity to the aliggimer. This was obtained from Dow Corning International Ltd.

It is a colourless liquid with a density of 1 gcm^{-3} and viscosity at $25^{o}C$ of 3 centistokes.

The catalysts which can be used to accelerate the cure of DC1107, recommended by the manufacturers, are fatty and soaps of lead, zinc or calcium.

First trials with rice starch and DC1107 were carried out in order to disclose the optimum processing conditions.

100 gms of commercial rice starch in dry granular form was mixed with 0.5 gm of DC1107 and 0.5 gm of zinc stearate. The mixture was placed in a 750 ml reaction flask, fitted with electric stirrer and thermometer and clamped in an oil bath set at $150^{o}C$. This temperature

was high enough to keep the reaction mixture at about 135°C. The coating action was taken to be complete after 20 minutes. After this period of time there was a clear change in the visible flow-properties of the starch powder. When a pinch of the powder was added to water, it remained on the surface of the water as an unwetted mass when the system was subject to lively agitation.

The treatment was extended to Taro starch, using the above procedure with some modification. The amount of DC1107 and zinc stearate was increased as the particle size decreased, to allow for the relative increase in surface area. In the case of Taro starches it was found experimentally that stirring for 40 minutes was required to complete the coating reaction.

3.3 Moisture content

3.3.1 Test Method.

The apparatus used was a Townsend and Mercer direct reading vacuum moisture-tester (figure 1). This instrument uses infra-red heating and a torsion-wire balance for the zero adjustment. The scale was set at 0% with 5 gm weight placed on the pan, zeroing knob was turned so as to bring the two index pointers in line. The weight on the pan was then replaced by an equal amount of starch sample so that the pointers were brought back to the same level. The sample was then subjected to heating under vacuum for about 20 minutes. The scale disc was then rotated until the pointers were again in line,

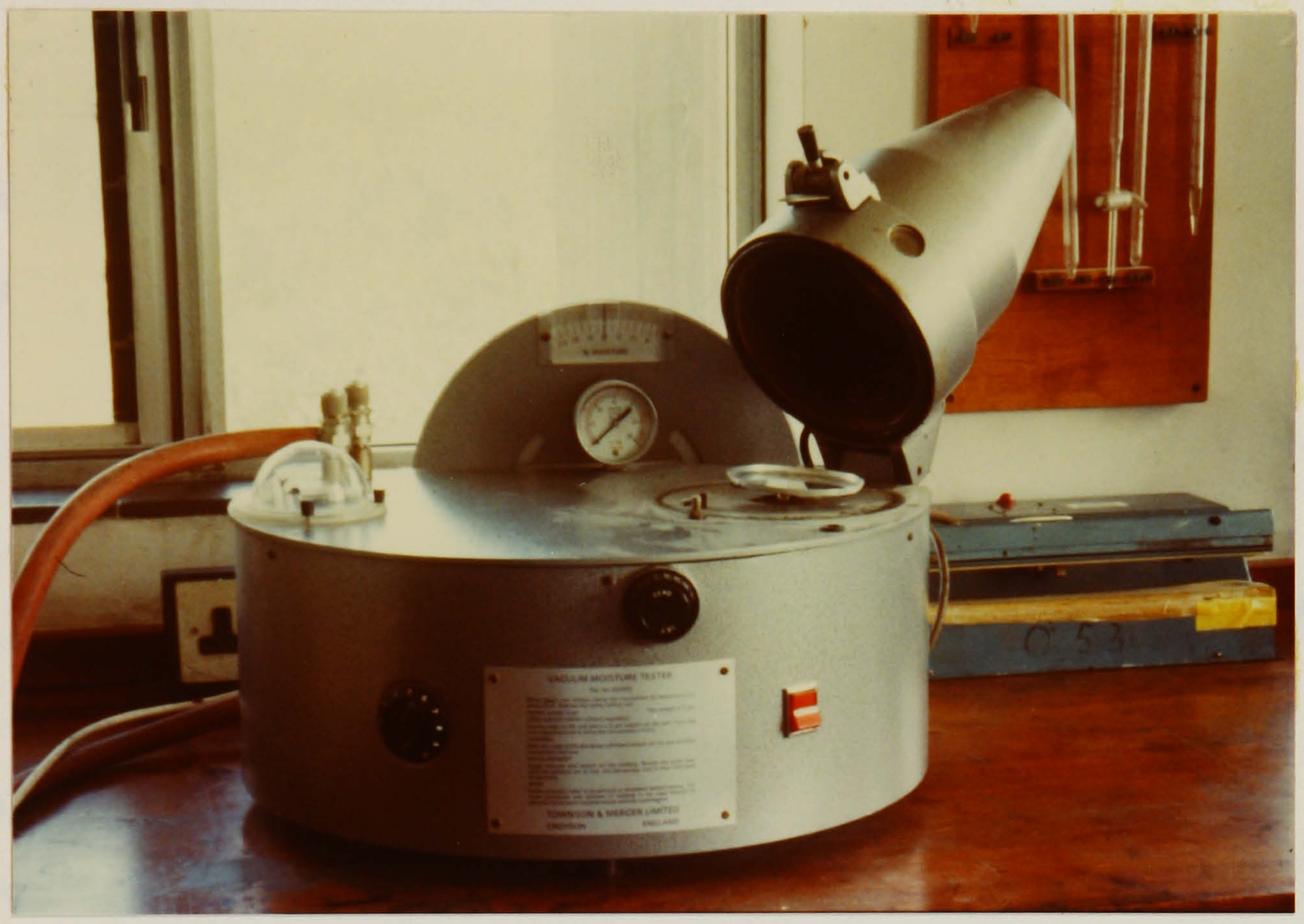

Fig (1) Townsend and Mercer direct-reading vacuum moisture tester

whereupon the percentage weight loss could be read directly from the scale. This was taken as a measure of water content of the starch.

3.4 Spray-drying technique.

Acid treated rice starch was dried using a spray dryer (Anhydro size 1) figure (2).

The principle of spray drying may be described as follows (102). A suspension is dispensed into a mist by an air-atomizer. The nozzle of the atomizer is situated in the middle of a drying chamber so as to spray upwards, thus giving the particles the longest trajectory obtainable in a compact plant. This method of atomization has the advantage that no high pressure hydraulic pump is necessary to atomize the fluid. Hot air is mixed continuously with the mist of atomized liquid, and a practically instantaneous evaporation of the volatiles takes place. The non-volatile part is left in the form of small dry particles of powder. On account of the rapid evaporation, the heat in the air is absorbed so quickly that the temperature in the drying zone is very low throughout the entire period of drying. It is only when the particles are dry that their temperature gradually rises towards the temperature of the outlet air. The ambient air is heated by passing over an electric heater mounted close to the air distributor on the upper part of the chamber. The temperature of the drying air is controlled from the instrument panel by varying the electrical power input to the heater. The temperature can be varied between 125^{o}C and 300^{o}C.

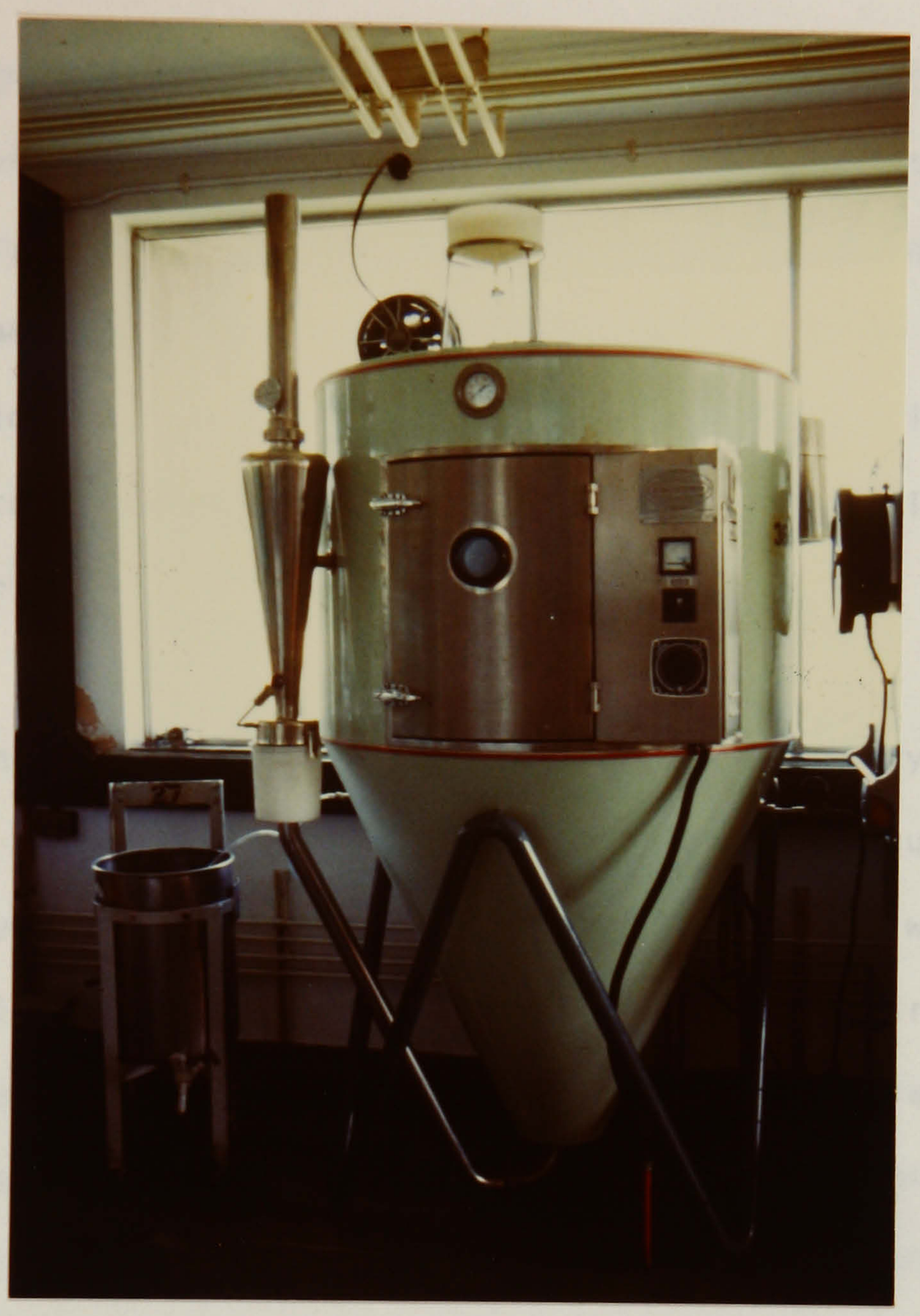

Fig (2) "Anhydro" laboratory spray dryer, laboratory model

The powder falls down towards the outlet aperture in the conical bottom of the chamber and from there it goes with the outlet air to the cyclone separator. Then the powder falls into a container, while the drying air is discharged from the top of the cyclone. The cyclone outlet is equipped with an air lock allowing a full powder container to be exchanged during the operation of the spray drier.

Using the "Anhydro" pilot unit spray drier, the drying chamber hot air supply was first switched on and adjusted up to the desired inlet temperature of 130°C. Then distilled water was drawn in to the drying chamber, by adjusting the compressed air pressure to the atomizer until the corrected outlet temperature of 70°C was constant, the starch suspension was fed into the drying chamber in the place of the water without interruption. When the last of the starch suspension to be dried was about to pass through, distilled water was introduced in inpurge the feeding tube and atomizer. The reason for this is that the residue of starch suspension should rapidly form a gel when heated and thus clog the atomizer and block the feeding tube. At this stage the current for the heating elements was switched off, and the supply of water was also gradually reduced, so that the temperature of the outlet was kept at the same level after the inlet air temperature had dropped to about 130°C, the water supply was cut off. When the inlet temperature fell to 80°C, the plant was stopped by turning the master switch back to the zero position.

The following spray drying conditions were chosen for preparing spray dried, acid treated starch:

inlet temperature	130°C
outlet temperature	70°C
atomizer - spray air-pressure	4 kg cm^{-2}
electrical input to air heater	3 kW

The powder obtained by spray drying under these conditions was further dried in a vacuum oven for a period of 72 hours at a temperature of 100°C.

3.5 Light-scattering technique for particle size measurement.

The experimental arrangement was as shown in figures (3). The light source was a He-Ne gas laser model B17/L with the following specifications:

power output	1 milliwatt uniphase
wavelength	6328 A
Mirror configuration	one spherical and one plane mirror forming a himeispherical resonator
Laser tube	D.C. incited
Beam diameter	2 mm at exit amperture

manufactured by Scientific and Cook Electronics Ltd.

The laser was mounted on an optical bench and with laser beam parallel to the bench axis so that its vertical position could be

Fig (3) Apparatus used in the small-angle light-scattering experiments

adjusted. As it was difficult to obtain an incident beam of reasonably uniform intensity profile, the scattering sample was positioned at a relatively long distance (50 cm) from the light source and a pinhole used to eliminate extraneous scattering from the main beam itself. The sample holder was adjustable in a plane normal to the beam axes by means of adjustable mountings with vertical and horizontal travel motions. The scattered ray passed through a polaroid analyzer attached to the sample holder.

Small-angle light scattering patterns are obtained when a beam of laser light is directed in a perpendicular manner at a thin flat sample of a dispersion of a spherulitic substance in liquid of matching refractive index. It is necessary to place an analyzer between the sample and the screen or detector system.

To process the result quickly an apparatus was devised to automate data-collection. Electronics were designed and constructed by G. Griffin with the Electronics Service Facility of the Electrical Engineering Dept. at Brunel University. The principle of the design of the apparatus was to arrange for a photodetector to scan the image and to convert the detector intensity signals together with detector coordinates into a binary 8-bit ASC II code so as to drive a paper type punch.

Figure (4) is a schematic diagram of the involved electronics. The detector output particularly for a weak diffraction pattern was

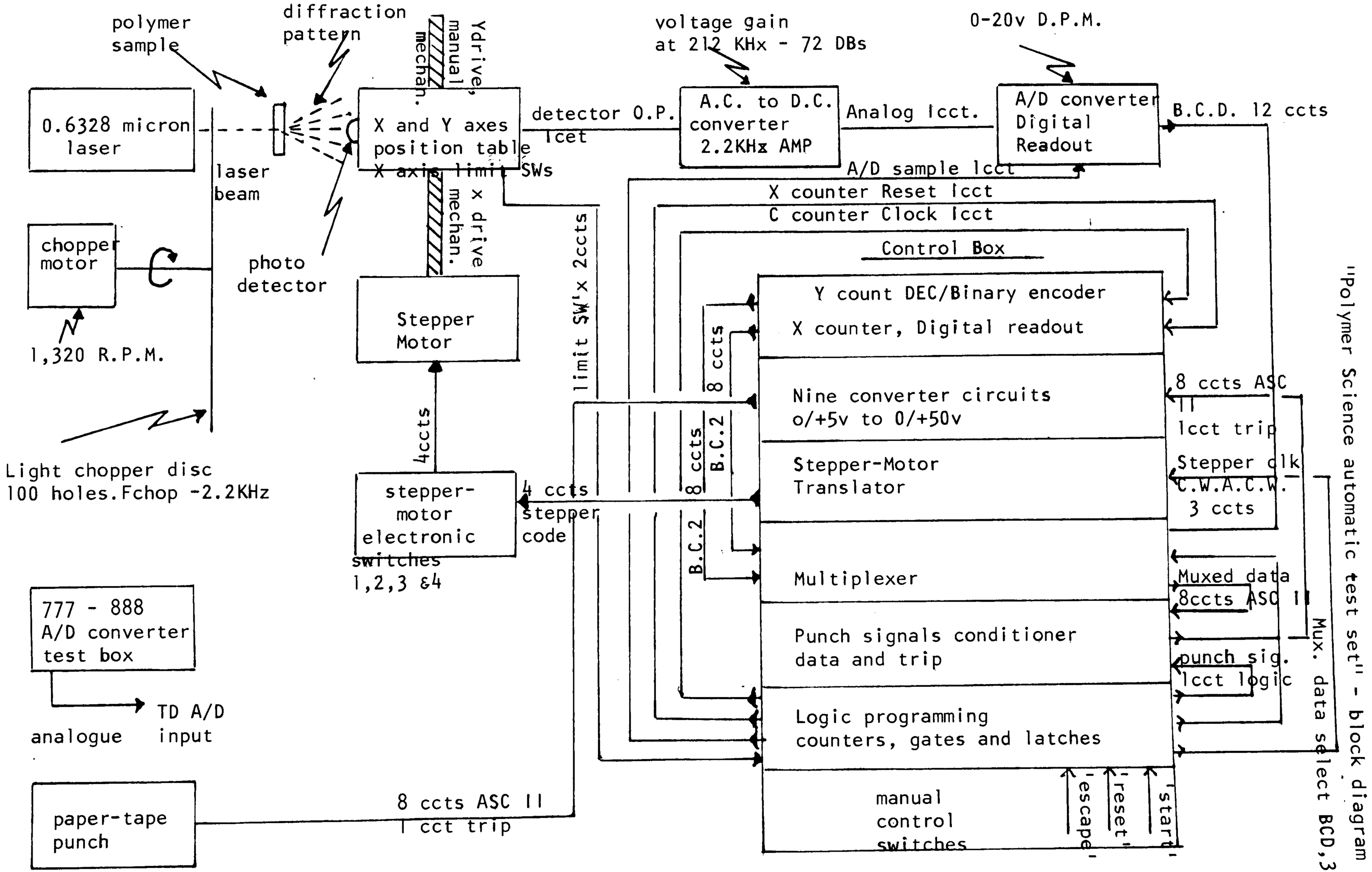

Fig 4)Schematic diagram of laser light scattering apparatus digital electronics

"Polymer Science automatic test set" - block diagram

rather small, sometimes only a few microvolts. In order to provide high amplification of these weak signals a tuned A.C. amplifier was used. This necessitated converting the D.C. signal from the detector to an A.C. signal which was achieved by chopping the laser beam at the frequency of the tuned amplifier (2,200 HZ), using a rotating chopper disc driven by a Synchronous motor. The final stages of the amplifier converted the A.C. signal back to a D.C. one which was then at the level (0-10V) required to drive an AID converter.

Digital circuits in the control-box provide drive signals for a stepping-motor that positioned the horizontal axis of the photo-detector. The position of the photodetector horizontal was manually adjusted and its numerical value was entered into the control-box by a thumb-wheel-operated decimal to binary encoder. All the information was then in binary form with two characters for each of the horizontal and vertical positions and three characters for the photo-detector signal. Each of the seven 4-bit binary characters as multiplaned would then be added to four extra bits of information, three of which indicate numerals and are fixed and one parity bit for error correction as required. The information was then fed, bit-parallel, character-serial to a paper tape punch. Each act of encoding (seven characters sampled and printed) was initiated by an internal clock derived from the horizontal axis counter. The logic programming in the control-box consisted of various counters and gates which controlled the sequence of events and responded to any manual input signals from the

control buttons and also to signals, from the limit switches on the horizontal traverse.

Sample preparation for light-scattering studies.

The starch samples were all available in the form of dry granular powders. They were further dried in a vacuum-oven before mounting for the light-scattering experiments. The suspensions of the starch were prepared by adding a weighed amount of the starch to a known weight of tung-oil selected because it possessed a refractive index of 1.54. This value was close to the average refractive index of the starch granules (other mounting fluids were used under some conditions). Either a microscope slide and a cover-slip or two microscope slides were used to mount a sample of starch granules suspended in tung-oil and the slides were sealed off using ohu adhesive.

The refractive indices of the starch granules were measured by optical microscopy using the Becke test (103). The refractive index of the immersion liquids were measured in a Bausch and Lamb Abbe refractometer.

3.6 Acid treatment of Rice starch

Linero (9) found that the blending of starch with polyethylene could give rise, under certain circumstances, to an increase in the yield strength of the composite material. In the present work an attempt has been made to explain this result by investigating

the nature of the starch-polymer interface. One possibility to be considered was that the crystalline regions of the starch might act as nucleating sites for polymer crystallization and thus affect the mechanical properties of the composite. It was decided to acid-etch the starch before compounding in order to remove, preferentially, the amorphous regions of the starch granules.

3.6.1 Procedure

Reagent-grade concentrated sulphuric acid was mixed with five parts of water (on a weight basis) to make 16% sulphuric acid. This was used to treat starch as follows:

50 grm of rice starch was suspended in one litre of 16% sulphuric acid). The mixture was kept inside an incubator at a temperature of (39-40^{o}C) and resuspended by occasional shaking by hand. After 24 hours and 48 hours, the starch was collected by filtration. The starch was then weighed with water until the washings were acid-free. After washing with water the starch residue was resuspended in a mixture of 25 ml of water and 25 ml of alcohol. The starch was collected by filtration and was dried by washing with a few ml of alcohol. The residue was kept in a vacuum oven for 18 hours at a temperature of 80^{o}C. When large quantities of rice starch were treated the residue was dried using the spray drier as described under section (3.4).

3.7 Compounding of thermoplastics and starch

The incorporation of dried starch into the appropriate thermoplastics was accomplished by pre-blending the powder such that a blend of randomly distributed particles resulted. The blended materials were placed in the nip of a two-roll mill heated and subjected to shear and mixing until the starch was thoroughly dispersed. After an average milling time of 25 minutes the material was taken off as a hide, about 3 mm thick, using the stripping knife and allowed to cool. Strips of materials were granulated and stored in polyethylene bags. Masterbatches of starch and HDPE prepared by this method. The roll-temperature was 165^{o}C for the front roll and 180^{o}C for the back roll.

3.8 Injection Moulding

Injection moulding is a process for producing identical articles using a hollow mould. Because of their high viscosity, polymer melts cannot be poured into such a mould; that is, gravitational forces are inadequate for affecting appreciable flow rates. Thus the melt must be injected into the mould cavity by generating high pressures in it with a plunger.

The injection moulding machine used in the present study was made by the Sandretto Co., (figure 5). It consists of two parts: the injection unit and the clamping unit. The function of the former is to melt the polymer and inject it into the mould, while

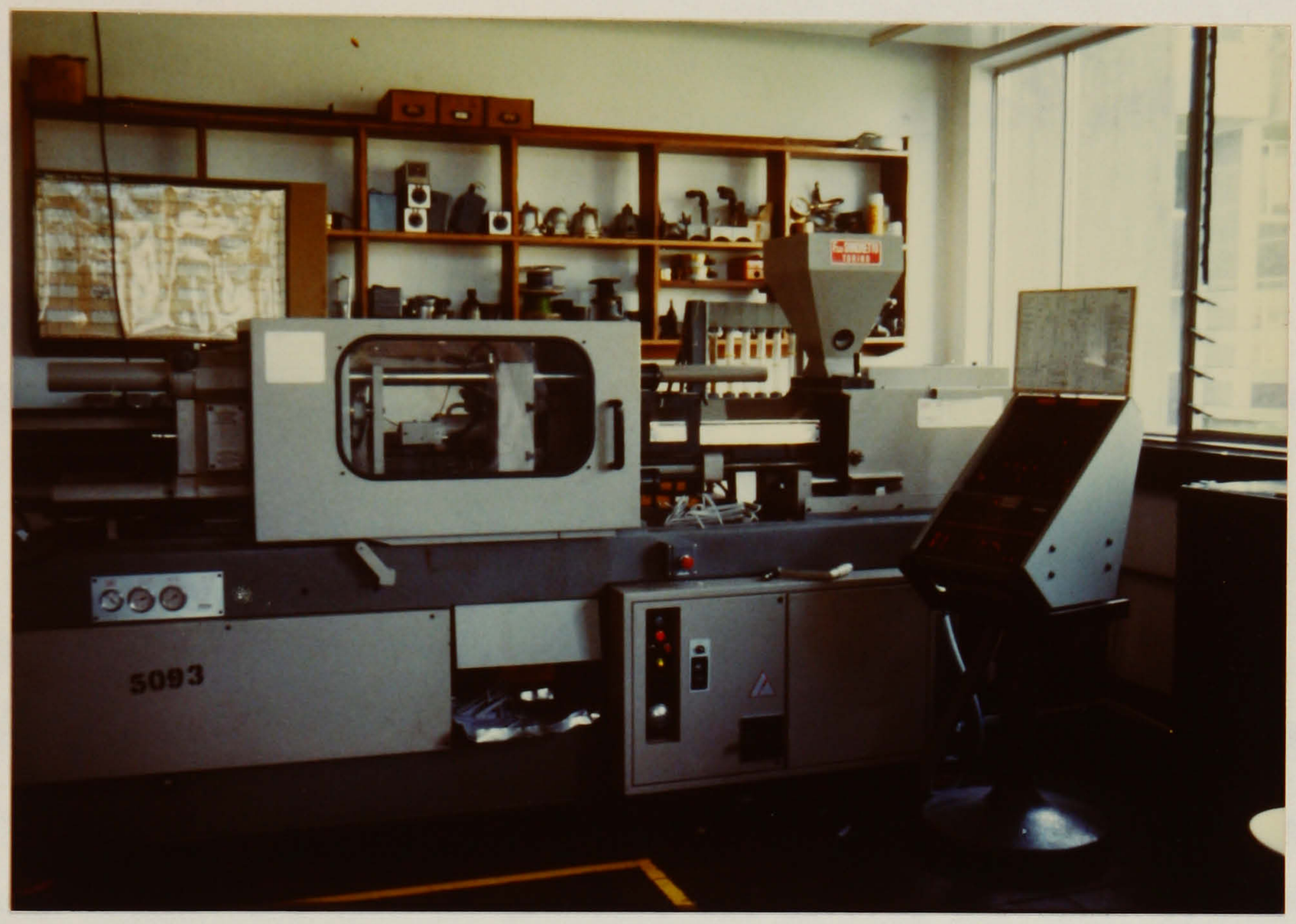

Fig (5) Injection-moulding machine used (Sandretto Co.)
in preparation of tensile and flexural test specimens

the clamping unit supports the mould, opens and closes automatically, and ejects the finished products. This machine was provided with a modern injection unit of the in-line reciprocating screw type. The screw both rotates and undergoes axial reciprocal motion. When it rotates, it acts like a screw extruder, melting and pumping the polymer. When it moves axially, it acts like an injection plunger. The screw is, in general, rotated by a hydraulic motor and its axil mortron is activated and controlled by a hydraulic system.

3.8.1 Test specimen preparation

The preparation of the required number of test specimens for the evaluation of mechanical properties, x-ray analysis, microscopy observation, and thermal analysis was carried out under optimal conditions in an injection moulding machine as described in the previous section. The machine was set with a multiple cavity mould to make under normal production conditions three mouldings with different test piece shapes at each cycle (figure 6.a,b)

The "dumb-bell" shaped tensile test-piece mouldings conformed to the dimensions and recommendation specified in the relevant ASTM Standard D638-64, for the material. The conditions under which the injection moulding process is carried out determines the finish of the mould test-pieces. Changing the injection moulding parameters may thus have dramatic effects on the physical properties of the moulding test-pieces.

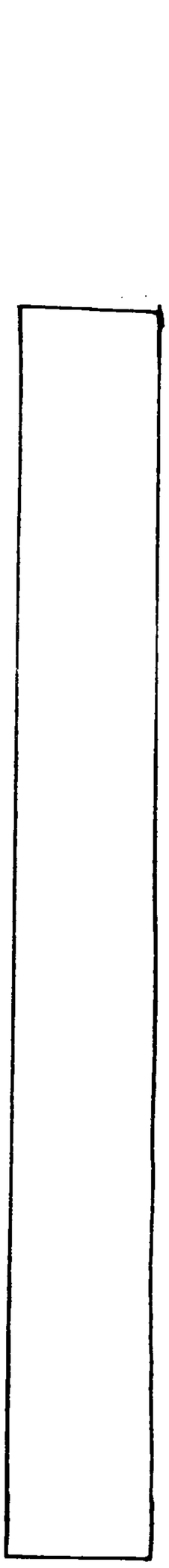

ASTMD 790

Fig (6a) Flexural modulus test specimen

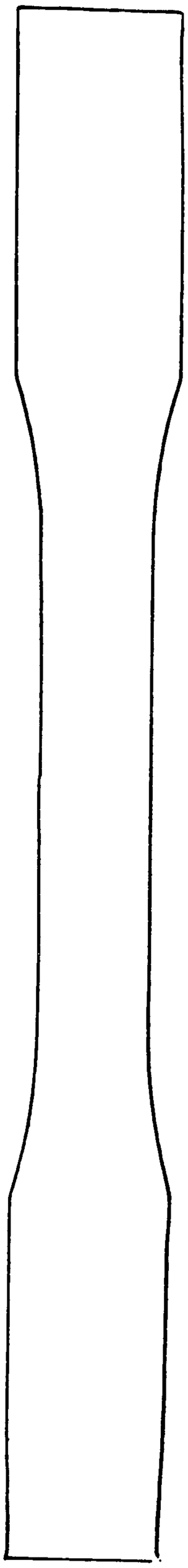

ASTMD 638

Fig (6b) Tensile test specimen

To scale

P1	-	Between-cycle time	4
P2	-	Mould-closed time after injection	20
P3	-	End of total mould opening stroke position	70
P4	-	End of high-speed mould opening stroke position	56
P5	-	End of slow-speed mould opening stroke position	36
P6	-	End of preferred forward stroke position	80
P7	-	End of first high-speed mould closing stroke position	70
P8	-	End of first slow-speed mould closing stroke position	56
P9	-	Mould protection low pressure commencement position	50
P10	-	High-speed phase mould opening speed	30
P11	-	High-speed phase mould closing speed	80
P12	-	Slow-speed phase mould opening and closing speed	83
P13	-	Reduction mould protection pressure	96
P30	-	Air blow time	40
P31	-	Air blow start position during mould opening	0.00
P32	-	Hydraulic ejector control start position during mould opening	70
P33	-	Time preceding hydraulic ejector and stroke	0.00

Table (3.1) -(1)

P34	-	Ejector out time (repeat ejectors)	0.30
P35	-	Nozzle heating (time %)	0.0
P36	-	Forward zone temperature	185
P37	-	Middle zone temperature	165
P38	-	Supply zone temperature	149
F8	-	Parameter change entry	65

Table (3.1) -(2)

Table (3.2) illustrates the conditions under which the injection machine was operated.

3.9 Description of light and electron microscopy of starch and polymers.

3.9.1 Light microscopy:

Although starches from various plants have similar chemical composition the form of the individual granules varies from sample to sample so that a microscopical examination is a valuable diagnostic procedure for any laboratory dealing with the starches and starch products. Microscopical examination enables one to determine among other features, granule shape and granule size-distributions.

Two light microscopes were used, one a Zeiss universal microscope which formed part of the optimax image analyzing system, and was fitted with mechanical stages, polarizer and analyzer. This microscope was used for particle size distributions and measurements. The other microscope used was a Reichert for study of polymer morphology and taking photographs.

3.9.2 Sample preparation

Mounting the starch for examination is a very simple procedure. A small drop of glycerol-water (1:1) solution as recommended by

MacMaster (104), is placed on a microscope slide and a small quantity of the starch sample is transferred on the point of a knife to the drop and thoroughly mixed by means of a needle. The drop is then covered with a cover glass. The sample is then ready for observation. The quantity of starch taken should be such that whilst the field of view shows numerous granules, these should not be so crowded together as to overlap since this would interfere with observation and with measurement.

For most of the starch-filled polyethylene mouldings the mounting medium was a drop of Canada balsam placed on a microscope stick.

3.9.3 Preparation of thin sections for microscopy using the microtome.

The importance of ensuring that the compounding process has produced an adequate dispersion has long been realised. In most cases visual examination of the compound does not discriminate between a good and a poor dispersion unless extremely thin sections are available for microscopic examination. The technique of preparing microtome sections and studying the dispersion of the filler under the microscope is not new. A conventional microtome was used to cut sections between 10-12 microns thick for observation, using light microscopy, of starch-filled HDPE. It is well known that the condition of the knife is one of the most important factors controlling the production of a good section. Experience with the microtomy of starch-filled HDPE proved no exception to the rule.

The microtome knife was sharpened for every series of sections cut from a single sample.

3.9.4 Scanning Electron Microscopy (S.E.M.)

The scanning electron microscope (S.E.M) is one of the latest tools for examining, photographing and, more recently, chemically analyzing small particles. The S.E.M. uses secondary electrons emitted from the surface of a sample to form seemingly three-dimensional images. It bridges the gap between light microscopy and T.E.M., and, in addition, performs some functions of the electron microprobe. The S.E.M. has a wide range of electron microprobes. The S.E.M. has a wide range of magnification (20 to 100,000X) and a depth of field approximately 300 times that of the light microscope. Resolution of better than 20 nm is possible on commercially available instruments, as compared with resolution for the visible light microscope of 250 nm. Although this does not compare with the resolution possible with the T.E.M., ultrahigh resolution is not usually necessary for the examination of starch particles. Sample preparation for S.E.M. is more straightforward than for T.E.M. and makes the S.E.M. particularly useful for examining starch particles and polymer matrices containing starch particles.

Scanning electron micrographs were taken on stereoscan instrument (Cambridge S250) (figure 7).

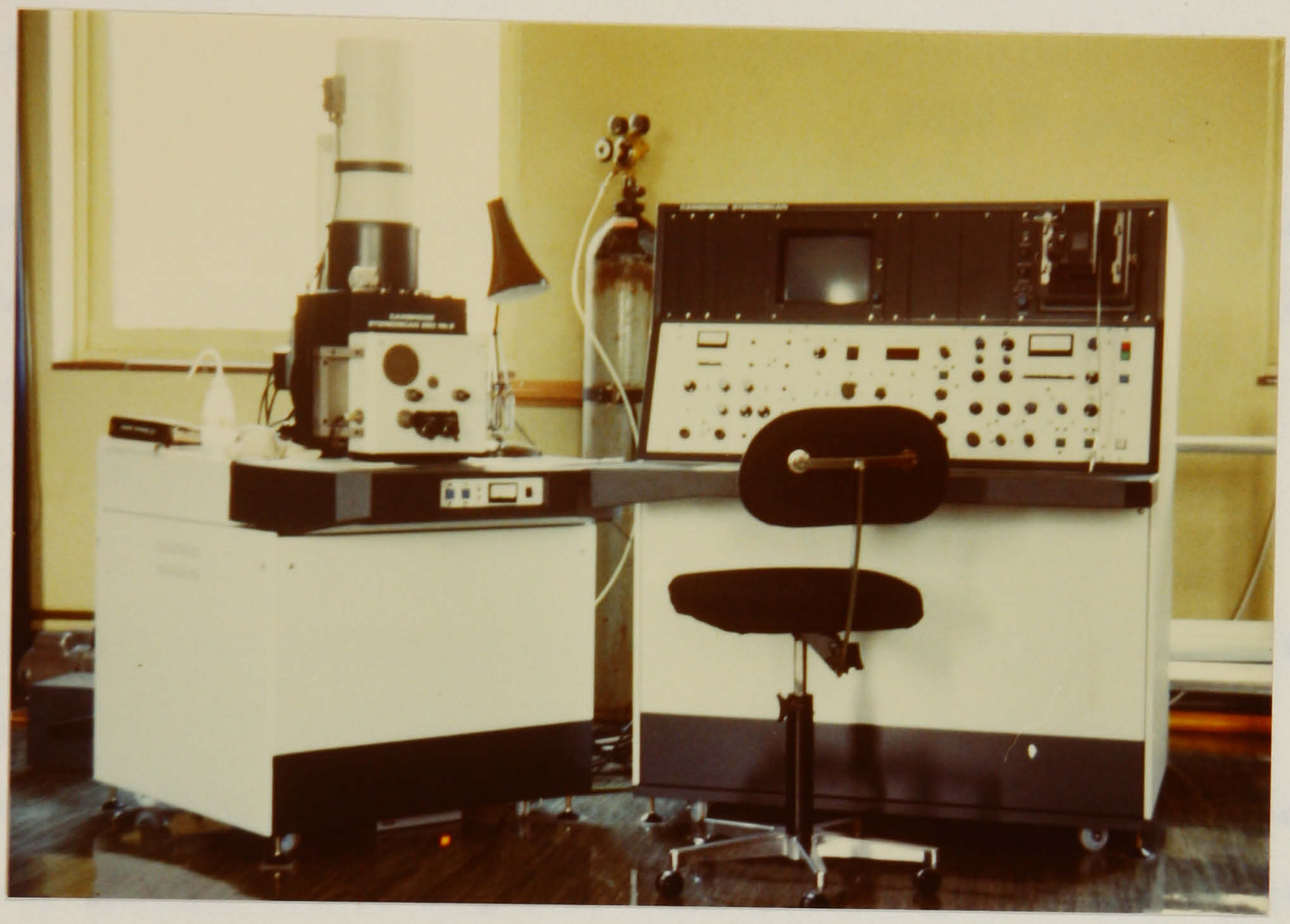

Fig (7) Scanning electron microscope used Stereoscan S250

(Cambridge Instruments Ltd.)

3.8.5 Sample preparation for S.E.M.

Only minimal sample preparation is necessary for S.E.M. The sample as a whole may be simply glued to a specimen stub and coated with a conducting material to prevent the accumulation of local electrostatic charge on the sample.

A thin coating of the sample with gold-palladium, one of the most effective methods for S.E.M. sample coating, has a high yield of secondary electrons and will give more information on surface structure.

To ensure that the particles did not fall off in the vacuum, a small piece of double-sided adhesive was placed on the specimen stub and the starch sample sprinkled on to the tape. Excess particles could then be removed simply by tapping the specimen stub lightly. After the particles were mounted the substrate was placed in a vacuum evaporator and then was coated with gold-palladium for 12 minutes.

Samples of high density polyethylene containing starch were prepared in a similar way. After etching the sample according to the method (3.9.5) it was placed on the specimen stub with the aid of double sided adhesive tape and then coated for 15 minutes with gold-palladium using vacuum evaporator.

3.9.5 Solvent-Etching

The solvent-etching technique is based on the principle that amorphous polymer chains are more soluble than the crystallized ones. A solvent will remove molecules as a whole from the amorphous regions without breaking covalent bonds. When a polymer is crystallized from the melt, crystalline structures like spherulites are covered by a thin layer of almost amorphous chains. The crystalline structures can therefore be revealed by selection dissolution of the amorphous material.

To prepare starch filled HDPE for viewing by scanning electron microscopy, the following etching process was employed. Injection moulded samples of polyethylene and starch filled polyethylene were placed into a 50 ml beaker containing the etching reagents which consisted of a solution of 54 parts (by weight) of sulphuric acid, 22 parts chromic acid and 72 parts water. The beaker was then placed in an air-circulating oven at a temperature of 70^{o}C for periods varying from 20-40 minutes. The etched samples were thoroughly washed in water and then air-dried.

The other etching reagents reported by Olley and Bassett (105) were prepared by dissolving a given weight percentage of potassium permanganate in a known volume of acid. This is either concentrated sulphuric acid or a mixture of one or two parts by volume of concentrated sulphuric acid and one part of orthophosphoric acid. The acid was placed in a conical flask and stirred with a glass

3.9.6 Transmission Electron Microscopy (T.E.M.)

T.E.M. can be used to help in the determination of the structure of materials. In most cases the T.E.M. can be used to derive information of several different kinds which relate to most of the sciences concerned with elucidating microstructure. The external surface of a body can be studied and information obtained concerning the external morphology of the specimen and also microscopic details of the surface roughness can be investigated. Materials of interest here are HDPE and starch particles in HDPE. The electron microscope used in the present study was a JEOL 100CX, chosen because of its ready accessibility in the laboratory (figure 8).

3.9.7 Replication

In some instances it is desirable to examine the surface of a bulk, fractured or etched sample, the sample was etched as described in section (2.9.8). Replicas of etched samples were prepared as follows: The technique was to cover the acetone-moistured surface of the etched sample with a ready-prepared collodion film (Bex film). Following evaporation of the solvent, the plastic replica was peeled off, and coated with a carbon film using a standard vacuum coating apparatus. The carbon film then was placed on a metal support grid, plastic side down, and exposed to a film of solvent (Acetone) which slowly dissolves the plastic leaving only the carbon replica. The replica was then shadowed with gold-palladium at an angle of $20^{o}C$.

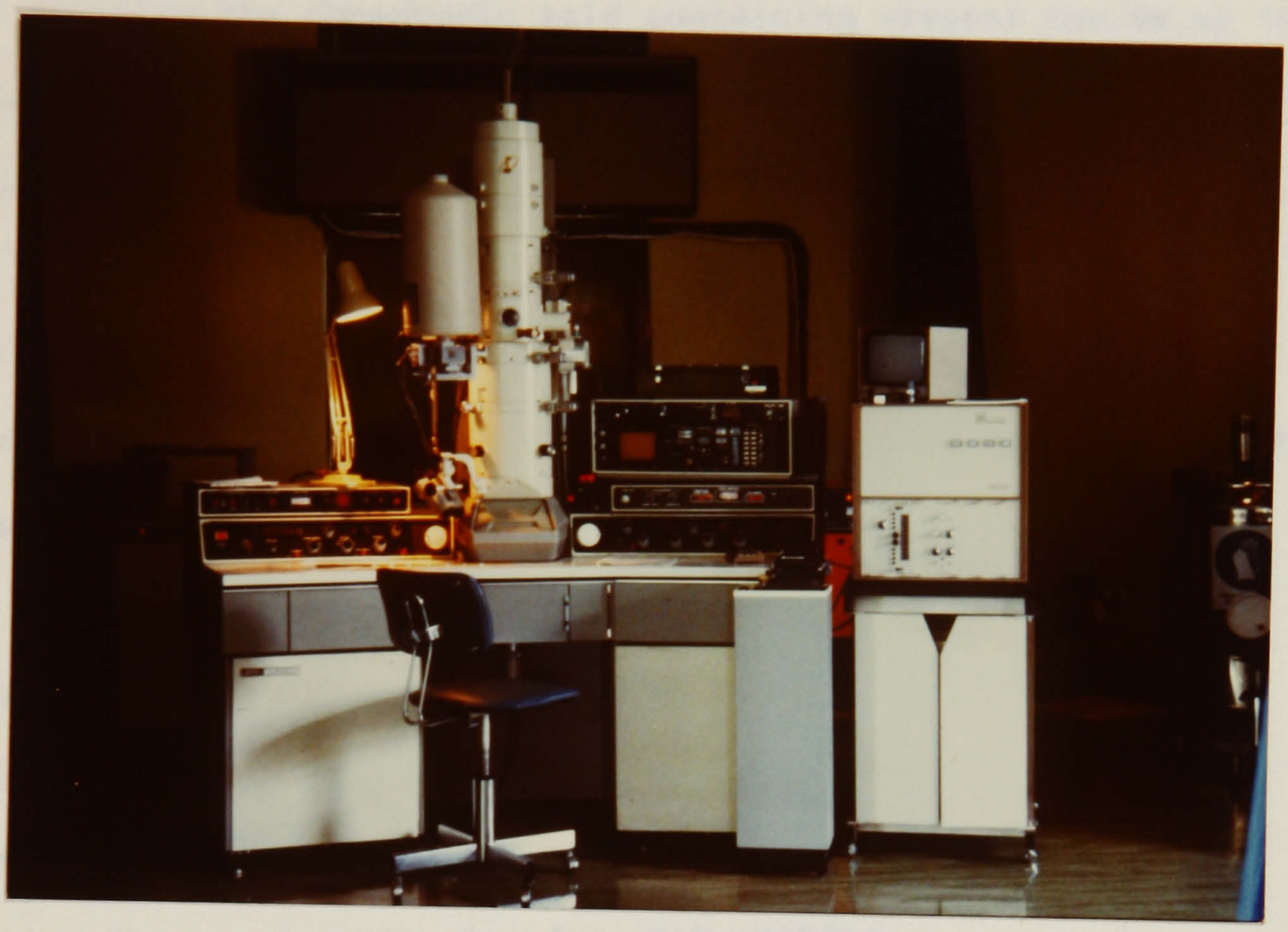

Fig (8) Transmission electron microscope used

(JEOL 100 CX)

covered magnetic stirrer. The potassium permanganate is shaken into the swirling acid, the flask stoppered, and the mixture stirred until all the permanganate is dissolved. The time taken to dissolve the phosphoric acid containing reagent may be up to one hour. Dissolution of the permanganate is faster if dry phosphoric acid is used.

Injection moulded samples of polyethylene and starch filled polyethylene was placed in the above reagent in a glass tube and heated in water bath at $70^{o}C$ for 20 minutes.

The sample was washed successively with hydrogen peroxide (to reduce any manganese dioxide or permanganate present) several changes of distilled water and finally acetone. 2 minutes is generally an adequate time for each washing.

3.10 Measurement of Mechanical properties of polymer samples in uniaxial tension (106).

A standard method of determining the tensile properties of plastics is specified by ASTM Standard D638-64. The specimen may be rectangular or circular in cross section and usually has a reduced section at the centre and larger dimensions at the ends, where the specimen engages the grips of the apparatus that applies the stress.

The elongation in the specimen at various values of the applied load or stress, is measured over a constant gauge-length of the specimen

by means of mechanical gauges, optical gauges, or electrical strain gauges. The resulting measurements are plotted in the form of a nominal stress - nominal strain plot. If the cross-sectional area is monitored, one can plot the data in terms of nominal stress (106) given by $\sigma = \frac{P}{A}$

where p is the applied load and A is the original cross-sectional area.

The elongation (e) is given by $e = l - lo$ where l is the instantaneous length of the gauge section at any moment the lo the original length.

The uniaxial tensile strain, ε, is defined as the elongation per unit of length, and hence $\varepsilon = \frac{l - lo}{lo}$.

A typical tensile stress-strain curve for a thermoplastic polymer is given in (figure 9). Over some finite range of strain the plot is essentially linear, hence over this range we may write

$$\sigma = Ee$$

Where E, the so-called Young's modulus of elasticity is given by the slope of the initial portion of the stress-strain curve.

The important mechanical properties in a flexural list are the modulus of elasticity, Eb and flexural strength, Sb. For a simply supported beam of span length L subjected to a central load the deflection at the centre is given by:

$$\delta = \frac{PL^3}{48\ EbI}$$

where I is the moment of inertia of the beam cross-section and, for a rectangular beam of width b and depth d, is given by $bd^3/12$. Thus the modulus of elasticity in bending Eb may be calculated from the initial slop $m = \frac{p}{f}$ of the load deflection curve. In terms of this slope and the dimensions, Eb is given by:

$$E_L = \frac{mL^3}{4\ bd^3}$$

At any value of P within the linear portion of the load deflection curve, the maximum fibre-stress is given by the usual strength of materials formula

$$S = {}^3/_2 \left(\frac{PL}{bd^2} \right)$$

where p load

L support span

b width of beam tested

d depth of beam tested

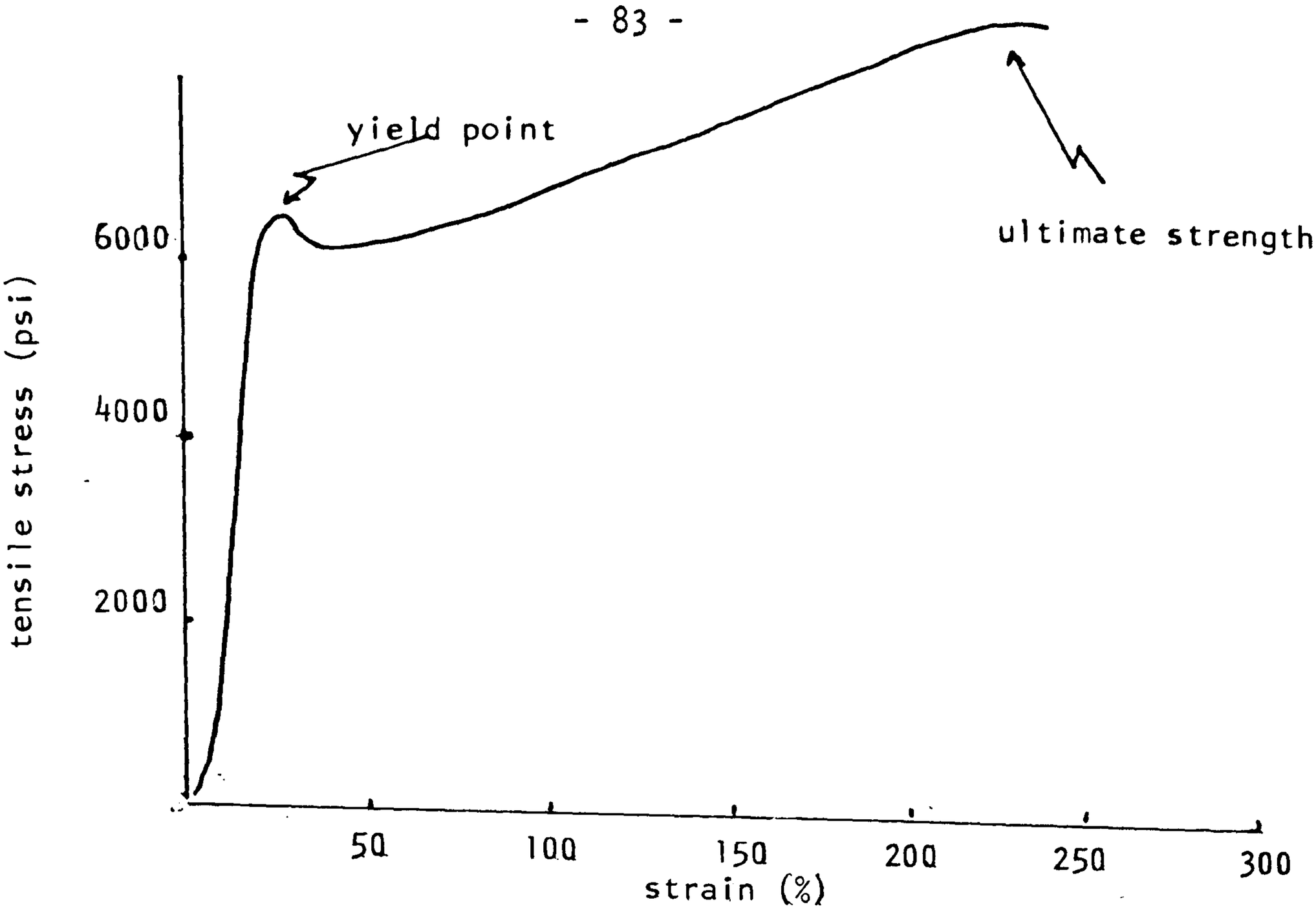

Fig (9) "Typical stress-strain curve for semicrystalline polymers"

The "dumb-bell" shaped (figure 6b) samples were firmly attached to the cross head of an "Instron" using the standard specimen grips and elongated at a constant rate of 50 mm/min, until the ultimate tensile strength of the material was reached. Load-extension curves were automatically recorded by the instrument in each case under an appropriate chart speed of 5" min^{-1}.

3.10.1 Mechanical properties of polymer samples in flexure. Standardized procedures for determining flexural properties of plastics are given in ASTM Standard D790-86. The specimen is required to be in the form of a rectangular bar which is loaded at the centre and simply supported at or near the ends.

Measurements are made of the deflection δ of the beam at the centre, usually with a micrometer dial gauge, as the load p is applied by the test machine. The experimental data is then generally plotted in the form of a load-elongation plot.

3.11 Differential Scanning Calorimetry (D.S.C.)

It was decided to obtain information about the thermal characteristics of starch-filled polymers using differential scanning calorimetry (D.S.C.)

A small sample specimen (between 1 and 20 mg) was subjected to a controlled series of temperature changes. By maintaining the temperature of the sample holder equal to that of an identical reference holder, heat evolved or absorbed as the result of physical or chemical changes in the sample may be detected and recorded.

Figure (10) shows the Perkin-Elmer Model DSC-2 which was used in the present study. This incorporates certain features which rendered it particularly convenient for the present study, notably the computer control and automatic recall facility of the thermal programming and the ease with which data from D.S.C. scans could be stored on magnetic discs.

The instrument may be calibrated in K^{o}, C^{o} or F^{o}, and the sample temperature may be programmed to increase or decrease at rates as slow as 0.3125^{o}/min or as fast as 320^{o}/min and may also be maintained isothermally to within a few hundredths of a degree. In addition both upper and lower limit switches can be terminated or reversed at any desired temperatured. The instrument is capable of operating from -175 to $715^{o}C$ at sensitivities that are variable from 2 to 0.01 mcal/sec per inch of chart paper.

Fig (10) Differential scanning calorimeter used

(Perkin-Elmer Model D.S.C.2)

3.11.1 Sample preparation for D.S.C.

Injection moulded samples of starch-filled polyethylene were thermally characterized by the D.S.C. technique. The bulk mouldings were hand-sliced using a sharp razor blade and thin rectangular pieces of material from the centre part were then sectioned until sample weight (about 8 mg) was obtained. These thin slices were then placed in a sealable aluminium pan in order to achieve thermal contact between the sample and the pan. Care was taken to cut the slices always from the same central part of the moulding (perpendicular to the direction of injection flow).

The sealing of the slices was performed using a Perkin sample pan crimper which crimps an aluminium pan cover on the pan and sample to provide a convenient encapsulated sample with high thermal contact and minimum gradients within the samples.

The operational conditions for D.S.C. as carried out in the present work were:

Minimum temperature	$323^{o}K$
Maximum temperature	$458^{o}K$
Heating rate	20 degree/min.
Cooling rate	320 degree/min.

3.12.0 X-ray diffraction methods used to study starch and starch-polymer composites.

3.12.1 The Debye-Scherrer Method

This method of powder analysis is also referred to as the Hull-Debye-Scherrer method because it was independently devised by Hull (107) in the United States and Debye and Scherrer (108) in Germany between 1915 and 1917. The characteristic geometrical features of this technique are portrayed in fig (11).

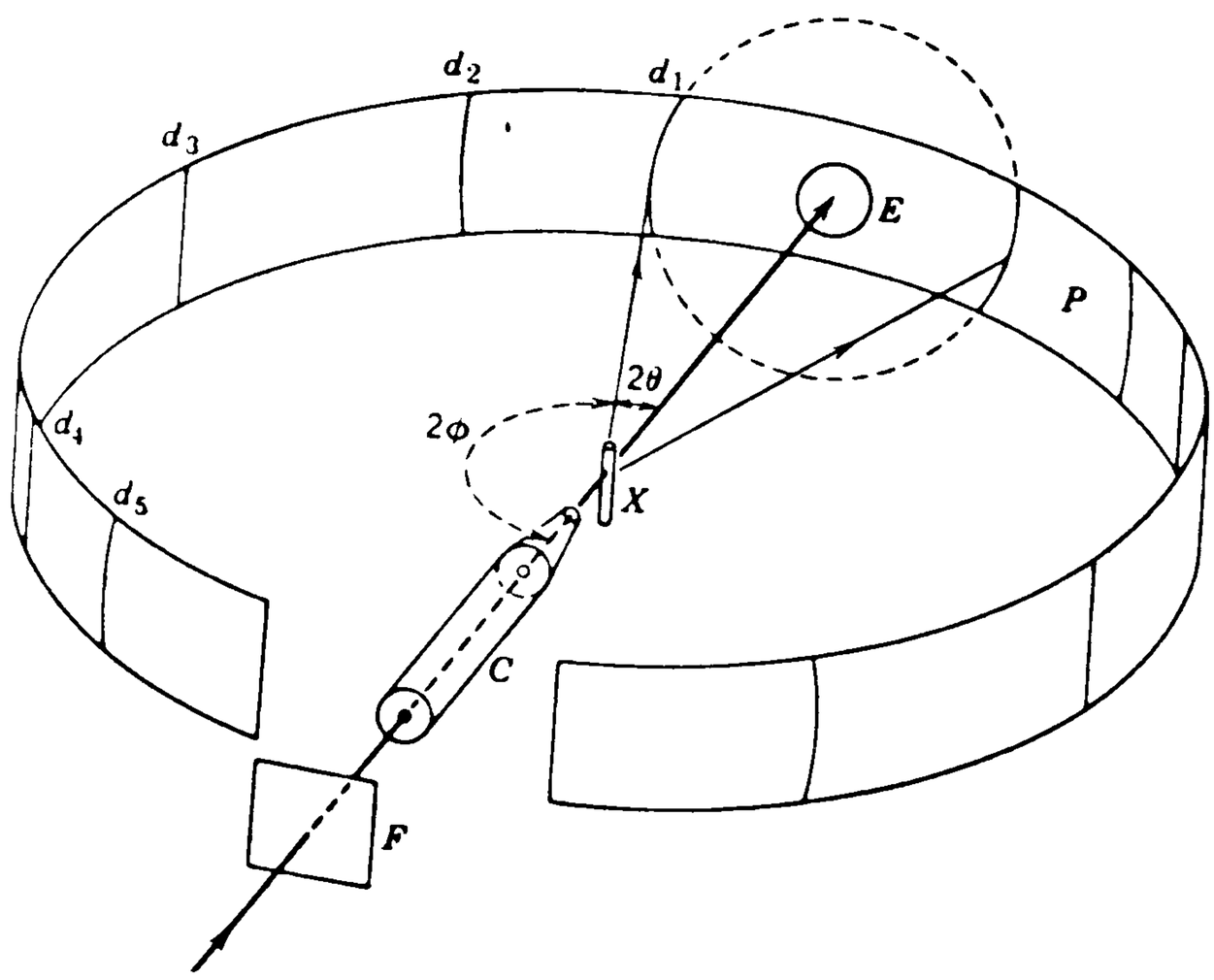

Fig(11) Geometrical features of the Debye-Scherrer technique

The incident beam is usually passed through a filter F to eliminate the characteristic $K\beta$ radiation, after which the K_α rays are collimated by the pin-hole system C. The resulting narrow pencil

of rays impinges on the small cylindrical sample X, and sections of the various diffraction cones are intercepted by the cylindrically disposed strip of photographic film p. This arrangement makes it possible to record, not only sections of the halos diffracted in the forward direction, but also most of those in the back-reflection region (for which $2\theta > 90^{o}$). The powder specimen is customarily rotated about the cylindrical axis in order to increase the number of particles contributing to each reflection. The features shown in (figure 11) are typical of the Debye-Scherrer techniques, but some, such as location of the filter, nature of the collimator, and positions of the ends of the film, may be varied in order to achieve particle advantages. The invariant features of the method include a collimated beam of monochromatic x-rays impinging upon a small powder sample which is located at the centre of a cylindrically arranged strip of film.

The chief merits of the Debye-Scherrer method are:

1. the small amount of sample powder required (as little as 0.1 mg can be used)
2. the almost complete coverage of all the reflections produced by the specimen, and
3. the relative simplicity of the apparatus and techniques required.

The Debye-Scherrer method was used in the present study to investigate changes in the crystallinity of starch due to acid treatment.

3.12.2 Sample preparation for the Debye-Scherrer camera. Starch samples were mounted on a fine glass tip cemented into the standard pin. The pin, together with the sample was inserted in its usual place in the 57.3 mm powder camera. The camera with its beam-trap removed, was placed on the specimen centering device. A strong light was shone through the exit-port to give a good image of the mounted particle. The sample must be centered accurately in the x-ray beam in order to obtain sharp lines and thus short exposure times. The insert, pre-loaded with x-ray film, was then placed in the camera, and exposed for 24 hours. The x-ray source (Cu target, Ni filtered Kα). The tube was run at 20 MA beam current and 40 KV.

3.12.3 Brief Description of the wide-angle or flat-film camera These cameras are sometimes referred to as Lane, monochromatic-pin hole, or transition cameras. The experimental arrangement is shown in figure (12)

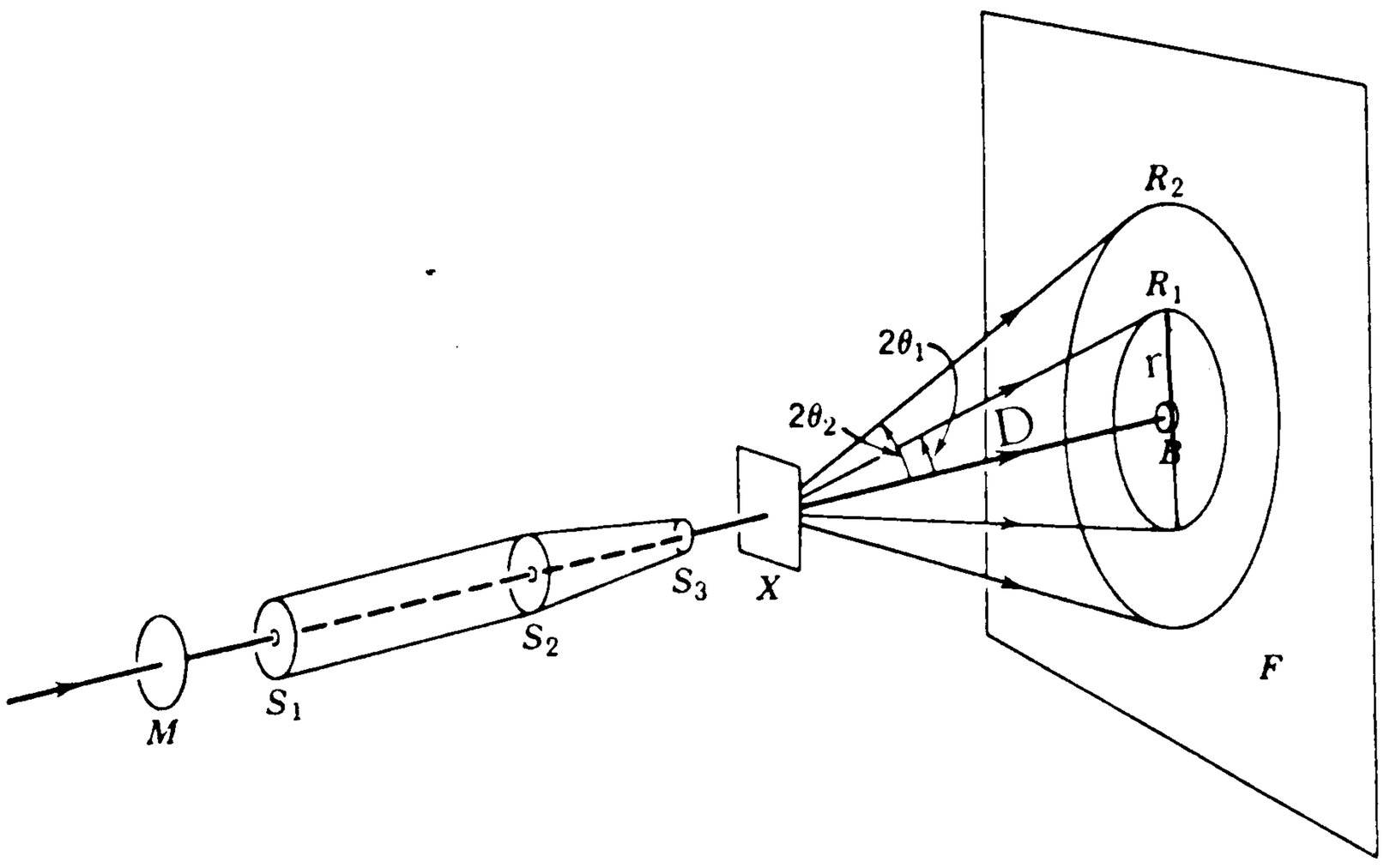

Fig(12) Forward-reflection arrangement of the monochromatic-pinhole technique

The direct beam passes through the B-filler M; is collimated by a pinhole system with apertures S, and S_2 and S_3 ; penetrates the polymer specimen P; and is finally intercepted by the small concave lead button B. Air-scattered x-rays tend to darken the central region of the film around B. This darkening can be either reduced by placing the beam stop as close as possible to specimen without obscuring any significant details near the centre of the diffraction pattern or else eliminated by evacuating the camera of air.

With reference to fig (12), it can be seen that the values of 2θ corresponding to particular diffraction effects on the film can be determined accurately only if the distance D is known precisely, since $\tan 2\theta = r/D$. However, because of the wide physical variability of polymer specimens, in practice it is difficult to measure D with high accuracy or to maintain it during the location of subsequent specimens that one of the same thickness and mounted in an identical manner it is possible to obtain a reproducible sample-to-film distance with the aid of a special gauge block (In this case 3 cm).

The x-ray source (CU target, Ni-filtered K_α radiatron). The tube was run at 20 MA beam current and 40 KV.

CHAPTER 4

RESULTS AND DISCUSSIONS

4.0.0. Introduction

Starch is the reserve food-substance for many plants. Even when the adult plants contain sugars only, as is the case for a number of monocotyledons, they often produce starch in the early stages of development. The storage of starch by plants in the form of granules is a convenient method since starch is an insoluble source of energy.

The fact that chemical composition, crystalline pattern, and shape of starch granule and particle size has got significant importance in the starch industries makes it a fascinating object to study. Of the starches, taro root crops have long been a staple food of the natives of all the Polynesian islands as well as in the West Indies and the Orient. Since Taro is propagated almost exclusively by vegetative means, each locality has tended to perpetuate its own forms, or "horticultural varieties". Some of these forms have remained localized; others have spread, and many of them have been given new names. In the past the valuation of the various Taros in Hawaii has been based on their quality as cooked table Taro or in making poi. A few are raised primarily for their leaves, used for luau and the early Hawaiians had varieties for medicinal purposes and for religious ceremonies. The two types of Taro cultivation common in Hawaii have formed another basis for segregating varieties: Wetland varieties (submerged culture), all of which are good for poi: and upland varieties (non-submerged culture) which are used primarily as table Taro, only a few of them being suitable for poi.

Within recent years, numerous scientific investigations (109,110) have indicated the superiority of Taro over other starchy crops, particularly polished rice, which are stable foods in the Pacific regions. The superiority of Taro starches in applications as a filler for plastics will be discussed in the next chapter. The emphasis on this fact by local physicians and nutritionists and use of Taro starch in the plastics industry led to an increased demand for Taro and a new interest in the cultivation of the crop. With commercial development, a need has arisen for varieties particularly adapted to the production of Taro flour, beverage powders, and other dried Taro products.

In addition, the problems involved in Wetland culture particularly the menace of disease - and the necessity of extending plantings by utilizing new lands have made important the selection of varieties which will grow well in the moist, cool uplands.

Experiments have recently been conducted by the Hawaii Agricultural Experimental Station on selection and development of desirable varieties through cross-pollination (111/2) as well as through natural vegetative mutation (111). Systematic work along these lines must, however, be preceded by a classification of the many varieties present in Hawaii. In 1914, MacCaughey and Emerson (113) listed about 300 varietal names of Taro in Hawaii.

Experiments have also been conducted in this department on the gelatinization temperature and the ratio of Amylose to Amylopectin (18).

Considerable interest exists, therefore, in studying the peculiar differences which exist among these many varieties. In the present study we have attempted to extend this line of investigation by characterizing some of the physical properties, of 112 Taro starch varieties, with particular attention to the measurement of granule size by narrow angle light-scattering.

Section I

4.1.0 Starch preparation

Generally, different starches are isolated from their sources, such as seeds, tubers, or other carbohydrate reservoirs of plants, by various processes that are determined by the sources and the end uses of the individual starches. Most of the industrial procedures disintegrate the starch source before suspension in water for further processing. Apart from the removal of shells, seed coats, brans, germs and/or other obvious major impurities, the success of starch production can be enhanced by the use of physical and/or chemical means that aim to weaken the physical and/or chemical bonds that hold starch granules. More specifically, the efficiency or starch isolation depends on the success of separating individual starch granules from the proteinacious matrices in which they are produced. In working with Taro starch, it was found that processes which we adopted for extraction of Taro starch not only gave good yield but also we were able to get free lump starch: of course a later one depends on the method of drying, which will be discussed later.

4.1.1. Drying

Drying is an important part of starch technology because starch derivatives and starch by-products are usually manufactured by treatment with water which afterwards has to be removed. This is usually done in two stages. The first of these is dewatering, i.e. the removal of moisture by centrifugation or filtration; removal of moisture by heat, follows at the second stage after the removal of moisture by mechanical means.

After centrifugal dewatering, Taro starches were dried in an air-circulating oven at 50°C, to a moisture content of about 8%. They were further dried at100°C for 72 hours to a moisture content of less than 1%, and then ground in a coffee grinder. Microscopical observation showed no damage to starch granules.

However, in the case of acid-treated starch, it was noticed that this method of drying produced starch granules which were clumped into large aggregates which were unsuitable for use as fillers in plastics.

Consequently, it was necessary to decide upon another method of drying which would minimise the hydrogen bonding and other forces tending to increase the tenacity with which the starch retained water. One way in which this could be accomplished was by chemical dehydration, i.e. dehydration of the dewatered starch cake by successively washing with ethyl alcohol, followed by filtering and air-drying to eliminate the volatile solvent.

Another method to avoid lumping in the acid-treated starch was to keep the starch granules in a state of movement at the same time as drying takes place. This last procedure was adopted for acid-treated starch by using a spray-drying machine. This method of drying also had the advantage of simplicity.

The principle of spray-drying is explained in section (3.4). Finally, it is important to point out that the starches dried with the spray-dryer were then post-dried in a vacuum oven at 100°C for a minimum period of 72 hours, because it was found that the spray dried starches had a moisture content about 8% which was too high for their intended use as fillers for thermoplastics.

4.1.2 Moisture

Starch moisture contents, above a certain level, have a catastrophic effect on the strength of several composites as observed by Sharafi (113). All the commercial starches and most of the treated starches were moisture analyzed and kept in an air-circulating oven at100°C for a period of 72 hours, before compounding with the appropriate thermoplastic. This method of drying produced a lump-free starch with a moisture content below 1%, in a relatively short time, providing that the sample to be dried had a moisture content low enough to show signs of being powdery, otherwise it will form agglomerates or cakes. The moisture content of Taro starches after extraction is 33-38%. Table (4.1) shows the moisture content of various starches before and after drying.

Table (4.1)

Determination of moisture by the "Townsend, Mercer " vacuum moisture tester.

a. Initial moisture content (%) of the commercial starches

Potato	Maize	Rice
13.4	11.4	9.8

b. Moisture content of Taro starches after drying at $40^{o}C$.

Bun Long	Lehua Maloi	White Masi	West Samoa
8.1	8.3	8.3	7.9

c. Final moisture content (%) of samples that were dried in an air-circulating oven at $80^{o}C$ for 72 hours before being mixed with polymer.

Potato	Maize	Rice	Acid-treated Rice	Lehua Mahe
0.5	0.5	0.5	0.9	0.7

d. Moisture content of acid-treated rice after spray-drying is 8.2

4.1.3 pH Determination of starch

The pH's of suspensions prepared by dispersing 2.5 g of the appropriate starch in 50 ml. distilled water was measured with a laboratory pH meter, and were found to be as follows:

Potato	Maize	Acid-treated Rice after washing	Lehua Maoli
5.7	5.4	5.8	5.1

4.1.4 Starch surface preparation

The reinforcing effect of starch particles on the mechanical strength of thermoplastics should depend primarily on the interface between the starch granules and the matrix polymer. Since the starch particles have a hydrophilic surface which mostly does not possess the properties that would permit sufficiently strong bonds between the individual granules and the non-polar thermoplastics, Linero (9) examined several physical and chemical methods to treat starches with reagents that should form a hydrophobic coat and thus increase the wettability of the starch granules by the polymer melts. Potato, maize and rice starch were available in a surface treated form, but Taro starch had to be surface treated in the laboratory using the dry-treatment method described below.

4.1.5 Dry treatment

Methyl Hydrogen polysiloxane (DC1107)

Spreading-times of the coating agent around the starch granules and

the optimal thickness of the resulting coatings were studied by Linero (9). His studies give valuable information regarding treatment cost and the interaction to be expected between filler and matrix polymer. Linero observed that calcium and lead stearates showed a low catalyst effect. Even at high concentration these metal soaps did not accelerate appreciably reaction of the silicone with the starch surface. On the basis of his information the zinc stearate was adopted as a wetting agent and catalyst to DC1107. See section (2.6.3) chapter 2.

4.1.6 Acid treatment of rice starch

In an attempt to explain the results of Linero (9) where the addition of starch to polyethylene gave unexpected increases in the yield strength, attempts have been made to increase this effect by acid-etching the surface of the starch granules to remove amorphous materials and possible thus encourage any epitaxial growth-influence on the crystal nucleation of the polymer melt.

Native rice starch granules were treated with 16% sulphuric acid at 40^{o} for one, two, three, four, five, six and seven days.

X-ray diffraction patterns were obtained using a Debye-Scherrer powder camera. The samples were exposed for 20 hours to the X-ray beams (40 KVP, 20 mA). Samples were sealed in thin-walled glass capillaries to prevent moisture changes in the samples during irradiation.

Result and discussion.

The heterogeneous hydrolysis of starch granules by aqueous acid cannot be regarded as the simple, uniform erosion of material from the granule's surface. Dexter French (32) conjected that this heterogeneous hydrolysis takes place preferentially at the more amorphous, gel-like portions of the starch granule, whether they be at the surface or in the interior. It is believed that crystalline portions are protected against acidic attack by at least two factors. First, the packing of the starch chains within the crystalline regions may be so dense that it does not permit the ready penetration of hydrated protons and accompanying axions. The gel-like, amorphous part of starch granules can readily take up acid molecules with consequent local glycositic hydrolysis. The crystallites would only be attacked at the surface of the crystallite or its junction with an amorphous regions.

The second factor is that for hydrolysis to occur, it is necessary for the glucose residues to undergo a change in conformation from a chair to half chair (39). As long as the glucose units are held in a crystalline matrix, such a conformational change would require a very high energy of activation, and hence would have a very low probability.

Such processes of hydrolysis sharpen the crystallinity of starch samples, (figure 1) as judged by x-ray diffraction.

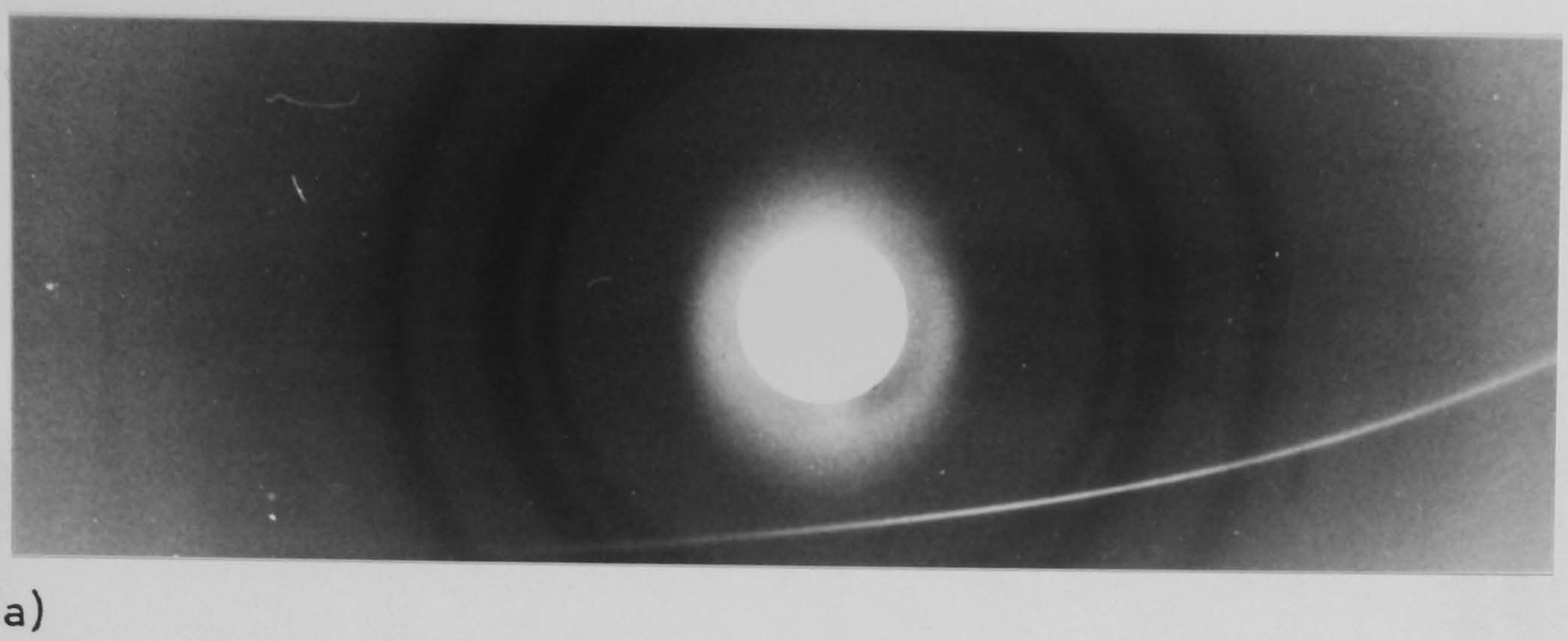

(a)

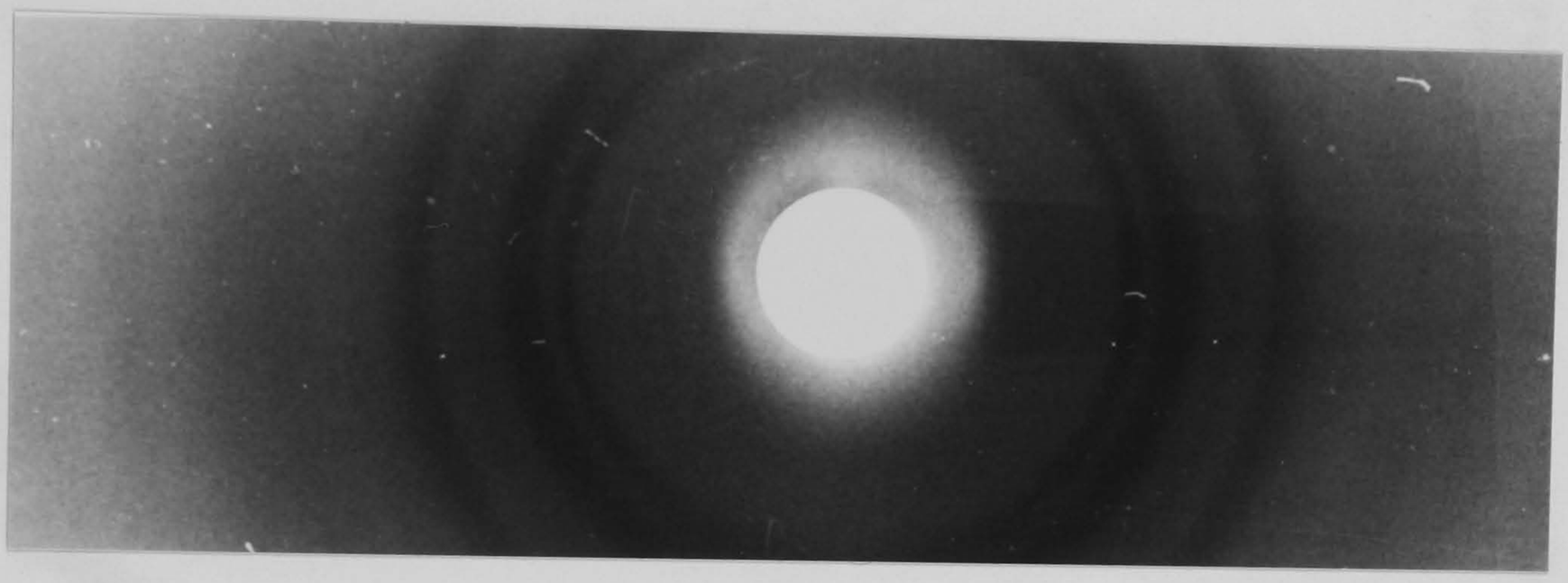

(b)

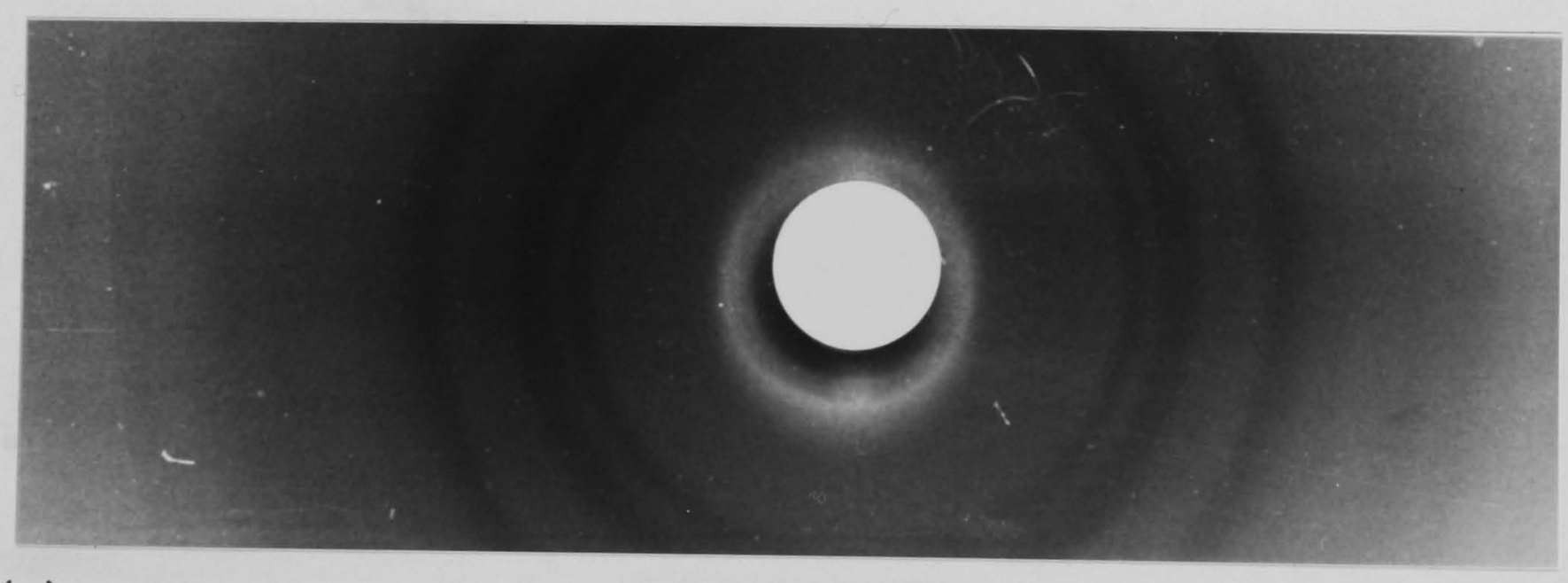

(c)

Fig (1) (a) x-ray diffraction pattern (Debye-Scherrer) of rice starch granules

(b) x-ray diffraction pattern (acid treated) of rice starch for 24 hours

(c) x-ray diffraction pattern (acid treated) of rice starch for 48 hours

Microdensitometer trace of x-ray diffraction pattern obtained from plate (a) fig (1)

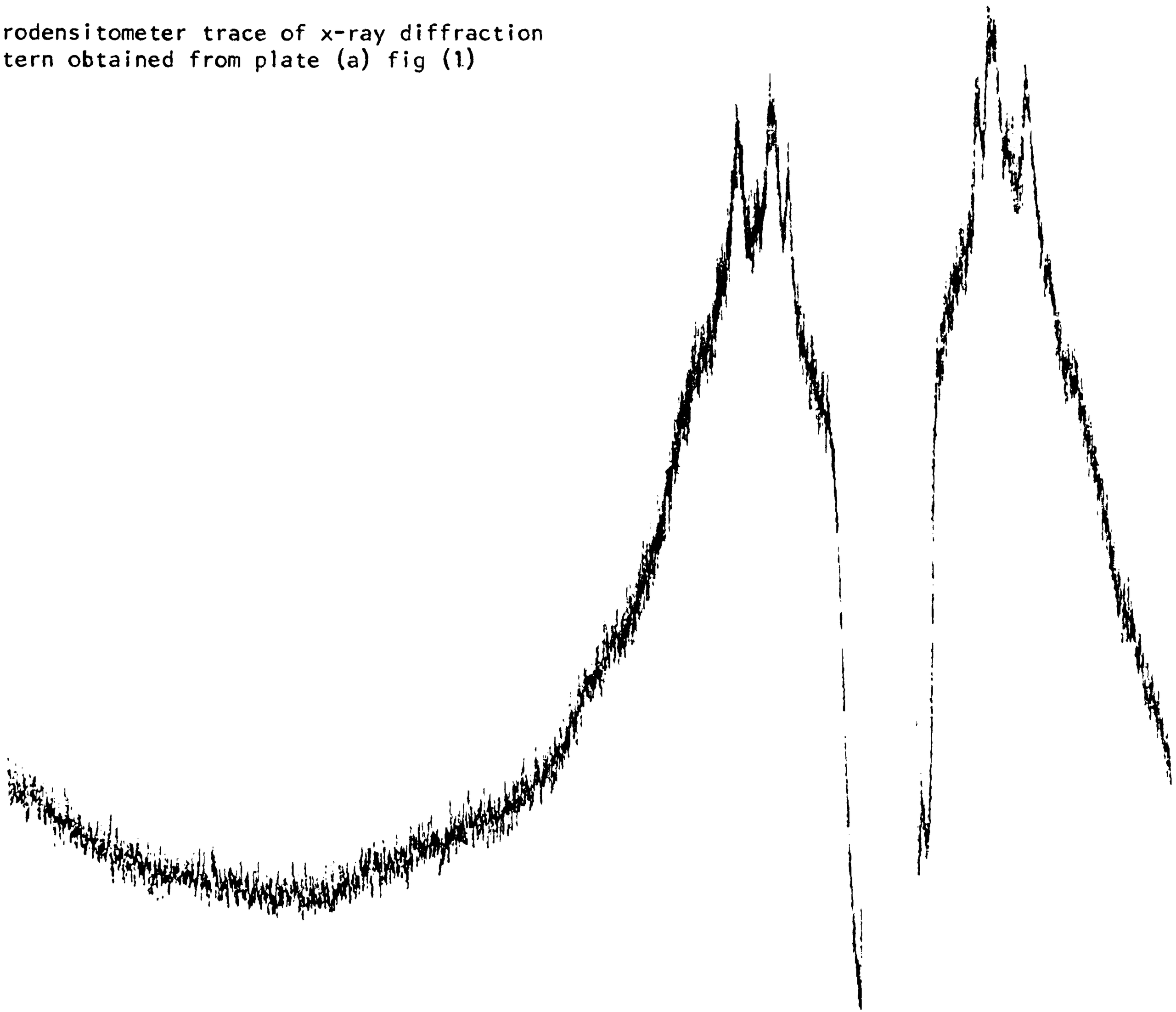

Microdensitometer trace of x-ray diffraction pattern obtained from plate (b) fig (1)

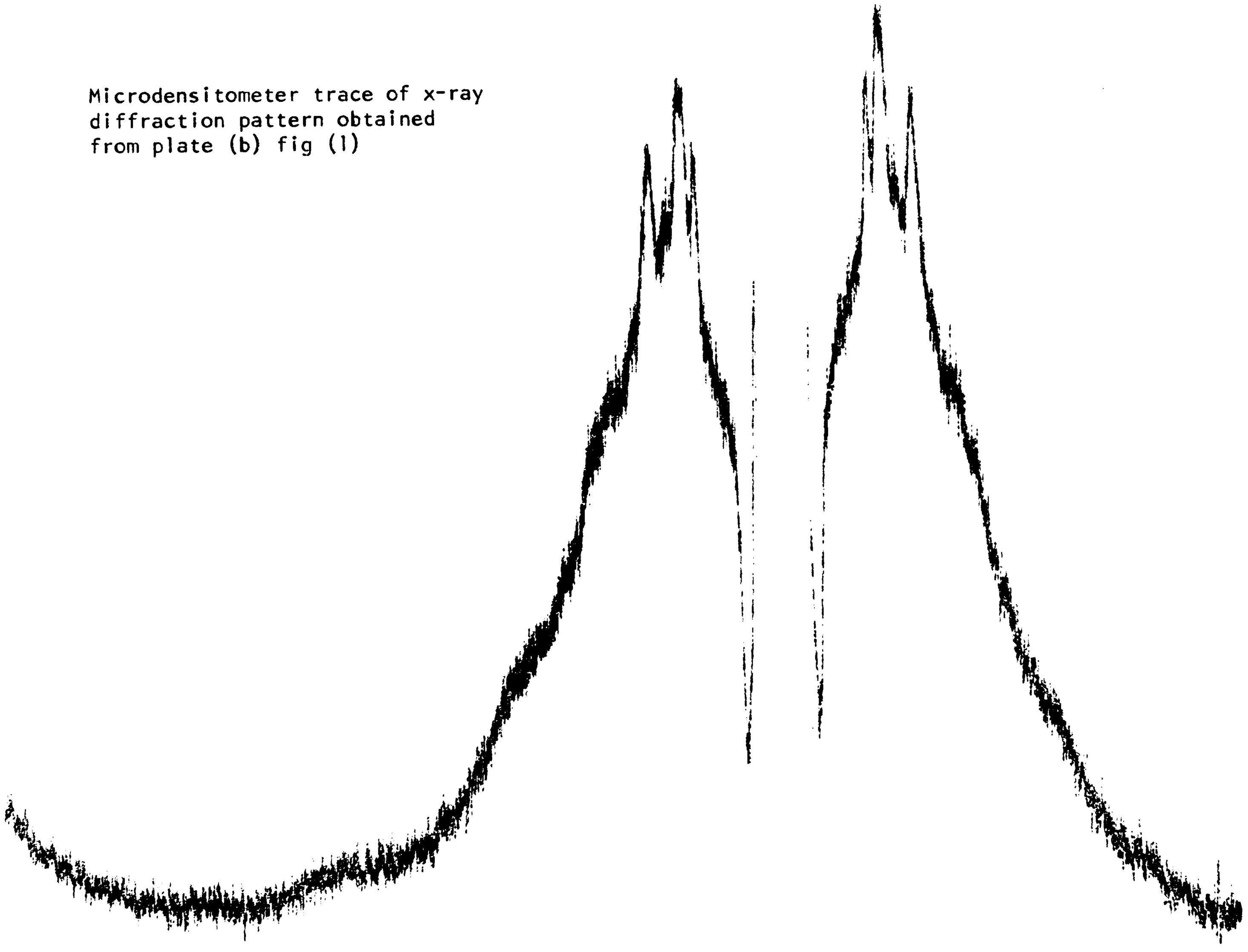

Microdensitometer trace of x-ray diffraction pattern obtained from plate (c) fig (1)

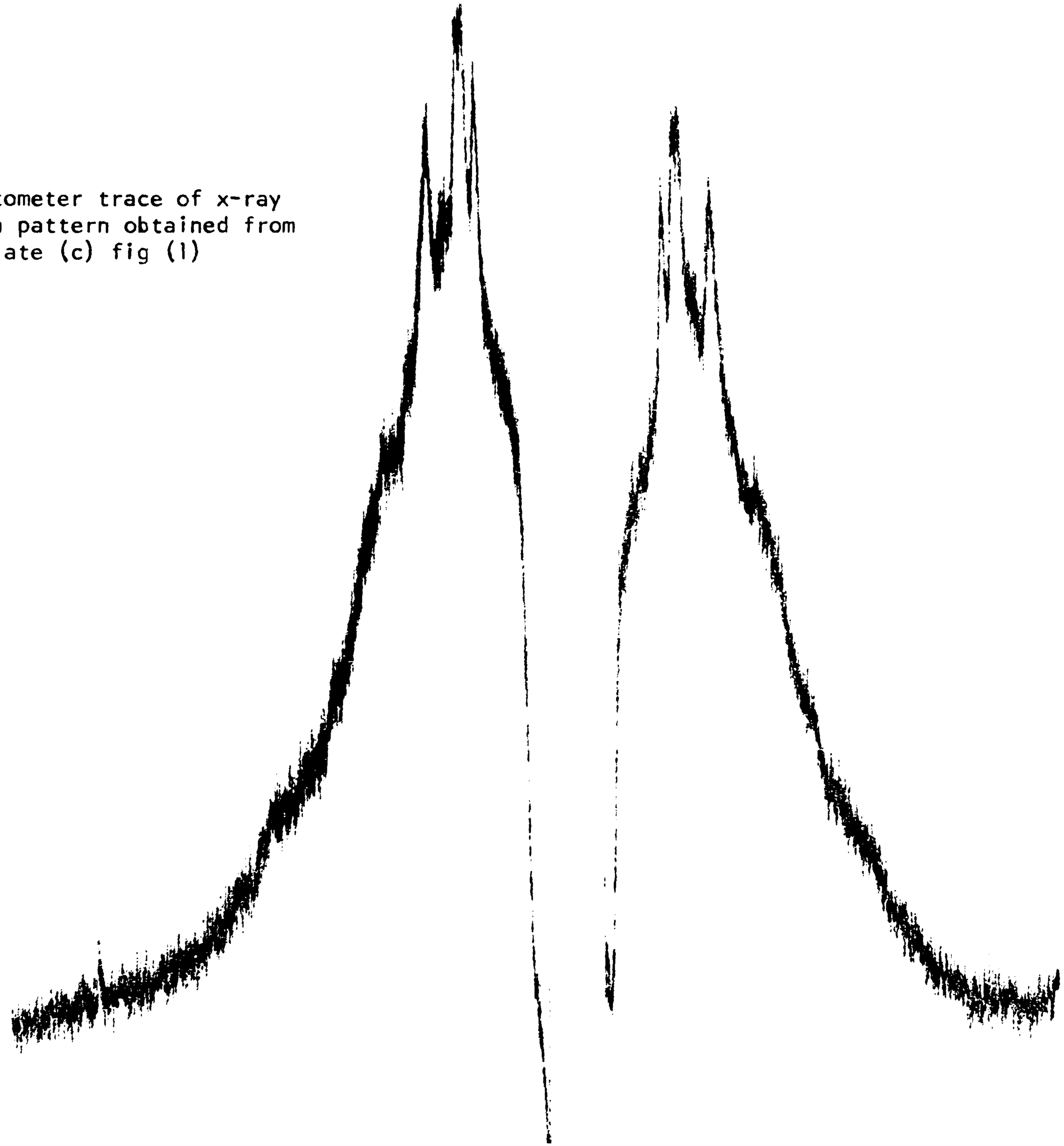

Plate (a) shows the diffraction pattern of native rice starch granules. Plate (b) is the diffraction pattern of acid-treated rice starch (one day's acid exposure), it is evidence that crystallinity of treated starch has increased as can be seen from microdensitometer trace of plates (a),(b),(c).
Plate (c) is the diffraction pattern of rice starch which has been treated for two days; it shows that the rings are sharper than in plate (a) and plate (b). However, further treatment of rice starch for longer periods did not make any significant difference to that of plate (c). It can be concluded that most of the erosion of the amorphous or gel-phase starch granule takes place in the first two days and any further hydrolysis processes are very slow.

It has been reported (32) that during acid hydrolysis at room temperature (24-25^{o}C), the amorphous gel phase is gradually eroded, leaving the crystalline amylodextrin. This process is very slow and takes up to 90 days to complete. However, it can be accelerated by treating starch granules at the higher temperature of 40^{o}C.

4.1.7 Microscopical examination

Although starches from various plants may have similar analytical data the form of the individual granules varies from sample to sample; and a microscopical examination is a valuable diagnostic

procedure for any laboratory dealing with starches and starch products. Microscopical examination includes the study of characteristic shape and granule size-distribution.

4.1.8 Optical microscopy observation

4.1.9 Potato starch

The granules of potato starch vary greatly in size and shape: the largest are often egg-shaped and are visible to the unaided eye. The majority are flattened ellipsoids and the smallest may be perfectly spherical (plate 1). The granules generally occur singly. Granules' size ranges from 15 micron to 100 micron.

The eccentric hilum towards the narrow end of the grain is normally well marked and surrounded by numerous concentric rings; these being very distinct on some grains. The cross observed with crossed polariser and analyser is well defined.

4.1.10 Maize starch

Maize exhibits the polygonal type of starch granule (plate 2), which is usually 4- or 5- sided. A striking point is the greater uniformity in size of the maize starch granules, generally 10 micron to 15 micron.

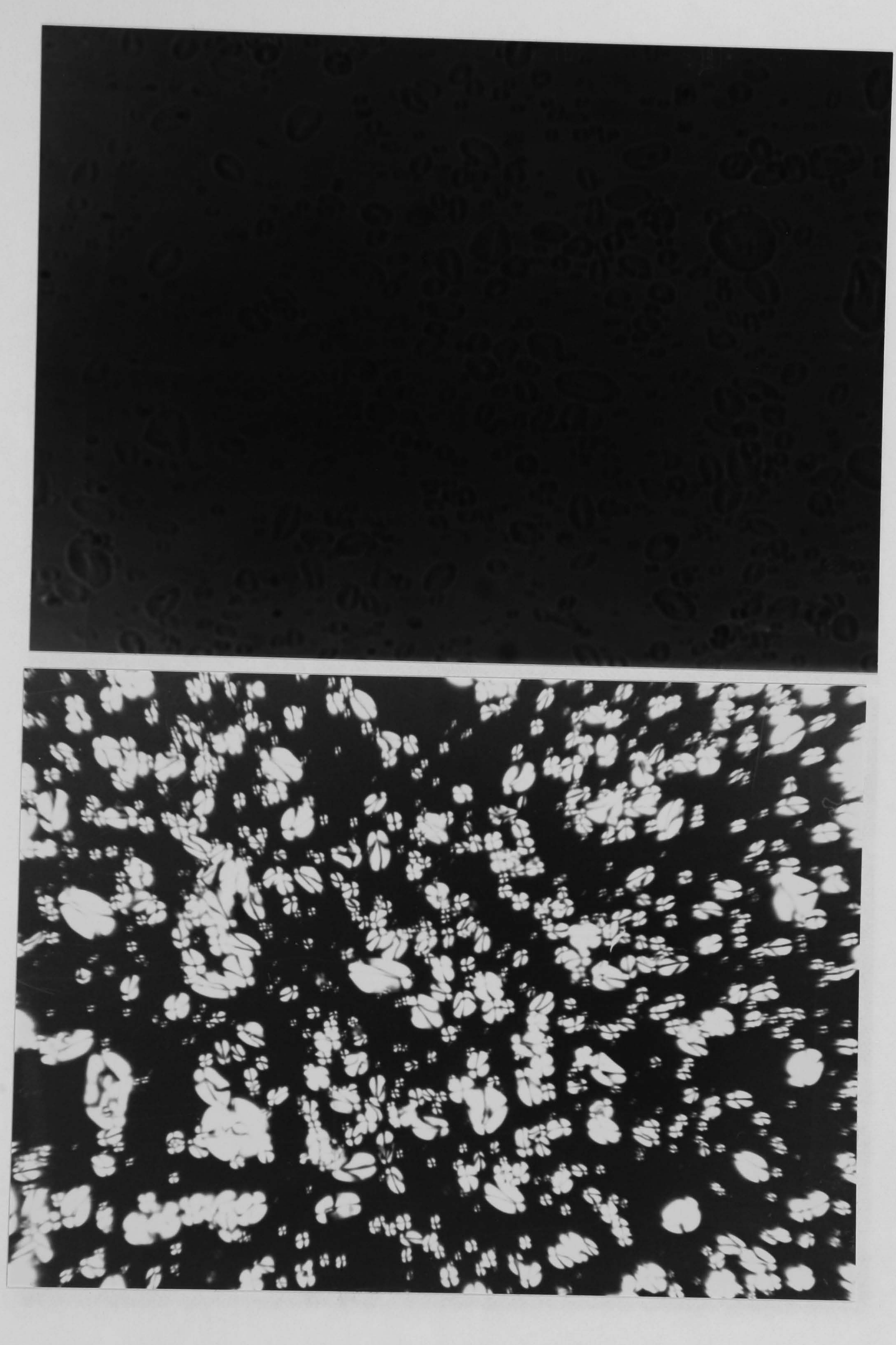

Plate (1) Optical photomicrograph of starch granules from commercial potato starch (x100).
(top): normal light (bottom): polarized light

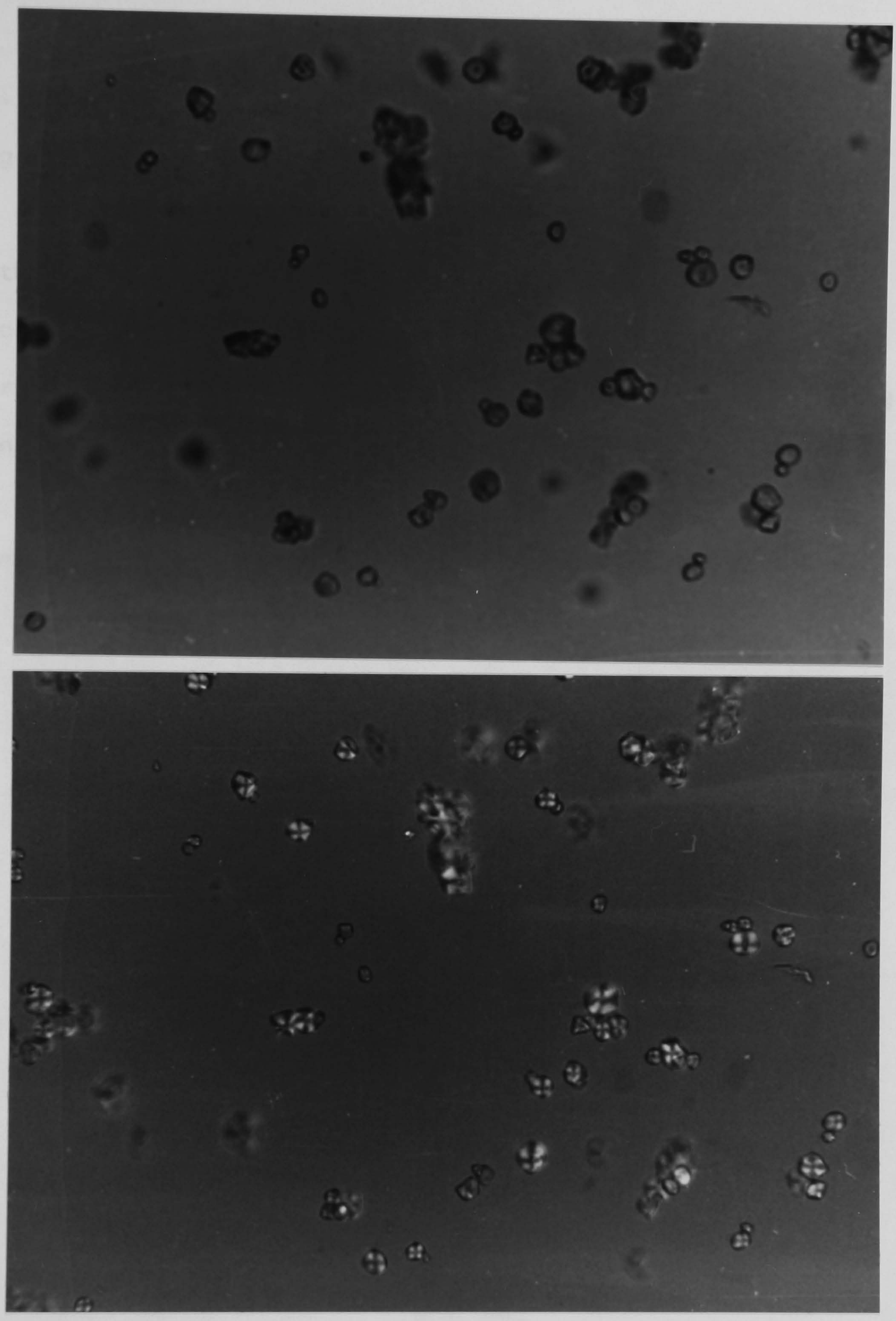

Plate (2) Optical photomicrograph of starch granules from commercial maize starch (x220)

(top): normal light (bottom): polarized light

4.1.11 Rice starch see plate 3

The granules of rice starch are small. Table (4.2) shows particle size distribution. The central hilum is difficult to observe and the hilum is visible only after treatment with dilute acid. Compound grains comprising several granules are sometimes observed owing either to inadequate steeping or to improper drying during manufacture, and have relatively low birefringence.

Table (4.2) particle size distribution of rice starch

Size class	Mean size	Number of particles
2.5 - 3.5	3	237
3.5 - 4.5	4	278
4.5 - 5.5	5	229
5.5 - 6.5	6	137
6.5 - 7.5	7	106

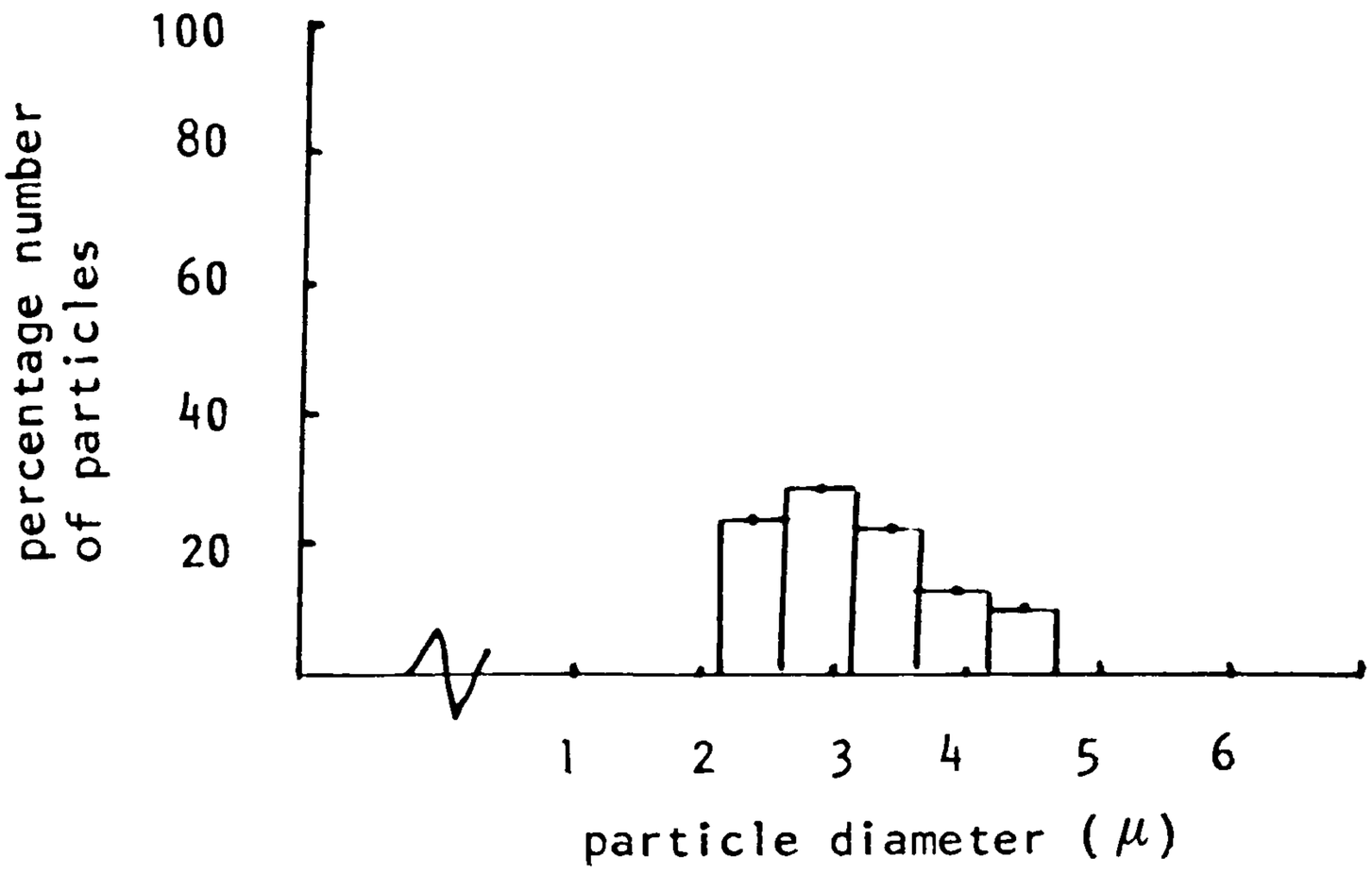

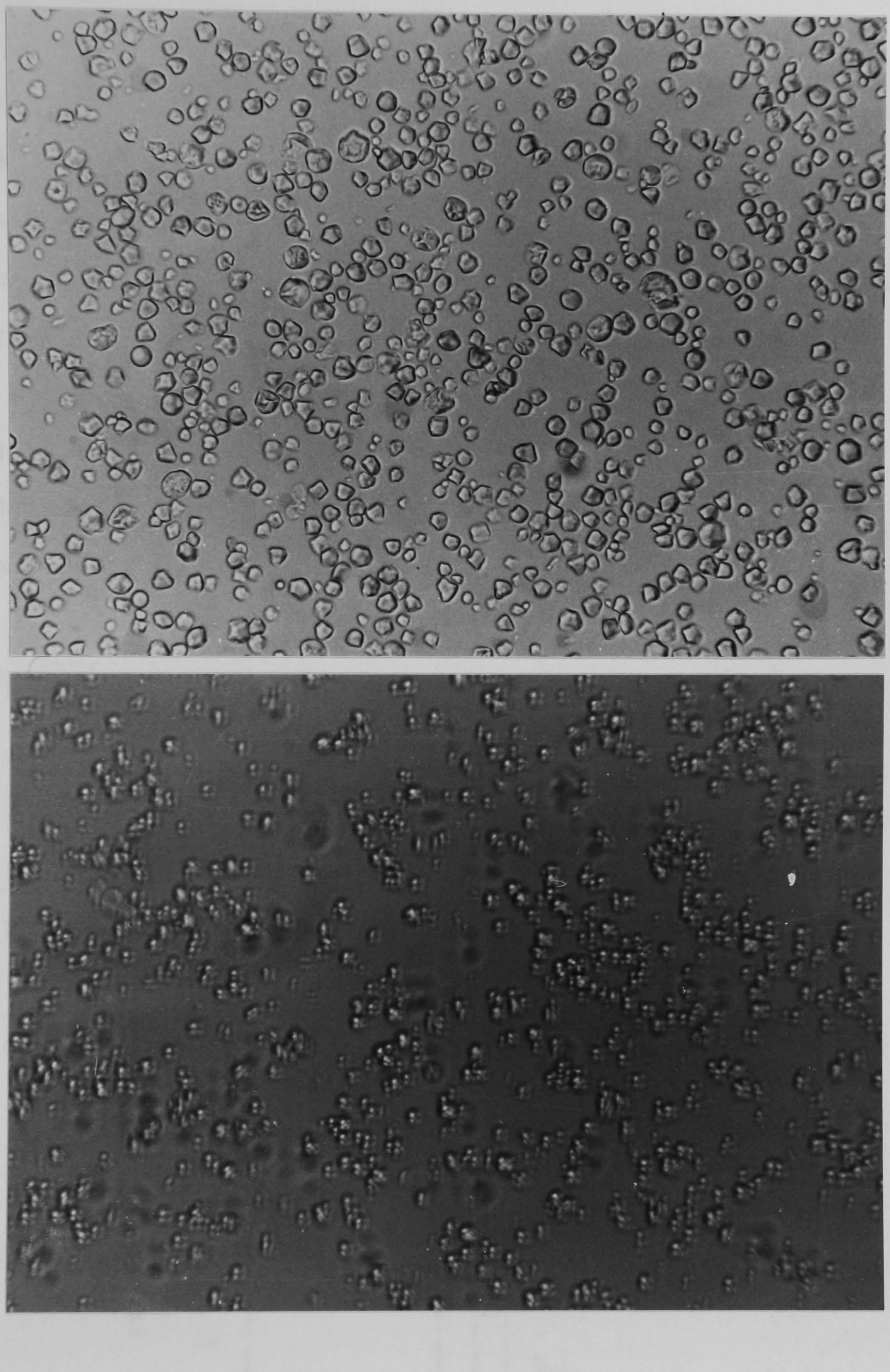

Plate (3) Optical photomicrograph of starch granules from rice starch (c420)

(top): normal light (bottom): polarized light

Mountant was glycerol/water (1:1)

4.1.12 Taro starches see plate (4-9)

Of the 112 Taro starches available, Bun-long, White Maoi, Lehua Maoli, and West Samoa, were observed under optical and S.E.M. microscope. The reason for choosing these starches is that they can be produced commercially.

4.1.13 Bun-long

Bun-long is the smallest among these four. Table (4.3) shows particle size distribution. The granules are mostly polygonal.

Table (4.3) particle size distribution of Bun-long

Size class	Mean size	Number of particles
1.5 - 2.5	2	521
2.5 - 3.5	3	223
3.5 - 4.5	4	101
4.5 - 5.5	5	60

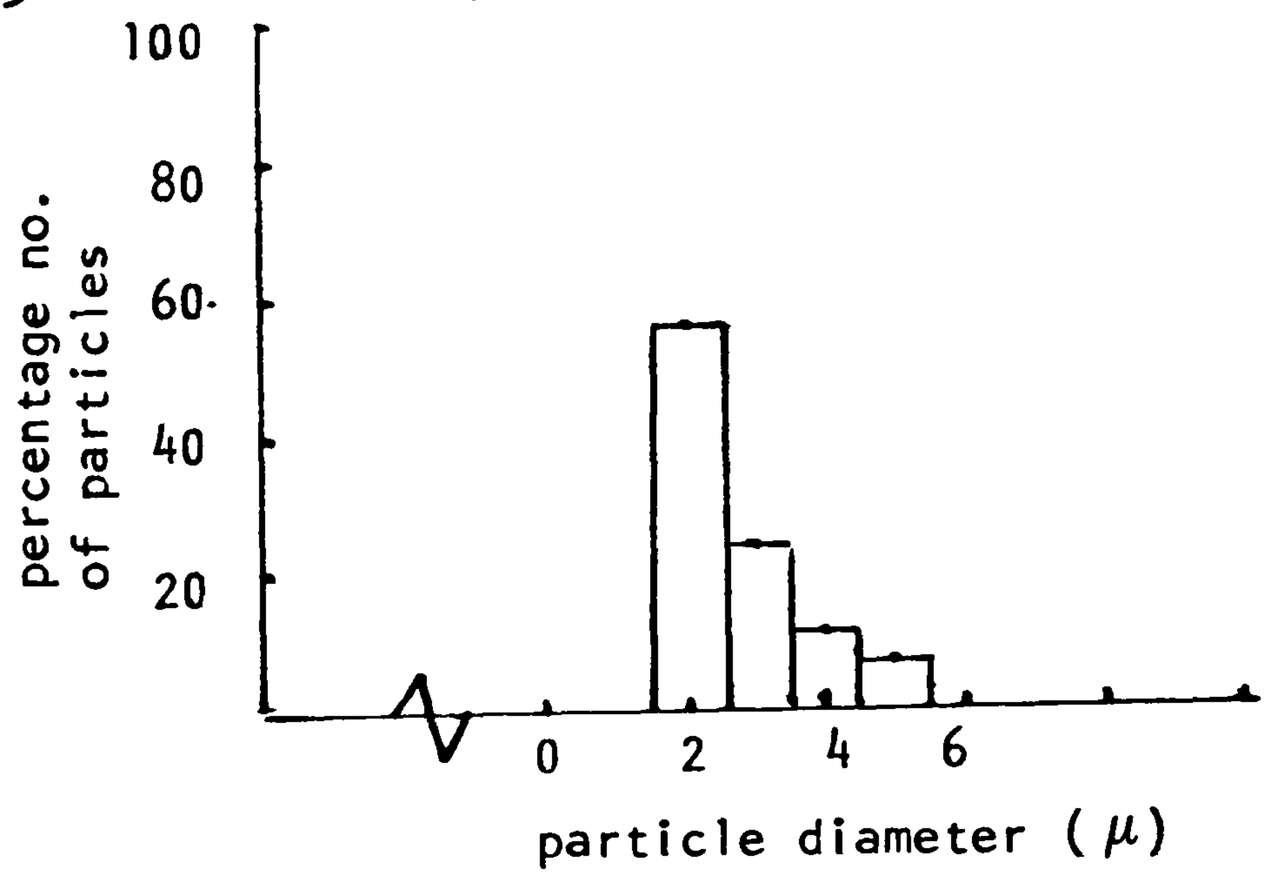

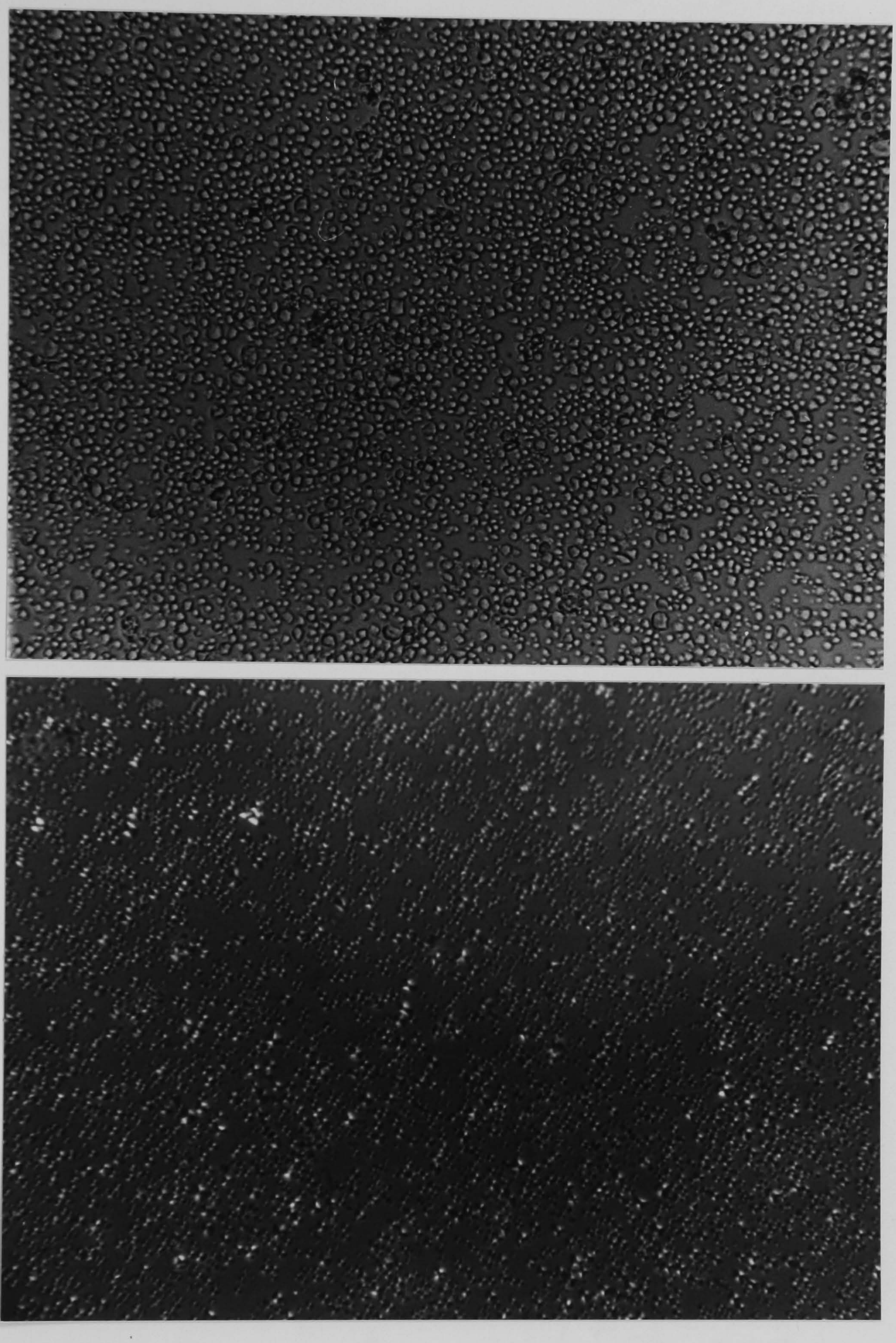

Plate (4) Optical photomicrograph of starch granules from Colocasia esculenta var, Bun Long x(420)

(top): normal light (bottom): polarized light

4.1.14 Lehua Maoli

The granules are very similar to those of Bun-long and have polygonal shape. Table (4.4) shows particle size distribution of Lehua Maoli.

Table (4.4) Particle size distribution of Lehua Maoli

Size class	Mean size	Number of particles
1.5 - 2.5	2	1058
2.5 - 3.5	3	503
3.5 - 4.5	4	231
4.5 - 5.5	5	99
5.5 - 6.5	6	55

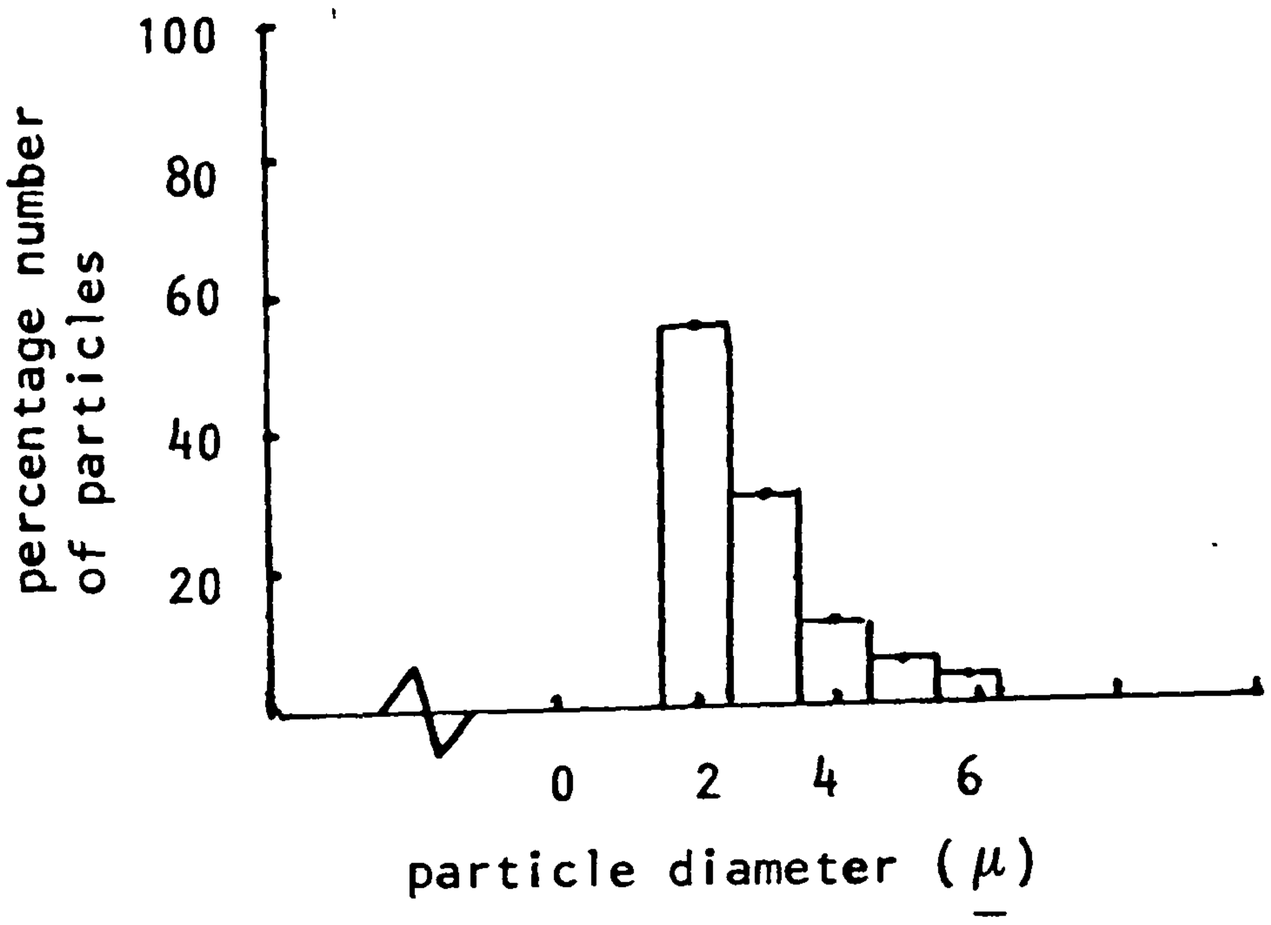

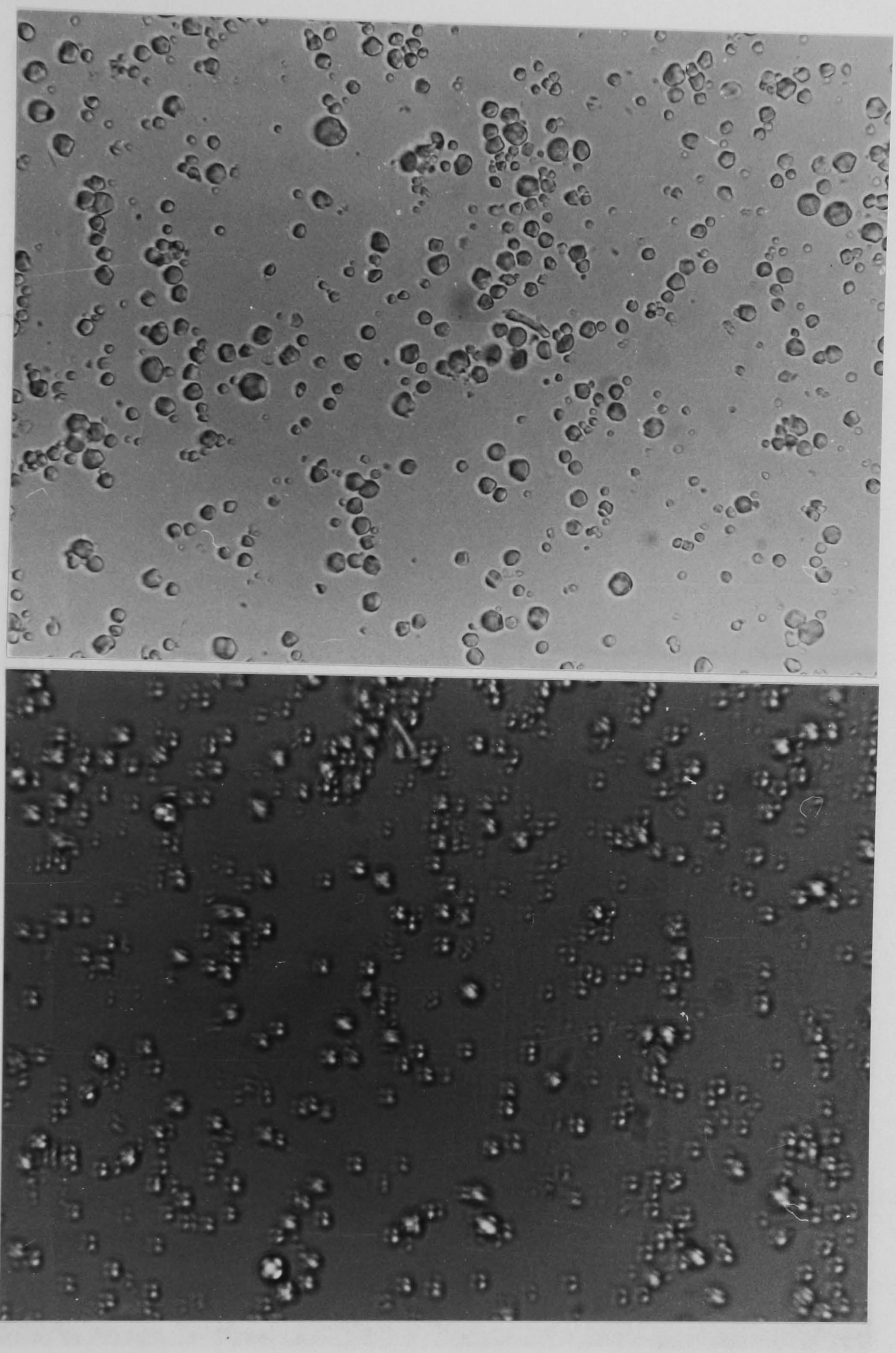

Plate (5) Optical photomicrograph of starch granules from un-named cultivar ex. W. Samoa (x420)
(top): normal light (bottom): polarized light

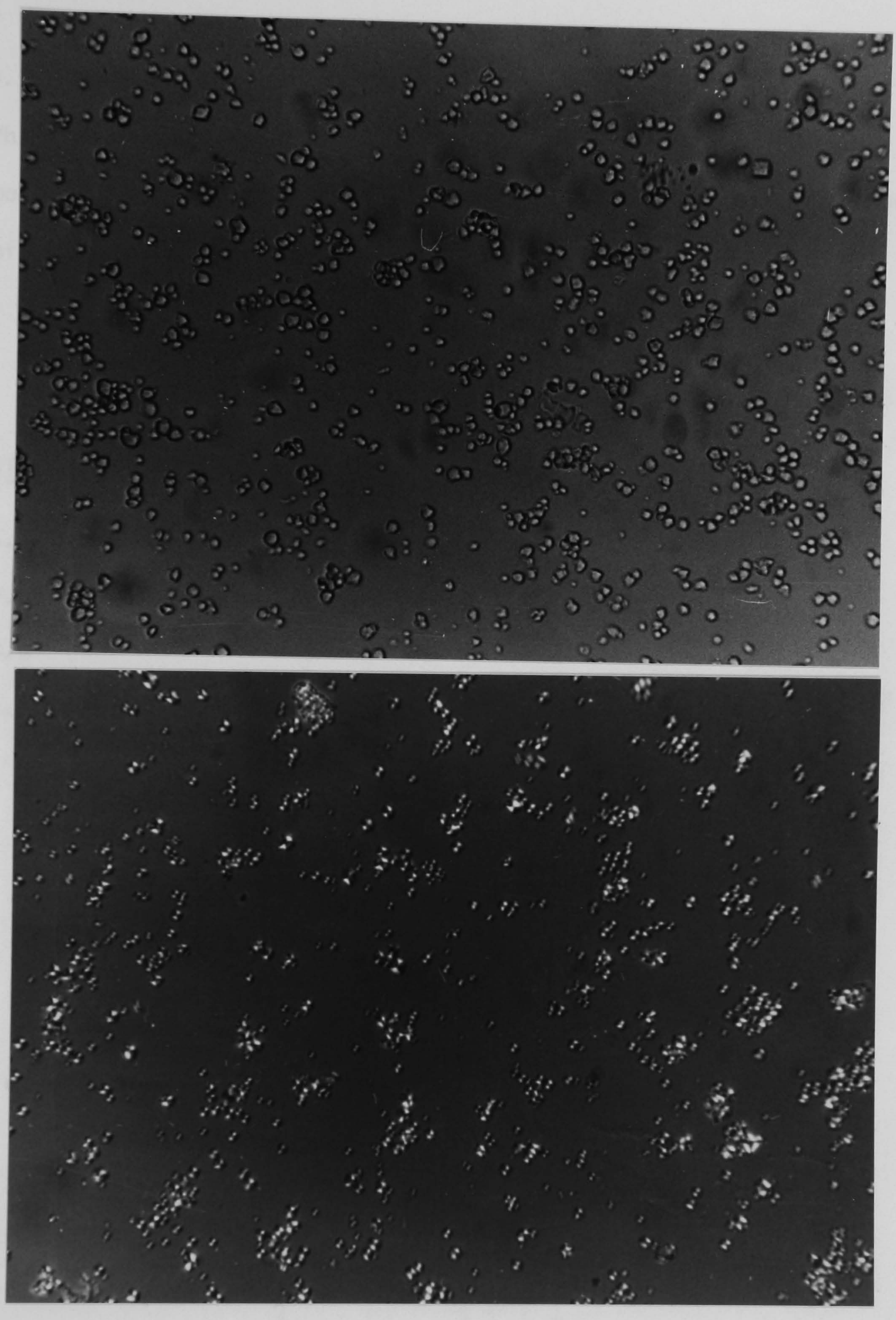

Plate (6) Optical photomicrograph of starch granules from Colocasia esculenta var. Lehua Moai (x470)

(top): normal light (bottom): polarized light

4.1.15 White Maoi

White Maoi is very similar to Lehua Maoli. The granules are mostly polygonal. Table (4.5) shows particle size distribution of White Maoi.

Table (4.5) particle size distribution of White Maoi

Size class	Mean size	Number of particles
1.5 - 2.5	2	527
2.5 - 3.5	3	309
3.5 - 4.5	4	183
4.5 - 5.5	5	107

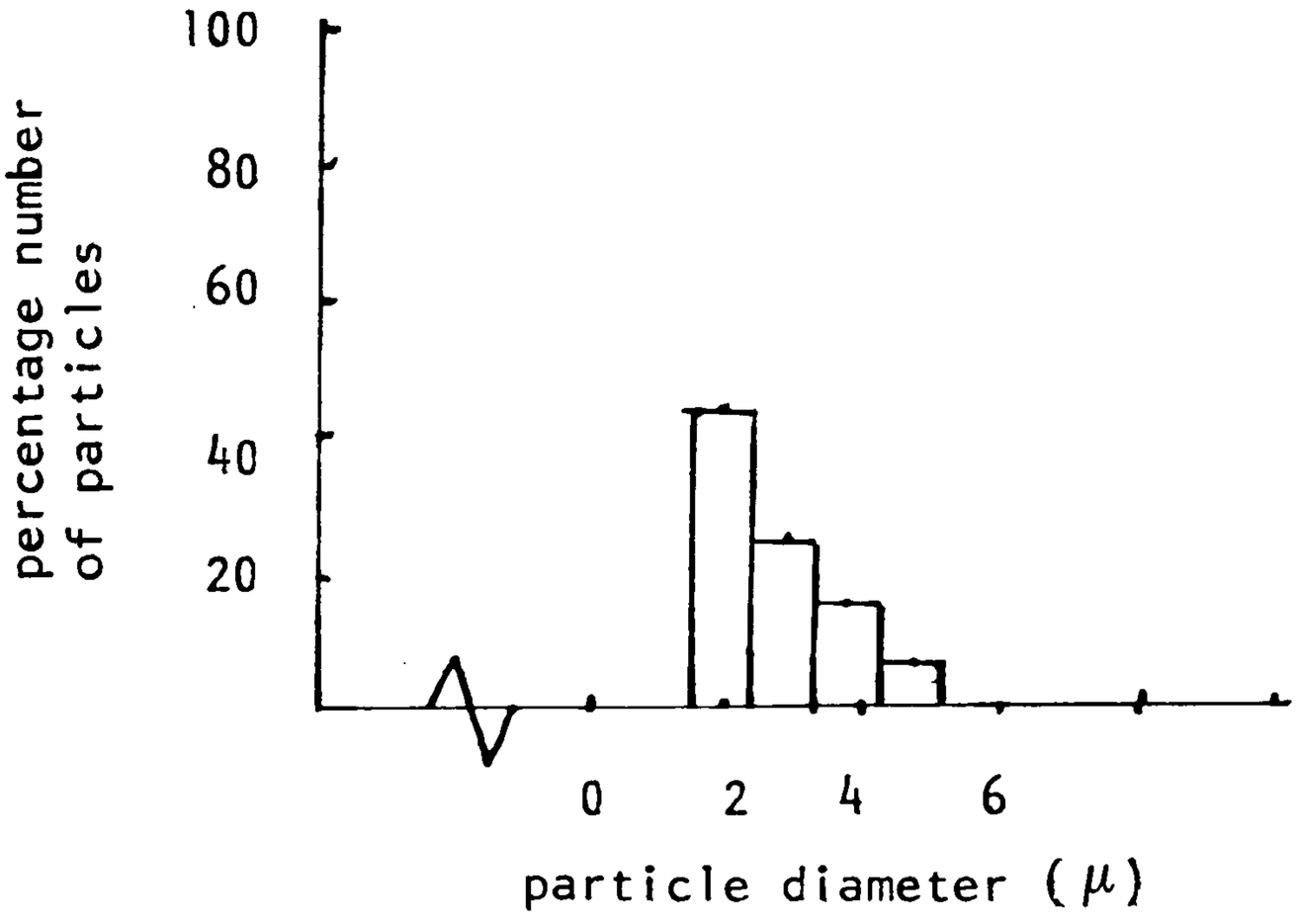

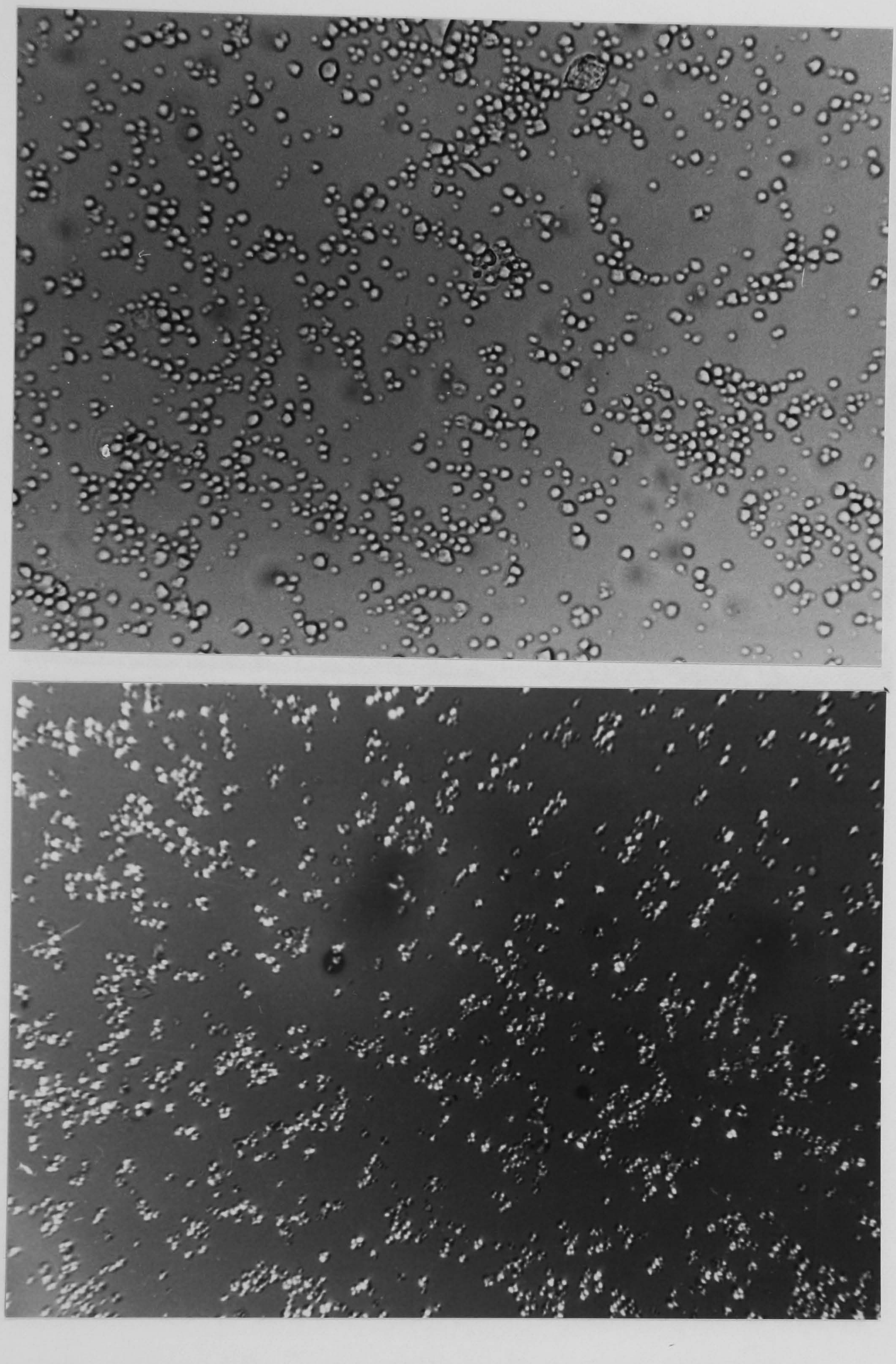

Plate (7) Optical photomicrograph of starch granules from Colocasia esculenta var. White Moi x(420)

(top): normal light (bottom): polarized light

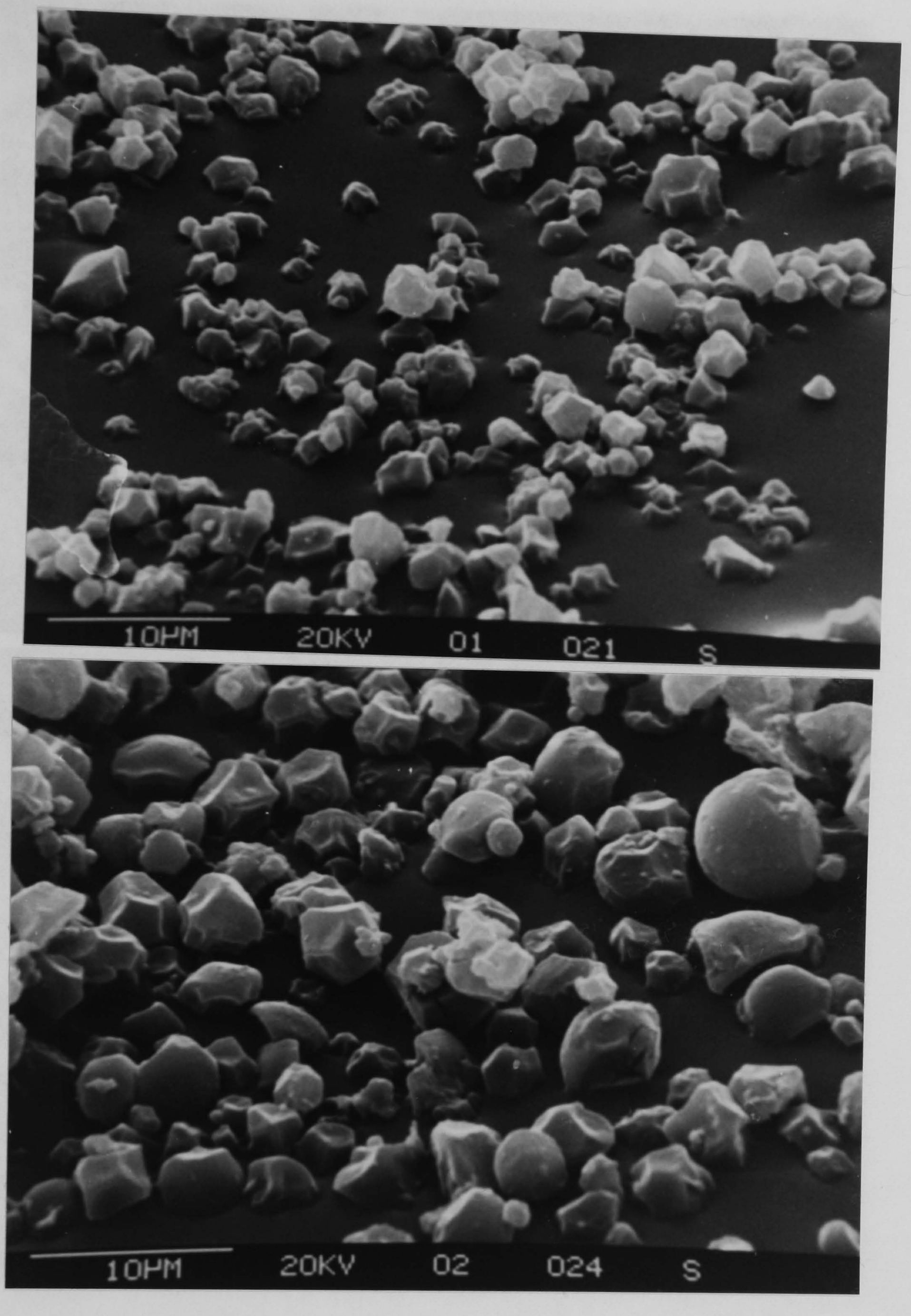

Plate (8) S.E.M. view of Colocasis esculenta var. Bun Long

starch granules (top)

Un-named cultivar ex W. Samoa (bottom)

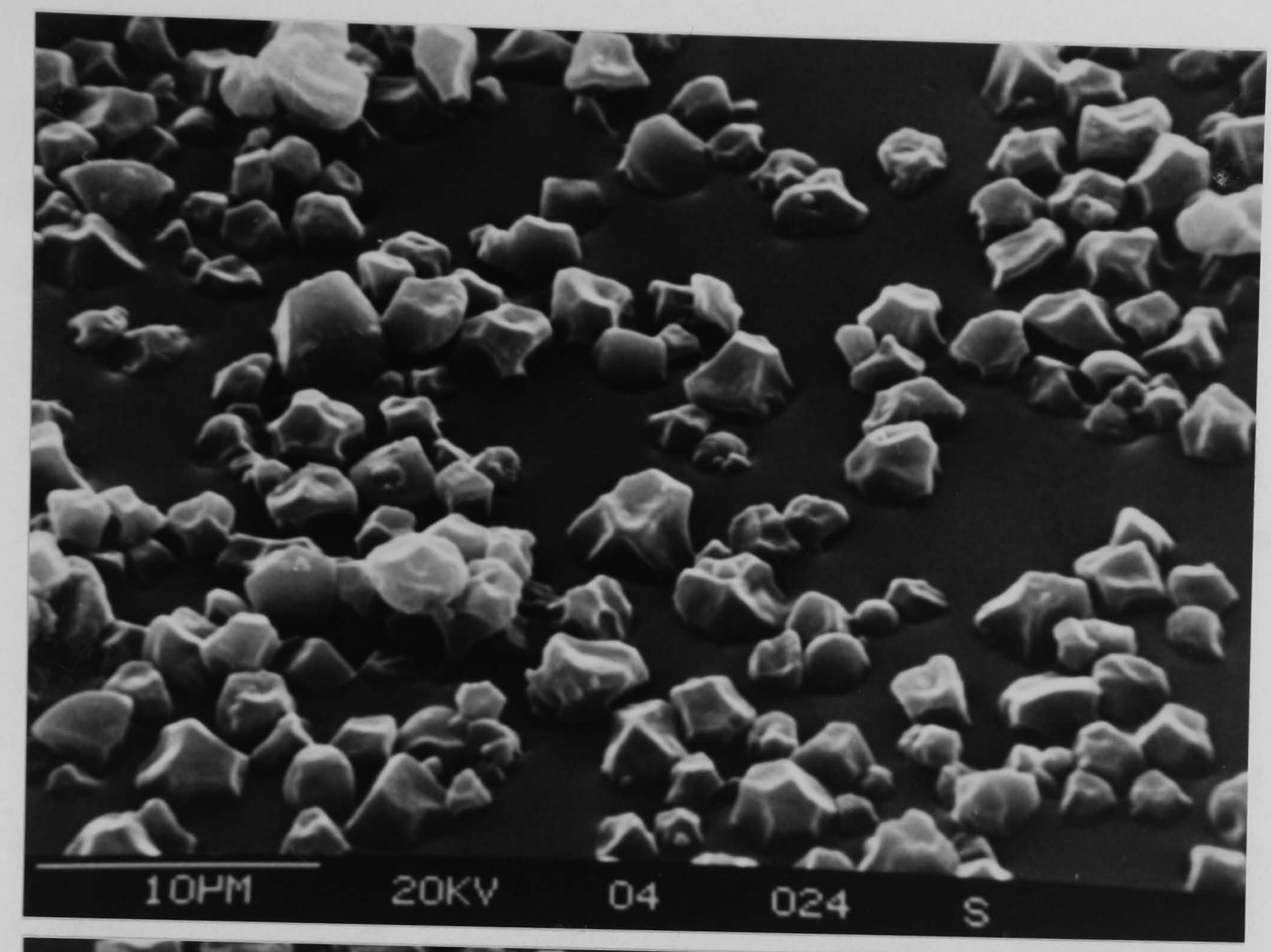

Plate (9) S.E.M. view of Colocasis esculenta var. Lehua Moai starch granules (top).

Colocasis esculenta var. White Moi (bottom)

Section 2

4.2.0 Starch sample analysis

Small-angle light-scattering can replace certain microscopic starch sample analysis methods. The scattering envelope from a sample of granules is the result of contributions from all the granules in the scattering beam whereas in the optical microscope the granules are viewed individually and in "optical sections" projected on to the plane of focus. Scattering analysis is therefore faster whenever collective properties of the granular collection are sought and when it can be demonstrated that this property, as derived from scattering analysis, is a reliable average measure. This has been shown for the average size of a granular sample (81).

The size of a spherulite obtained by scattering may be derived as shown on page (45) and it is often used as an approximation for the average size of spherulites in polymeric film (10,71,73,75).

A spherulite must be characterized optically as an anisotropic sphere. This is because the crystallites have preferred orientation along the spherically arranged fibrils and impart optical anisotropy to them. Realizing this, Stein and Rhodes developed the small-angle light-scattering theory based on a model of an anisotropic sphere

immersed in either an isotropic or an anisotropic medium. An accurate experimental test of the validity of their equations would have required availability of individual, separable spherulites that could be immersed in media of different refractive indices. Unfortunately separable spherulites were not available, and investigators had to use spherulitic polymer films and fibres as substitutes (10,114,115). A comprehensive examination of the SALS scattering from polymer films was published in 1965 (116). In this study Vv SALS patterns were obtained from both negative and positive spherulites of polypropylene, nylon 610, polyethylene terophalate) and nylon 66, as well as from spherulites of polyethylene and penton. The experimentally observed Vv SALS patterns were then compared with patterns calculated by using the Vv SALS equation of Stein and Rhodes. On the basis of these observations, Samuels (84) concluded from a theoretical study that patterns corresponding in form to these observed experimentally could be produced by changing the anisotropy of the spherulite surroundings while keeping the magnitude and sign of the spherulite birefringence constant, In other words, the spherulite surroundings had to be assumed anisotropic in order to fit the existing theoretical equations to the experimental patterns.

In a polymer film the spherulites are space filling. This means that the background environment of any spherulite in the film

would be the average polarizability of all the surrounding spherulites. Thus, if there is an equivalent number of spherulites in all directions, the average background polarizability is expected to be approximately isotropic. However, since polymer films are not ideal systems experimentally, it was possible to rationalize the theoretically required anisotropic character of the background on the basis that (1) the spherulites are not independent scatterers as required by the theory (2) internal strains might be produced during cooling to produce an anisotropic background, (3) multiple-scattering and interparticle interference effect might predominate, or (4) orientation of noncrystalline chains might occur during crystallization, a factor not considered in the theory. Though these rationalizations might explain the theoretically required background anisotropy a careful examination the magnitude of the background anisotropy that was theoretically required to produce acceptable patterns made this approach physically untenable. For in order to produce acceptable patterns from the theoretical Vv SALS equation, Samuels (84) assumed that the background anisotropy was greater than that of the spherulite. A re-evaluation of the Vv SALS equation was reported by Samuels (84), and the conclusion of the study was that there was an error in the sign in the original Vv SALS equation (2.1) which was corrected but unrecognized in a later rederivation of the theory (83)

Due to this error, the polarizability anisotropy term, which is listed in equation (2.1as $(\alpha_1 - \alpha_2)$ had the incorrect form of

($\alpha_2 - \alpha_1$). It should be noted that, as a consequence of the Samuels study, Stein et al (116) had re-examined their earlier derivation and agree with Samuels that there was an error in the original SALS equation.

Starch granules. The similarity between the shape of the theoretical Vv SALS patterns calculated by using the corrected equation, which contains the physically reasonable assumption of background isotropy, and the Vv SALS pattern observed experimentally from polymer films, suggests that the anisotropic sphere model can now be used to describe the observed small-angle light scattering from a spherulitic system. Still needed, however, to test the theory, is a quantitative characterization of the correspondence between theoretical and observed changes in the Vv SALS patterns. This required observation of the scattering from separable spherulites of known optical character, as the refractive index of the surrounding isotropic medium is changed. Fortunately, a second study by Borch and Marchessault (23) has shown that starch granules which grow as isolated spherulites, produce Hv SALS and Vv SALS patterns. Thus, by using starch granules immersed in media of known refractive index as an ideal scattering system, it is possible to test quantitatively the anisotropic sphere scattering theory.

Samuels (84) examination of a large number of starch systems (maize,

wheat, rice, tapioca, waxy rice, and potato) showed that rice starch yields the most uniform scattering patterns when immersed in silicone oil. The average diameter of the rice starch spherulites ranged from 3 to 6 micron. Their average refractive index was determined as 1.530; the radial refractive index was 1.533; the tangential refractive index was 1.527; and the average birefringence was 1×10^{-2}. The average refractive index of the medium was calculated from the measured average refractive index of both the silicone oil and the rice starch by using the Gladstone-Dale relation (117) as MAV = 1.5295

$$\frac{w(n_{AV} - 1)}{\rho} = \frac{w_p(n_p - 1)}{\rho_p} + \frac{w_s(n_s - 1)}{\rho_s}$$

where , w, w_p, w_s are the sample, polymer, and solvent weights and ρ, ρ_p, ρ_s are the sample, polymer, and solvent densities, V, V_p, V_s are the sample polymer, and solvent volume (e.g. $V = w/\rho$).. This relation can be rewritten as $n_{AV} = \beta n_p + (1 - \beta)n_s$ where $\beta = V_p/V$, is the volume fraction of polymer. The densities of the rice starch and silicone oil were taken as 1.50 g/cc and 1.156 g/cc respectively. By substituting the measured refractive index values of both the spherulite and the background for the appropriate polarizability terms in the theoretical Vv SALS equation, it was possible to compute theoretical Vv SALS patterns and compare them directly with experimental patterns produced under the same optical conditions.

Other experimental conditions required by the anisotropic sphere theory, is that the spherulites should be present at a concentration low enough for them to act as independent scatterers. At the same time, the concentration must be high enough to obtain maximum information from the Vv SALS pattern. Clearly, from the point of view of independence of spherulites, the lowest concentration of spherulites is preferred, while from an experimental point of view the highest concentration is desirable. Samuels (84) solved this problem experimentally. The time required for the most intense region of the Vv SALS pattern to reach a given intensity was plotted against the weight fraction of starch in the sample. The time taken to reach a given intensity would be expected to decrease as a direct function of the concentration of starch in the region where the spherulites act independently (i.e. direct addition of intensities). When the scatterers no longer act independently the intensity will not be proportional to the fraction of scatters and the rate of change of the time to a given intensity as a function of concentration will decrease. Different concentrations of starch immersed in three media were examined by Samuels. The media consisted of silicone oil mixtures of low (n_s = 1.5090), high (n_s = 1.5350), and intermediate (n_s = 1.5290) refractive indices. The data was plotted, the highest concentration of starch still present on the initial linear region of the plot (weight fraction of 0.20) was chosen as the concentration used to test the small light scattering theory.

Samuels (84) results demonstrate conclusively that the SALS theory of anisotropic spheres, as represented by equation (2.1) correctly represents the observed scattering from spherulites.

4.2.1 Hv scattering from starch granules.

The Hv scattering pattern was obtained when polarizer and analyser were crossed. The intensity of the scattered light was measured as explained in the experimental sections.

Using the granule-backing obtained by measurement in the optical microscope (R=1-1, 1.25,1.64,2.5,5), the scattering intensity predicted by equation (2,9) page 44 was calculated and is plotted in figures (2,3,4,5). The intensity for only one lobe was calculated since the pattern is fourfold symmetric.

The similarity with the experimentally recorded intensity is obvious in figures (2,3,4,5)and the conclusion is therefore drawn that the Stein-Rhodes equation (equation2.9) accurately predicts the scattering envelope of the starch granules. However, the direct application of equation (2.9) is always complicated by the presence of a distribution of particle sizes and the necessity of adopting average value of R.

For a collection of granules the complication that arises because larger granules contribute more to the scattering envelope is

illustrated in figures(4,5). The figures indicate that the value of R obtained experimentally is slightly higher than the theory predicts. However the analysis of the single-granule scattering envelope by Borch (34) demonstrates that the disagreement is not due to an inadequacy of the scattering theory (there is, however, a discrepancy due to anisotropy fluctuations, which depend upon the granule size).

Borch (34) in comparing the scattering envelopes of single granules and granular samples showed that for the single granule the envelopes appear much more "grainy" or non-homogeneous. The non homogeneity of the pattern is dependent on the number of scattering bodies in the beam, since it is not observable for a granular sample. It was proposed that this effect is due to an interaction between the incoming and the scattered beams (118,119) When several bodies are located in the scattering beams the effect is destroyed because of the random positions of the particles which partially destroy distinct phase relationships created by a single particle.

4.2.2 Influence of granule shape on the Hv scattering.

The Stein-Rhodes equation is derived for a perfect spherical body possessing a centre of symmetry, However, many starch varieties consist of granules of nonspherical shape due to the occurrence of preferred growth directions. Potato-starch samples which contain a significant number of such deformed granules produce

the fourfold symmetric cloverleaf like the much more spherical shaped granules of Taros.

4.2.3 Granule structure

Although the scattering technique represents a significant advance in analysis of the starch granules the information regarding the granular structure which may be derived from Hv scattering envelope is limited. The structure of the native granule is at present unknown and many conflicting hypotheses have been proposed in the past. Small-angle light-scattering techniques at least contributed towards eliminating some of these hypotheses even if it is unable to produce concrete evidence for a particular structure. However, Hv scattering proved to be quite good for measurement of average particle size.

Table (4.6) lists the average particle size of one hundred and twelve types of Taro starches calculated by the light-scattering technique.

Intensities obtained from experiments were analysed by computer to obtain a least-squares fit to an equation of the form $y = ax^n + bx^{n-1} + cx^{n-2}$ ... Since the curve was assumed to be roughly parabolic around the maximum so that the above equation could be reduced to the equation $y = ax^2 + bx + c$ (1). From equation (1) the maximum was calculated as part of the computer programme used in the above curve fitting analysis. This meant

that average spherulite radius could be obtained from the Hv SALS pattern. The distance from the centre of Hv SALS pattern to the intensity maximum of one of the lobes, in conjunction with the known sample to film distance, can be used to calculate the polar angle. Once the value of the polar angle, θmax, has been obtained, the value of Ro can be calculated by using the equation (2.10) see section (2.7.1).

$$Ro = 1.025\lambda/\pi \sin(\theta max/2)$$

Table (4.6)

No.	Horticultural varieties	Average particle diameter μ
1	A'Alii	3.37
2	Akado	4.96
3	Apowale	2.88
4	Apu	2.62
5	Apuwai	4.135
6	Aweu	3.8
7	Bun-Long	2.46
8	Burra	3.10
9	Eleele Makoko	3.02
10	Eleele Naidea	2.78
11	Elepaio	3.38
12	Fai Faasi 2	2.92
13	Fa Eleele	3.16
14	Fai Faasi 1	3.05
15	Falan	3.34
16	Haokea	2.77
17	Hapuu	3.98
18	Iliuaua	1.75
19	Kakaura Ula	3.20
20	Kai-Uliulu	3.379
21	Kai Ala	3.6
22	Kai Kea	2.64
23	Kala Lau	3.36
24	Kai KBS	3.368
25	Kaladao	3.04
26	KBS Bun-Long	3.73
27	Ketuangamea 2	2.82
28	Ketuangamea 1	2.97
29	Kuoho	2.69
30	Kumu Eleele	3.07
31	Lauloa Keokeo	3.04
32	Lauloa Dala	2.96

No.	Horticultural varieties	Average Particle diameter μ
33	Leo	3.44
34	Lehua Palaii	4.02
35	Lehua Keokeo	2.96
36	Lehua Maoli	2.72
37	Lauloa Palakea Keokeo	2.89
38	Lauloa Palakea Papa Mu	2.85
39	Lauloa Palakea Ula	3.06
40	Lauloa Palakea Eleele	2.8
41	Uahiapele	3.12
42	L73-369	2.42
43	L73-365	3.37
44	Manua Lanu Memata 2	3.5
45	Manua Lanu Mehata	3.52
46	Manakea Mata	5.1
47	Mana Okoa	4.8
48	Mana Eleele	3.45
49	Manini Opelu	3.72
50	Manini Toretore	3.08
51	Manini Kea	4.32
52	Manini Uliuli	3.35
53	Manini Owali	2.89
54	Manapiko	4.03
55	Matangi Fauna	3.64
56	Matale 1	3.97
57	Mana Uliuli	3.94
58	Mana Ulaula	5.1
59	Mana Lauloa	3.48
60	Mana Keokeo	3.18
61	Miyako	3.77
62	Moana	2.7
63	Naea	2.62
64	Nawao	3.1
65	Nihopuu	3.54
66	Niue Ulaula	3.463

No.	Horticultural varieties	Average particle diameter μ
67	No 330	3.71
68	No 7 - 398	4.27
69	No 8 - 398	3.497
70	No 7 - 391	2.746
71	No 365 - 1	3.28
72	No 3 - 396	3.37
73	OHE	2.67
74	OOPUKAI	3.095
75	Pang Daga	2.85
76	Papapueo	3.85
77	Papakoloa Koae	2.93
78	Paakai	3.07
79	Piko Uaua	2.87
80	Piko Elele	3.2
81	Piko Keokeo	3.13
82	Piko Keo	2.63
83	Piko Ulaula	2.83
84	Piko Lehua Apei	3.5
85	Piialii	3.089
86	Piialii Ula	2.84
87	Pilipino Short Stem	3.63
88	Pilipino Red	3.18
89	Pola Samoa	3.16
90	Pololu	4.19
91	Pula Mumu	3.99
92	Purple Manaluo	4.08
93	Red Moi	3.77
94	Sawa Pah Uetata	3.34
95	Sasa Uliuli	3.08
96	Sasa Paepae	2.92
97	Sasa Uliuli	3.95
98	Taro Hoia	2.92
99	Talo Manua	3.35

No.	Horticultural varieties	Average particle diameter μ
100	Tahitian	3.28
101	Teatea 2	3.11
102	Teatea 1	4.27
103	Tsurunoko	3.21
104	Ulaula Moano	3.58
105	Ulaula Poni	3.3
106	Ulaula Kumo	3.55
107	Vaevae Ula Uli	3.8
108	Wehiwa	2.93
109	West Samoa	3.82
110	White Moi	2.94
111	Yen 614	3.71
112	Yellow Benahi	3.38

Table (4.6) illustrates average particle sizes of 112 Taro varieties obtained from light scattering technique.

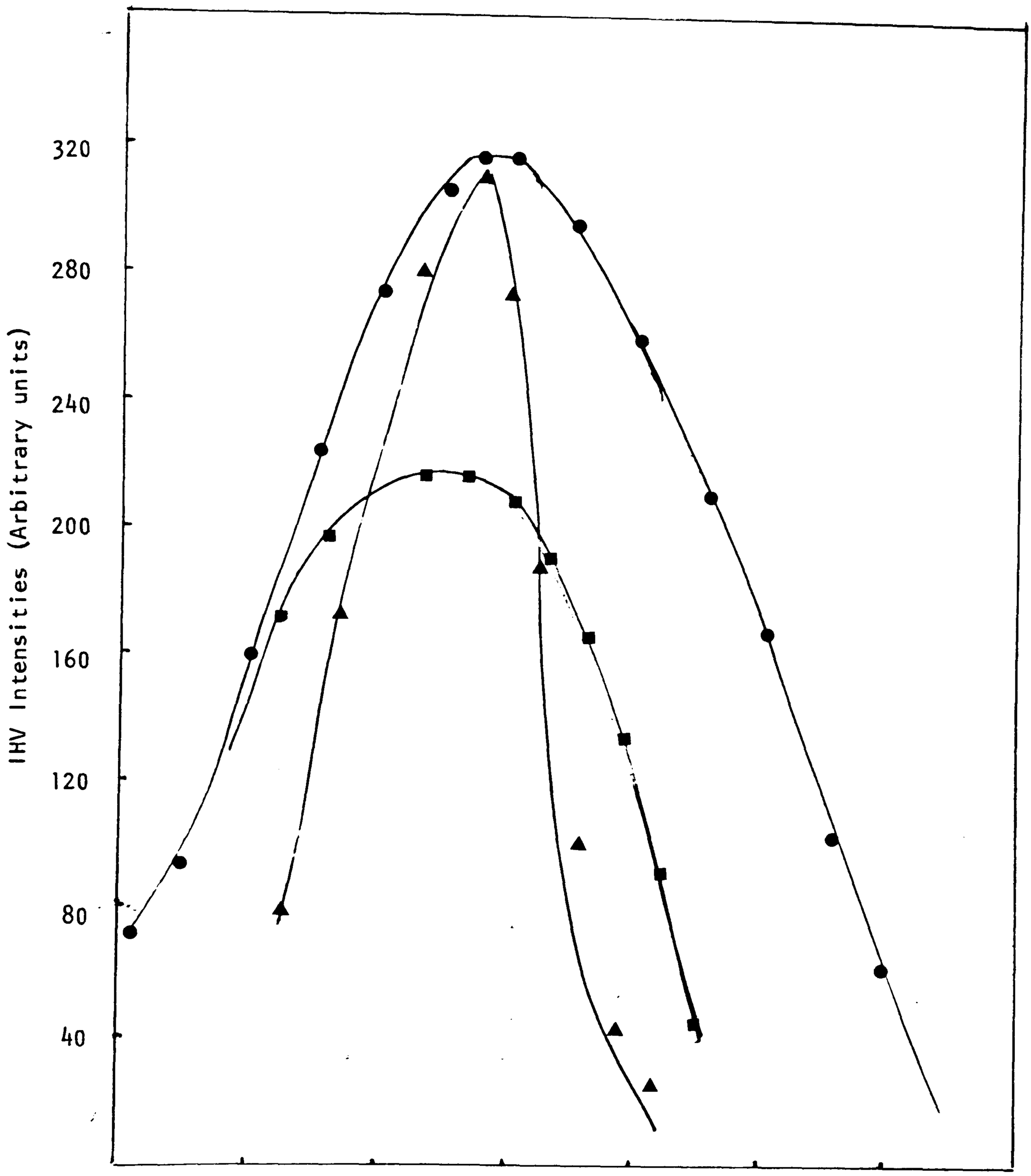

Fig (2) plot of radial angle vs. IHV (arbitrary units) for R = 1.1

theoretical ——●—— experimental ——▲——
curve derived from numerical fitting procedure ——■——

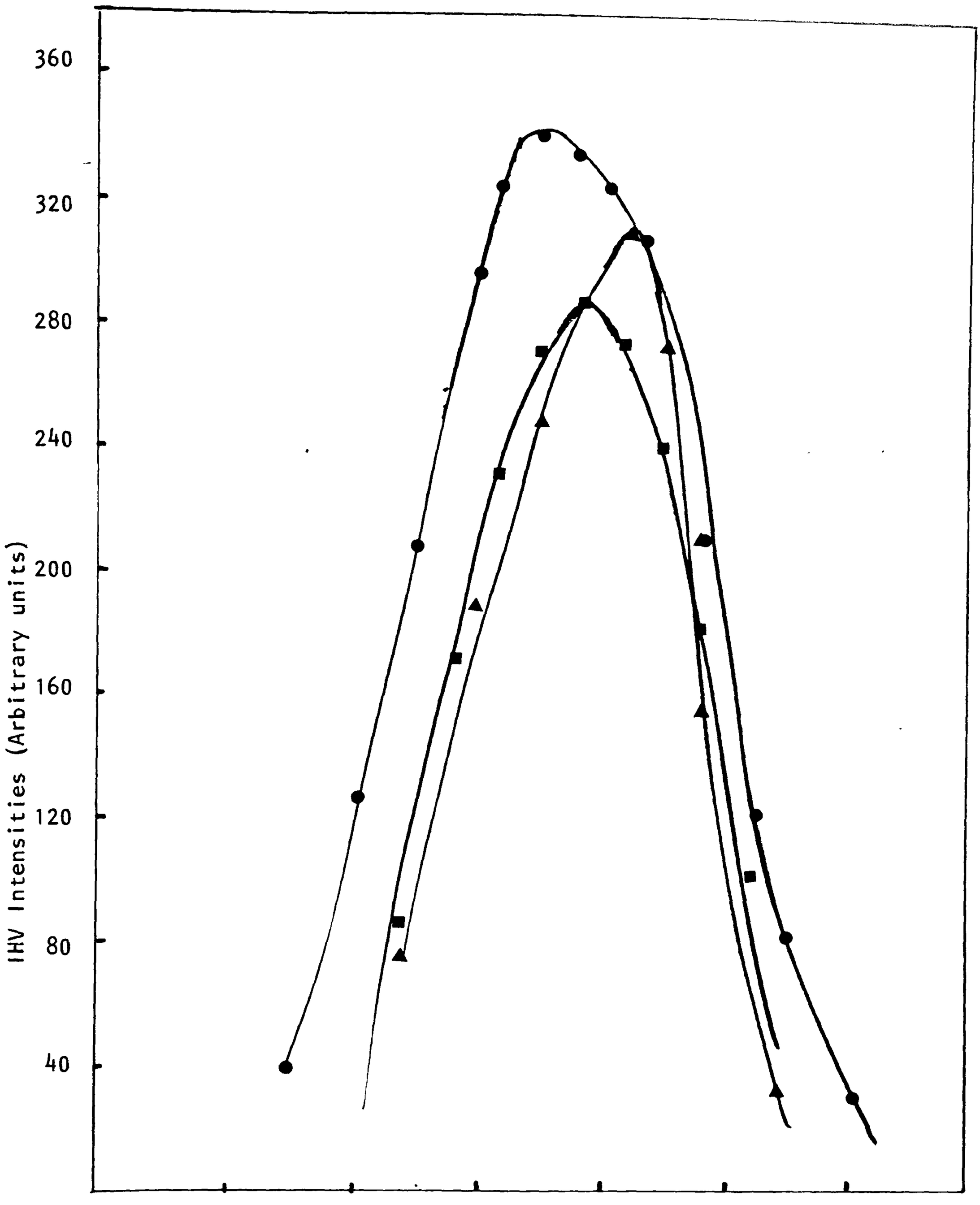

Fig (3) plot of radial angle vs. IHV (arbitrary units) for $R^{=}=1.64$

theoretical ——●——— experimental ——▲———
curve derived from numerical fitting procedure———■———

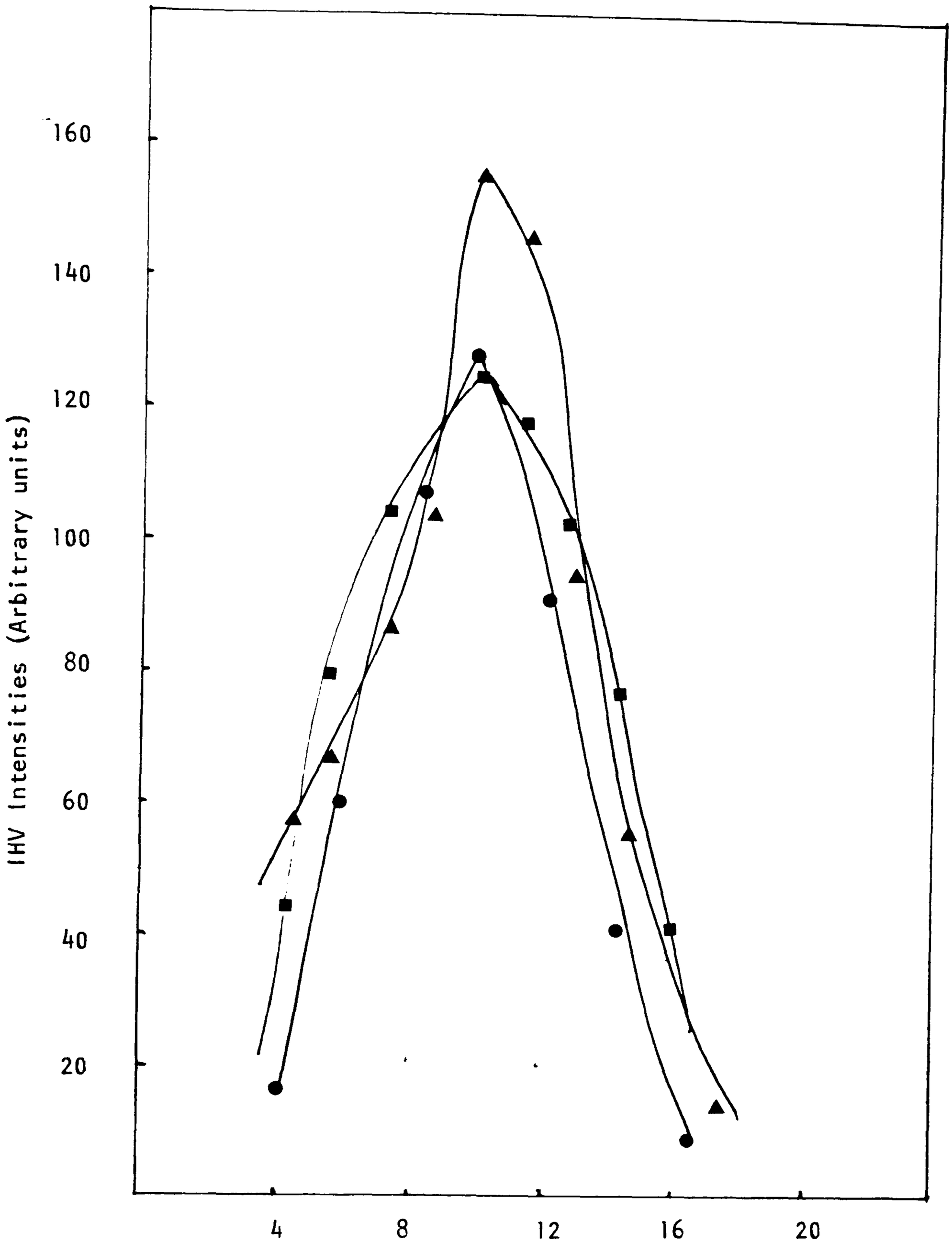

Fig (4) plot of radial angle vs. IHV (arbitrary units) for R =2.5

theoretical— —●— — experimental— — ▲— — —

curve derived from numerical fitting procedure— —■— — —

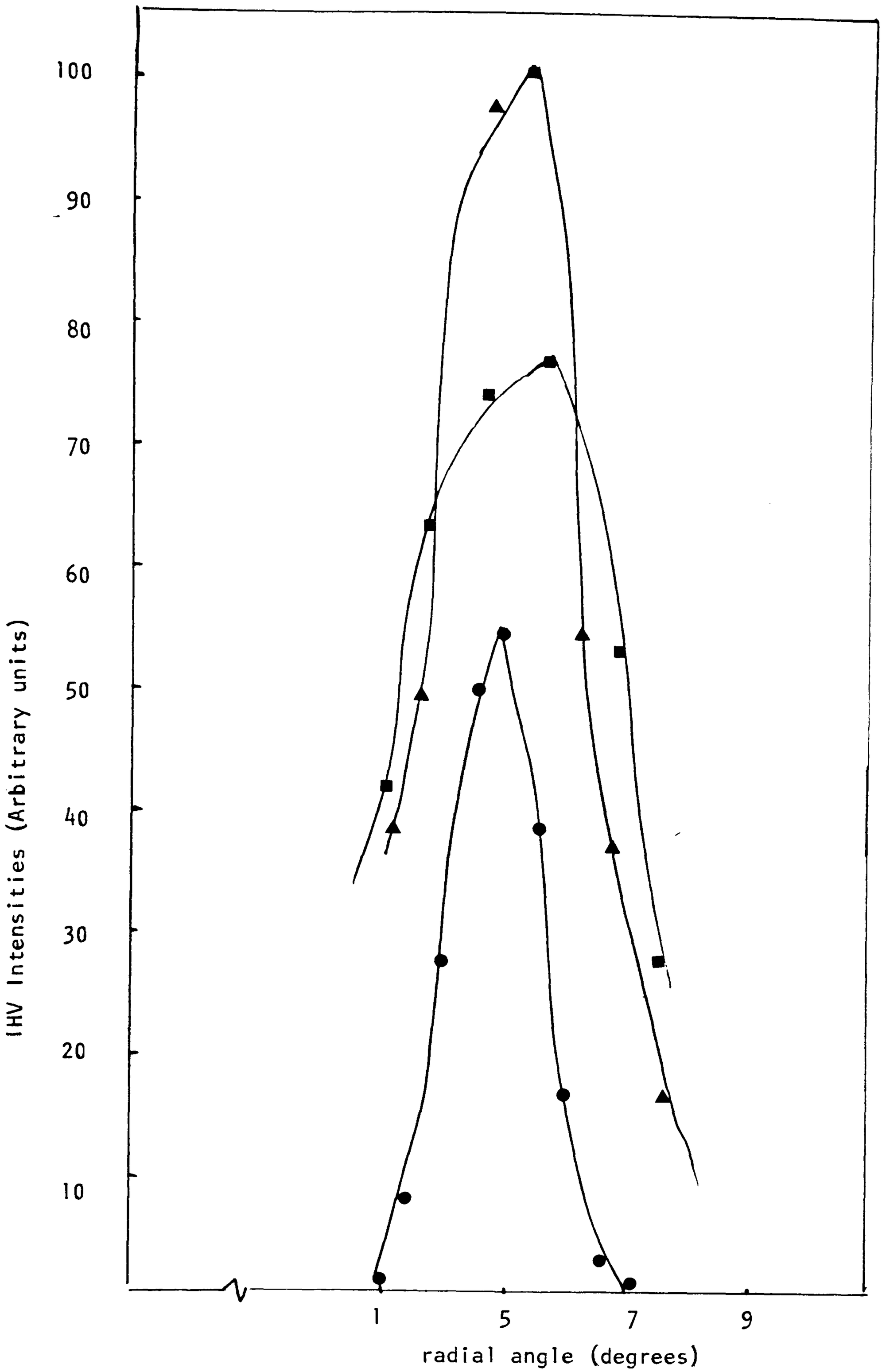

Fig (5) plot of radial angle vs. IHV (arbitrary units) for R= 5

theoretical — —●— — — — experimental— —▲— — —
curve derived from numerical fitting procedure— —■— — —

Section 3

4.3.0 Particulate-filled polymers

4.3.1 Introduction to the various types of composite systems.

A composite material may be defined as a material made up of two or more components and consisting of two or more phases. Such material must be heterogeneous at least on a microscopic scale. Composite materials may be divided into three general classes: 1. particulate-filled materials consisting of a continuous matrix phase and discontinuous filler phase made up of discrete particles. 2. fibre-filled composite 3. skeletal or interpenetrating network composite consisting of two continuous phases.

Many commercial polymeric materials are composites, although their composite nature may not be obvious. Examples include polyblends and ABS materials, foams, filled polyvinylchloride formulations used in such applications as floor tile and wire coating, filled rubber, thermosetting resins containing a great variety of fillers, and glass fibre-filled plastics. There are many reasons for using composite materials instead of the simpler homogeneous polymers. Some of these reasons are:

1. Increased stiffness, strength, and dimensional stability
2. Increased toughness or impact strength
3. Increased heat-distortion temperature
4. Increased mechanical damping.

5. Reduced permeability to gases and liquids

6. Modified electrical properties

7. Reduced cost.

Not all of these desirable features are to be found in any single composite. The advantages that composite materials have to offer must be balanced against their undesirable properties, which can include complex and difficult-to-predict rheological behaviour and the need for different fabrication techniques as well as a reduction in some physical and mechanical properties.

The properties of composite materials are determined by the properties of the components by the shape of the filler phase, by the morphology of the system, and by the nature of the interface between the phases. Thus, a great variety of properties can be obtained with composites. By alteration of the morphological or interface properties an important property of the interface which can greatly affect mechanical behaviour is the strength of the adhesive bond between the phases.

In order to improve the adhesion it is necessary to know all the interactions at the interphase. Types of interaction between filler and polymer can be divided into four groups depending on the type of filler and its interaction with the matrix .

1. The simple physical inclusion of filler particles or their agglomerates in a non polar polymer matrix causes weakening of the

system by acting is a diluent.

2. Physical inclusion of filler particles with a simultaneous wetting of the particle surface by the polymer causes some stiffening of the system, i.e. it increases the Young's modulus and decreases the ultimate elongation.

3. Strong physical adhesion of the polymer to the surface of the filler particle which causes a considerable reinforcement of the system.

4. Chemical bonding of the matrix to the filler particles.

When selecting a filler for a given polymer types 3 or 4 interactions are obviously preferred since the strongly-bonded systems have relatively good mechanical properties. Basically there are four ways to improve the adhesion between polymer and filler:

a. to increase the total adhesion forces by reducing the size of filler particles and/or the treating of the surfaces to increase the surface area of each particle (increasing roughness or porosity).

b. increasing the adhesion forces by improving the wetting of the filler particles by the polymer matrix (type 2 or 3 interaction).

This may be achieved by the introduction of the third component which adheres well to the filler and to the polymer. If each particle of the filler is surrounded by a thin layer of this third component, it acts as a kind of adhesive bond between filler and polymer.

Many and various types of fillers are used for the filling of the plastic materials (120,121). In the case of polyolefines the following fillers have been used: talc (122), asbestos (123,124), Kaolin (125,126), metal powders, (127,128), metal oxides (129), mica (130,131), aluminium hydroxide (132), carbon black (133), silica (134), glass (in the form of spheres or fibres (135,136), cellulose (137), straw with wood chips, wood sawdust and gypsum (138), lignin (139), wood flour (140), peanut shells (141). Usually one finds an increase of the Young's modulus, or an increase of hardness but a decrease of tensile strength and an increase in the brittleness of a composite. Such properties would seem likely to result from the adhesive bond formed at the interface. The interaction at the interface can be changed in various ways with an improvement in physical properties. In the case of polyolefines the covering of the filler particles with carefully chosen materials is often effective.

Organo-titanate layers

Organo-titanate layers are used for most fillers to polyolefines (142,143). If applied in amounts ranging from 0.5% to 3% they cause an increase of adhesion between polyolefine and filler followed by an increase of the elastic modulus and a decrease of the impact strength and the ultimate elongation (144).

Silane layers are used as coating agents for the mineral fillers, polymers and Organosilanes (145-147). The silanes have two

functional groups R^1 and OR, usually R^1 is a reactive organic group such as an amine $H_2N-CH_2-CH_2-CH_2-(OC_2H_5)3$, vinyl CH_2 - $CHSi-(OCH_3)_3$, or methyacrylate.

CH_3
|
CH_2 - C - $COO-CH_2-CH_2-CH_2-Si(OCH_3)_3$ group bonded to the silicon atom via a short aliphatic chain. OR group is hydrolysing alcoholate groups while R^1 groups react with the polymer matrix R^1 and OR groups are chosen to suit each particular filler and polymer.

Organic layers

Stearic acid and stearates of calcium, sodium and barime and their compositions are the popular modifiers. These compounds function as coupling agents between the organic and mineral phase. They also show a lubricating property in processing.

Methods for improving the strength of the composite by modifying starch fillers in order to obtain adhesion between the filler and its matrix was reported by Sharafi (113). The use of various silane derivated starch brought about some useful improvements in the strength of polystyrene composite reported by Sharafi. Linero studied the effect of adhesion further in order to find the optimal conditions for the surface treatment of starch for a variety of uses.

An attempt was made to increase adhesion of starch and polymer by acid treatment of rice starch. It is believed that acid attacks

the amorphous part of starch, and causes roughness on the surface of the granule.

4.3.2 Mechanical properties of HDPE containing various starches with different particle sizes have been measured. (see section 3.10.0). Table (4.7) shows these properties.

4.3.3 Strength and stress-strain behaviour of starch-filled HDPE.

Although particle-size alone has little, if any, effect on the modulus of a composite in the absence of agglomeration, particle size has a large effect on tensile strength, fig (6). Tensile strength increases as particle size decreases. The reason for this is not entirely clear, but the increase in interfacial area per unit volume of filler as particle size decreases must be an important factor (148). A second factor may also be important, and that is the creation of voids in the polymer, the larger the particle the bigger the voids, as is shown schematically in (fig 7 a,b).

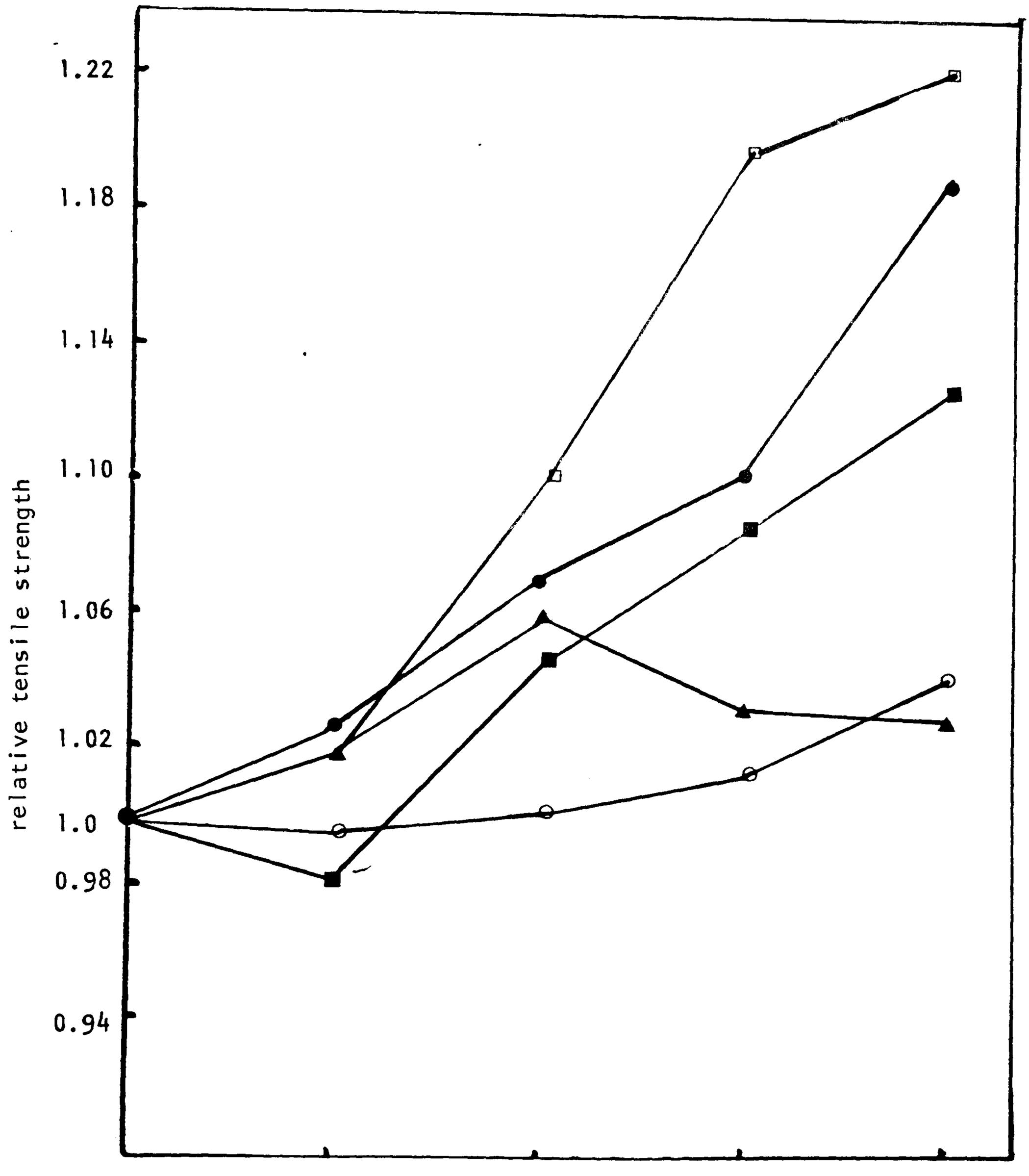

Fig (6) Effect of various starches on tensile strength of HDPE

Symbols used are as given in table (4.7)

Table (4.7) The effect of different particle size starches on the mechanical properties of HDPE

Filler	Mean particle diameter	% concentration of starch W/W	% elongation at break	Young's Modulus from tensile test $MNmm^{-2} \times 10^7$	Young's Modulus from flexural test $MNmm^{-2} \times 10^7$	Yield strength $MNmm^{-2} \times 10^7$	Tensile strength $MNmm^{-2} \times 10^7$	Symbols used in
Hydrophobic		none	69.1	5.764	5.343	2.468	2.055	
Lehua		5	59.28	5.583	6.959	2.304	2.106	
Maoli	2.8	10	45.68	6.333	6.957	2.319	2.211	●
(taro)		15	41.68	7.408	7.546	2.35	2.286	
		20	34.8	8.188	8.31	2.483	2.4653	
Hydrophobic		none	69.1	5.764	5.343	2.468	2.055	
Rice		5	65.43	6.695	7.27	2.332	2.001	
Starch	5	10	48.876	6.006	7.76	2.3454	2.1706	■
		15	47.37	7.055	8.56	2.365	2.341	
		20	37.595	7.90	8.89	2.393	2.341	
Acid		none	69.1	5.764	5.343	2.468	2.055	
treated		5	61.37	5.25	6.79	2.334	2.1006	
Rice	5	10	49.55	6.41	7.436	2.42	2.2706	□
Starch		15	32.22	7.31	8.03	2.468	2.4715	
		20	28.34	7.83	8.77	2.532	2.4916	

Filler	Mean particle diameter	% concentration of starch W/W	% elongation at break	Young's Modulus from tensile test $MNmm^{-2} \times 10^{-7}$	Young's strength from flexural test $MNmm^{-2} \times 10^{-7}$	Yield strength $MNmm^{-2} \times 10^{-7}$	Tensile strength $MNmm^{-2} \times 10^{-7}$	Symbols used in
Hydrophobic Maize Starch	11	none	69.1	5.764	5.343	2.468	2.055	
		5	61.5	6.051	6.945	2.291	2.051	
		10	55.996	6.869	7.563	2.249	2.055	○
		15	54.327	6.942	8.299	2.178	2.0929	
		20	42.394	7.16	8.8	2.142	2.156	
Hydrophobic Potato	50	none	69.1	5.764	5.343	2.468	2.055	
		5	57.5	5.99	6.8	2.317	2.106	
		10	58.56	5.7655	7.43	2.399	2.1866	▲
		15	55.56	6.079	7.7	2.228	2.1313	
		20	47.19	7.53	8.35	2.124	2.1069	

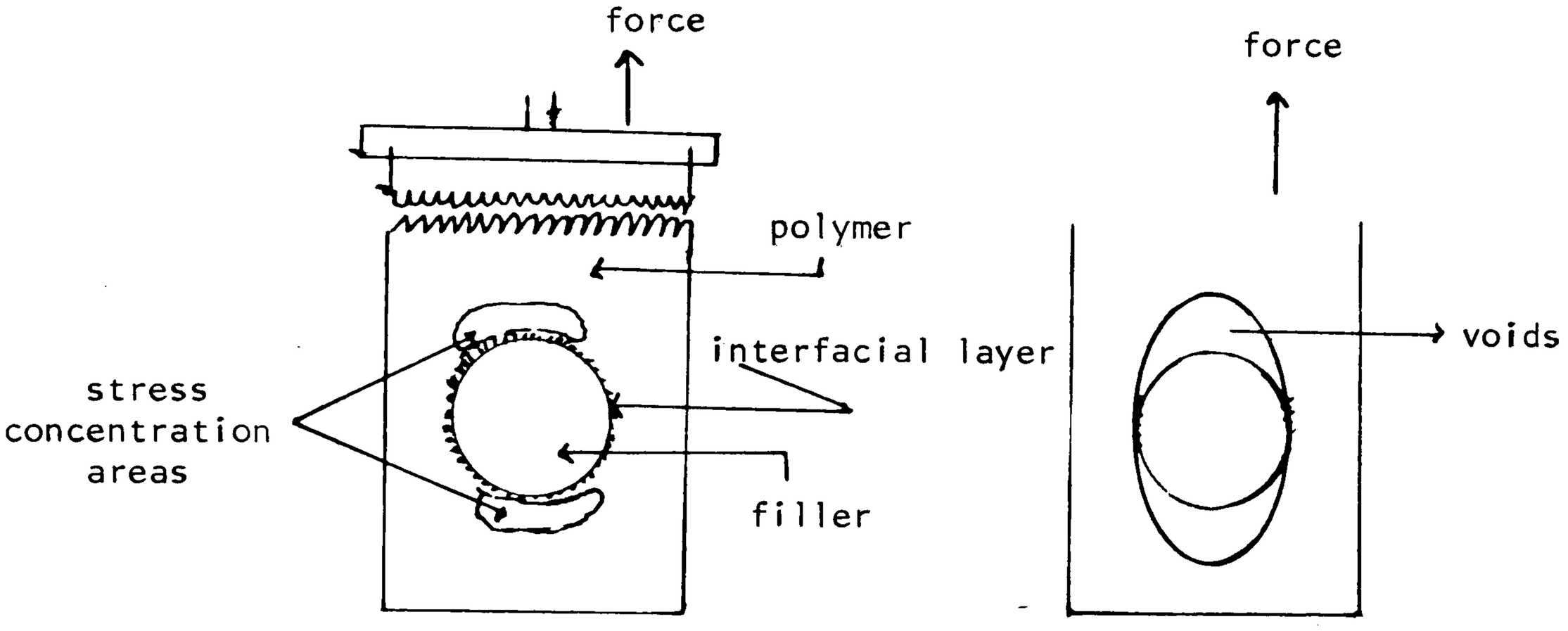

7(a) 7(b)

Figure (7a) shows the state of the polymer in the neighbourhood of a starch particle before the tensile stress is applied. The dotted lines depict the region of polymer which will experience the maximum stress concentration once the tensile stress is applied. Fig (7)b shows that voids may form at these regions of high stress concentration along the direction of stress.

Particle agglomeration tends to reduce the strength of a filled material even though the agglomerate may be strong enough to increase the initial modulus. Agglomerates are weak points in the material and break fairly easily when a stress is applied to them. A broken agglomerate particle then behaves as a strong stress concentrator. In addition, since agglomerates are larger than the primary filler particles, they produce weaker materials than composites containing the dispersed particles.

We have always attempted to use the roll milling process to eliminate starch agglomeration as is shown in plate (27,28) section (4.4.4). Thus, a given composite can have a range of stress-strain properties depending upon the intensity and time of mixing and upon the kind of surface treatment given the filler particles for at least two reasons: 1. the mixing may break up agglomerates and change the degree of dispersion 2. the mixing may change the amount of air entrapped in the composite.

4.3.4 Yield strength.

The presence of fillers often causes the appearance of a yield point in the stress-strain curves of elastomers and ductile polymers. The yielding phenomenon might be due to a crazing effect or to a dewetting effect in which the adhesion between the filler and matrix phases is destroyed so that there is a dramatic decrease in the modulus of the material. At the same time, voids are created and the specimen undergoes dilation (149-151) Although pure LDPE and HDPE possess an intrinsic yield point fillers in these materials may cause changes in yield strength possibly by analogous mechanisms.

The increase in yield strength in LDPE at high concentrations of starch filler was observed by Linero (9).

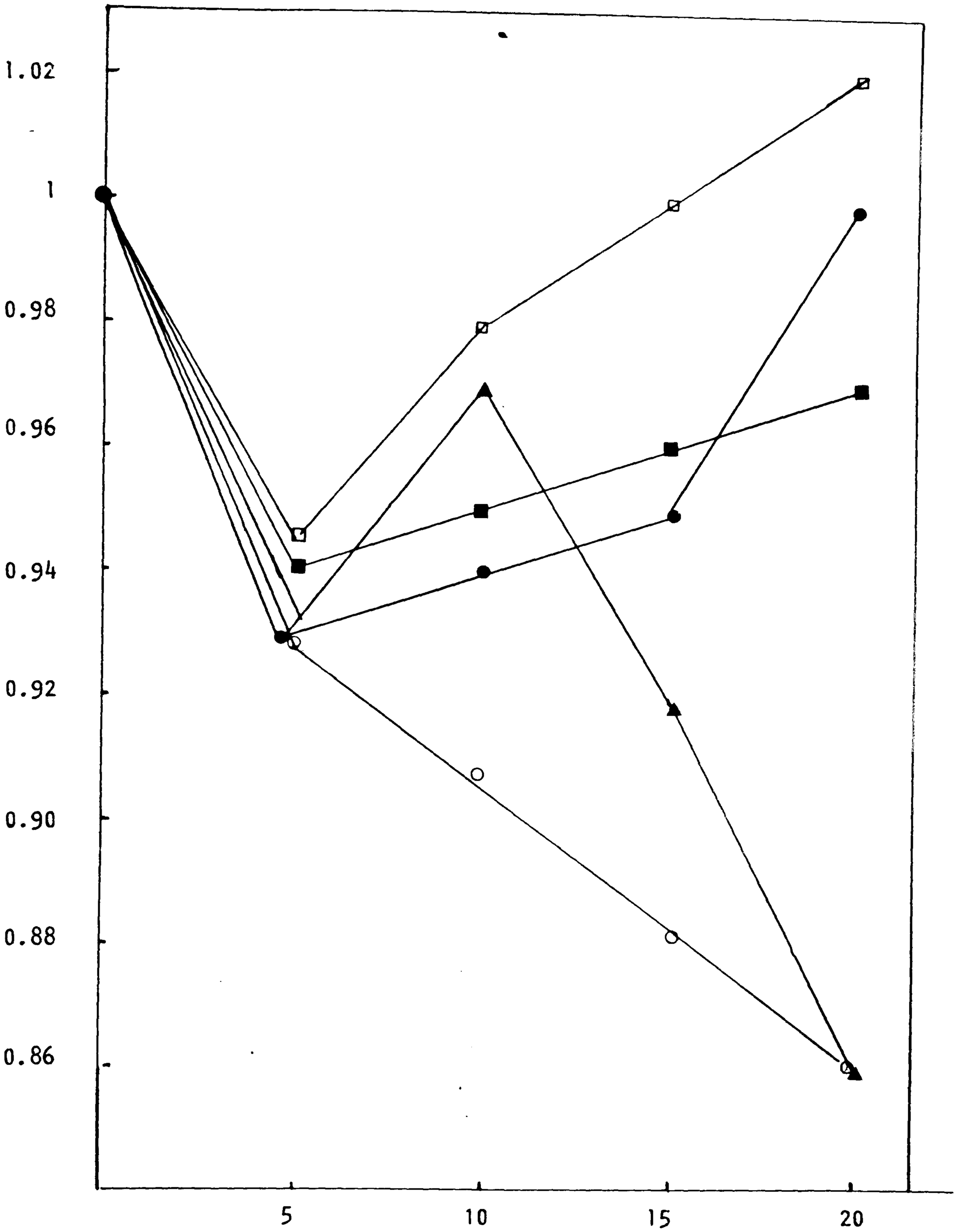

Fig (8) Effect of various starches on yield strength of HDPE

Symbols used are as given in table (4.7)

In contrast to Linero's work with LDPE, the presence of starch in HDPE resulted in no increase in yield strength as shown in fig (8). Only acid treated rice starch at a concentration of 20% by weight resulted in slight increase in yield strength.

4.3.5 Elongation at break.

The decrease in elongation at break with rigid fillers arises from the fact that the actual elongation experienced by the polymer matrix is much greater than the measured elongation of the specimen (152). Fig (9) illustrates the elongation at break of starch filled HDPE as a function of filler concentration. Although the specimen is part filler and part matrix, all the elongation comes from the polymer provided that the filler is rigid and particles of filler do not fragment.

4.3.6 Moduli of starch filled HDPE

For polymers containing nearly spherical particles of any modulus, the Kerner equation (153) or the equivalent equation of Hashin and Shtrikman (159) can be used to calculate the modulus of a composite if there is good adhesion between the phases.

It is assumed that starch is a rigid filler and that there is good adhesion between the starch and HDPE. The equation of Hashin can be used to predict the Young's modulus of the composite:

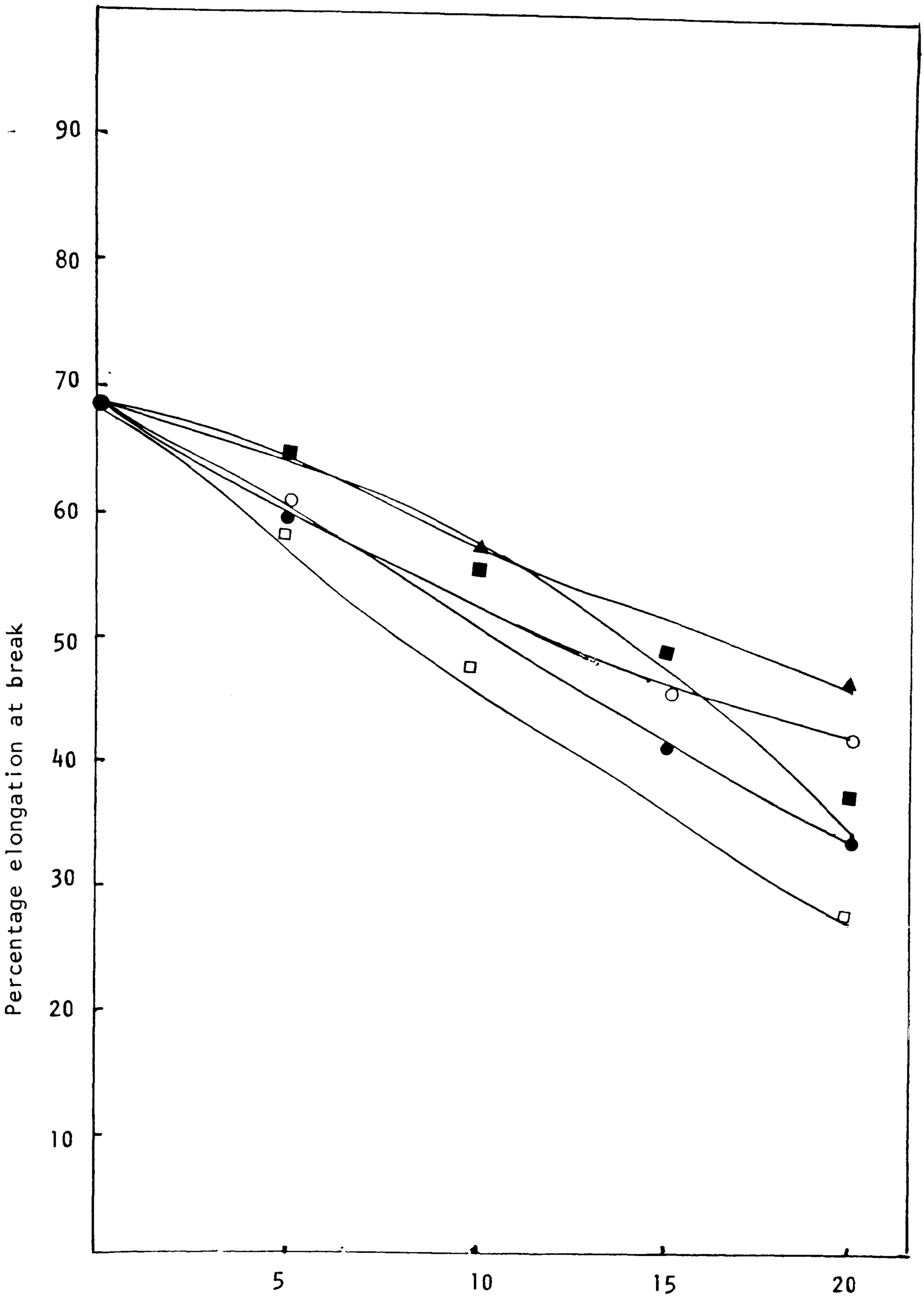

Fig (9) Effect of various starches on percentage elongation at break of HDPE

Symbols used are as given in table (4.7)

$$\frac{Ec}{Em} = 1 + 3 \frac{(1-\gamma)}{(1+\gamma)} \frac{(5\gamma - \gamma)}{(4- 5\gamma)} Cv$$

where

E_c - Young's modulus of composite

E_m - Young's modulus of matrix

Cv - volume fraction of filler

γ - Poisson's ratio for the matrix

The predicted Young's modulus Ec was calculated using above formula. Fig (10) illustrates the Young's modulus obtained experimentally calculated using literature values for $\gamma = .45$, together with Ec predicted on the basis of Hashin's equation given above.

According to the formula the predicted moduli are slightly higher than the experimental results obtained by tensometry. However, moduli obtained from flexural testing matched those obtained from the theory of Hashin. It may be concluded that a good adhesive bond exists between filler and polymer in the cases studied.

The theories of composite elasticity indicate that the elastic moduli of a composite material should be independent of the size of the filler particles (155). However, experiments generally show an increase in modulus as the particle size decreases (156) Fig (11,12) illustrates this effect.

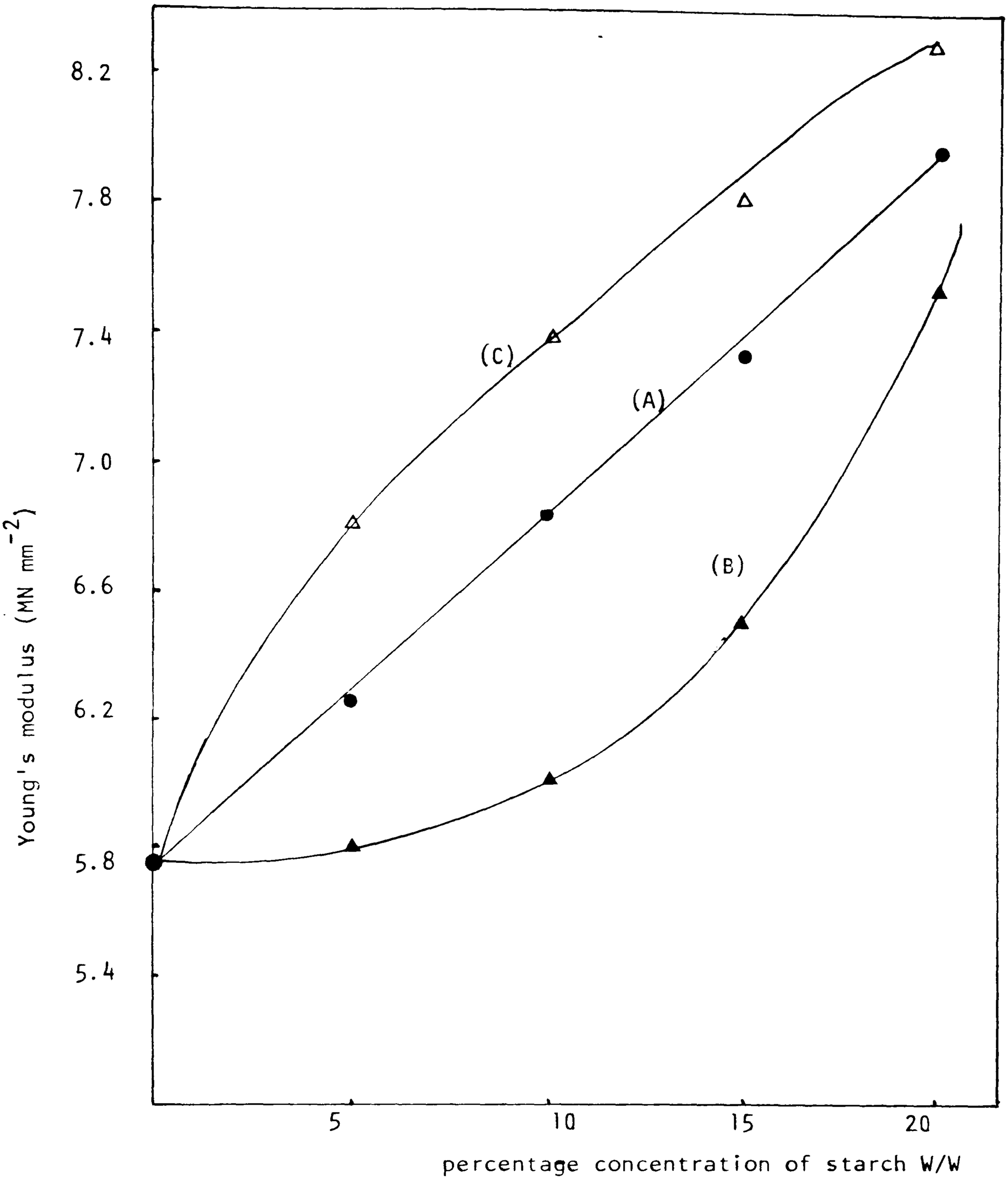

Fig (10) Comparison of the theoretical model for Young's modulus of potato starch filled HDPE with the experimentsl.

(A) theoretical (B) Experimental, tensile modulus
(C) Experimental, flexural test modulus

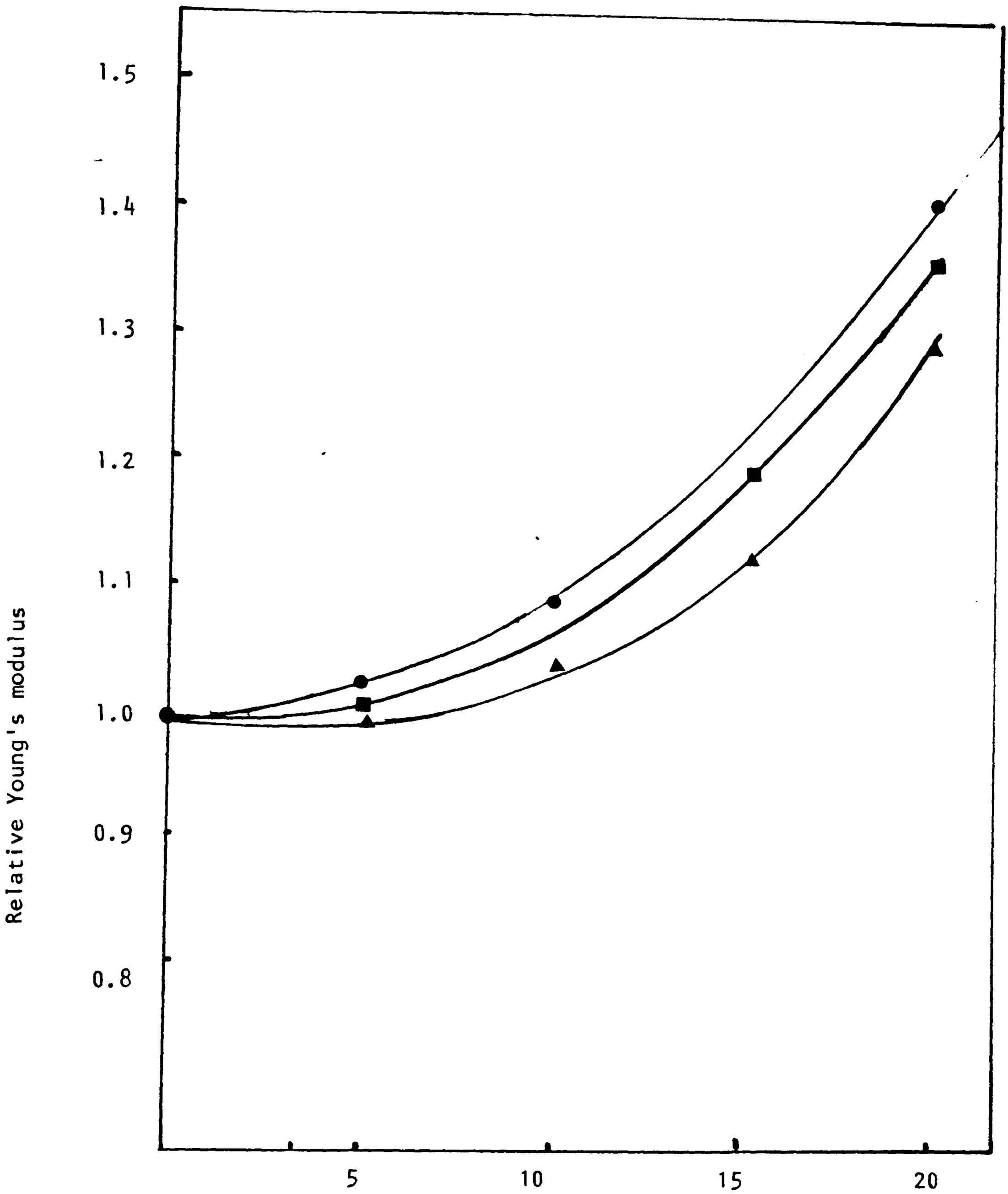

Fig (11)-1 Effect of various starches on Young's modulus of HDPE (obtained from tensile test)

Symbols used are as given in table (4.7)

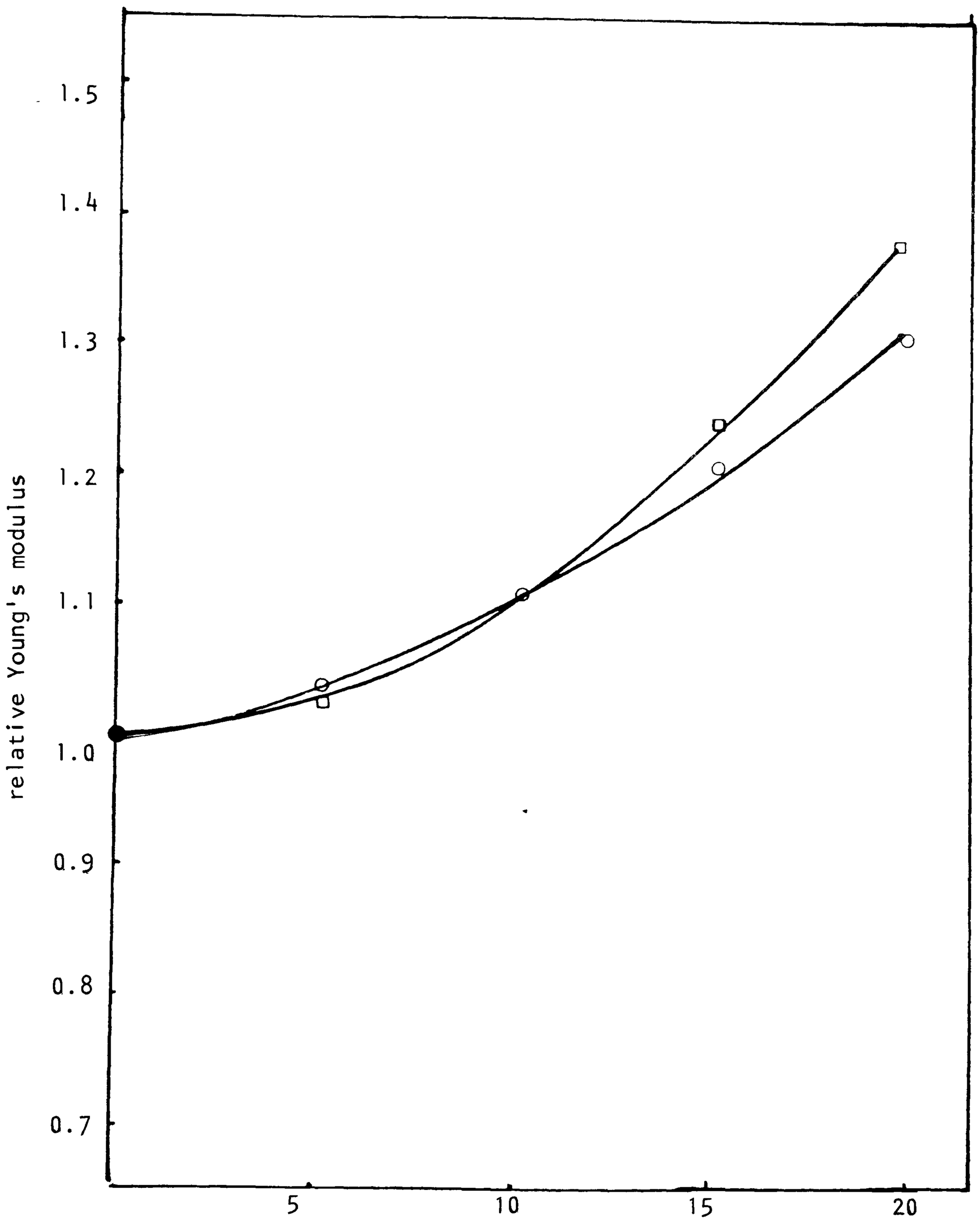

Fig (11) -2 Effect of various starches on Young's modulus of HDPE (obtained from tensile test)

Symbols used are as given in table (4.7)

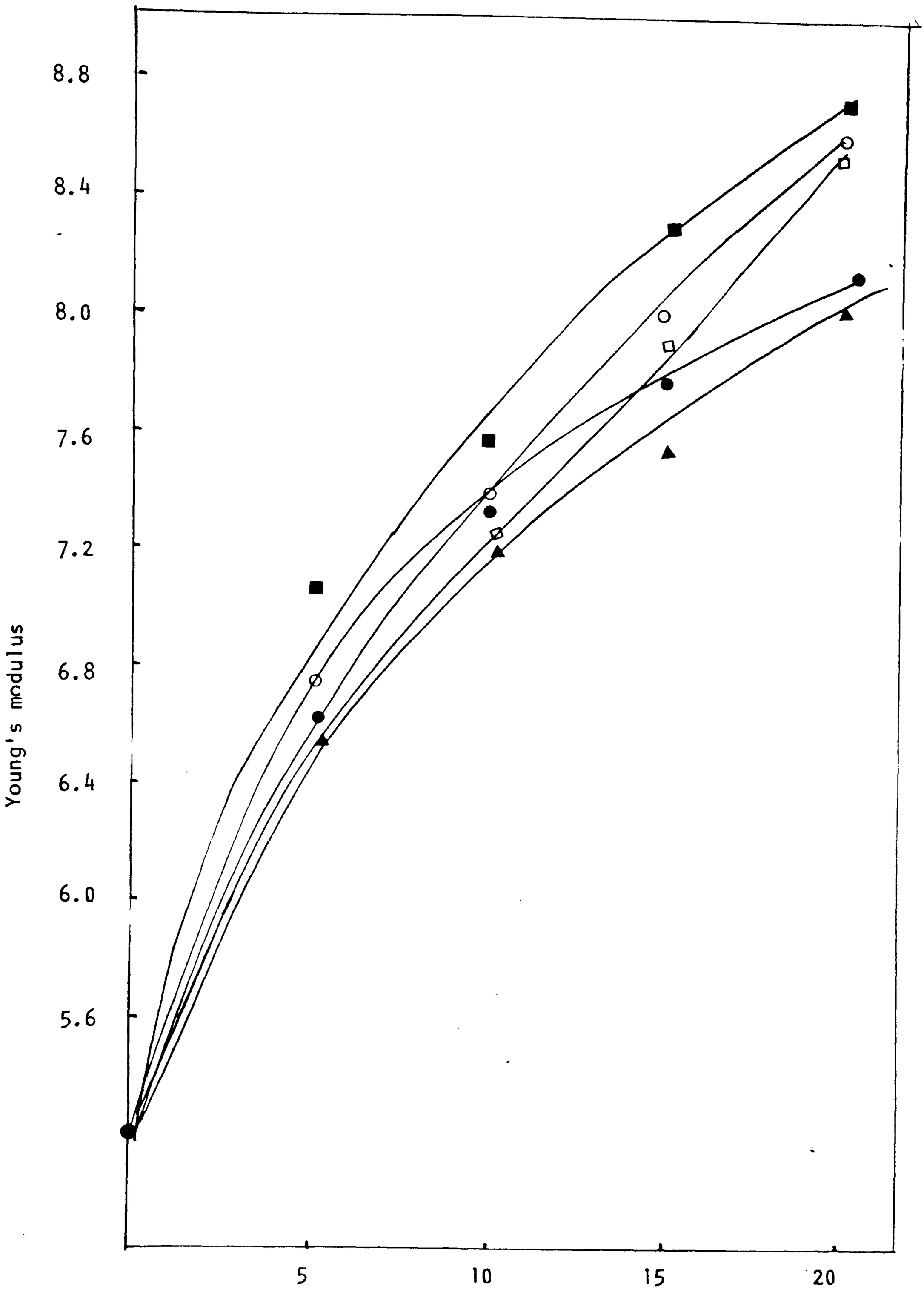

Fig (12) Effect of various starches on Young's modulus obtained from flexural specimens.of HDPE

Symbols used are as given in table (4.7)

There are several possible reasons for this discrepancy between theory and experiment: 1. As particle size decreases the surface area of a given mass of the particles increases. If the polymer is changed in some manner at the interface, then the properties should change with particle size because of the change in surface area provided that the elastic properties of the composite depend on the interfacial area. 2. As particle size decreases agglomeration of powder tends to increase with a corresponding decrease in maximum packing volume. Thus agglomeration may account in part for the difference observed between theory and experiment. In the case of the experiments reported here very little agglomeration was allowed to occur suggesting that the first explanation is correct and the simple theory must be inadequate in some respect.

Section (4)

4.4.0 Microscopic observation of starch-filled HDPE

Many methods have been suggested for assessing the degree of dispersion and extent of agglomeration of fillers in plastics and possible morphological modifications due to the presence of the filler in the polymer. The results of optical microscopy taken in conjunction with S.E.M. and T.E.M. results have been used for such studies.

4.4.1 Light microscopy observation

Thin sections, about 10 micron thick, of unfilled HDPE and 1% starch-filled HDPE were prepared by microtomy. Sections were taken from within a region of area 72 mm^2 in the centre of the bar-shaped tensile test moulding specimen (perpendicular to the flow direction). Thin sections were observed using light microscopy and Canada balsam as a mounting medium.

Plates (11,13) show clearly that the starch granules do not change their apparent birefringent pattern or shape during compounding or moul d ing processes. Plate (10) shows the microstructure of unfilled HDPE observed using crossed polars (the striations visible in this photograph result from the effect of the knife-edge profile on the specimen). Plate (12,14) shows the microstructure of HDPE in the presence of starch comparing plate (12,14) with plate (10), there is evidently a significant difference between the filled and unfilled material. A white area around the starch granules can be observed in these photographs. The depth to which this region

extends seems to be dependent on the size of the starch granules.

Chanzy and Reval (157) studied the morphology of the polyethylene shells encapsulating starch granules where the polymer had been chemically synthesized on the surface of potato starch granules.

When the polyethylene encapsulated starch granules were observed with polarized light in an optical microscope, Chanzy and Reval showed that the polyethylene encapsulation shell was strongly birefringent and displayed the Maltese cross effect. Their conclusion was that the layer had a negative birefringence, i.e. in the birefringent area the polyethylene was mainly oriented tangentially to the starch surface. This behaviour was correlated with the stretching of the encapsulation membrane during the growth. This stretching caused ruptures inside the polymer shell, and formation of dry cracks with edges limited by an array of microfibrils. The cracks deepen towards the starch granule centre, whereas the microfibrils run tangentially to the encapsulated granule. These microfibrils contain highly oriented polyethylene and are responsible for the negative birefringence of the polyethylene shell. Although the conditions of preparation of their samples were different from that used in the present work, similar observations were made. Here we are not concerned with the sign of the birefringence of polymer contigno us with the starch granule layer, but we believe that microfibrils grow tangentially to the starch surface, and orient the HDPE locally. Linero (9) suggested that

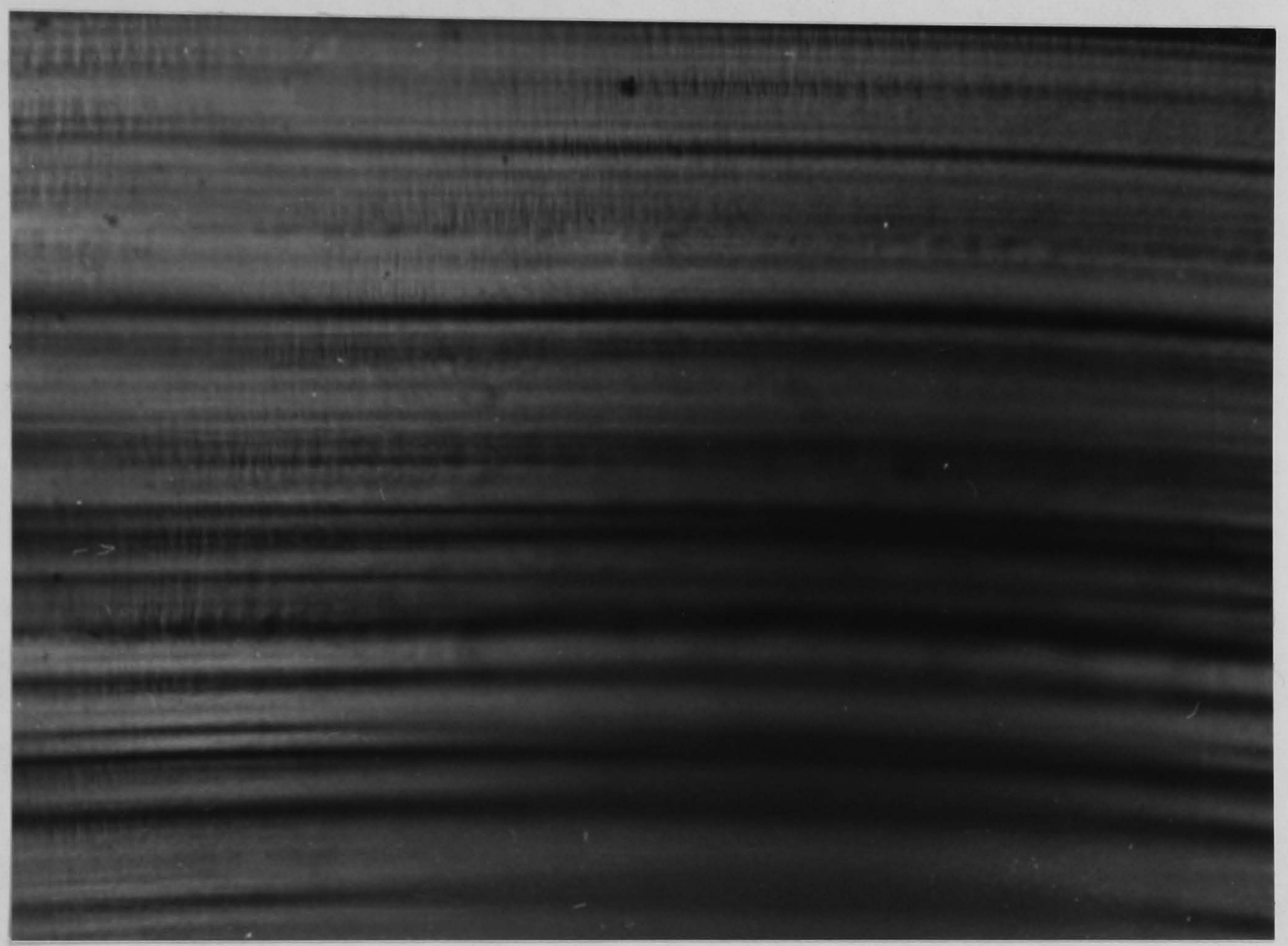

Plate (10) Optical Photomicrograph of microtome cross-section of HDPE (polarized light) (x 420)

Mountant, Canada balsam

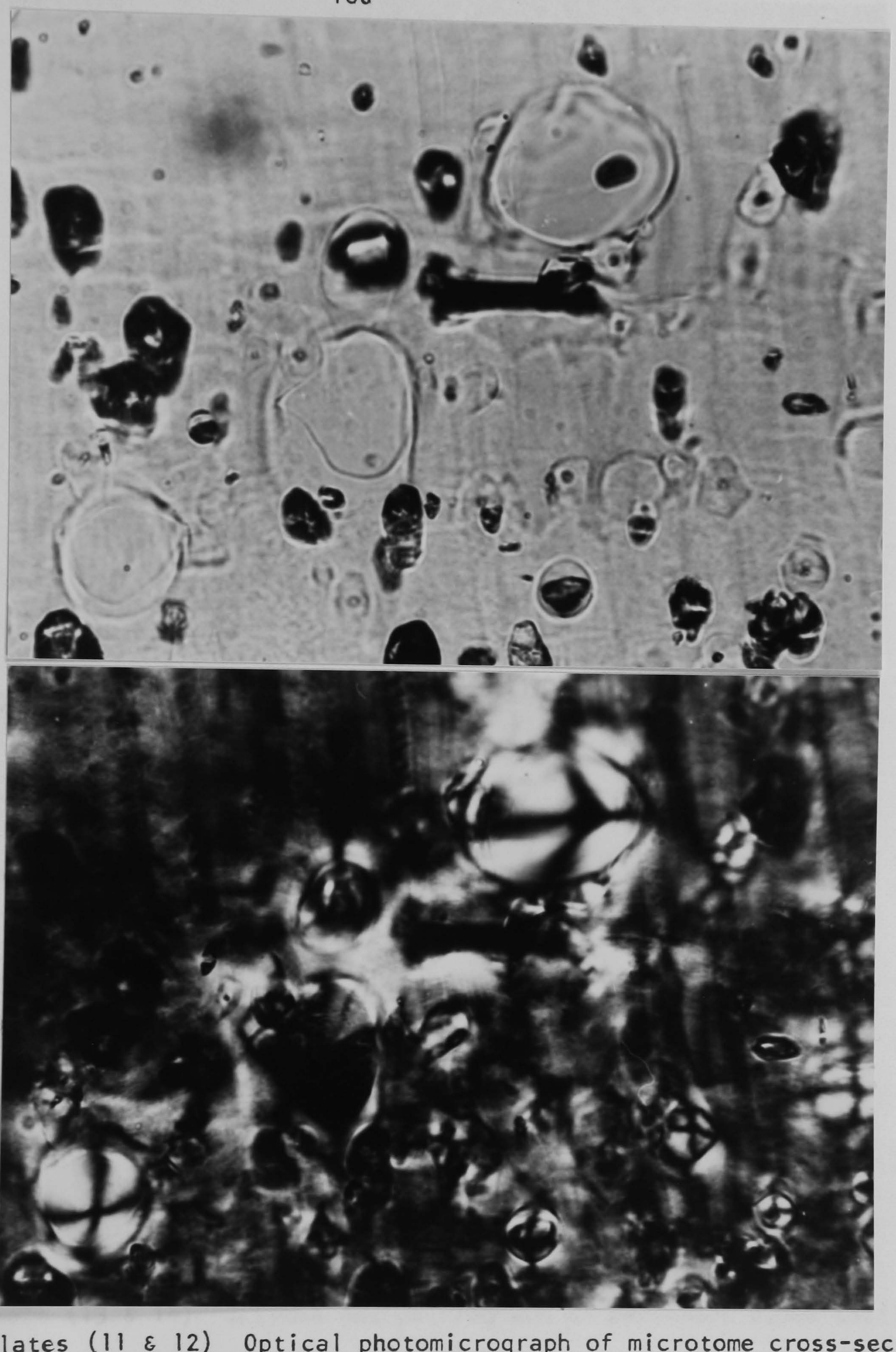

Plates (11 & 12) Optical photomicrograph of microtome cross-section of 1% potato starch filled HDPE (x 420)

(Top): normal light (bottom): polarized light, mountant Canada Balsam

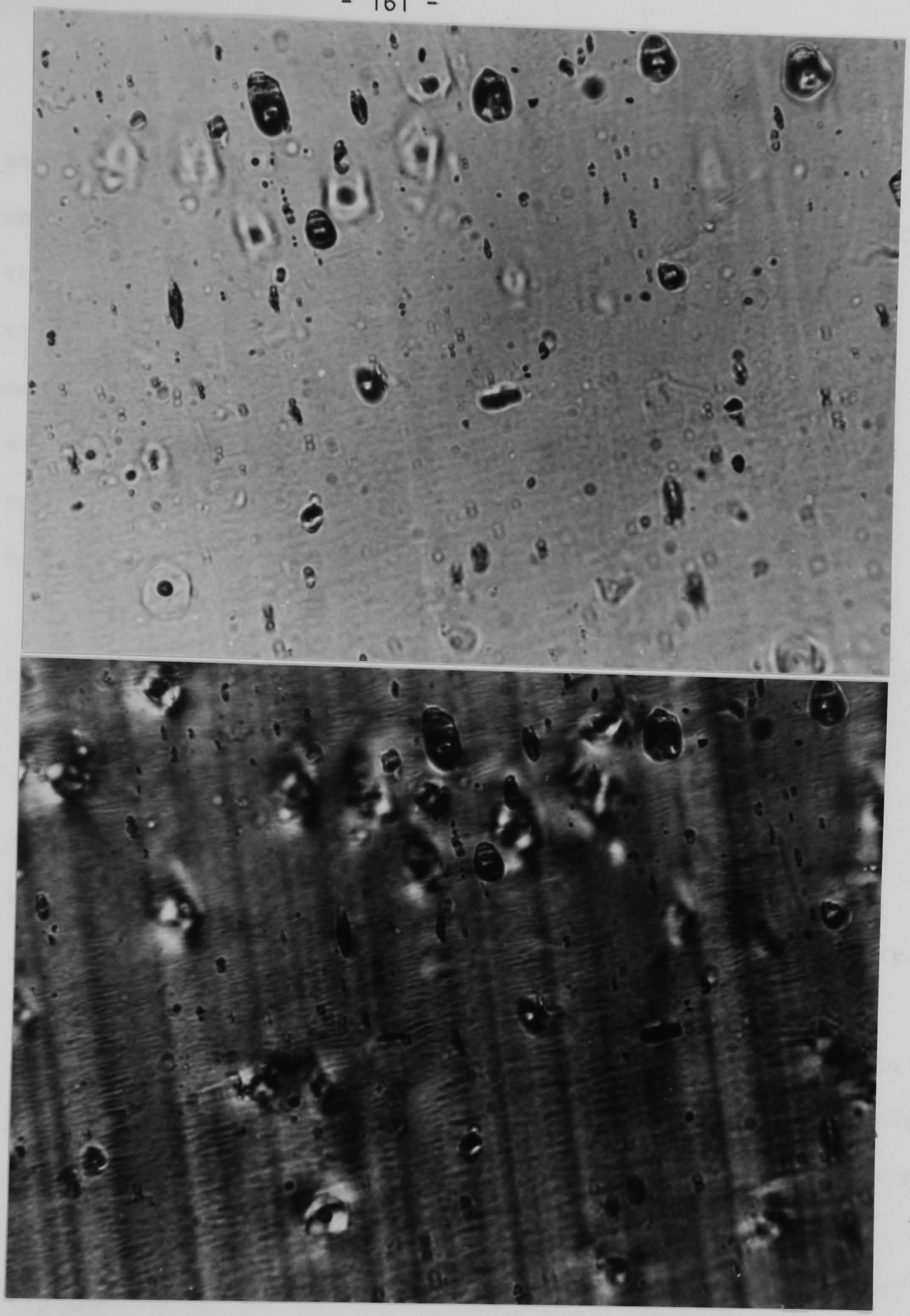

Plate (13 & 14) Optical photomicrograph of microtome cross-section of 1% maize starch filled HDPE (X420)

(top): normal light (bottom): polarized light

polyethylene melt wet the starch granules very readily during the milling processes, then during the milling or injection process the polymer melt is forced to crystalline and orient around the starch granules. The above observations suggest that the final morphology of the matrix polyethylene, near the starch granules might be different to the unfilled polymer. These observations encouraged us to investigate these effects in greater detail by electron microscopy.

4.4.2 Observation of the starch filled HDPE by Scanning Electron Microscopy.

To prepare the polymer surface for viewing by scanning electron microscopy, moulded samples were etched with hot chromic, sulphuric acid solution (see section 3.9.5). This etching treatment on starch filled HDPE reveals a fibrillar substructure. The oxidative etching in hot chromic sulphuric acid has caused the amorphous material to be dissolved in part, leaving the fibrillar core which has resisted attach. Plates (15-18) show a sample of HDPE polymer containing potato starch which enables us to comment on the appearance of isolated granules in the matrix. As is evidenced by these photomicrographs, the morphology of the matrix polyethylene, near the starch granules, is different from the rest of the polymer matrix. Here the fibrillar structure displays a radially propagating pattern with the granules at its centre.

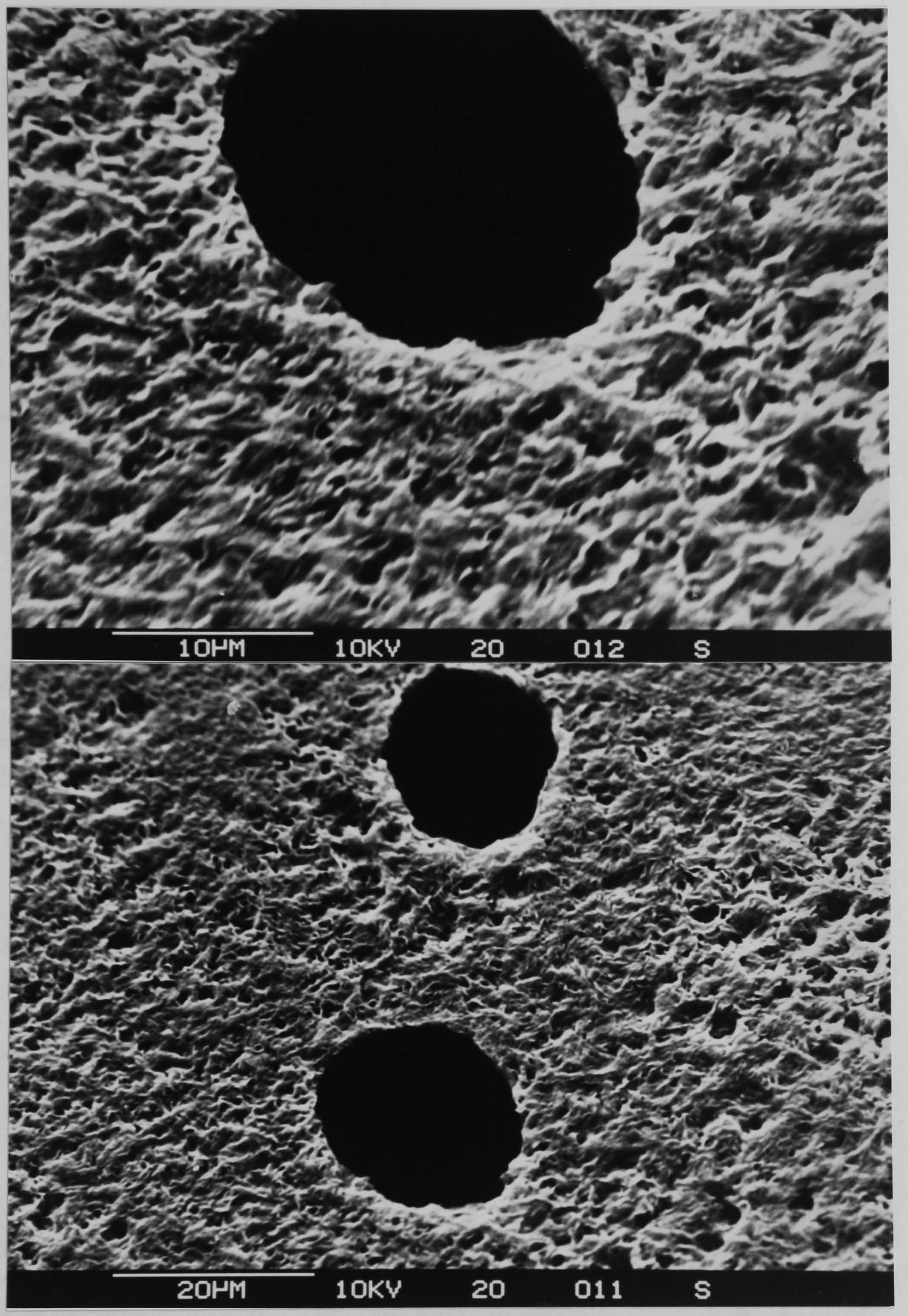

Plates (15 & 16) S.E.M. view of potato starch-filled HDPE etched with hot chromic and sulphuric acid showing microstructure of polymer in the presence of starch.

The black areas respresent the location of starch granules before etching removed them.

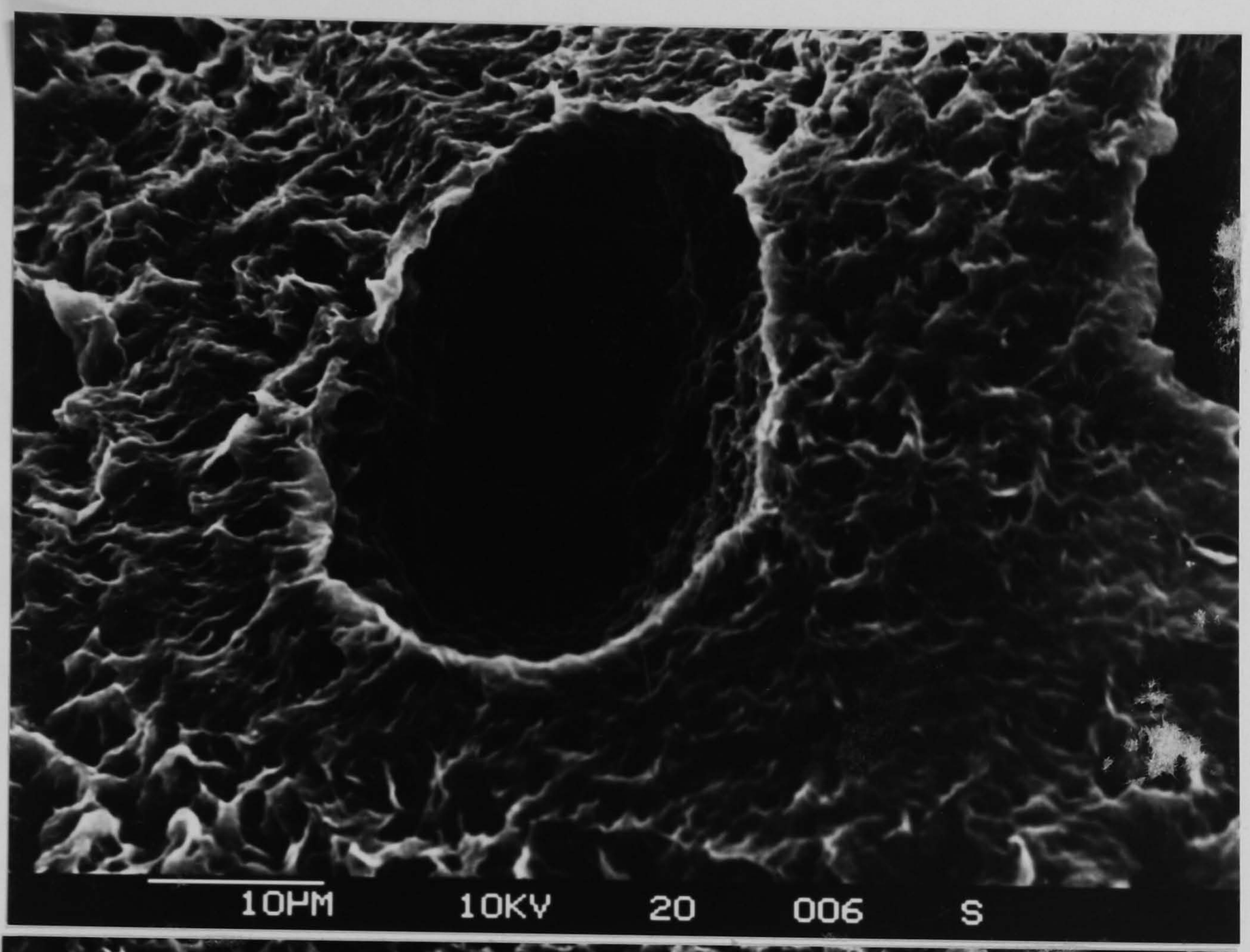

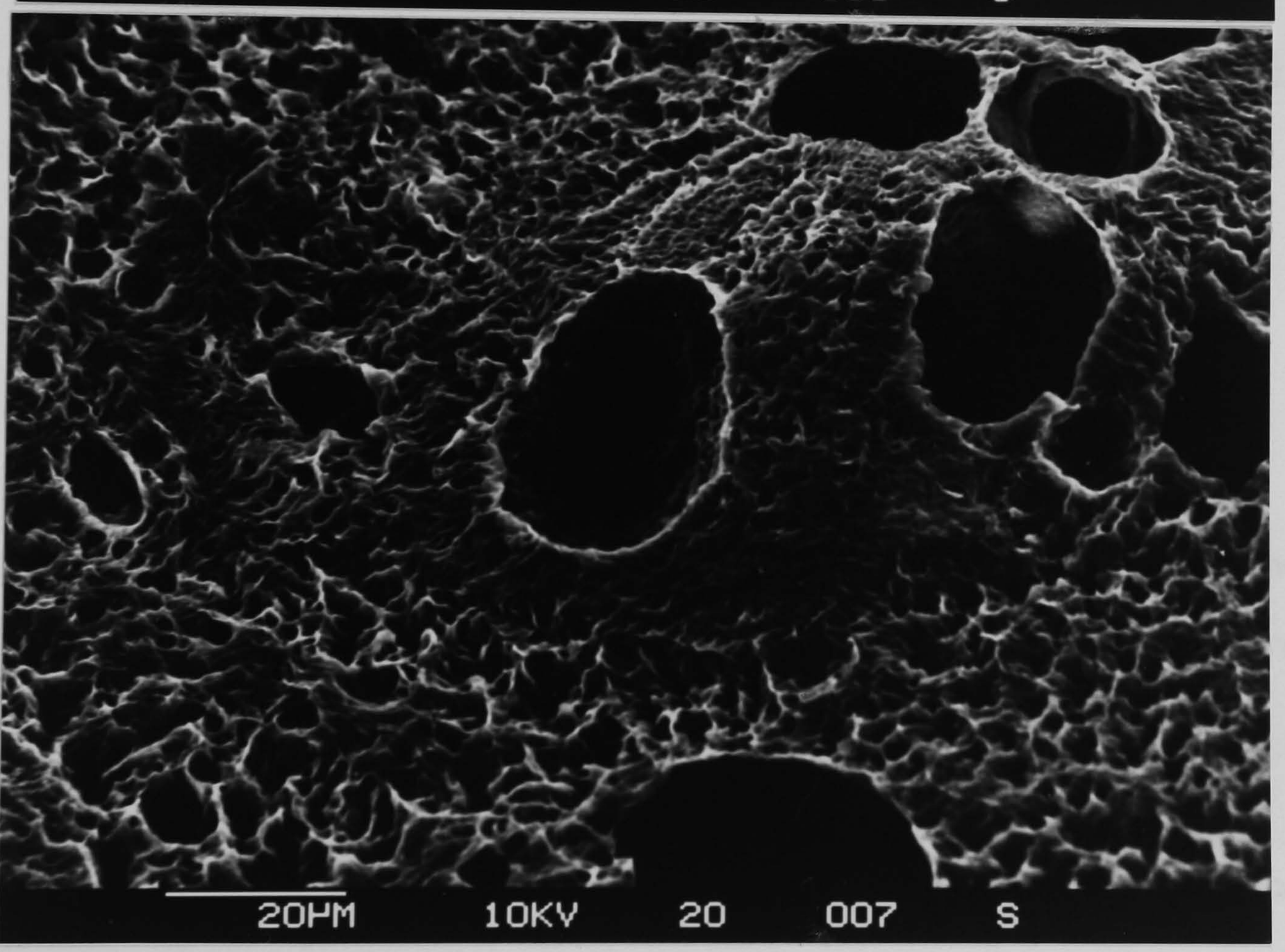

Plates (17 and 18) S.E.M. view of potato starch-filled HDPE etched with hot chromic acid and sulphuric acid showing the microstructure of the polymer in the presence of starch

Plate 15-18 shows clearly the black area which represents the position where a starch granule existed in the polymer before the etching treatment removed it.

Linero (9) suggested the possibility of formation of regions of trans crystallinity in the starch filled polyethylene. Wide differences in the density of spherulite nuclei on the surface relative to the bulk may be observed so that in extreme cases a unidirectional or trans crystalline growth may occur leading to surfaces of different texture, orientation, and probably of crystalline perfection as well (158). Generally there is no disagreement that trans crystallinity is essentially spherulitic in character and originates from a crowding of primary nuclei at the surface (158). Considerable disagreement does exist concerning the factor which contributes to the formation of a relatively high nucleation density at the surface.

In most crystalline polymers and especially in polyolefines, the formation of primary nuclei is dominated by the presence of foreign matter (present either by accident or design).

Presence of starch at the melt surface therefore may well induce trans crystallinity.

4.4.3 The technique of permanganic etchings

In order to reveal more lamellar structures present in polyethylene and other polyolefines a technique involving the use of permanganate as an etchant has been devised (105) which allows representatives of melt-crystallized morphologies to be studied with the electron microscope. Olley and Bassett (105) reported that artefacts of about 10 micron in diameter can develop if permanganic etching procedure was adopted (see section 3.9.5). etching recipe).

It is necessary when using the permanganic etching technique to study the morphology of these artefacts so that they may be recognized as such should they occur in some particular experimental situation and to discover whether the presence of starch makes any difference to the morphology of the polymer matrix or the artefacts.

This permangenic etching technique is a very sensitive monitor of surface topography. Plate (19,20)shows the number and size of artefacts as a function of the length of time, over which etching was carried out. It was reported (105), that there are systematic variations in number and size of the artefacts with the concentration of the etchant (high concentrations resulting in large numbers of artefacts). The distribution of artefacts over the field of view is generally uneven, showing a tendency to form along surface scratches, knife-marks or similar irregularities.

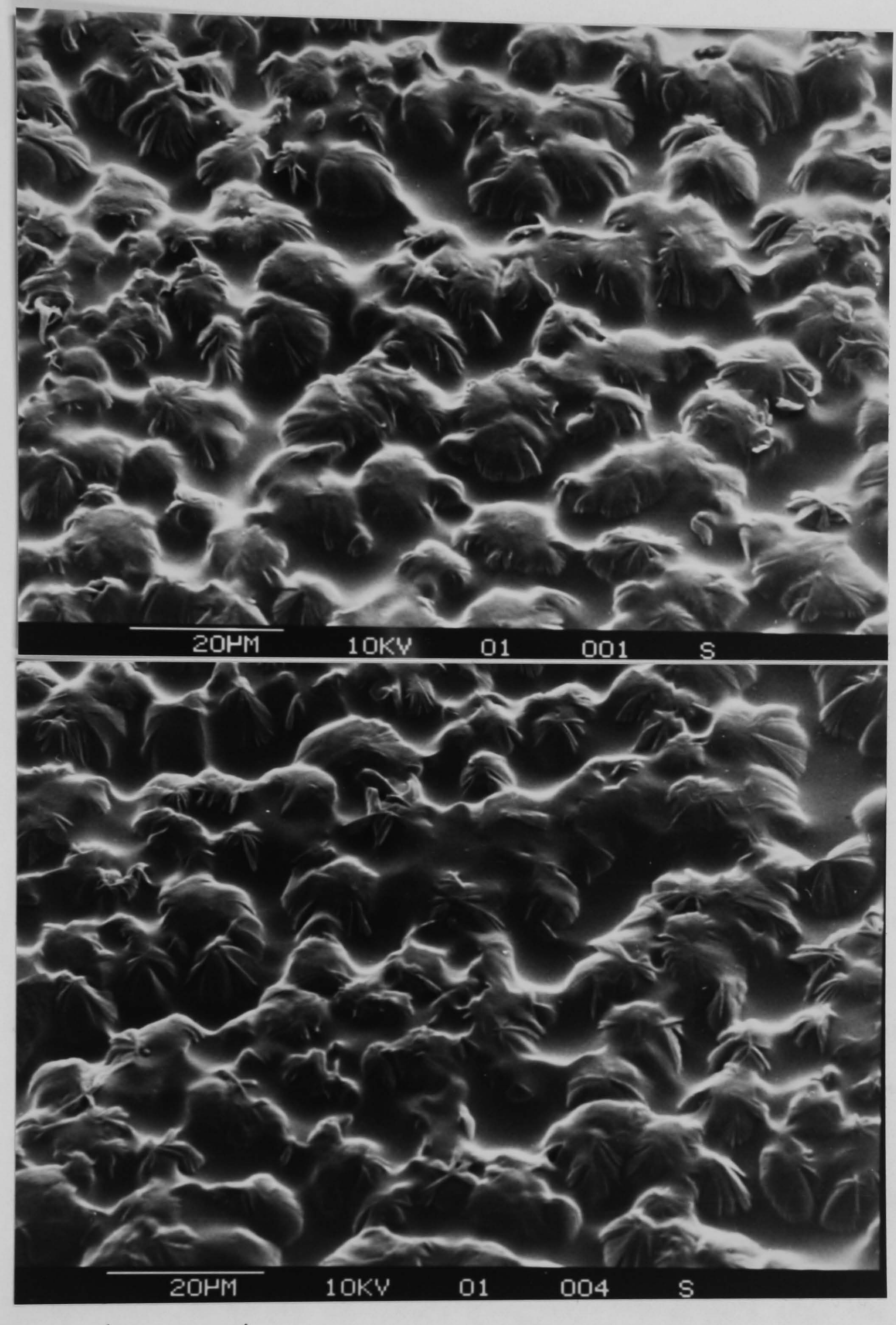

Plates (19 and 20) S.E.M. view of HDPE etched with permanganate and sulphuric acid, showing the creation of artefacts

Injection moulding samples facing the smooth surface of the cavity have been chosen for etching in order to avoid surface scratches.

Plate (21/2) shows starch-filled HDPE and it is clear that the artefacts are created in the presence and absence of starch. It is apparent from plate (21/2) that the structure of polymer matrix is affected in the area near the starch granules where once again the round black area represents the position of starch granules as they were before etching treatment. Here the fibrillar structure has a radially propagating structure with the granules at the centre which tends to support the previous arguments.

Olley and Bassett also reported an improved etchant for polyolefines, which avoids the creation of artefacts (see section 3.9.5) Plate (23) shows the matrix of HDPE without starch, the structure is uniform and there is no sign of variation in structure. However plate (24) shows that the structure of polymer matrix is different in the area which has been influenced by the presence of starch. It may be tentatively concluded from our microscopic investigations on the structure of starch-filled HDPE that the starch granules exert some effect on the morphology of polymer locally.

The various problems of interpretation of photomicrographs using different microscopy techniques are well known and it is necessary to state that our conclusions need to be taken in conjunction with

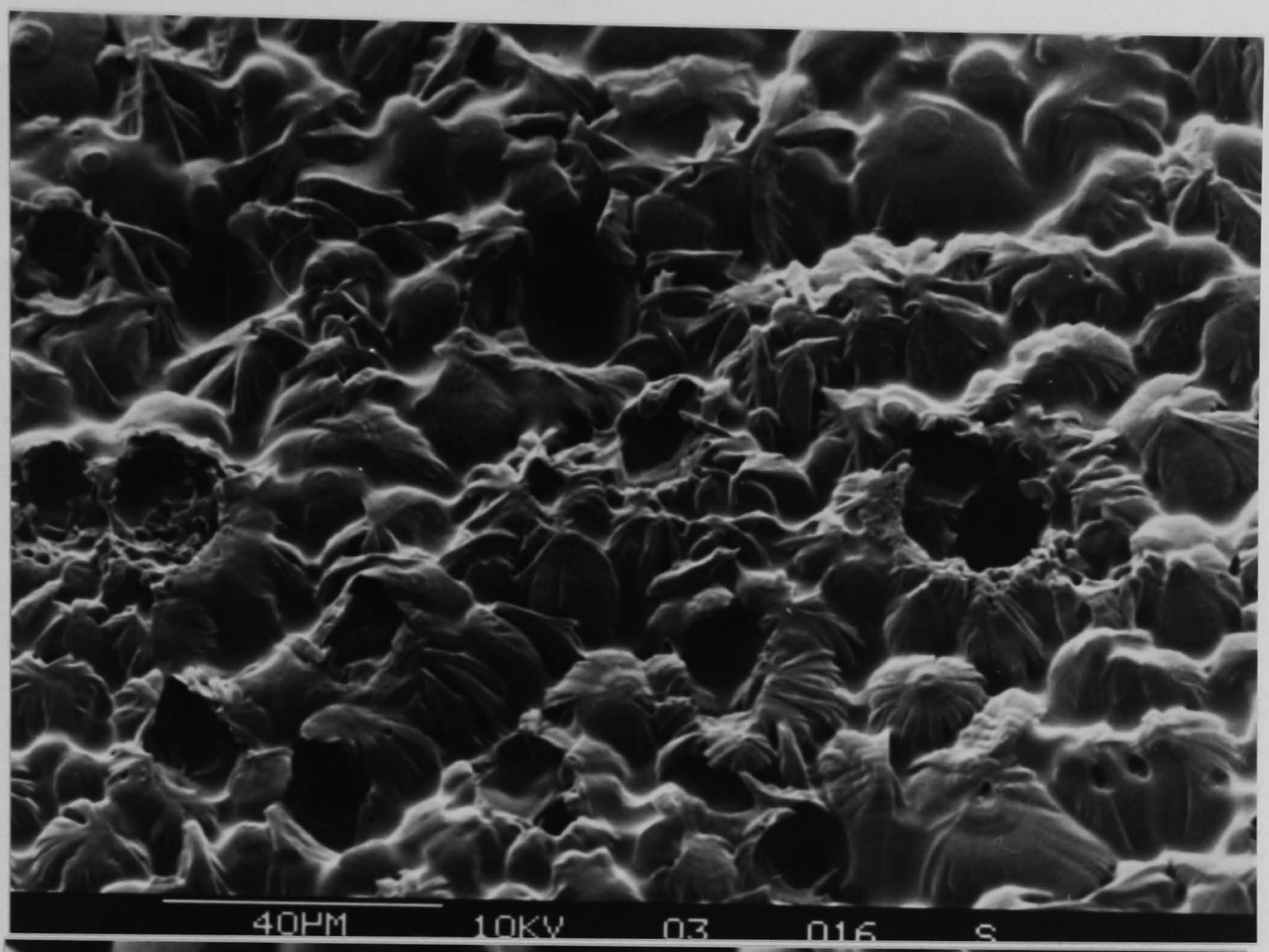

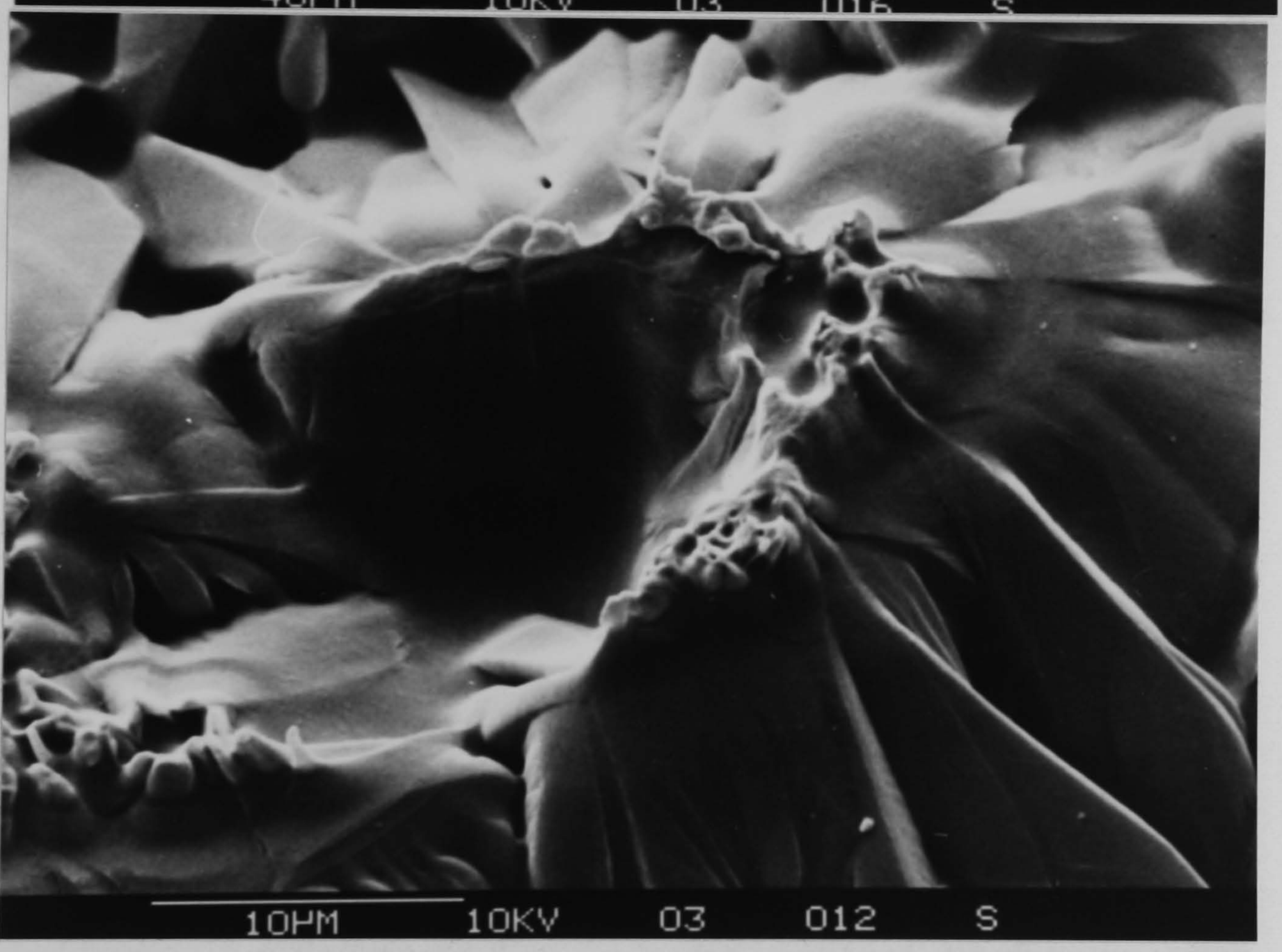

Plates (21 and 22) S.E.M. view of maize starch-filled HDPE, etched with permanganate and sulphuric acid, showing the morphology of artefacts in the presence of starch

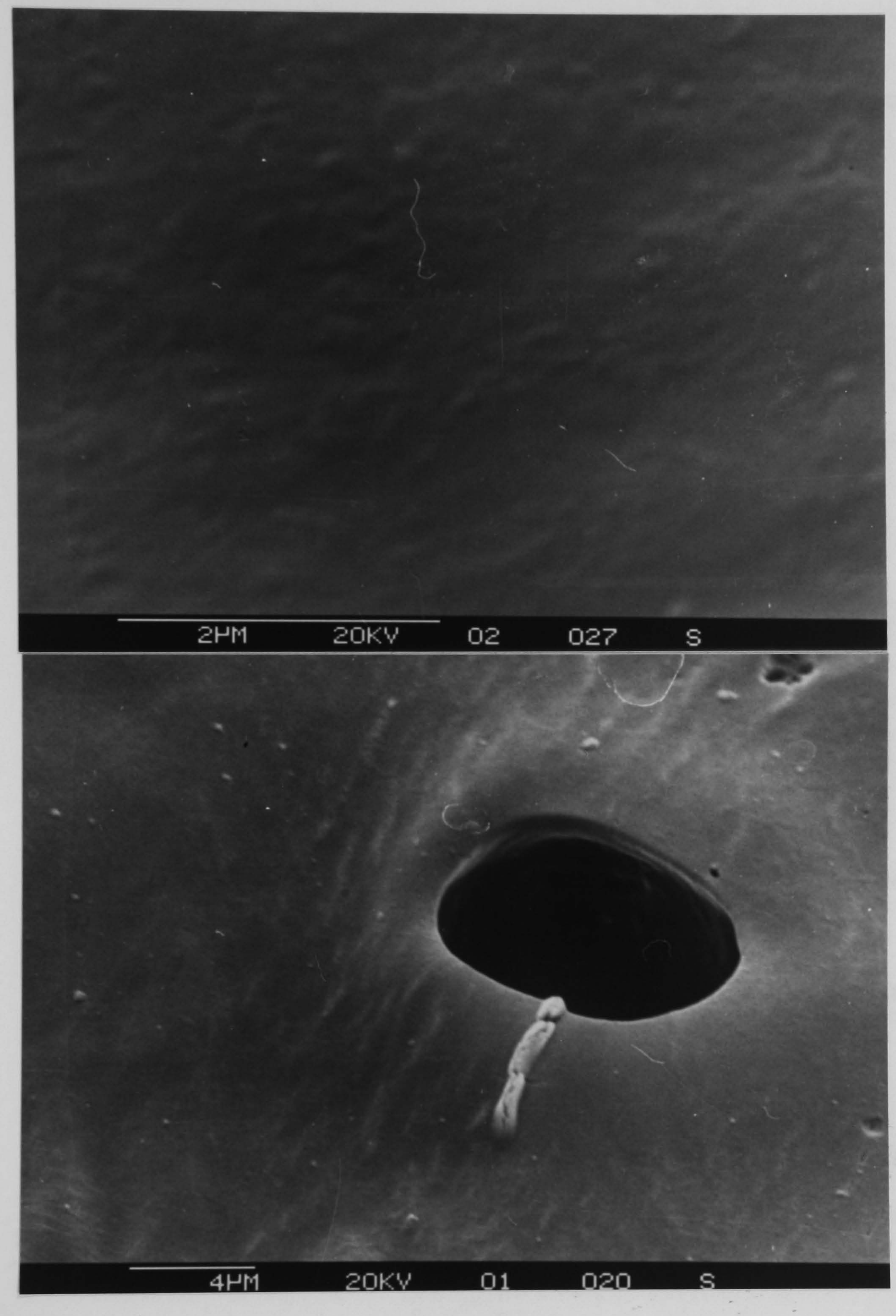

Plate (23) S.E.M. view of HDPE etched with permanganate, sulphuric acid and orthophosphoric acid.

Plate (24) S.E.M. view of maize starch-filled HDPE etched as in plate (23)

with the substantiating evidence for starch polymer interaction provided the other investigations reported in this thesis and elsewhere.

Several attempts have been made to prepare a replica of the polymer surface, see section (3.9.7) for observation using TEM, although the replica method shows the structure of the surface of the polymer.

We have not succeeded in finding the area of the field in which starch was present. The difficulty might be attributed to the method of sample preparation; when the sample is etched it is possible that the starch granule falls out of the polymer matrix. so that when acetone-softened the replica film material (BCX) on the surface of the polymer, the film does not penetrate the hole created by the loss of the starch.granule. Plate (25) shows a surface replica of HDPE etched with potassium permanganate and sulphuric acid. Although the presence of the artefacts mentioned above seen using the S.E.M. technique, it has been impossible to observe them under T.E.M. A comparison of plate (25,26) clearly shows that the presence of orthophosphoric acid causes a change in the appearance of the etched polymer under T.E.M.

4.4.4 Dispersion of starch granules in HDPE

Injection moulding samples which were etched with hot-chromic sulphuric acid in order to observe morphological changes in polymers

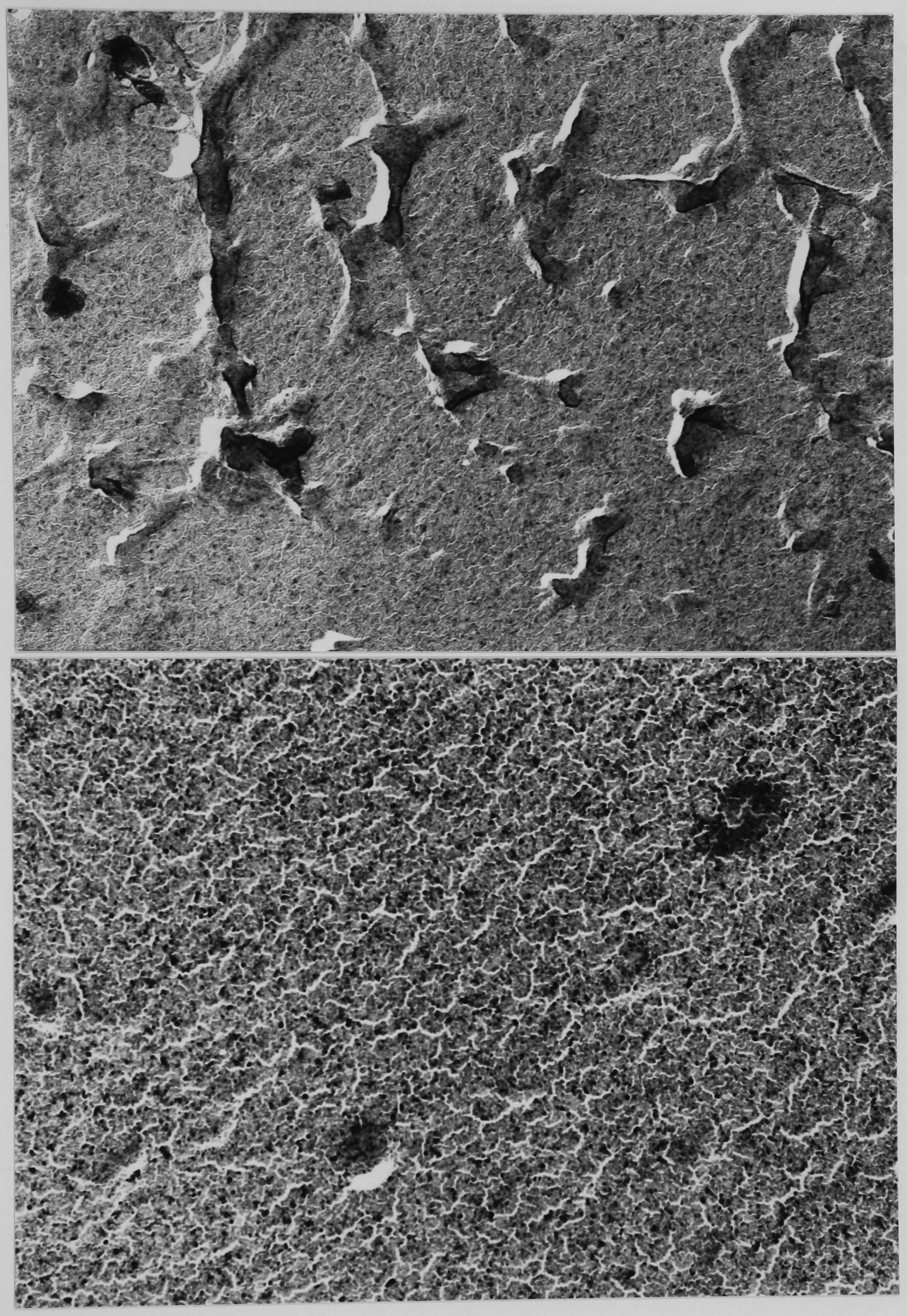

Plate (25) T.E.M. photomicrograph of replica of HDPE etched with permanganate and sulphuric acid. $\underline{0.25\mu}$

Plate (26) T.E.M. photomicrograph of replica of HDPE etched with permanganate and sulphuric and orthophosphoric acid $\underline{0.1\mu}$

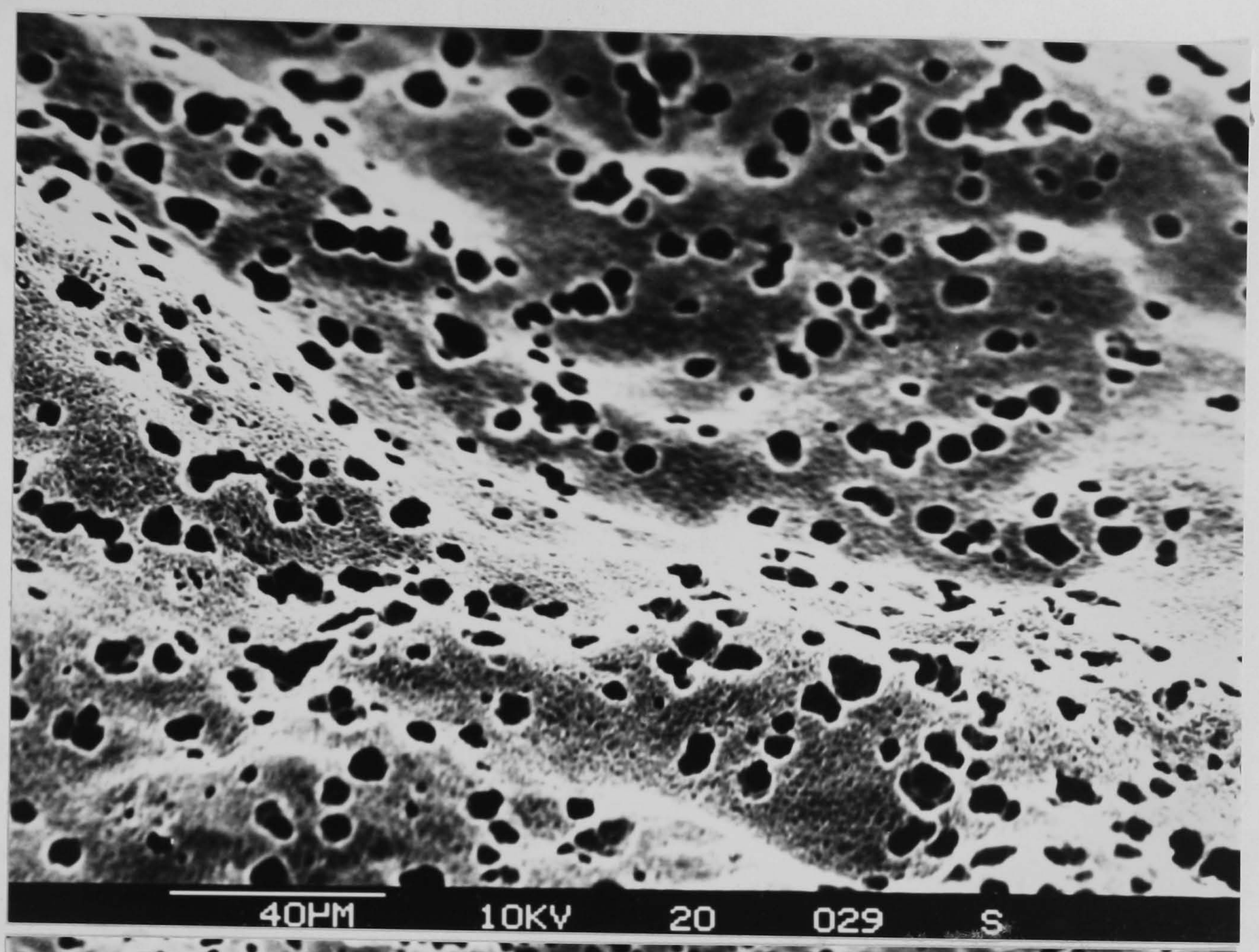

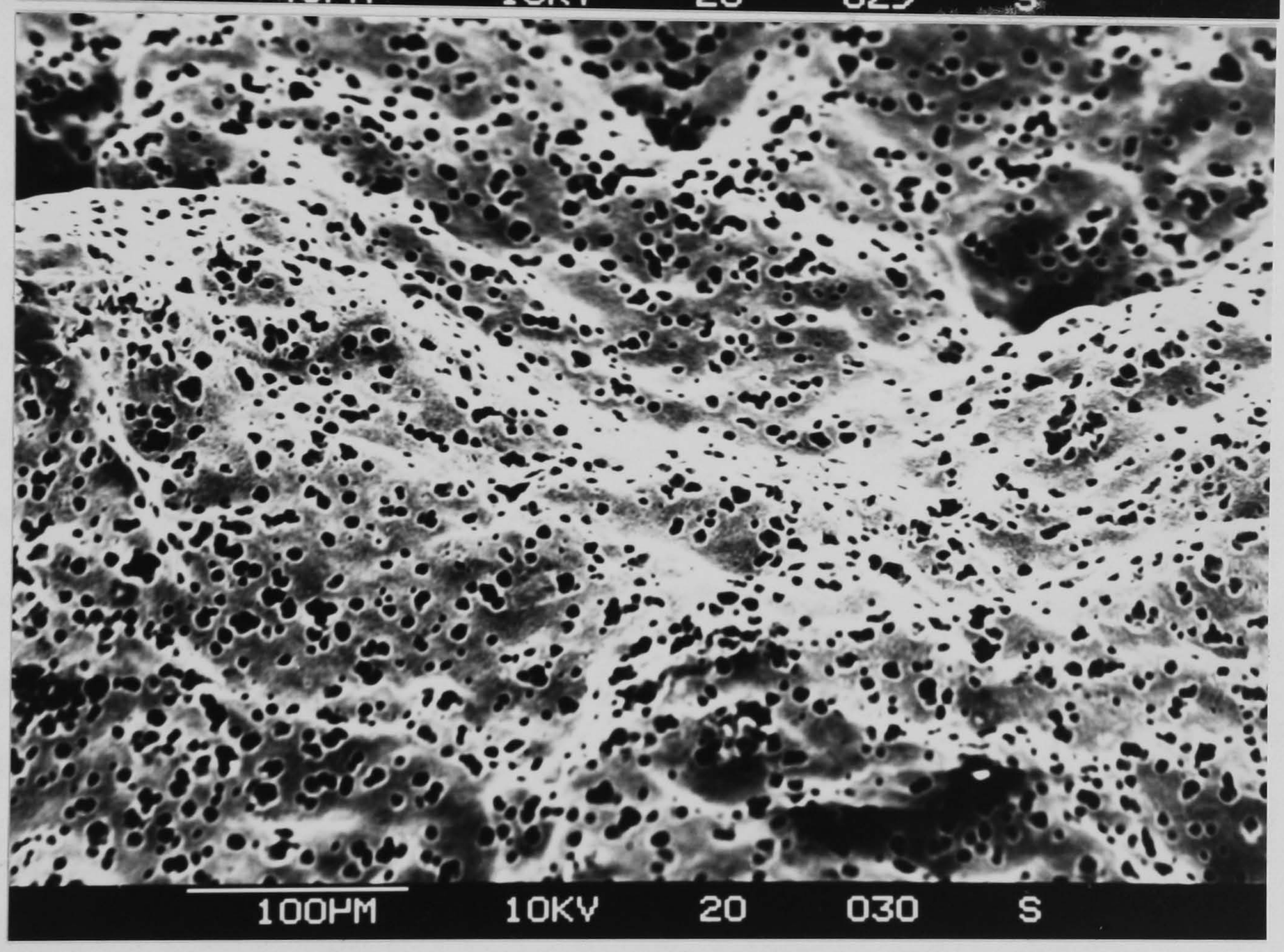

Plates (27 and 28) SEM view of rice starch-filled HDPE etched with hot sulphuric and chromic acid showing the dispersion of the filler in the polymer matrix.

could be used to see the dispersion of starch granules in the polymer matrix. Plates (27,28) illustrate the dispersion of rice starch in the polymer matrix. As can be seen from these plates (20% by weight of rice) it has been well dispersed in the HDPE matrix. Similar results have been obtained with the other starches-HDPE systems investigated.

Section 5

4.5.6 Thermal analysis of starch filled HDPE

Introduction

The science of thermal analysis of the melting behaviour has been developed over a long period of time, a recent review of the application of thermal analysis to polymers even as a fundamental reference cites the work of Le-Chatelier (1887) on differential thermal analysis (159). However, extensive applications of thermoanalytical techniques to polymers has taken place only during the past 15 years (1980) (160). The term "thermal analysis" applies to a family of techniques, all of which monitor primarily physical properties as a function of temperature (or of time at a defined temperature). Applications of these techniques have been mentioned in section (2.8.1).

In this section we concentrate on differential scanning calorimetry (D.S.C.), because the D.S.C. equipment available was particularly suited to the present study. An abundance of experimental

information on polymers has become available through the use of D.S.C., but little information is available on the effect of fillers on polymer thermal properties, and the section is largely devoted to study of starch filled polymers using D.S.C.

4.5.1 Quantitative methods of thermal analysis of starch-polymer composites.

Of primary importance in the characterization of semicrystalline polymers is the determination of the weight fraction crystallinity (x_1) at a particular temperature T_1. This parameter (x_1) influences a variety of polymer properties and hence its determination is fundamental in understanding and correlating polymer properties. One method of finding x_1 is based on the measurement of the heat of fusion of the polymer sample by D.S.C. Like most methods of crystallinity determination for polymers, a two-phase structural model is employed (amorphous-crystalline). Use of this model requires that certain assumptions be made. These include (161).

1. That the polymer consists of distinct amorphous and crystalline regions and that each may be assigned a particular heat capacity at any particular temperature.

2. That the polymer exists in a stress-free state

3. That the heat capacity of the amorphous regions can be extrapolated from or is identical to that of the melt

4. That the amorphous and crystalline heat capacities are additive by definition,

$$X_1 = \Delta Hf_1 / \Delta Hf_1^{o} \qquad (5.1)$$

where ΔHf_1 is the measured heat of fusion of the polymer at temperature T_1 and ΔHf_1^{o}, is the heat of fusion of a notional 100% crystalline polymer determined at T_1. Practically, ΔHf_1 is found as follows (160). First the melting curve of a known weight (Yr) of a pure, well-characterized material such as indium ($Tm = 156.6^{o}C$; $\Delta Hf_r = 6.80$ cal/g) is determined. The area under the melting endotherm (Ar) can be determined and the heat of fusion (ΔHfr) found in the literature. It can be seen that:

$$Yr(\Delta Hfr) = KAr \qquad (5.2)$$

Where K is an instrumental constant that relates thermal energy to the area of recorded output. One can then solve for K. A polymer sample of known weight (Yp) is then scanned through its melting region. The area under the endotherm (Ap) is again determined. By analogy to (5.2):

$$Yp\ (\Delta Hfp) = KAp \qquad (5.3)$$

Where ΔHfp is the heat of fusion of the polymer. Since K is an instrumental calibration constant and Yp and Ap are known,

one can solve for ΔHfp. A problem that is frequently encountered with polymers is to decide how one defines Ap, or in other words, to decide how to join the pre- and post-transition baselines

Consider the general equation relating measured heat capacity to thermal measurement (162).

$$H = XHC + (1-x)Ha + \frac{dx}{dt}\Delta Hf \qquad (5.4)$$

where H is the measured heat capacity (t) the temperature, and Hc and Ha the heat capacities of the crystalline and amorphous material, respectively. In the melting region the last term in (5.4) becomes dominant, but at least in the case of polyethylene, is a minor contribution to H up to 30°C below the melting temperature (162). Hence it is customary to determine the last term in (5.4) from the heat capacity contributions by drawing an appropriate straight base line tangential to the pre- and post-melting baseline of the melting curve (fig 12). However, the construction of this baseline can be a somewhat subjective procedure.

Several procedures have been suggested by different authors (163). However, since we are comparing polymers with and without fillers in the measurement of heat of fusion, and the base lines are drawn in an identical way, in each case it is considered possible to

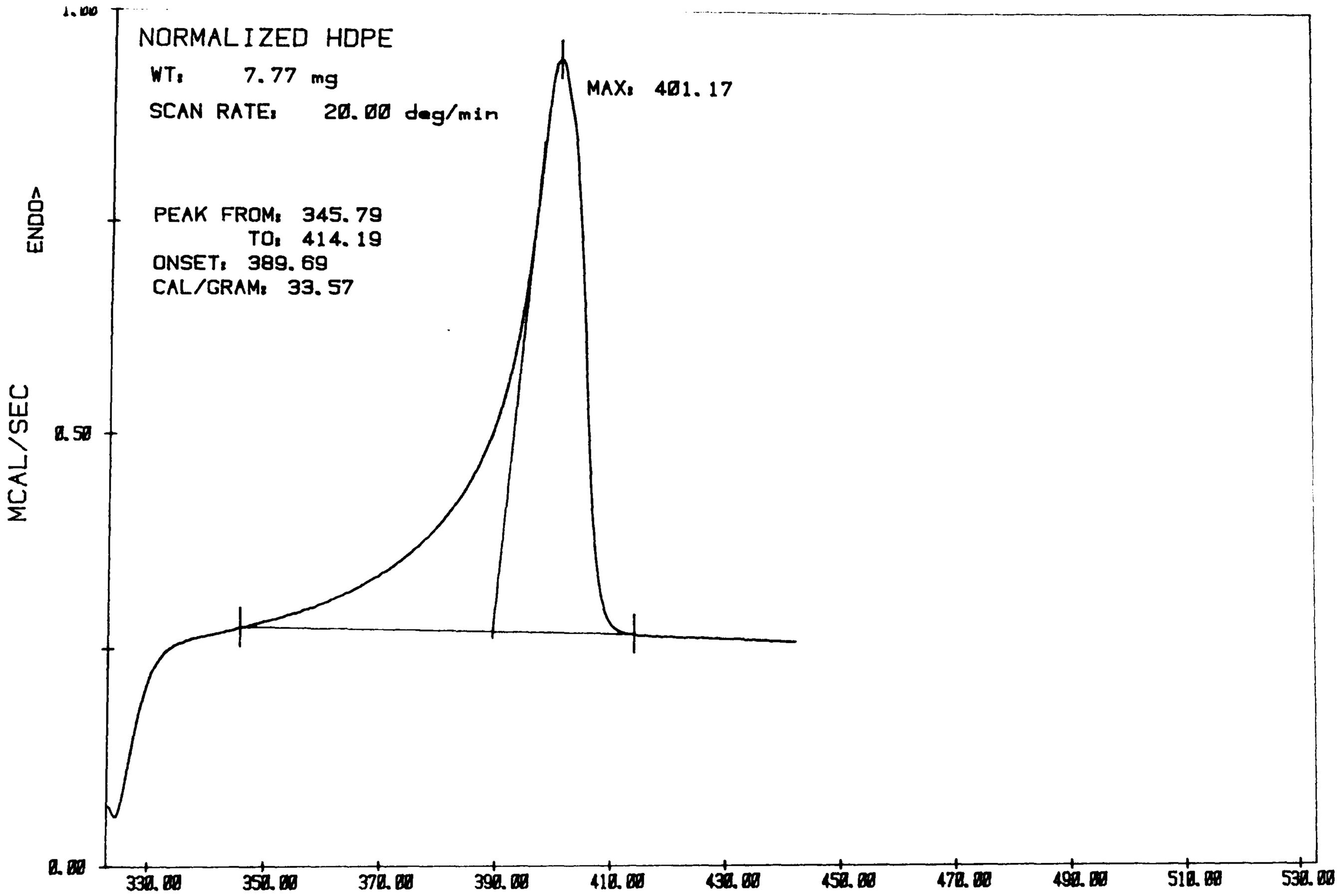

A. HASHEMI *FILE: HDPEP.DA*

DATE: 09/09/82 TIME: 13:21

Fig (12) DSC melting curve of HDPE

obtain a reasonably accurate measurement.

The "total ΔHf_l" method for crystallinity will often involve the determination of small differences between large quantities, which is undesirable from the point of view of accuracy. However, careful analysis of the data obtained on a variety of samples should lead to a greater understanding of the fusion process for each class of polymer and this in turn may even lead to a simple "baseline" means of measuring ΔHf_l.

4.5.2 Melting point and percent crystallinity

Polyethylene is a semi-crystalline thermoplastic polymer, which upon the application of heat, undergoes a process of fusion, or melting, where the crystalline character of the polymer is destroyed. While polymers melt over a temperature range due to difference in the size and regularity of the individual crystallites, the melting point of a polymer is generally reported as a single temperature where the melting of the polymer is complete.

An additional parameter for the characterization of polyethylene is its percent crystallinity. Many important physical properties of polyethylene are dependent on the percent crystallinity. For example, low crystallinity polyethylene is characterized by high impact strength and optical clarity and high crystallinity polyethylene is characterized by stiffness.

Both the melting point and percent crystallinity may be determined from a single D.S.C. scan on the sample. Fig ($_{13}$) illustrates a typical D.S.C. determination of the polyethylene. The melting point is taken at the peak temperature where melting is complete, or at least nearly so - in this case 401.17^{o}K. The area under the melting peak is equal to the heat of fusion of the sample, generally abbreviated ΔHf_1, in units of calories/gram. The D.S.C. method for determining the percent crystallinity of a semi-crystalline polymer is based upon the measurement of the heat of fusion, ΔHf_1, and the reasonable assumption that this quantity is proportional to the percent crystallinity. If by some process of extrapolation, estimation or analogy with model compounds, the heat of fusion, ΔHf^{o} of a hypothetical 100% crystalline sample is known, the percent crystallinity may be calculated from equation (2).

Fortunately - for polyethylene at leat - this quantity, ΔHf_1^{o} has been determined by D.S.C. measurements on a 100% crystalline polyethylene (164) and found to be 68 calories/gram.

With the aid of the computer system, the area under the curve, representing the heat of fusion, is directly printed out.

Measurement of heat of fusion of starch filled HDPE.

The heat of fusion calculated using the scan D.S.C. has first

been multiplied by the total weight of polymer and starch in the sample. The result was divided by weight of polymer present in the same sample. It was assumed that since starch does not melt, it does not contribute to the heat of fusion of the composite, i.e. the observed heat of fusion was attributed to thermal transitions of the polymer alone. Support for this assumption is provided by the comparison of the D.S.C. scan of starch filled polymer and starch alone, shown in figure (13).

Percent crystallinity of starch filled HDPE was calculated using equation 5.1), and illustrated in figure (14). Table (4.5) shows ΔHf_1, and melting point for HDPE and starch filled HDPE.

Increasing the concentration of taro starch with an average particle size of 3.2 micron in HDPE caused a gradual increase in the total heat of fusion of the polymer calculated as explained above.

However, increasing the concentration of potato starch with an average particle size 50 micron and maize starch (average particle size 15 micron) did not make any significant difference to the total heat of fusion regardless of the amount of the starch. It may be concluded that particle size does play a part in determining the thermal properties of the filled polymer (and in turn in determining the mechanical properties of the filled polymer, see section (4.3.0)).Although it is necessary to take into account the

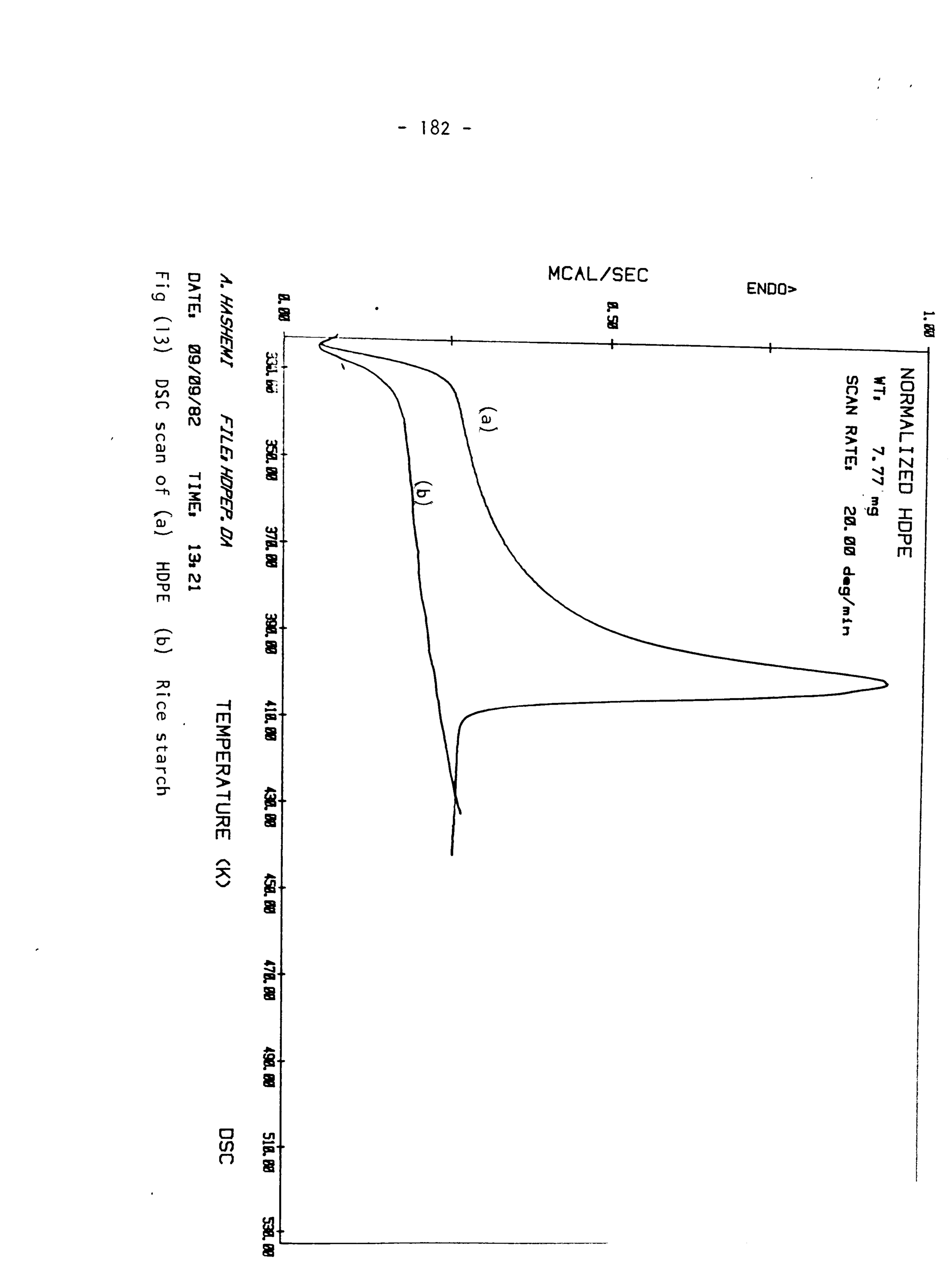

Fig (13) DSC scan of (a) HDPE (b) Rice starch

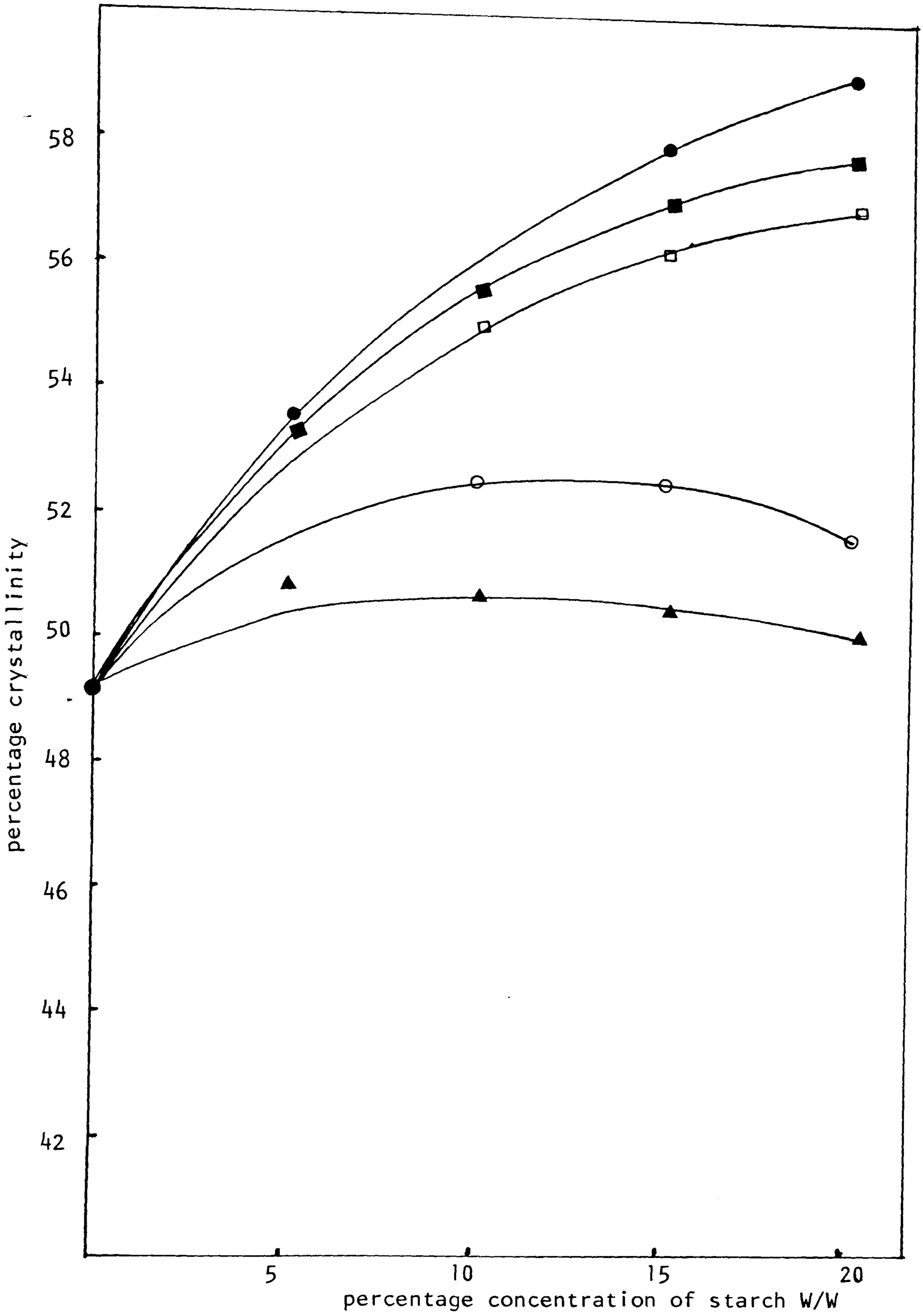

Fig (14) Effect of various starches on percentage crystallinity of HDPE

Symbols used are as given in table (4.7)

Table (4.8)

Effect of different starches on the thermal properties of HDPE

Filler	Starch concentration W/W	Melting point K^{o}	Heat of fusion Cal/gram	%crystallinity
Lehua Mali starch	None	401.12	33.57	49.36
	5	404	36.81	53.82
	10	404	39.14	57.55
	15	404	39.48	58.05
	20	402	40.15	59.004
Acid treated Rice Starch	None	401.12	33.57	49.36
	5	400.39	36.64	53.95
	10	401.13	37.4	55
	15	405.73	38.2	56.176
	20	406.6	38.92	57.23
Rice Starch	None	401.12	35.57	49.36
	5	404.31	37.08	54.52
	10	401.43	37.8	55.54
	15	403.19	38.92	57.23
	20	400.32	39.162	57.59
Maize Starch	None	401.12	35.57	49.36
	5	403.91	36.4	53.52
	10	400.57	35.96	52.88
	15	400.54	35.82	52.67
	20	400.77	35.33	51.95
Potato Starch	None	401.12	35.57	49.36
	5	401.19	34.94	51.3
	10	400.0	34.5	50.73
	15	400.56	34.28	50.41
	20	400.99	34.12	50.17

fact that different starch types have somewhat different effects on the polymer into which they are blended.

Increasing the concentration of rice starch with average particle size of 5 micron, acid-treated rice starch in HDPE causes a gradual increase in the total heat of fusion of the polymer. In the case of acid-treated rice starch it was expected that the effect of the filler on the total heat of fusion of the polymer would be greater than that observed with the other starches, because greater mechanical yield and tensile strength and hence the presumably increased starch-polymer interaction (see section) but in fact differences we observed were rather small.

It is interesting to compare and contrast these results on thermal properties of the starch-filled HDPE with the result obtained on the effect of starch granules on the mechanical strength of the filled polymer.

Only in the case of acid-treated rice starch-filled HDPE was an increase in the mechanical yield strength observed. The effect of acid-treated rice starch on the heat of fusion of the filled polymer was, by contrast, quite similar to that of untreated rice-starch, which suggests that the mechanism which mediates the increase in yield strength as a result of blending acid-treated rice starch with HDPE has a different physical origin to that study involved in increased crystallinity in the polymer.

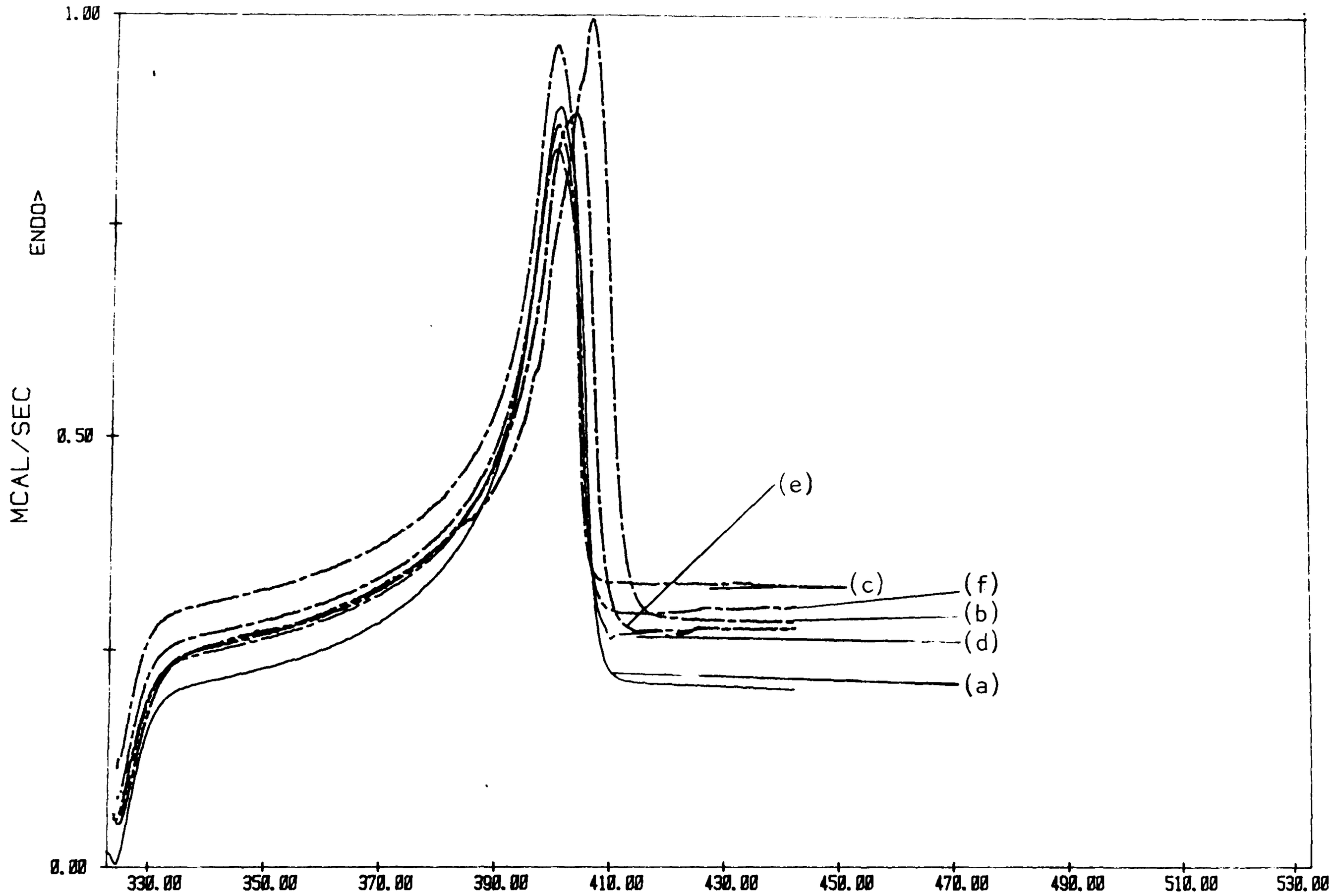

Fig (15) Comparison of melting curve of HDPE containing (a) none, (b) 1 % (c) 5 % (d) 10% (e) 15 % (f) 20% acid treated rice starch

Fig (15) illustrates the D.S.C. thermograms of acid treated rice starch filled HDPE, indicating variation of melting points for various concentrations of starch.

Section 6

4.6.0. X-ray diffraction studies of starch filled HDPE.

Introduction

Solid polymer can exist in an amorphous state characterized by a disorder arrangement of molecules and in a crystalline state characterized by three-dimensional order. Crystallization causes changes in the properties of polymers, e.g. in hardness, softening temperature, density and optical clarity. During the 1940's and early 1950's polymer chemists considered all partly crystalline polymers to be two-phase systems made up of small crystallites embedded in an amorphous matrix. Each of these crystallites was supposed to consist of a bundle of parallel chains, shown schematically in (figure 16a), with each crystallite so small that a single molecule passed through several crystals (165).

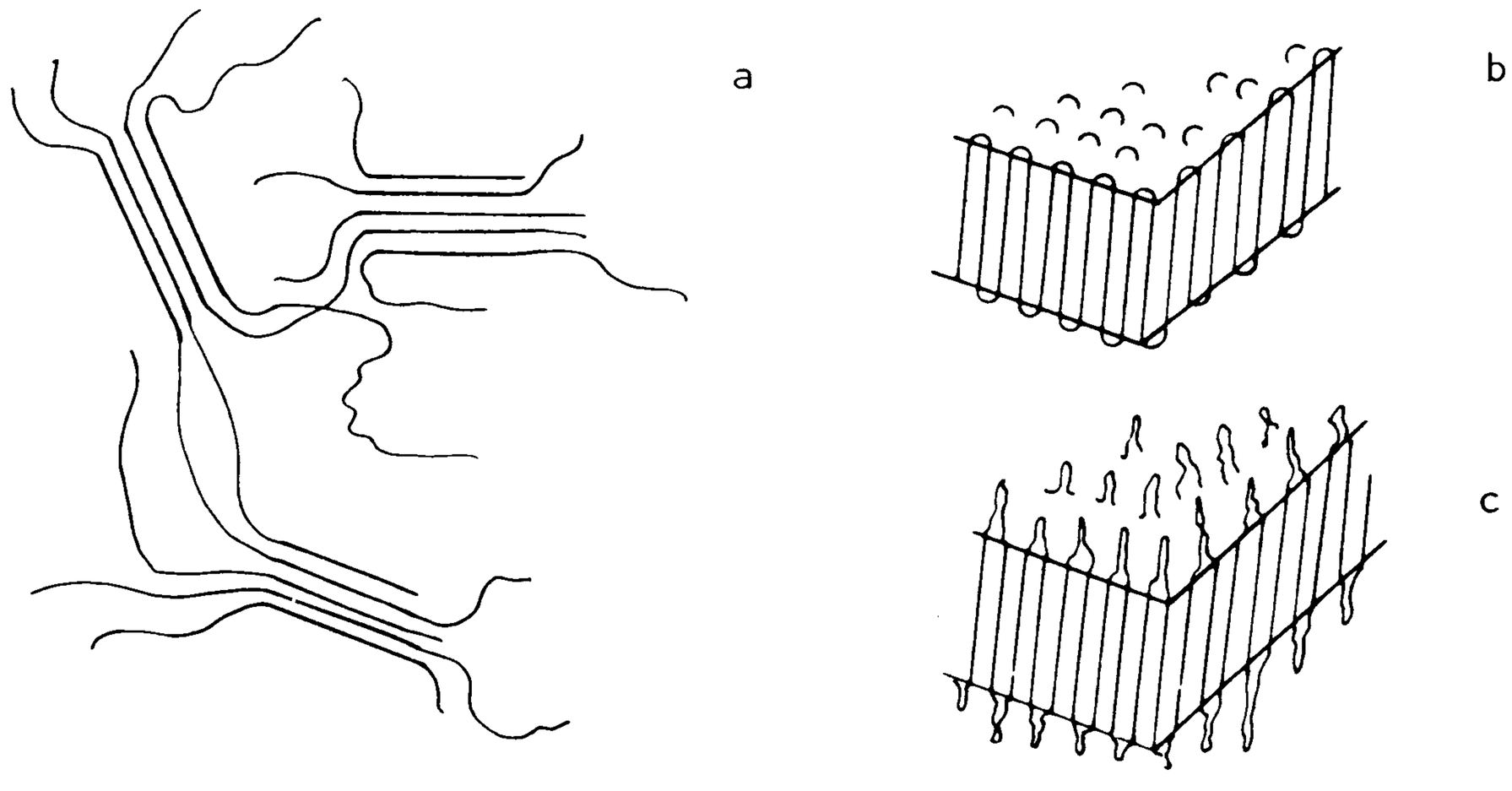

Fig. 16 Various representations of chain conformation in crystalline polymers.

This concept of polymer crystallinity, called the fringe micellar theory, predicted that a polymer could never become 100 per cent crystalline because, as crystallization progressed, the portions of molecules in amorphous regions would become strained and this strain would finally prevent further crystallization (165). During the period when the fringe micellar theory was generally accepted, partly crystalline polymers were characterized by the percentage of crystallinity and various methods for determining the percentage of crystallinity were devised (165). However, as measurements and observations accumulated, it became apparent that the fringe micellar theory was inadequate. In the late 1950's single crystals were prepared from solutions of various polymers, and the molecules in these crystals were shown to be arranged perpendicular to the broad face of the crystals and to be folded back on themselves accordian-wise, as shown in fig (16) b and (16)c.

A modern view (166) would have us regard highly crystalline polymers in a similar way to that in which crystals of low molecular weight compounds have long been regarded, i.e. as a single crystalline phase with defects. Defects in polymers (167) may be lattice defects like the defects that occur in crystals of low molecular weight compounds, screw or edge dislocations, grain boundaries stacking disorders, etc.

Not all workers subscribe to the viewpoint that a partly crystalline polymer is a single (crystalline) phase with defects. These workers prefer to treat semicrystalline polymers, and even highly crystalline polymers, as mixtures of crystalline and amorphous phases (168). It seems probable that the truth lies somewhere between these two extreme views.

Experimental techniques that yield important information about crystalline polymers are: x-ray diffraction, infrared absorption, density measurement, electron microscopy, electron diffraction, nuclear magnetic resonance spectroscopy and observation of birefringence (165). However, the presence of starch as a filler in polymers make it impossible for some of these techniques to be used. In the following paragraphs the feasibility of some of the above-mentioned techniques as means to examine the morphology of starch-filled polymers will be discussed.

x-ray diffraction

X-ray diffraction (169) is a most important technique for the study of crystallinity. When an x-ray beam strikes matter, the beam is scattered by electrons. If the matter were entirely without order, a photographic plate placed perpendicular to the beam would darken uniformly. Amorphous solids and liquids are, however, rarely devoid of order. There is even in liquids, transient short-range order over a distance of about 5 Å. Even completely amorphous polymers

scatter x-rays and produce diffuse haloes on a photographic plate.

When a beam of x-rays strikes a crystal in which the atoms are arranged in a three-dimensional lattice, the x-rays are reflected from different planes in the crystal and interfere with one another in the reflected beam. There are maxima in the intensity of x-rays scattered by a crystal when the relationship between the angle of incidence, or the reflected beam and distance between layers in the crystal, d, is such that reflections from different layers reinforce one another. These maxima occur when the following equation is satisfied:

$$n\lambda = 2d \sin \theta \qquad (1)$$

Where is the wavelength of the x-ray and n is an integer, 1,2,3..... This is an expression of Bragg's law. The x-ray diffraction pattern from a single crystal consists of an array of spots symmetrically arranged. The intensities and positions of these spots can be used to map the distribution of electrons in a crystal and, hence, to determine the position.of atoms (170). The preparation of a map of electron density requires much labour and a highly crystalline sample. However, even if crystals are not large enough to be studied singly, much can be learned from the diffraction of x-rays by finely divided powders of crystalline materials.

It is usually reasonable to assume such powders consist of a multitude of tiny crystals with faces oriented at all angles to the incident beam. Some of these crystals are oriented so that one set of parallel planes is at just the angle, θ, to produce reflections. Because there are many crystals in the powder sample with this particular orientation of one crystal axis, and because the crystals are small, the point reflections arising from the individual, small crystals, coalesce on the photographic film to produce a ring. Since, in general, crystals have several sets of reflecting planes, many diffraction rings are produced. The centres of these rings are located at the point at which the undiffracted beam intersects the photographic plate, and the radii of the rings are determined by the fact that, when the incident beam strikes the plane in a crystal at an angle θ, the beam is reflected at an angle 2θ. Their geometry is illustrated diagramatically in section (3.12.2). Samples of the thin film were prepared by melting the HDPE between two glass slides and cooled at room temperature. Attempts were made to work with identical samples under identical conditions. The thin film thus prepared was exposed to x-ray as explained in section (3.12.3)

Plate (29) shows a comparison between the x-ray powder diffraction pattern obtained from HDPE and 1% rice starch-filled HDPE.

Plate (30) shows a comparison of the x-ray powder photographs of HDPE and 15% rice filled HDPE.

Plate (32) shows a comparison of the x-ray powder photographs of HDPE and 20% rice starch filled HDPE.

The purpose of these studies was as follows: to attempt to discover whether or not there is any orientation in polymer resulting from the presence of starch filler in the polymer.

Judging from the similarity between the x-ray patterns obtained from the samples with and without the filler, it appears that at least as far as it is possible to judge from the x-ray reflection observed, no induced orientation in particular direction is evident.

To discover whether or not there is any change in the degree of crystallinity resulting from the presence of starch, it is difficult using the standard densitometer to trace all the x-ray diffraction lines. However, from those lines which could be traced, it seems that the line profile sharpens due to the presence of starch, and this can be seen visually in plate (31), despite the fact that the amount of HDPE has been reduced as the concentration of starch increases.

The results from D.S.C. confirm that there is an increase in the heat of fusion of the polymer and in turn in the degree of crystallinity, see section (4.4.0).

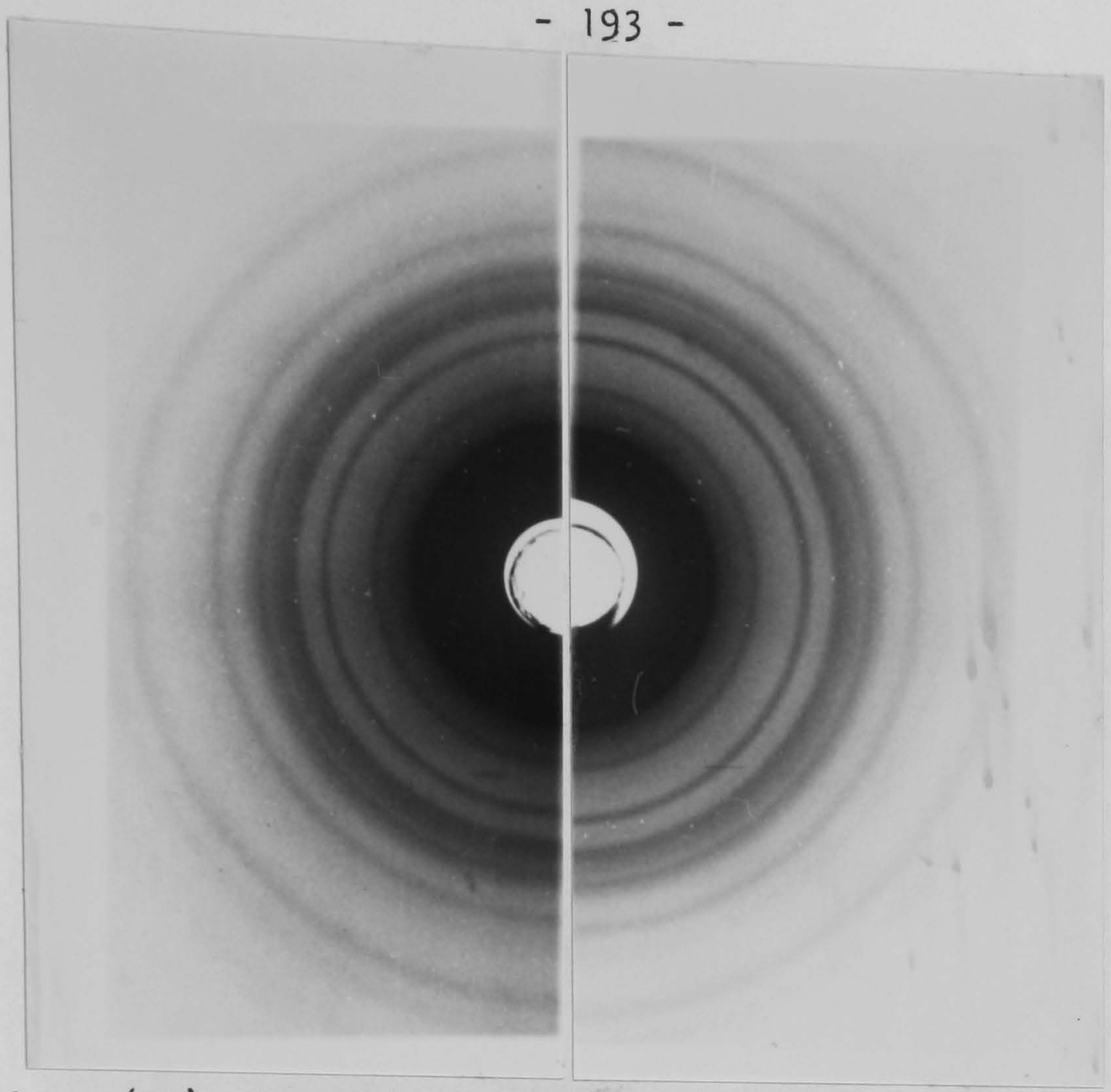

Plate (29) Comparison of flat-plate x-ray diffraction pattern for HDPE and 10% rice starch-filled HDPE

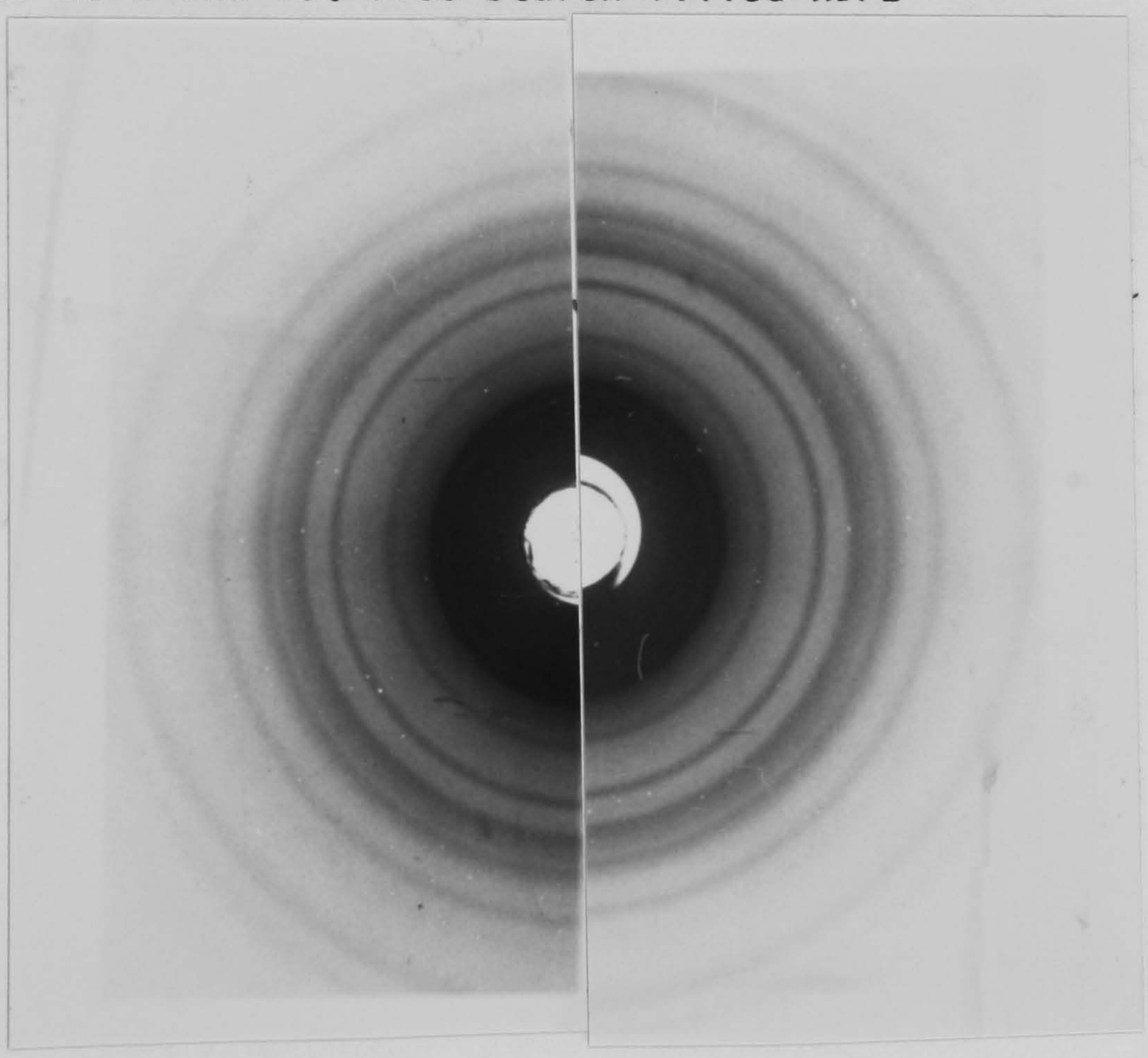

Plate (30) Comparison of flat-plate x-ray diffraction pattern for HDPE and 15% rice starch-filled HDPE

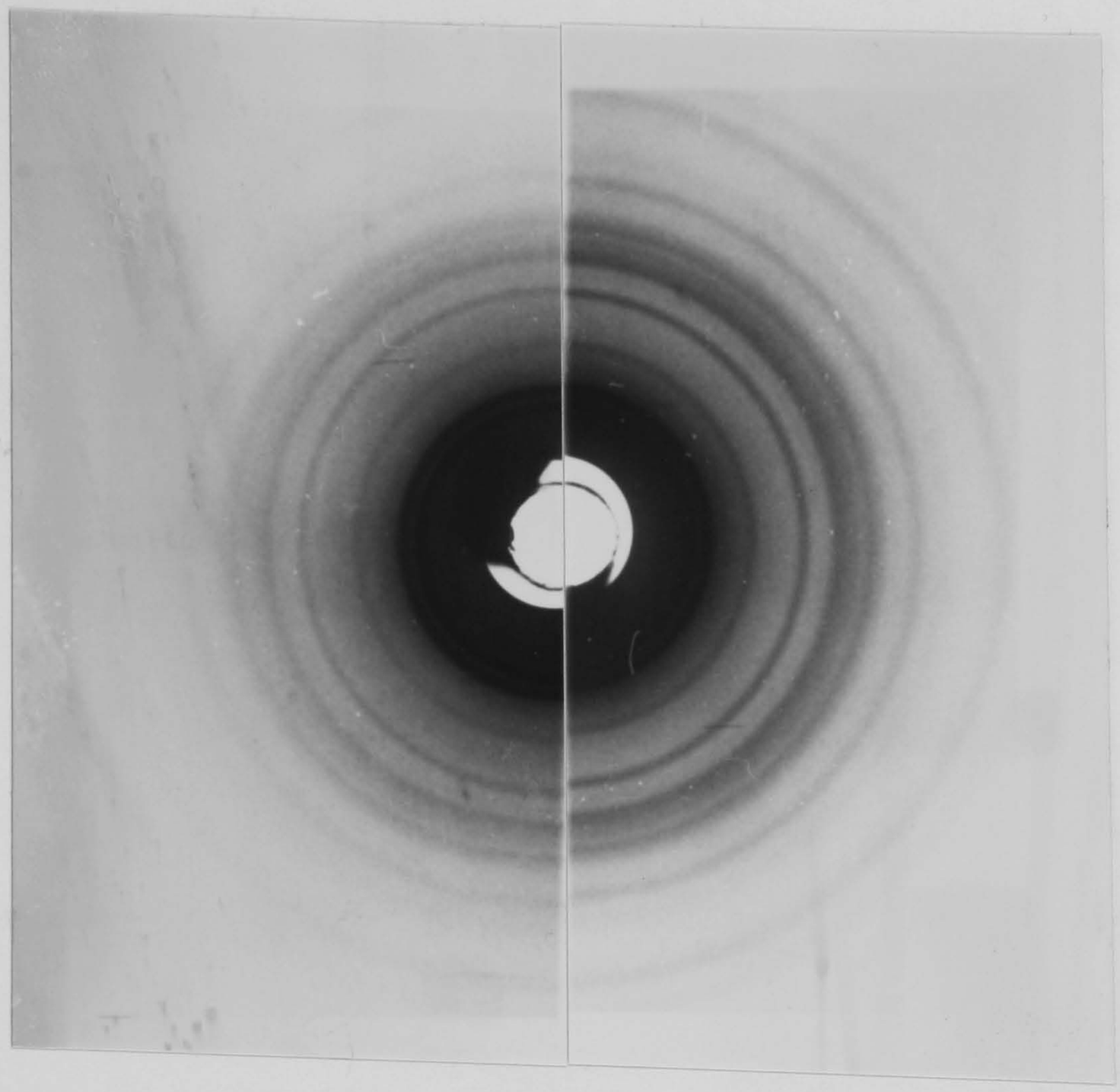

Plate (31) Comparison of flat-plate x-ray diffraction pattern for HDPE and 20% rice starch-filled HDPE

CHAPTER 5

CONCLUSIONS AND SUGGESTIONS

FOR FURTHER WORK

Conclusion and Suggestions for further work

The evidence offered in this thesis strengthens the conclusion from earlier work that whole grain starch is a most promising filler, for high density polyethylene. The results now show that certain varieties of starch can be used as true reinforcing fillers. When we consider the modest cost, wide botanical variety and its clear position as a renewal resource, it seems likely that starch will find many applications in such polymer composites. The new evidence shows that by controlled acid treatment of starch granules one can achieve better adhesion between the filler and the polymer matrix, and this is most probably due to the increase in the surface roughness. This argument is based on the observed increase in mechanical strength of HDPE, when treated starch has been incorporated.

It is already known that the starch can perform better as a filler for polymers if the surface of starch granules have been treated so that they become more easily wettable by polymer melts. There seems to be only modest incentive to attempt to achieve fully covalent coupling between the starch filler and its matrix because of the close match in physical properties between this filler/ matrix pair, not surprising when both elements are in fact organic polymers. It has been shown that Taro starches are much better fillers than other starches, because of their small particle size and corresponding larger specific surface area available to

interact with the matrix.

The technique of small-angle laser light scattering proved to be of invaluable assistance in dealing with the very large number of different starches. Improvements in the experimental method have allowed reliable recording of the Hv scattering data from starches including the very small Taro, thus permitting an accurate evaluation of particle size from scattering data in terms of the Stein-Rhodes theory. This theory was originally devised for studying spherulitic crystalline polymers. On the basis of the excellent agreement between particle diameters calculated from scattering measurements using the theory and such diameters derived from microscopy using various starches, it is concluded that the theoretical Hv equation accurately describes the scattering from spherulites such as starch granules. Attempts to record Vv scattering from starch granules failed because of experimental limitations, so that certain aspects of particle structure could not be derived, however the Hv scattering analysis of starch samples was of obvious technical value and average particle size could be determined in a fast and convenient manner for any spherulitic granular sample possessing predominantly spherical shape shape. The main advantage of light scattering over microscopy is the ease and convenience of technique. However, it can only give average particle size and particle size distribution had to be measured by microscopy.

In order to seek some explanation of the unexpected physical changes in the polymer matrix, evidence obtained from x-ray diffraction patterns and differential scanning calometry was examined. There was definite indication of an increase in the degree of crystallinity.

On the basis of the optical and electron microscopy work, it has been possible to see morphological changes on matrix polymer near to the starch particle. The results presented in this investigation are, admittedly, incomplete and contain some puzzling features which should be clarified by further work. Some suggestions are as follows:

1. It would be interesting to investigate a series of different starches which contain different amounts of amylose because one aspect of the acid treatment process is that it removes amylopectin from the starch grain surfaces and this could be more important than the development of surface roughness. There are starches available which contain up to 90% of amylopectin.

2. It is still not known if there is any chemical reaction taking place between the filler and polymer, a closer investigation might reveal evidence of reactions at the interface which may help a better understanding of the relationship between the two components.

3. It would be useful to investigate the mechanical stress pattern created at the interface by transfer through the matrix polymers. Some guidance could be derived from other studies in the composites field involving stiff elastic particles embedded in a slightly stiffer polymer matrix.

4. The technique of light scattering could be used for examining other aspects of these starch-composites, such as measurement of gelatinization temperatures of particles in situ by providing the apparatus with programmed hot stage.

5. Because of the known abnormal behaviour of very thin films of polyolefines, for example they exhibit semiconductor properties and higher permeability than the bulk material, it would be interesting to examine certain physical properties of the composites containing high loadings of the very small particle starches. There is considerable literature on the diffusion of water and gases through composites which would be applicable.

1) Griffin,G.J.L. "Degradation of Polyethylene in Compost Burial" J. Polym Sci. Symposium No 57, 281-286 (1976)

2) Griffin,G.J.L.and Turner, R.D. "Macrobiodegradation of Plastics" 4th Intl Bioder. Conference, Berlin, August(1978) (in press)

3) Griffin,G.J.L. British Patent 1 489 050 (1973)

4) Griffin,G.J.L. U.S. Patent 4125495 (1973)

5) Griffin,G.J.L. "Synthetic Resin-Based Compositions, USPatent 4016117, 4021388 and 4125495

6) Griffin,G.J.L. "Synthetic Polymers and the Living Environment" Pure & Appl. Chem., Vol.53 pp399

7) Dennenberg,R.J., Bolhast,R.J., and Abbott,T.P., "A New Biodegradable Plastic Made from Starch Graft Poly/methyl Acrylate copolymers", J. Appl. Polym. Sci. 22,2,459, (1978)

8) Afandi,R.D., "Starch-carried Fire Retardant Additives in Polyester Resins. M.Phil Thesis, Dept. of Non-Metallic Materials, Brunel University, Uxbridge, U.K. January (1982)

9) Linero,C.G.O. "Suitability of Tropical Starches as Fillers and Reinforcement for Thermoplastics and Polyester Resins- PhD thesis, Dept. of Non-Metallic Materials, Brunel University, Uxbridge, U.K. October (1979)

10) Rhodes,M.B., and Stein,R.S., J. Appl. Phys., 31 1873 (1960)

11) Whistler,R.L., and Paschall,E.F. Eds. "Starch Chemistry and Technology" (Academic Press, New York, 1965)

12) Ott,E, Spurlin, H.M., and Grafflin, M.E., Eds., "Cellulose and Cellulose Derivatives" (Interscience Publishers, New York, 1954)

13) Bear,R.S. and French,D.J. Am. Chem. Soc., 63, 2298 (1941)

14) Rundle,R.E. and French,D., J. Am. Chem. Soc., 65, 1720 (1943);
Rundle,R.E. and Edwards,F.C., Ibid., 65,2200 (1943);
Rundle,R.E., 69,1769 (1947)

15) Harries,P.M., Mark, E., Jr., and Blake,F.C., J. Am. Chem. Soc. 50, 1583 (1928)

16) Hames,C.S., New Phytologist, 36, 189, (1937)

17) Freudenburg,K., Schaaf,E., Dumpert,G and Ploetz,T., Naturwissensch aften, 27, 850 (1939)

18) Ogbonna,C., Private Communication, Ecological Materials Research Institute, Brunel University, Egham, Surrey, (1983)

19) Badenhuisen,N.P. "Chemistry and Biology of the starch granule" in "Protoplasmatalogie", Band II (Springer verlag, Wien 1959)

20) Mark,H., Chem, Rev., 26, 184 (1940)

21) Katz, et al, series of papers in Z. Physik, Chem. Ser. A (1930-1939)

22) Sterling,C., Starke, 12, 182 (1960)

23) Borch, J. "Light Scattering by Starch Granules", Ph.D. Thesis State University of New York, College of Environmental Science and Forestry. (1970).

24) Badenhuizen,N.P. and Dutton,R.W. "Protoplasma.", 47, 156 (1956)

25) Chandarkar,K.R., and Badenhuizen,N.P. Cereal Chem. 44,27 (1967)

26) Zobel,H.F., "Methods Carbohydrate Chem", Vol. IV, Whistler,R.L. Ed. (Academic Press, New York, 1964) p109

27) Sair,L., Cereal Chem 44 8 (1967)

28) Blackwell,J., Sarko, A. and Marchessault,R.M., J. Molecular Biol. 42, 379 (1969)

29) Nageli, Liebig's Ann. Chem., 173, 218 (1874)

30) Brown, H.T. and Morris,G.J., J. Chem. Soc. (London), 55,449

31) Klason,P., and Sjoberg,K., Ber. Deutsch Chem. Ges., 59,40 (1926)

32. Kainuma,K. and French,D., "Preparation and Properties of Amylodextrins from Various Starch Types", Biopolymer 10, 1673-1680 (1971)

33) Lintner,C.J., J. Prakt. Chem. 34, 378 (1886)

34) Samec,M., Katz,J.R., and Derksen J.C., Z. Physik, Chem., A158, 321 (1932)

35) French,D. "Chemistry and Industry of Starch", 2nd ed., Kerr,R.W., Ed., Academic Press, New York, p.157 (1950)

36) Sterling,C., "Starch and its Derivatives" 4th ed., J.A.Radley Ed., Chapman and Hall, London p 139 (1968)

37) Hickerson,R.F. and Hable,J.A., Ind. Eng. Chem, 39, 1507 (1967)

38) Marrinan,H.J., "Recent Advances in the Chemistry of Cellulose and Starch", Honeyman,J.Ed., Interscience Publisher, Inc., New York, p.147 (1959)

39) Bemiller,J.N., "Starch:Chemistry and Technology", Whistler, R.L. and Paschall,E.F.,Eds.,Academic Press, New York and London, p 495 (1965)

40) BeMiller,J.N., Advan. Carbohydrate Chem., 22,25 (1967)

41) Ingersoll,H.G., J. Appl Phys. 17, 924 (1946)

42) Howsman,J.A., Textile Res. J., 19,152 (1949)

43) Seidemann,J. Starke-Atlas: Principle of Starch Microscopy and Description of Varieties of Starches, P. Parcy, Berlin, (1966)

44) MacMaster,M.M. "Microscopic Techniques for Determining Starch Granule Properties" in Methods in Carbohydrate Chemistry IV.; Whistler,R.L. Ed., Am. Press, New York (1964)

45) Moss,G.E., "The Microscopy of Starch in Examination and Analysis of Starch and Starch Products: Radley,J.A. Ed; App. Sci. Publishers Ltd., London (1976)

46) Schleiden,J.M., "Principles of Scientific Botany, Longman, Brown, Green and Longmans pub., London (1849)

47) Sterling,C. "The Structure of the Starch grain in Starch and its Derivatives". Radley,J.A. Ed. Chapman and Hall, London (1968)

48) Yamaguchi,M., Kainuma,K. and French,D. Journal of Ultra-structure Research, 69, 249-261 (1979)

49) Hall,D.M. and Sayre,J.G.? Textile Rep. J. 40, 147-157 (1970)

50) "Official Method of Analysis", Horwitz,W., ed., Association of Official Agricultural Chemist, PO Box 540, Benjamin Franklin Station, Washington 4, D.C. 9th Ed., pp 169, 282 (1960)

51) Standard Analytical Methods of the Member Companies of the Corn Industries Research Foundation, Inc., R.J.Smith Ed., Corn Industries Research Foundation Inc., 1st Ed., (1952)

52) Sair,L and Fetzer,W.R., Ind. Eng. Chem., Anal. Ed. 14, 843, (1942)

53) Ulmann, M. and Shierbaum, F. Starke 9, 23 (1957)

54) Fischer,K. Angew, Chem., 48, 394 (1935)

55) Johnson,C.M., Ind. Eng. Chem. Anal. Ed. 17, 312 (1945)

56) Judd,D.B., "Colour in Business, Science and Industry" John Wiley and Sons Inc., New York, N.Y. p 191 (1952)

57) Schoch,J.J. and Leach,H.W., Cereal Chem., 38, 40 (1961)

58) Whitney,L.D., Bowers,F.A.J. and Takahashi,M. "Taro Varieties in Hawaii" Hawaii Agricultural Experiment Station of the University of Hawaii, Bulletin No. 84

59) Higashinara,M., Umeki,K., and Yamamoto, T. "Isolation and Some Properties of Taro Root Starch, Denpun Kagaku (J. Japan Soc. Starch Sci) 22:61 (1975)

60) Radley,J.A. "Starch and its Derivatives", Chapman and Hall, London (1940)

61) Griffin,G.J.L. "Biodegradable Synthetic resin sheet Material" US Patent 4016117 (1977)

62) Watt,J.A.C., J. Tex. Inst. 48, 175 (1967)

63) Dow Corning 1107 Fluid: Bulletin 05-169, Dow Corning International Ltd., Brussels-Belgium (1967)

64) Griffin,G.J.L. "Non-food Applications of Starch, especially Potential Uses of Taro" in small-scale Processing and Storage of Tropical Root Crops Ed. Plucknett,.DL. p 275, Hawaii (1978)

65) Zigman,W.A., Ind. Eng. Chem. 55 (10) 18, (1963)

66) Stein,R.S. "Newer Methods of Polymer Characterization", Ke, B., Ed. (Interscience Publishers, New York, 1964) p 185

67) Rhodes,M.B., Keedy,D.A., and Stein,R.S., J. Polymer Sci. 62, S73 (1962)

68) Erhardt, P.F., and Stein, R.S., J. Polymer Sci., Part B, 3, 553, (1965)

69) Adams, G.G. and Stain, R.S., J. Polymer Sci. Part A2, 6, 31 (1968)

70) Keller, A. "Fibre Structure", Hearle, J.W.S. and Peters, R.H. Ed. (Butterworth, London 1963) p346

71) Clough, S.,van Aartsen, J.J. and Stein, R.S. J. Appl. Phys. 36, 3072 (1965)

72) Rhodes, M.B. and Stein, R.S. J. Appl. Phys. 39,4903 (1968)

73) Samuels, R.J. J. Polymer Sci., Patt A2, 6, 1101 (1968)

74) Picot, C. Ph.D. Thesis, Centre de Recherches sur les Macromolecules, Strasbourg, France (1968)

75) Keizzers, A.E.M. PhD. Thesis, The Technical University of Delft, Holland, (1967)

76) Debye, P. and Bueche A.M., J. App. Phys. 20, 518

77) Stein, R.S. and Wilson, P.R. J. Appl. Phys. 33, 1914 (1962)

78) Stein, R.S. and Wilson, P.R. J. Appl. Phys. 33, 1914 (1962)

79) Beebe, E.V., Coalson, R.L., and Marchessault, R.N., J. Polymer Sci. Part C, 13, 103 (1966)

80) Borch, J. M.S. Thesis, State University of Forestry at Syraceuse University, Syraceuse, New York (1967)

81) Borch, J. and Marchessault, R.H. J. Colloid Sci., 27,355 (1968)

82) Giunier, A., Fournet, G., Walker, C. and Yudowich, K. "Small-Angle Scattering of X-ray, Wiley, New York p19 (1955)

83) Van Aartsen, J.J. Office Navel Res. Tech. Dept. No. 83, March 1 (1966)

84) Samuels, R.J. "Small-Angle Light Scattering from Optically Anisotropic Spheres and Disks. Theory and Experimental Verification". J. Polym. Sci. Part A2, Vol 9, 2165-2246 (1971)

85) Ke, B., J. Polym. Sci, 42, 15 (1960)

86) Ke, B., J. Polym. Sci. 61, 47 (1962)

87) Wunderlich, B. and Kashdan, W.H., J. Polym Sci. 50,71 (1961)

88) Coste, J. Ind. Plastiques Mod. (Paris) 9, 37 (1957)

89) Hoffman, J.D. and Week, J.J., J. Res. Natl Bur. Std., A66 13 (1962)

90) Flory, P.J. Trans. Faraday Soc. 51, 848 (1955)

91) Richardson, M.J. Flory, P.J. and Jackson, J.B., Polymer 4, 221 (1963)

92) O'Neill, M.J. Anal. Chem. 38, 1331 (1966)

93) Mandeluern, L., Allou, A.L., Jr. and Gopalan, M., J. Phys. Chem. 72, 309, (1968)

94) Bair, H.E., SPE Technical Papers 16, 115 (1970)

95) Prime, R.B., Wunderlich, B., and Melillo, L. J. Poly. Sci. Pt. A-2, 7. 2091 (1969)

96) Casey, K. Elston, C.E. and Phibbs, M.K., Polymer Letters, 2, 1054 (1964)

97) Groeninekx, G., Berghmans, H. and Smets, G., in abstracts of the IUPAC Macromolecular Symposium, Leiden, Holland, Sept. p742 (1970)

98) Fava, R.S.? Polymer, P 137 (March 1968)

99) Gray, A.P. and Casey, K. Polymer Letters 2, 381 (1964)

100) Parker, R.S. and Johnson, J.E. (eds) Analytical Calorimetry, Vol. 1 (Plenum Press New York, 1968)

101) Knox, J.R. Instrument News, 17 No. 4 (Perkin-Elmer Corp.) (1967)

102) "Anhydro" Laboratory Spray Dryer Operating Manual

103) Wahlstrom, E.C., Optical Crystallography, 4th ed. Wiley, New York, (1969)

104) MacMaster, M.M. "Microscopic Techniques for Determining Starch Granules Properties,"in Methods in Carbohydrate Chemistry IV; R.L.Whistler (ed), Am. Press, New York (1964)

105) Olley, R.H. and Bassett, D.C. "An Improved Permanganic Etchant for Polyolefines" Polymer, Vol. 23, November (1982)

106) Sauer, J.A. and Pac, K.D., Mechanicals Properties of High Polymers in Introduction to Polymer Science and Technology, Ed. by Kauffman, H.

107) Hull, A.W. Phys. Rev. 9, 84, 564 (1917); 10, 661, (1917)

108) Debye, P., and Scherrer, P. Phys. 7, 17, 277 (1916); 18, 291 (1917)

109) Jones, M.R., Larsen, N.P. and Pritchard, G.P. "Taro and Sweet Potatoes versus grain foods in relation to health and dental decay in Hawaii" Dental Cosmos (4): 395-409 illus (1934)

110) Miller, C.D. Food value of poi, taro and limu, Bernice P. Bishop Museum, Bull.37, 55pp, illus (1927)

111) Annual Report, Hawaii Agricultural Experimental Station pp 17-18 (1938)

112) MacCaughey, V. and Emerson, J.S. A Revised list of Hawaiian Varietal Names of Kalo. The Hawaiian Forester and Agriculturist 11: 338-341 (1914)

113) Sharafi, M. "A Study of the properties of starch/polystyrene composites." M.Phil thesis, Non-Metallic Material Department Brunel University, U.K. (1976)

114) Samuels, R.J. "In Supramolecular structure in Fibers" Poly. Sci. C, 20, P.H. Lindenmeyer, Ed. Interscience, New York, p.253 (1967)

115) Samuels, R.J. "In Small Angle Scattering from Fibrous and partially ordered systems". J. Polym. Sci. C, 13, Marchessault, R.H.? Ed., Interscience, New York, p37, (1966)

116) Stein, R.S., Clough, S.B. and Picot, C. J. Polym. Scie. A-2, 9, 1147 (1971)

117) Partington, J.R. "An Advanced Treatise on Physical Chemistry Vol. 4, Longmans, Green, p 72 London (1953)

118) Schwar, M.J.R., Pandya, T.P. and Weinberg, F.J., Nature, 215 239 (1967)

119) Thompson, B.J. and Zinky, W.R. Appl. Opt. 7, 2426 (1968)

120) "Fillers for Plastics" Ed. Wake, W.C., Liffe Books, London, The Plastics Institute (1971)

121) Encyclopedia of Polymer Science and Technology Vol. 6, P750 Interscience Publishers, a division of John Wiley and Sons Inc New York, London, (1967)

122) Bragg, T.P. and Held, M.D. Plast. Eng. 9, 30 (1974)

123) Arnaud, P. Rev. Plastics Mod., 174, 1092 (1970)

124) Axelson, J.W. Polymer Plast. Techn. Eng. 2, 93, (1975)

125) Jap, Plast. Ind. Ann. 17, 73 (1974)

126) Grillo, T.A. "Silane Modified Kaolin Pigments" Rubber Age (Aug 1971)

127) Van Hazlestesvelt, C.H. SPI-R.P. Div Preprint, Vol. 13, 12-D (1958)

128) Delmonte, J. SPI, R.P. Div. Preprint, Vol. 14, 14-B (1959)

129) Boehme, R.D., J. Appl. Polymer Sci. 12, 1097 (1968)

130) Okuno, K., Woodhams, R.T., Polym. Eng. Sci. 4, 308 (1975)

131) Maine, F.W., Shepherd, P.D., Composites 5, 193 (1974)

132) Sakaguchi, F. Jap. Plast. Age 12 (4), 44 (1974)

133) Klason, C. J. Kubat, J. Appl. Polym Sci, 19, 831 (1975)

134) Bostwicks, R. and Carey R.H. Ind. Eng. Chem. 42, 848 (1950)

135) Roberts, K.D., M.S. Thesis, Washington University, St. Louis (1973)

136) Roberts, K.D., Hill, C.T., Ann. Tech. Conf. Soc. Plastic Engineers, Montreal, May (1973)

137) Eisa, B., Parchessault, R.H., J. Appl. Polymer Sci, 7, 2025 (1975)

138) Mureyama, T. Jap. Plast. Age. 1, 27 (1974)

139) Wilcox, G.R. SPI-R.P. Div, Preprint, Vol. 12, 15-C (1957)

140) Rev. Plast. Mod. 223, (1) 118 (1975)

141) Lightsey, G.R., Hines, A.L., Plast. Engng, 5, 40 (1973)

142) Plast. Tech. 22 (8) 71 (1976)

143) Plast. Tech. 22 (4) 81 (1976)

144) Stieg, F.B. Off. Digest 29, 439 (1957)

145) Dow Corning Corp, US Patent 061505

146) Union Carbide Corp. US Patent 862027

147) Motoyoshi, M. Jap. Plastics Age, 33, 5 (1975)

148) Boonstra, B.B. and Medalia A.I., Rubber Chem. Techn. 36, 115 (1963)

149) Smith, T.L. Trans Soc. Rhed., 3, 113 (1959)

150) Farris, R.J., J. Appl. Polymer Sci. 8, 25 (1964)

151) Farris, R.J. Trans Soc. Rheol. 12, 203, 315 (1968)

152) Nielsen, L.E. J. App. Polymer Sci. 10, 97 (1966)

153) Kerner, E.H., Proc. Phys. Soc. B69, 808 (1956)

154) Hashin, Z. and Shtritman, S. J. Mech. Phys. Solids, 11, 127 (1963)

155) Lewis, T.B. and Nielson, L.E. J. App. Polymer Sci., 14, 1449 (1970)

156) Flocke, H.A., Kaut. Gumni Kunstr. 18, 717 (1965)

157) Chanzy, H.D. and Revol, J.F. "Potato starch Encapsulation with Polyethylene", Die Starke ZG. Jabg. nr. 6 (1974)

158) Fitchmun, D.R. and Newman, S. "Surface Crystallization of Polypropylene, " J. Polym. Sci. Part A-2, Vol 8 1545 (1970)

159) Lechatelier, H. Z. Phys. Chem 1, 396 (1887)

160) Runt, J. and Harrison, I.R. Thermal Analysis of Polymers, in Method of Experimental Physics Vol. 16 Part B

161) Gray, A.P. Thermochim. Acta 1, 563 (1970)

162) Wunderlich, B "Macromolecular Physics" Vol. 1, p401, Academic Press, New York (1973)

163) Brennan, W.P., Miller, B and Whitwell, J.C. Ind. Eng. Chem. Fundam. 8, 314 (1969)

164) Wunderlich, B. and Cromier, J. Poly. Sci A-2,5 , 987 (1967)

165) Miller M.L. "The Structure of Polymer", Polymer Science and Engineering Series, Eds. Reinhold, Book, Corp., New York, London p493 (1968)

166) Stuart, H.A., Ann. N.York Acad. Sci. 83, 3 (1959)

167) Wunderlich, B. Polymer, 5, 125 (1964)

168) Mandelkern, L. "Growth and Perfection of Crystals" Eds, Dorcmus, R.H., Roberts, B.W. and Turnbull, New York, Wiley, (1958)

169) Nyberg, S.C., "X-ray analysis of organic structures" New York, Academic Press, (1961)

170) Alexander, L.E. "X-ray diffraction Methods in polymer science, Eds. Wiley, J. New York, London, Sydney, Toronto, (1969)